Contract NAS8-26266

MCR-72-107

Final
Report

May 1972

INVESTIGATION OF CHARACTERISTICS
OF FEED SYSTEM INSTABILITIES

Prepared by

R. D. Vaage
L. E. Fidler
R. A. Zehnle

Prepared for

National Aeronautics and Space Administration
George C. Marshall Space Flight Center
Marshall Space Flight Center, Alabama 35812

MARTIN MARIETTA CORPORATION
P. O. Box 179
Denver, Colorado 80201

FOREWORD

This final report is submitted in accordance with the
requirements of the Statement of Work for Contract NAS8-26266,
and documents the work accomplished during the contract period
1 July 1970 through 1 June 1972. This study was performed for
the George C. Marshall Space Flight Center of the National
Aeronautics and Space Administration, and was administered
technically by Mr. Raymond Spink of the Science and Engineering
Directorate, Astronautics Laboratory.

ABSTRACT

In the investigation of structure-propulsion system coupled longitudinal oscillations (POGO), the relationship between the structural and feed system natural frequencies is of major importance. The structural frequencies can be adequately defined by existing analytical techniques. The feed system frequencies are usually very dependent upon the compressibility (compliance) of cavitation bubbles that exist to some extent in all operating turbopumps. The lack of an accurate analytical prediction method for determining cavitation compliance has delayed the completion of POGO stability analyses until after turbopumps have been built and tested.

This document includes: a complete review of cavitation mechanisms; development of a turbopump cavitation compliance model; an accumulation and analysis of all available cavitation compliance test data; and a correlation of empirical-analytical results. The analytical model is based on the analysis of flow relative to a set of cascaded blades, having any described shape, and assumes phase changes occur under conditions of isentropic equilibrium. The model is restricted to incipient blade cavitation and does not include the effects of blade tip clearance or back flow.

Analytical cavitation compliance predictions for the J-2 LOX, F-1 LOX, H-1 LOX and LR87 oxidizer turbopump inducers do not compare favorably with test data. The model predicts much less cavitation than is derived from the test data. This implies that mechanisms other than blade cavitation contribute significantly to the total amount of turbopump cavitation. A current related technology contract (NAS8-27731) is extending the empirical evaluation of test data presented in this document.

TABLE OF CONTENTS

LIST OF TABLES

LIST OF FIGURES

1. Introduction

1. INTRODUCTION

1.1 <u>Purpose</u> - Longitudinal oscillation instabilities (POGO) due to closed loop coupling between structural modes and propulsion feed system modes have been encountered on most liquid propellant launch vehicles (Reference 1). Experimental evaluation of feed system dynamics in these vehicles has shown that turbopump cavitation is usually the major source of feed system compliance which, along with the effective fluid mass, determines the feed system resonant frequencies. Compliance (C) is defined as the rate of change of fluid mass (W) with respect to pressure (P) for a constant volume; i.e.,

$$C = \frac{\partial W}{\partial P} \qquad \frac{lb_m \ in.^2}{lb_f} \qquad or \ in.^2 \qquad (1.1)$$

Cavitation bubble compliance (C_b) is given by the rate of change of the mass of propellant stored in the turbopump (W_p) with respect to inlet pressure (P_s). Changes in W_p can be related to changes in cavitation vapor volume (V_v) by

$$C_b = \frac{\partial W_p}{\partial P_s} \approx - \frac{\rho \, \partial V_v}{\partial P_s} \qquad (1.2)$$

where ρ is the liquid density and the mass of vapor is small relative to the mass of liquid.* Some previous analytical and semi-empirical attempts (Section 2.3) have been made, usually using average geometry parameters and flow conditions through the turbopump, to predict the amount of cavitation. Confidence in these methods has never been sufficient to eliminate the requirement to perform dynamic response tests on new turbopump

---

* In some of the literature C_b is defined as $\partial V_v / \partial P_s$ which can be related to the values presented in this report by multiplying by the appropriate propellant density.

configurations. The lack of available test hardware during design phases is one of the major reasons that POGO suppression has been worked as a post flight effort on all past launch vehicles. The technology effort documented in this report is aimed at producing increased confidence in pre-test POGO stability analysis on future launch vehicle programs like the Space Shuttle Vehicle. This study is closely related to three other current Space Shuttle Technology programs: contract NAS8-26250, "Research on Cavitating Pump Instabilities", Hydronautics Incorporated; contract NAS8-25919, "Analysis of Propellant Feedline Dynamics", South West Research Institute; and contract NAS8-27731, "Empirical Evaluation of Pump Inlet Compliance", Aerospace Corporation.

1.2 <u>Objectives</u> - The intent of this investigation is to establish the relationships between turbopump inlet compliance and the pump parameters and fluid properties that control or define the compliance mechanism. The correlation is to be established with an analytical and/or semi-empirical model which is verified with existing test data. It is desired that the correlations be formulated and presented such that the frequency response characteristics of a cryogenic feed system can be evaluated for a given vehicle configuration. It is desired that the deviation in feed system resonant frequency between analytical and empirical results not exceed ±10%.

1.3 <u>Scope</u> - This study deals primarily with the determination of turbopump cavitation compliance, the largest element of uncertainty in dynamic modeling of feed systems. Feed system models, incorporating cavitation compliance, are well understood and range from very simple models (Paragraph 4.1.3) to

fairly complicated models (References 2 and 3). A general feed system computer model was provided to NASA under contract NAS8-23511. Also, detailed feed system modeling is currently being performed under contract NAS8-25919. For these reasons, no complex feed system models are presented in this report.

1.3.1 Since cavitation compliance is required for determination of feed system frequency response characteristics for use in POGO stability analysis, only linear response characteristics are of interest. Also, only the normal flight operating range of a turbopump is considered. These two conditions permit the analysis of turbopump cavitation to be restricted to the region of incipient cavitation, and does not consider the region of gross cavitation where turbopump operating performance is significantly reduced. The analytical model developed deals with thermal vapor cavitation between the turbopump blades. It does not include gaseous cavitation, or cavitation resulting from back flow or blade tip clearance flow, although these effects are discussed.

1.4 General Approach - The general approach taken to meet the study objectives within the scope specified was to:

 a. Review all literature relative to turbopump cavitation;

 b. Develop an analytical model to predict cavitation compliance;

 c. Analyze all available cavitation compliance test data;

 d. Perform an evaluation of the test data;

 e. Correlate the analytical and test results.

The model development portion of this study is a continuation of a portion of a general POGO technology contract conducted for the Air Force Rocket Propulsion Lab (References 4 and 5).

The analytical cavitation model is a fluid dynamic/thermodynamic model which employs the compressible flow equations in finite difference form and solves them iteratively. Isentropic conditions of thermodynamic equilibrium between the vapor (cavitation) and liquid phases are assumed. The solution yields the amount of vapor at many grid points in a turbopump streamsheet of revolution (an annulus between two blades). A combination of several streamsheets at different blade radii gives the total turbopump cavitation, which when related to a change in inlet pressure, results in cavitation compliance. This approach accounts for varying conditions of fluid flow and blade geometry throughout the turbopump.

2. Review of Cavitation Mechanism

2. REVIEW OF CAVITATION MECHANISM

2.1 <u>Turbopump Operation</u> - Turbopumps used in present rocket
propulsion systems are generally of the mixed flow design. The
pump fluid while in the impeller has, in addition to angular
velocities, both axial and radial velocity components as opposed
to the predominantly radial velocities associated with centri-
fugal water pumps. In most cases, the turbopump will have an
inducer section upstream of the main impeller that improves
fluid angle of attack and increases the pressure at the inlet
to the impeller. This allows further reduction in NPSH before
blade stall and a loss in head rise (pressure increase from
inlet to discharge) occurs. In some configurations, the impeller
and inducer are of one piece construction, the inducer blades
transitioning into impeller blades with additional impeller
blades starting at some distance into the turbopump. The pres-
sure rise through the inducer makes it probable that the majority
of the turbopump cavitation occurs in the inducer. This is
because the average pressure at the impeller inlet is generally
too high for any local blade surface pressure to be reduced to
the vapor pressure.

2.1.1 Shrouded blades of proper design, operating at the
design point and free of vapor represent an analytical idealiza-
tion in that channel type flow exists between the blades. Most
turbopumps, however, are not designed with completely shrouded
blades, and the channel flow idealization cannot be realized.
In this situation, the flow picture is complicated by a tip
clearance flow between the moving blades and the stationary
shroud. The tip clearance flow, which is from the pressure
side of a blade to the suction side, often induces a vortex

near the outer edge of the blades on the suction side. If the blades are improperly designed or are being operated off the design conditions, a liquid-filled separation cavity may be attached to the leading edge. This is more likely when the blade leading edges are quite sharp. Although the impeller will still pump fluid with an associated pressure rise, it is accomplished at a reduced efficiency.

2.1.2 The complexity of the flow situation increases with the appearance of vapor phases. If the velocity gradients are not large and the inducer blades have large radii of curvature associated with the leading edge region, the vapor phases, which consist of dissolved gas coming out of solution and/or a change in phase of the pump fluid, will appear as a region of bubbles moving with the fluid. On the other hand, if a liquid-filled separation cavity exists before the appearance of vapor, the cavity may fill with vapor when it evolves and expand with further reduction in suction pressure. Such cavities that originate near the leading edge of the blade may reattach on the downstream side of the blade or, if severely low pressures exist, extend downstream into the discharge portion of the pump. Although separation cavities may not exist before the appearance of vapor, the density change and disturbances associated with the evolution of vapor may induce separation of the boundary layer and create a cavity. In both types of two-phase flow, the variations of density add considerable complexity to the analysis problem.

2.2 Sources of Cavitation - Cavities may exist in the turbopump liquid propellant due to the presence of either vapor bubbles produced by liquid boiling, hereafter referred to as thermal cavitation; or contaminant gas bubbles, hereafter referred to as gaseous cavitation.

2.2.1 <u>Thermal Cavitation</u> - Thermal cavitation results when the ambient pressure drops below the saturation pressure, or the fluid temperature rises above the saturation temperature. Pressure changes may be associated with quasi-steady fluid motion, transient fluid motion, or acoustic excitation. Temperature changes can result from heat transfer across the boundaries of the system, fluid motion, and phase changes of the fluid (latent heat of vaporization and condensation). For an isentropic process, a change in pressure produces a phase change, which results in a change in fluid temperature, which in turn tends to impede the phase change. With sufficient time, thermodynamic equilibrium is reached and there exists a given amount of vapor for a given pressure. For bubble growth and decay under conditions of non-thermodynamic equilibrium, the mathematics defining the rate of change of bubble size are given in Appendix A.

2.2.2 <u>Gaseous Cavitation</u> - Gaseous cavitation can occur from the following sources:

        a. Dissolved gases coming out of solution;

        b. Undissolved gases mixed with the propellant;

        c. Chemical reaction (corrosion) between the propellant and the turbopump.

Substantial concentrations of both dissolved and undissolved foreign gases, such as atmospheric air or blanket gases used to hold the fluid under pressure before entrance to the pump, may also be present in propellants which have been stored for either long periods of time or under very low gravity conditions. Changes in the ratio of dissolved to undissolved gas can result from changes in fluid velocity, acoustic excitation, or heat

transfer. Undissolved gas may also exist as a result of a Gas
Bubbling POGO Suppression Device (References 6 and 7). The
problem of corrosion is not normally encountered in current
propulsion systems. Even if storage and utilization of pro-
pellants are controlled so that an insignificant amount of
gaseous cavitation occurs, small amounts of dissolved gases may
be instrumental in the initial formation of a thermal cavitation
vapor bubble (Paragraph 2.3.2).

2.3 <u>Previous Cavitation Analyses</u> - Analysis of turbopump
cavitation compliance was initiated with a review of existing
knowledge on cavitation. Discussion of this review and the
conclusions derived follow.

2.3.1 <u>Turbopump vs Other Types of Cavitation</u> - Considerable
investigation has been performed in the field of cavitation.
Areas that have received the most attention have been pump
cavitation, hydrofoil and hydrodynamic propeller cavitation,
cavitation on such underwater vehicles as submarines and torpedos,
and cavitation induced by sound waves. The majority of investiga-
tions associated with pumps have been experimental or semiempirical
with the objective of preventing cavitation damage by determination
of incipient cavitation conditions (References 8 and 9). Investi-
gations of hydrofoils, propellers, and underwater vehicles have
been aimed at predicting lift and drag coefficients and reducing
noise associated with cavitation bubble collapse. Ultrasonic
cavitation research has been directed primarily toward assessing
sound energy and frequency requirements to induce cavitation, and
examining the attenuation and distortion of sound waves caused
by the cavitation bubbles.

2.3.2 <u>Nucleation</u> - If gas-filled voids exist in a fluid (References 10 and 11), changes in the concentration of dissolved gases and changes in phase within the fluid will take place at the boundary of the voids as well as at the fluid surface. The presence of voids in a fluid is suggested by the cohesive strength of water. Predictions of cohesive strength based on breaking the van der Waals intermolecular bonds exceed experimental observations by several orders of magnitude. The source of this large discrepancy is attributed to the presence of contaminants in the water that form voids of nuclei on the order of 10^{-5} to 10^{-2} cm in diameter. Since it is known that large amounts of air can be dissolved in water, it is hypothesized that the voids of nuclei are filled with contaminant gases such as air or mixtures of gas and fluid vapor. This hypothesis only partially explains the observed fracture strength of water. A nucleus containing contaminant gas and vapor will be in static equilibrium in the fluid if

$$P_V + P_G - P_\infty = 2\sigma/R \qquad (2.1)$$

where

P_V = vapor pressure

P_G = sum of partial pressures of contaminant gases

P_∞ = ambient pressure

σ = surface tension constant

R = radius of nucleus

If the nucleus contains only vapor and its radius is given by Equation (2.1), it is in a condition of unstable equilibrium and will either grow or collapse upon being disturbed.

2.3.2.1 Gas-filled nuclei on the order of 10^{-5} to 10^{-2} cm in diameter present in an undersaturated or saturated solution of

water (saturation in this context refers to the concentration of dissolved gas) dissolve in a few minutes or seconds depending on the radius of the nuclei and the dissolved gas concentration. The dissolving process is assisted by the surface tension force $2\sigma/R$. A nucleus of this size, if present in a supersaturated solution of water, grows by diffusion of gas into the nucleus and floats to the surface of the water where it escapes. The rate of rise of a nucleus of 10^{-5} cm in diameter is very slow and may take several hundred hours to escape from the liquid. Water that has been allowed to set a long time still fails to demonstrate the expected cohesive strength. A mechanism or mechanisms, there- fore, that prevents the diffusion of gas out of the nuclei and/or prevents nuclei from rising to the surface of the fluid must be acting. Two hypotheses advanced are:

a. Surface films composed of algae or other contaminants form around the nuclei and act as barriers to the diffusion process;

b. The nuclei are held in surface cracks of the fluid container or on dust particles suspended in the fluid.

The first hypothesis has been demonstrated by Bernd (Reference 12) in experiments where the cohesive strength of various fluids has been manipulated by control of the algae content. Rosenberg (Reference 13) has shown analytically and experimentally that the walls of the fluid containers can have cracks in which nuclei can be attached in a stable condition. In the same work, it was shown that dust particles or colloidal matter in the fluid can have cracks upon which the nuclei can be stabilized. An aspect of Rosenberg's investigation that will require further attention is the observed difference in susceptibility of various liquids to contamination by dust.

2.3.2.2 The nuclei are the focal points that govern changes in dissolved gas concentration and changes in phase (Reference 14). Regarding changes in phases, nucleation action occurs not only for the growth of vapor bubbles, but also for their collapse. The presence of contaminant dust particles in the bubble and on its surface serve as nuclei upon which additional condensation can take place.

2.3.2.3 The preceding discussion shows that cavitation in a turbopump will depend on the number of nuclei present in the fluid, their size, and conditions that will affect their dynamic behavior. It is important, therefore, that methods be developed for assessing the effects of fluid characteristics on nucleation.

2.3.3 Diffusion - A decrease in the concentration of dissolved gas in the pump fluid will result from diffusion of dissolved gas into nuclei present in the fluid. If the diffusion process continues, the nuclei will grow into gas bubbles and the phenomenon of gaseous cavitation will be observed. The diffusion process in a pump can be driven by changes in either pressure or temperature. Once the temperature and pressure conditions have been altered to a condition that favors diffusion of gas out of the cavitation bubble, the bubble will decrease in size. Although conditions return to those existing at inception of bubble growth, the contracting bubble may reach an equilibrium volume substantially greater than that of the original nucleus. This phenomenon is demonstrated by tests of the cohesive strength of water. Water that has been subjected to gaseous cavitation has a fracture strength considerably less than it had before cavitation. This results from the presence of nuclei after cavitation that are larger than those that existed before cavitation. Plesset and Epstein (Reference 15),

ignoring the effects of the motion of the bubble boundary on the concentration gradient in the liquid, have derived the equation governing the diffusion of gas into and out of a static bubble. Their results, if applied directly to turbopumps, show that the characteristic time for bubble growth is too large to cause cavitation. The boundary conditions for the derivation, however, differ considerably from those that will exist in a turbopump. The effects of bubble boundary motion and turbulence on the gaseous concentration gradient serve to accelerate the bubble growth. Future work, therefore, should incorporate these effects into a more accurate description of the diffusion process.

2.3.4 <u>Acoustic Cavitation</u> - As previously stated, changes in the ratio of dissolved to undissolved gas in a fluid can occur due to acoustic excitation. The generation of sound in a fluid results in an oscillatory pressure throughout the fluid. The pressure disturbances in turn result in an oscillation of the boundary of nuclei in the fluid. With a fluid saturated or supersaturated with dissolved gas, the nuclei may grow into gas bubbles given the proper amplitude and frequency of acoustic excitation. The growth is achieved through the rectified diffusion of gas into the bubble. During the low-pressure or expansion phase of bubble oscillation, conditions result in diffusion of gas into the bubble. During compression of the bubble, gas diffuses out; however, due to the large time surface area associated with the bubble expansion, a net inflow of gas occurs. Because of the extreme noises associated with rocket engines, this type of cavitation should not be ignored when analyzing rocket turbopumps.

2.3.5 <u>Thermodynamics</u> - The cavitation problem requires consideration of many thermodynamic effects. Literature on the subject of thermal cavitation may be divided into two areas. The first of these deals with the effect of heat transfer on cavitation bubble growth. The nonsteady heat diffusion problem with moving boundaries has been solved by Plesset and Zwick (Reference 16). The same authors have combined the results of the heat diffusion problem with the equations of motion for bubble growth to obtain a solution for the case of constant ambient pressure (Reference 17). Skinner and Bankoff (Reference 18) as well as Forster and Zuber (Reference 19) have taken slightly different approaches and obtained similar results. The bubble growth problem with variable ambient pressure and inclusion of terms containing P_v is still unsolved.

2.3.5.1 Other investigators such as Stepanoff (References 20 and 21) and Jakobsen (Reference 22), rather than examine thermal cavitation on a microscopic basis, choose to derive semiempirical macroscopic descriptions. The results of this approach suffer from inability to correlate a particular value of pump head dropoff with volume of vapor present over a wide range of operating conditions. Furthermore, the results cannot justifiably be used to predict the vapor volume, because a number of assumptions and empirical factors do not accurately describe the vapor formation process.

2.3.5.2 Future work on thermal cavitation should take two directions. The first, referred to as the equilibrium approach, should examine the thermal cavitation phenomenon assuming thermal equilibrium phase changes. For pumps that have gradual changes in pressure through the system and low fluid velocities, the

14

equilibrium approach may give entirely satisfactory results; and, thereby, negate the need for a microscopic examination. The second method should be a microscopic examination of cavitation in which large pressure gradients and velocities produce metastable changes of phase. For cryogenic fluids, the effects of heat transfer across the boundaries of the system should be included in both methods of analysis. The thermodynamic properties of the fluid should be examined closely to determine whether certain characteristics simplify or complicate the solution of the thermal cavitation equations.

2.3.6 Fluid Mechanics - Like thermodynamics, there are many branches of fluid mechanics drawn on for examination of turbopump cavitation. The flow of liquid through a turbopump to the inception of cavitation can be examined with the incompressible flow equations. In the pump, cavitation may appear in a number of forms. If the leading edges of the impeller blades are very sharp, a separation cavity may be attached to the suction side of the blade. Depending on the fluid velocity, pressure, and boundary layer conditions, the cavity may close on the downstream suction side of the blade or may extend through the pump in a condition known as supercavitation. Examinations of separation cavities as related to turbopump cavitation have been made by Stripling and Acosta (References 23 and 24). This method predicts the geometry of the cavity up to the point of maximum height based on fluid momentum considerations; however, the reattachment or cavity closure conditions remain arbitrary. The work of Wade (Reference 25) applies to the conditions of cavities closing on the blade. The most recent and most elegant application of the Stripling and Acosta method is that developed by Davis, Coons and Scheer (Reference 26). This application

couples the Stripling-Acosta model to a two dimensional impeller flow field including boundary layer displacement effects. The primary objective of this model was to predict blade loading under cavitating conditions. Comparing its results with test data showed that it accomplished this purpose very well. Its use for predicting cavitation compliance is much more questionable due to a greater sensitivity to the assumed closure conditions. After documentation of the Stripling and Acosta work, different investigators have claimed that various pieces of experimental data (mostly photographic data, e.g., Reference 32) support either the separation cavity theory or the thermal equilibrium mixed flow concept. Our own review of this data suggests that it is inconclusive for the most part in offering substantial supporting evidence for either theory.

2.3.6.1 Unfortunately, the assumptions for the mathematical models, such as a blade leading edge radius of curvature equal to zero are seldom if ever physically realizable. If the blade is very thick and has a large leading edge radius of curvature, the flow may remain attached, and cavitation will appear as a mixture of vapor bubbles and liquid that demonstrates compressible flow characteristics. In this type of cavitation, the growth and collapse of vapor bubbles require fluid-mechanic examination. Plesset (References 17, 27 and 28) has examined the growth phenomena under conditions of constant ambient pressure and bubble vapor density. Both Gilmore (Reference 29) and Hunter (Reference 30) have taken into account compressibility and shock effects encountered during bubble collapse.

2.3.6.2 The effect of gas bubbles on the sonic velocity in a fluid represents another area that has received attention in

cavitation investigations. Figure 2.1 shows the variation in sonic velocity as a function of gas content for a mixture of water and air. It is seen that the sonic velocity can drop to a very low value that may result in sonic choking in the turbo-pump. Ghahremani (Reference 31) uses the work of Jakobsen (Reference 22) and assumes that fully choked flow exists at head breakdown (no pressure rise through the turbopump). Somewhat arbitrary assumptions, requiring empirical correlation, are then made to relate the fully choked conditions to normal operating conditions of unchoked or partially choked flow. The Ghahremani approach is unique in that the theory includes the effects of blade tip clearance backflow which, according to his results, produce more cavitation than occurs on the blade suction surface.

2.3.6.3 Attention in future fluid-mechanic investigations of cavitation should be given to determination of the conditions necessary for and which influence the geometry of separation cavities; and development of the flow equations for a vapor-liquid mixture in a turbopump. Incorporated into these equations should be the effects of bubble growth and collapse on the sur-rounding fluid. Also, the approach related to sonic choking at head breakdown should be refined.

2.4 A General Cavitation Analysis - From the preceding review of existing investigations of cavitation, it is possible to construct a plan for solution to the general cavitation com-pliance problem. This plan, which itemizes the various areas of investigation and integrates these areas into a completely general analysis, is outlined in the following paragraphs. The analytical investigations conducted during this program were restricted to fluid-mechanics with thermodynamic cavitation, which occurs on an equilibrium basis.

2.4.1 Nucleation

    a. Number of nuclei;

    b. Size distribution of nuclei;

    c. Conditions in fluid or vapor that affect the dynamic behavior of nuclei.

2.4.2 Acoustic Cavitation

    a. Identification of sound sources;

    b. Assessment of power and frequency characteristics of each source;

    c. Wave transmission in the fluid mechanic system.

2.4.3 Diffusion

    a. Identification of dissolved gas species and assessment of their relative concentrations;

    b. Evaluation of diffusion rates into nuclei or out of gas bubbles under both laminar and turbulent flow conditions;

    c. Determine effects of contaminants on diffusion rates.

2.4.4 Thermodynamics

    a. Examination of thermal cavitation on a microscopic or dynamic basis;

    b. Examination of thermal cavitation on a thermal equilibrium basis;

    c. Thermodynamic properties of fluids;

    d. Heat transfer across system boundaries.

2.4.5 Fluid Mechanics

    a. Hydrodynamics of turbomachinery without cavitation;

    b. Hydrodynamics of turbomachinery with cavitation, but without separation cavities;

    c. Bubble hydrodynamics;

    d. Hydrodynamics of turbomachinery with separation cavities attached to blades;

    e. Compressibility effects in fluid including shock phenomena;

    f. Effects of tip clearance flow and backflow.
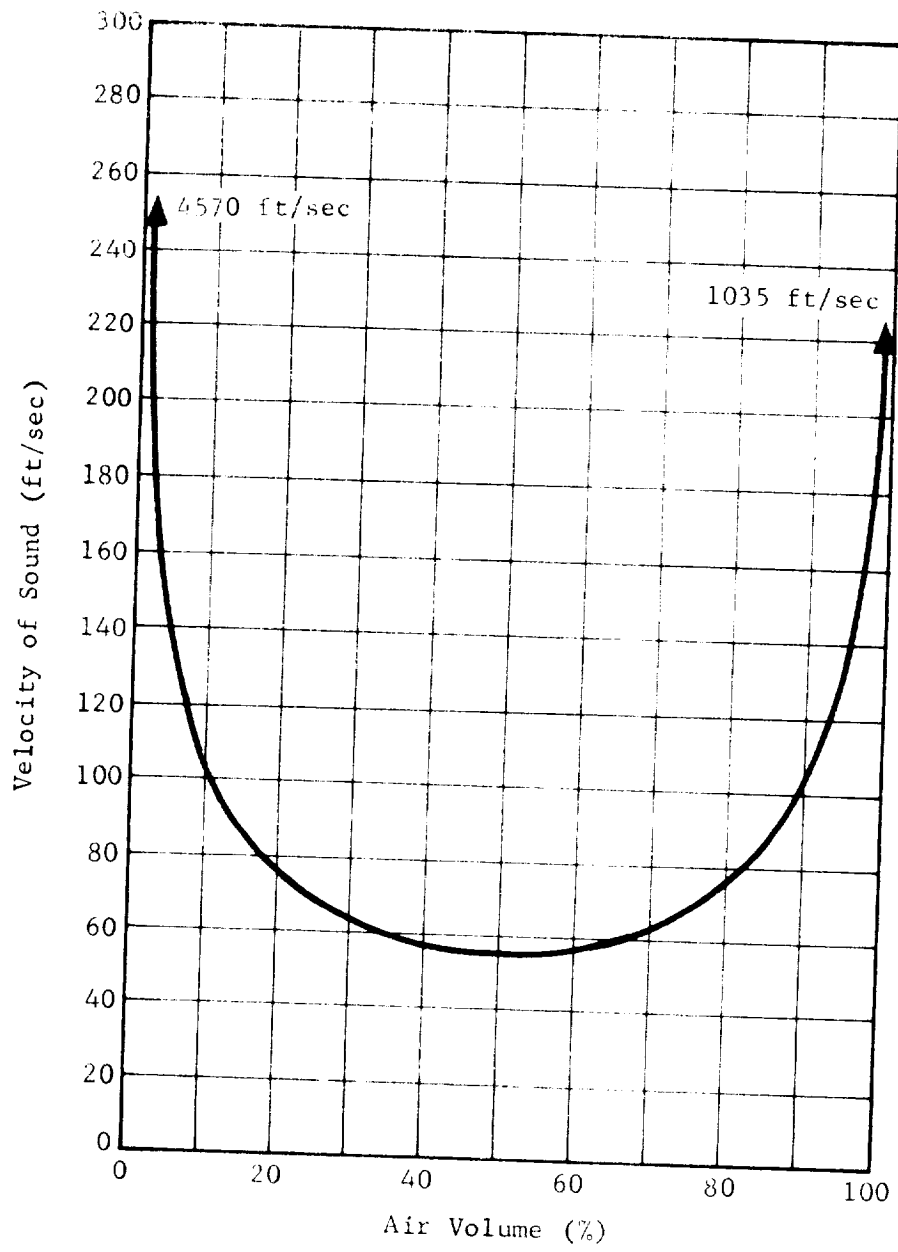
Figure 2.1   Variation of Isothermal Velocity of Sound in
Water Containing Air Bubbles

3. Turbopump Cavitation Model

3. TURBOPUMP CAVITATION MODEL

3.1 Model Requirements - As outlined in Section 2.4, a complete analysis of turbopump cavitation compliance will require a complex model of the turbopump based upon the physical equations describing the fluid mechanic and thermodynamic phenomena occuring in the pump. The purpose of this program was to develop such a model; but, on a very fundamental basis, in order to evaluate the validity of such a model and identify the associated programming and numerical analysis problems. If the feasibility and engineering usefulness of a basic program could be demonstrated the more complex effects of fluid viscosity, gas diffusion, and non-equilibrium thermodynamics could be added to the program with considerably more confidence of success.

3.1.1 A prime objective of the cavitation compliance model development was to derive mathematical descriptions that could be related directly to the physical situation in a turbopump. Semi-empirical approaches were discarded because of their inability to account for all the different design considerations. This is particularly true considering the lack of any empirical data which relates changes in cavitation compliance to changes in specific turbopump geometry parameters. The required mathematical descriptions, which are consistent with the objectives and scope of this study, are:

    a. Basic turbopump flow equations into which two-phase flow phenomena can be incorporated and which could later be expanded to include more complex flow situations;

    b. A thermal cavitation model which is independent of time and conditions of nucleation and which can be

combined with the flow equations to give a description of turbopump cavitation compliance;

c. A finite difference iteration algorithm which allows solution of the flow and cavitation equations for any given blade geometry and flow conditions.

3.2 Model Assumptions - The assumptions made in the development of the turbopump model pertain to the cavitation process, the fluid-mechanics, and the turbopump configuration. The assumptions were required in order to obtain a solution for cavitation compliance within the scope of this study. The first two assumptions related to the cavitation process determine the basic approach of the analytical effort.

3.2.1 Channel Flow - The fundamental assumption of the turbopump model is that channel flow exists approximately between the pump inducer and impeller blades. This assumption can be used to separate the three-dimensional flow problems into two-dimensional problems. The first problem is that of defining the flow streamlines in the meridional plane. This can be accomplished by the method described in Appendix A, or by a more approximate method wherein the streamlines and associated streamtube width (b in Figure 3.2) is related to the inducer or impeller hub and shroud geometry by a suitable function. With a meridional plane description of the streamlines, one can proceed with the development of the blade to blade flow equations along a surface generated by rotating a meridional plane streamline about the impeller axis. This development is presented below in Section 3.3.

3.2.2 Thermal and Velocity Equilibrium - The liquid-vapor phase change is assumed to occur under isentropic conditions of

thermodynamic equilibrium with both phases in velocity equilibrium. An equation that deals with nonequilibrium changes of phase (vapor bubble growth) for a single bubble is presented in Appendix B. This derivation includes the effects of heat transfer at the bubble wall, varying ambient pressure, and variable density of the vapor within the bubble. Unfortunately, a complete solution to the resulting integro-differential equation was not obtained. Solutions were found in the literature for simplified versions of the equation; however, the solutions sacrificed the inertial effects to gain a description of the thermodynamic effects or vice versa. The assumed condition of equilibrium applies to the bubble growth and decay both as the fluid passes through the turbopump encountering different local pressures, and as the local pressures change as a result of changes in the turbopump inlet pressure. Some test results (Reference 4) at very low static inlet pressure (6 to 10 psi) and large pressure oscillation amplitudes (10 to 20 psi peak to peak) indicate that the cavitation process is not in equilibrium, and that the amount of compliance is a function of the frequency of the pressure oscillations. The extrapolation of this data to small amplitudes and flight pressures is not possible. Since this model is more concerned with cavitation compliance (rate of change of cavitation with respect to pressure) than with the amount of cavitation, the equilibrium assumption should be more valid because the period of pressure oscillation is greater than the average bubble life (Paragraph 3.2.5).

3.2.3 Tip Clearance and Backflow - An additional restriction which is implied by the channel flow assumption is that there is no tip clearance flow or backflow within the pump.

The model only computes cavitation as a result of channel flow between cascaded blades and does not consider cavitation which may occur from either blade tip clearance flow or from backflow into the suction line (backflow is produced by tip clearance flow). These other sources may have a significant effect when considering unshrouded blades. Based on analysis, Ghahremani (Reference 31) theorizes that tip flow cavitation is much larger than blade cavitation. The only tests concerned with tip clearance flow evaluated the effect on performance for a gas medium (Reference 33) instead of a liquid, and for a variation in the axial clearance of the impeller tip (Reference 34) instead of a radial clearance of the inducer tip. A test program to investigate the effect of tip clearance flow and backflow would be very beneficial to the understanding of the complete turbopump cavitation process.

3.2.4 Incipient Cavitation - The model is developed for conditions of incipient cavitation only. This restriction is necessary because in deep cavitation local fluid velocities may approach the local speed of sound, whereupon the finite difference solution scheme becomes invalid. Since turbopumps do not usually operate in the region of deep cavitation, this is not considered to be a severe restriction.

3.2.5 Steady Flow - Since cavitation compliance is related to an oscillatory change in inlet pressure, unsteady flow conditions are implied. However, since the period of oscillation is typically 50 times greater than the time required for a fluid element to pass through the cavitation region, it is valid to assume quasi-steady flow; i.e., cavitation compliance can be obtained from a steady state solution at different turbopump inlet pressures.

3.2.6 <u>Inviscid Flow</u> - A further assumption which must be used is that the flow is inviscid. A solution of the complete viscous flow equations would compound the overall computational problems and is not warranted until the usefulness of the basic inviscid approach is demonstrated.

3.2.7 <u>Separation Cavities</u> - The computer model of turbo-pump cavitation was developed on the basis that no separation cavities were present in the blade system. This restriction is actually necessary only when the vapor phase is present in the pump. Solutions can be obtained with separation cavities for incompressible or non-cavitating flow; however, diverging solutions appear whenever two phase flow is encountered.

3.2.8 <u>Identical Blades</u> - The final assumption of the model development requires that all blades within the pump inducer or impeller are identical. This restriction was necessary in order to simplify the computer programming and to meet core limitations on the computer. In most pumps, the inducer section where most cavitation occurs is made up of identical blades. In the impeller section, however, partial blades are quite often placed between the main blades. The capability of treating non-identical blade systems can be added to the program, but would require an overlay technique and, consequently, some re-programming.

3.3 <u>Equation Development</u> - The development of the non-separated, thermal equilibrium cavitation flow equations for a blade-to-blade analysis are discussed below along with the pump blade coordinate transformations used to simplify the numerical solutions. Figure A.1 shows the coordinate system used for

derivation of the flow equations. The coordinate system is rotating about the Z axis with angular velocity ω. The velocities shown, therefore, are relative to the pump blades. The equation development derives two basic equations: a fluid flow equation, and an energy equation. The flow equation is derived from potential theory utilizing a continuity equation and the condition of irrotational flow. The energy equation is derived by relating the fluid energy to the inlet energy and the work done by the turbopump. Changes in thermal energy are obtained from the assumed condition of thermal equilibrium. The final form of the two equations is written in terms of the stream function, ψ, and the density ρ.

3.3.1 <u>Flow Equation</u> - From a solution to the flow problem in the meridional plane (Appendix A), a streamline and its associated streamtube can be defined as shown graphically in Figure 3.1. Rotation of the streamtube about the impeller axis results in a streamtube of revolution while a stream surface is generated by the meridional streamline. With reference to Figure 3.2, which shows a segment of the stream-tube, the flow continuity equation is derived as follows. Using the segment of the streamtube as a control volume, the conservation of mass is expressed by

$$\sum \left(\dot{W}_{in} - \dot{W}_{out} \right) = \frac{d}{dt} (W) = 0 \qquad (3.1)$$

where $\dot{W}$ is the flowrate. $\frac{d}{dt} (W)$ is the time rate of change of the weight of fluid in the control volume, which is zero for steady flow. In the M direction,

$$\dot{W}_{in} - \dot{W}_{out} = (\rho V_M \ b) \ r \ d\theta - \left[\rho V_M \ b + \frac{\partial}{\partial r} (\rho V_M \ b) \ dr\right] (r + dr) \ d\theta$$

$$= -\left[\rho V_M b \ dr \ d\theta + \frac{\partial}{\partial r}(\rho V_M b)dr \ r \ d\theta + \frac{\partial}{\partial r}(\rho V_M b)dr^2 \ d\theta\right] \quad (3.2)$$

In the θ direction,

$$\dot{W}_{in} - \dot{W}_{out} = \rho V_\theta \ b \ \frac{dr}{\sin \alpha} - \left[\rho V_\theta + \frac{\partial}{\partial \theta} (\rho V_\theta)d\theta\right] b \ \frac{dr}{\sin \alpha}$$

$$= - \frac{\partial}{\partial \theta} \left(\frac{\rho V_\theta \ b}{\sin \alpha}\right) d\theta \ dr \quad (3.3)$$

Using the above relationship, Equation (3.1) becomes:

$$\rho V_M \ b \ dr \ d\theta + \frac{\partial}{\partial r} (\rho V_M \ b) \ dr \ r \ d\theta + \frac{\partial}{\partial r} (\rho V_M \ b)dr^2 d\theta$$

$$+ \frac{\partial}{\partial \theta} \left(\frac{\rho V_\theta \ b}{\sin \alpha}\right) dr \ d\theta = 0 \quad (3.4)$$

Dividing through by $r \ d\theta \ b \ \dfrac{r}{\sin \alpha}$, and taking the limit as dr and $d\theta$ approach zero, Equation (3.4) becomes

$$\frac{\partial}{\partial r} (\rho V_M \ b \ r) + \frac{\partial}{\partial \theta} \left(\frac{\rho V_\theta \ b}{\sin \alpha}\right) = 0 \quad (3.5)$$

A stream function ψ that satisfies Equation (3.5) is then defined by

$$\frac{\partial \psi}{\partial \theta} = \rho V_M \ b \ r \quad (3.6)$$

$$\frac{\partial \psi}{\partial r} = - \frac{\rho V_\theta \ b}{\sin \alpha} \quad (3.7)$$

With the further assumptions that the fluid is inviscid and that its absolute motion is irrotational, another equation for

fluid motion can be derived. For absolute irrotational flow the circulation, Γ, around the fluid segment (Figure 3.3) must be zero.

If $\Gamma = 0$, then $d\Gamma = 0$, or

$$d\Gamma = 0 = \left[\frac{\partial}{\partial r} \left(r\omega + V_\theta \right) r\,\theta \right] dr - \frac{\partial}{\partial \theta} \left(\frac{V_M\,dr}{\sin \alpha} \right) d\theta \qquad (3.8)$$

Differentiating:

$$2r\omega + V_\theta + r \frac{\partial V_\theta}{\partial r} - \frac{\partial V_M}{\partial \theta} \frac{1}{\sin \alpha} = 0 \qquad (3.9)$$

At this point, a transformation of the pump blade coordinates facilitates programming of the problem for computer solution. The transformation will depend on the blade shape. However, the objective of the transformation is to straighten the blade such that the leading edge becomes the maximum of the blade angular coordinates and the trailing edge the minimum. For an inducer a transformation such as $dE = dZ$ and $dF = d\theta$ may be the most appropriate. For an impeller having logarithmic spiral blades, the following transformation is most convenient.

$$dE = \frac{1}{\sin \alpha} \frac{dr}{r} \qquad (3.10)$$

$$dF = d\theta \qquad (3.11)$$

Carrying the equation development through, using this last transformation, Equation (3.9) becomes

$$2r\omega + V_\theta + \frac{1}{\sin \alpha} \left[\frac{\partial}{\partial E} \left(V_\theta \right) - \frac{\partial}{\partial F} \left(V_M \right) \right] = 0 \qquad (3.12)$$

Combining Equations (3.6), (3.7) and (3.12) results in

$$2r_\omega \sin\alpha \quad - \frac{\sin\alpha}{\rho br} \frac{\partial\psi}{\partial E} + \frac{1}{\rho^2 rb} \frac{\partial\rho}{\partial E} \frac{\partial\psi}{\partial E} + \frac{\sin\alpha}{b\rho r} \frac{\partial\psi}{\partial E}$$

$$+ \frac{1}{b^2 \rho r} \frac{\partial b}{\partial E} \frac{\partial\psi}{\partial E} - \frac{1}{\rho br} \frac{\partial^2\psi}{\partial E^2} - \frac{1}{\rho br} \frac{\partial^2\psi}{\partial F^2}$$

$$+ \frac{1}{\rho^2 rb} \frac{\partial\psi}{\partial F} \frac{\partial\rho}{\partial F} = 0 \tag{3.13}$$

which in turn reduces to

$$2r^2_\omega b\rho \sin\alpha + \frac{\partial\psi}{\partial E}\left[\frac{\partial}{\partial E}(\ell n\rho)\right] + \frac{\partial\psi}{\partial E}\left[\frac{\partial}{\partial E}(\ell nb)\right] - \frac{\partial^2\psi}{\partial E^2} - \frac{\partial^2\psi}{\partial F^2}$$

$$+ \frac{\partial\psi}{\partial F}\left[\frac{\partial}{\partial F}(\ell n\rho)\right] = 0 \tag{3.14}$$

From the meridional plane solution a relationship between α, b, and r can be defined. Equation (3.10) can then be integrated to give E as a function of r with the condition that E = 0 at $r = r_t$. Also, from Equation (3.11) F = θ. The relationship between the stream surface on which E and F lie and the r,θ,Z coordinate system is shown for the general case in Figure 3.4. In the E,F plane, the pump blades are as shown in Figure 3.5. With a relationship between fluid density, stream function, and known inlet conditions, Equation (3.14) can be solved numerically in the E,F plane and the results transformed back to the r,θ,Z physical plane.

3.3.2 <u>Energy Equation</u> - The completion of the solution to Equation (3.14) depends on a relationship between the fluid density, ρ, the streamfunction, ψ, and known pump inlet conditions. The energy equation for a steady flow fluid system such as a turbopump is given by

$$h + \frac{V'^2}{2g} = h_{o_u} + W \tag{3.15}$$

where

h = static enthalpy/lb

V' = absolute fluid velocity

h_{o_u} = total enthalpy/lb at the pump inlet

W = work done on the fluid per pound of fluid/unit time

Equation (3.15) expressed in terms of components of the absolute velocity is

$$h + \frac{1}{2g}\left[\left(\omega r + V_\theta\right)^2 + V_M^2\right] = h_{o_u} + W \tag{3.16}$$

But the rate of work addition between a station, u, upstream (where all flow properties are known) and the station being considered is equal to the rate of change in moment of angular momentum between the stations or

$$W = \frac{\omega}{g}\left[r\left(r\omega + V_\theta\right) - r_u\left(r_u\omega + V_{\theta_u}\right)\right] \tag{3.17}$$

The quantity $r_u\left(r_u\omega + V_{\theta_u}\right)$ is commonly referred to as the pump prewhirl, which is either specified for the problem or is obtained from a viscous flow solution to the upstream flow problem. If it is assumed that the flow in the impeller undergoes isentropic changes of state and that for cavitation conditions the vapor and liquid phases are in thermal and velocity equilibrium, a relationship between pressure and average fluid density, ρ, can be obtained from a state diagram for the working fluid. Referring to Figure 3.6, which represents a temperature-entropy diagram for a typical pump fluid,

the isentropic compression process might be represented by the
vertical line CAB. Assuming the inlet properties of the fluid
correspond to Point A, the fluid experiences a decreasing
pressure as it enters the pump and ultimately reaches conditions
corresponding to Point B in the vicinity of the blade leading
edge. Cavitation is fully developed at this point. Downstream
of the blade leading edge region, the work input to the pump
goes into compressing the fluid that exists from the pump having
properties corresponding to Point C. Using oxygen as the pump
fluid and assuming that the flow process in the pump is isentropic
and that velocity and thermal equilibrium exist throughout, the
variation of density with pressure is shown in Figure 3.7. The
data of the figure is based on a saturation temperature corres-
ponding to 15 psia. The data from which the curve was derived
were taken from Reference 35. Similar relationships can be
obtained for different saturation temperatures as well as dif-
ferent fluids. Combining Equations (3.16), (3.17), and relating
h to P/ρ yields

$$h \ (P/\rho) \ - \ \frac{(\omega r)^2}{2g} + \frac{1}{2g} \left(V_\theta^2 + V_M^2 \right) = \text{CONST} \qquad (3.18)$$

where CONST = inlet energy conditions. Upon application of
Equation (3.6), (3.7), (3.10) and (3.11), Equation (3.18) is
transformed to its final form

$$h \ (P/\rho) + \frac{1}{2g} \left(\frac{1}{\rho br} \right) \left[\left(\frac{\partial \psi}{\partial F} \right)^2 + \left(\frac{\partial \psi}{\partial E} \right)^2 \right] - \frac{(r\omega)^2}{2g} = \text{CONST} \qquad (3.19)$$

3.4 _Solution Technique_ - In order to define the turbopump
cavitation flow field, Equations (3.14) and (3.19) must be
solved throughout the field between two blades of the pump and
for a number of streamtubes selected from the meridional plane.

The results are then integrated throughout the pump to obtain the total cavitation compliance. The solution of Equations (3.14) and (3.19) is accomplished in a finite difference form on the CDC 6000 series computer. The problem is initiated by transforming the pump blades from the physical plane (Figure 3.4) to the E, F plane (Figure 3.5) through Equations (3.10) and (3.11). Next, a gridwork is established between the blades as shown in Figure 3.5. Equations (3.14) and (3.19) are written in finite difference form at each grid point and a relaxation method of solution employed. Solution of the problem is accomplished by specifying the upstream and downstream boundary conditions, assuming values of ψ at each grid point within the boundaries, and checked to see if Equations (3.14) and (3.19) are satisfied at each point. If it is not, the left hand side of Equation (3.14) will be equal to a residual R. Then, values of ψ at each grid point are systematically adjusted until the residuals are reduced to an acceptable level. Once this condition is reached, a solution is achieved. This initial solution may not correspond to the correct angular velocity on the upstream boundary. A scheme is included in the program for adjusting the upstream boundary and reapplying the relaxation solution until the correct value of angular velocity is obtained. A complete discussion of the relaxation method of solving systems of partial differential equations is given in Reference 36. The equations and solution technique described above have been developed into a computer program known as the turbopump cavitation flow program. User instructions for the computer model are given in Appendix D, and program listings are given in Appendix E. The analysis of the computer results required to obtain the cavitation compliance of the total turbopump is given in Section 5.1.

3.5 <u>Model Applications</u> – In addition to cavitation com-
pliance, the turbopump model is capable of generating other
information which is of interest in the analysis of turbo-
pump response and the design of turbopump blades. Turbopump
discharge dynamic pressure gain can be determined as a function
of inlet pressure (pump gain, $\partial Pd/\partial Ps$), exit flow (pump resistance,
$\partial Pd/\partial wd$), and blade speed (speed gain, $\partial Pd/\partial N$). These parameters
are also important in POGO stability analysis. Unlike cavitation
compliance, there are currently methods available for estimating
these parameters; however, the use of a cavitating turbopump
model may result in a significant improvement. This model can
also be used for design analysis of turbopump blades. This
could include blade pressure loading, and the influence of blade
shape on cavitation, separation, etc.
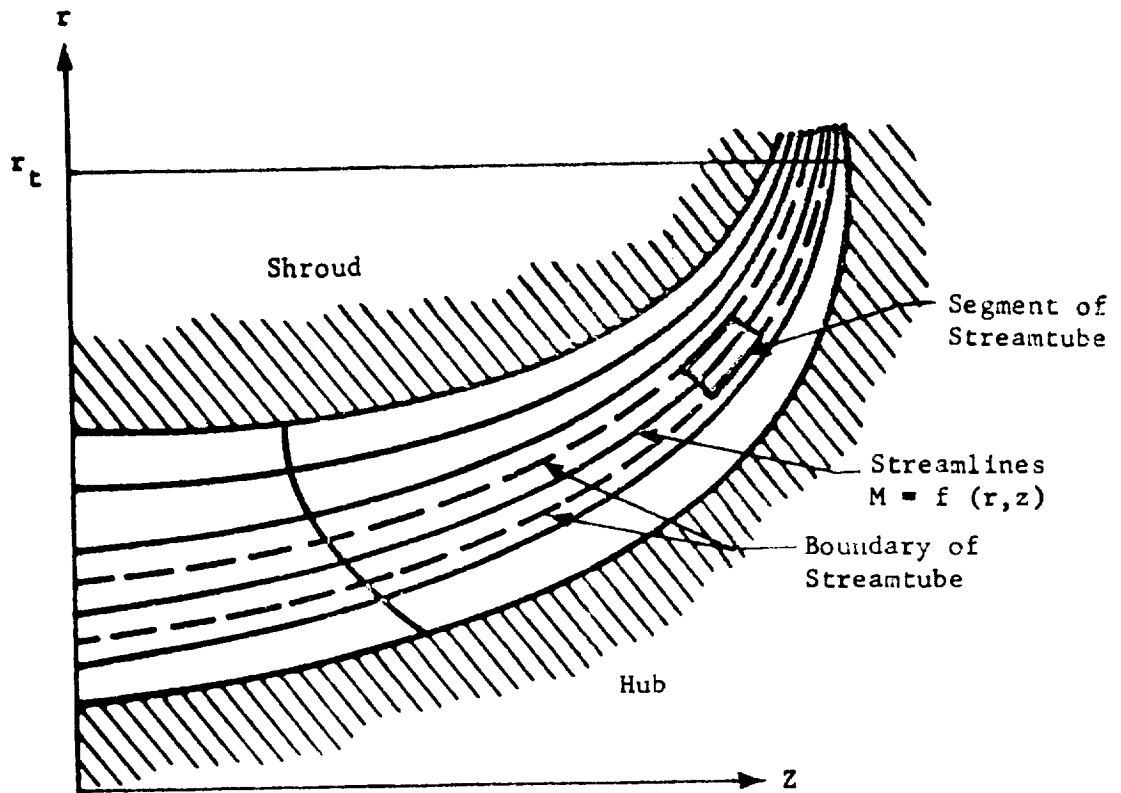
Figure 3.1   Meridional Plane of Pump Impeller
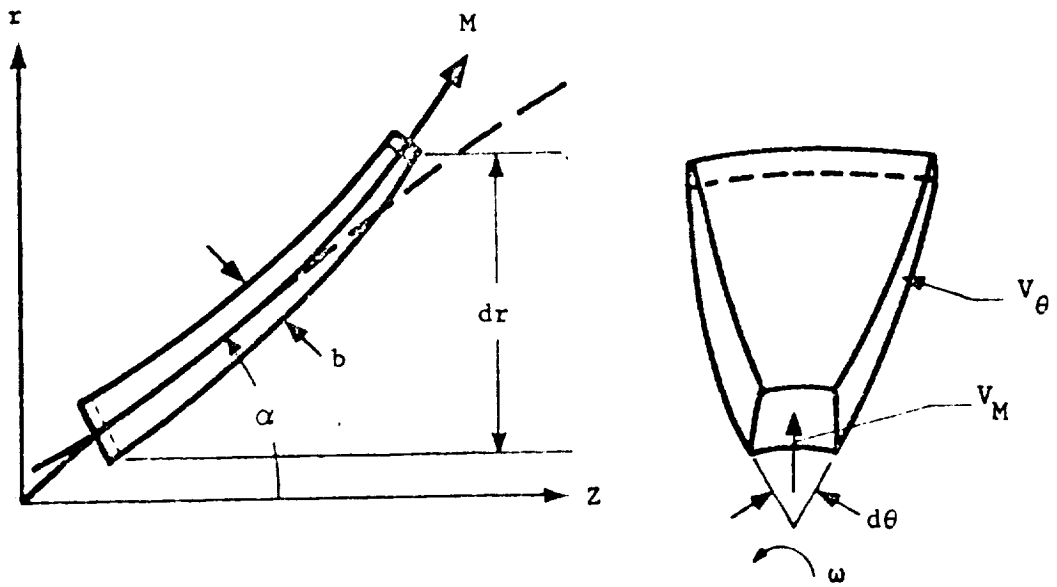
Figure 3.2   Segment Streamtube of Revolution for Continuity Equation

$$rd\theta \ (r\omega + V_\theta) + \frac{\partial}{\partial r} \left[(r\omega + V_\theta) \ \ rd\theta\right] dr$$

$$\frac{V_M \cdot dr}{Sin \ \alpha} \qquad \frac{V_M dr}{Sin \ \alpha} - \frac{\partial}{\partial\theta} \ \ \frac{V_M \cdot dr}{Sin \ \alpha} \qquad d\theta$$

$$rd\theta \ (r\omega + V_\theta)$$
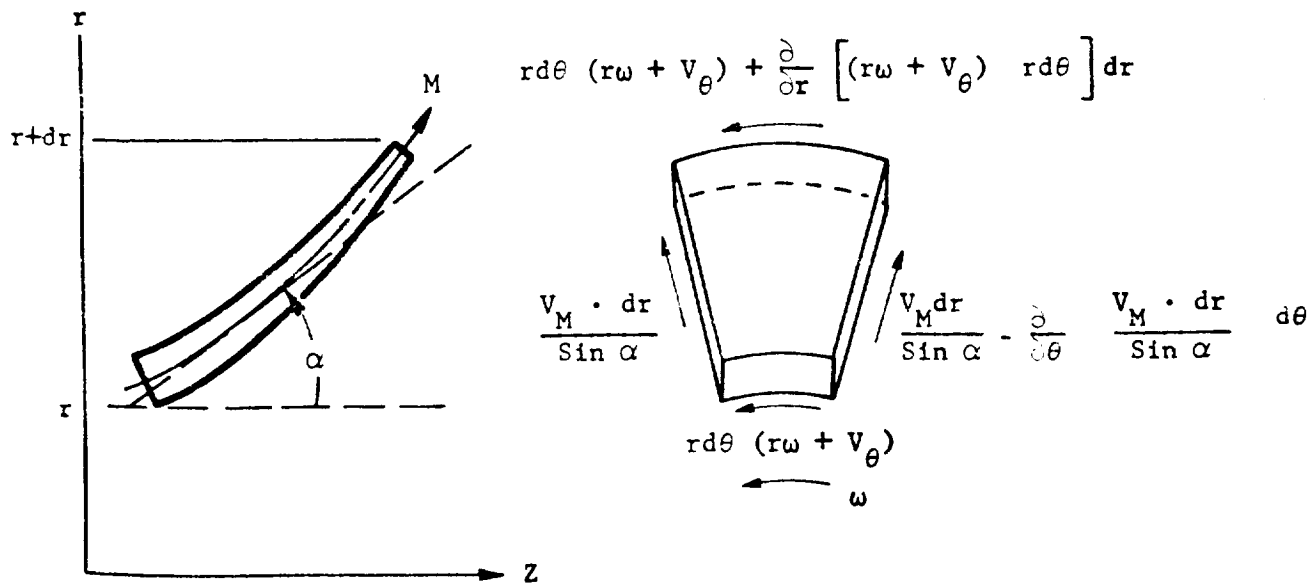
Figure 3.3   Segment Streamtube of Revolution for Irrotational Flow
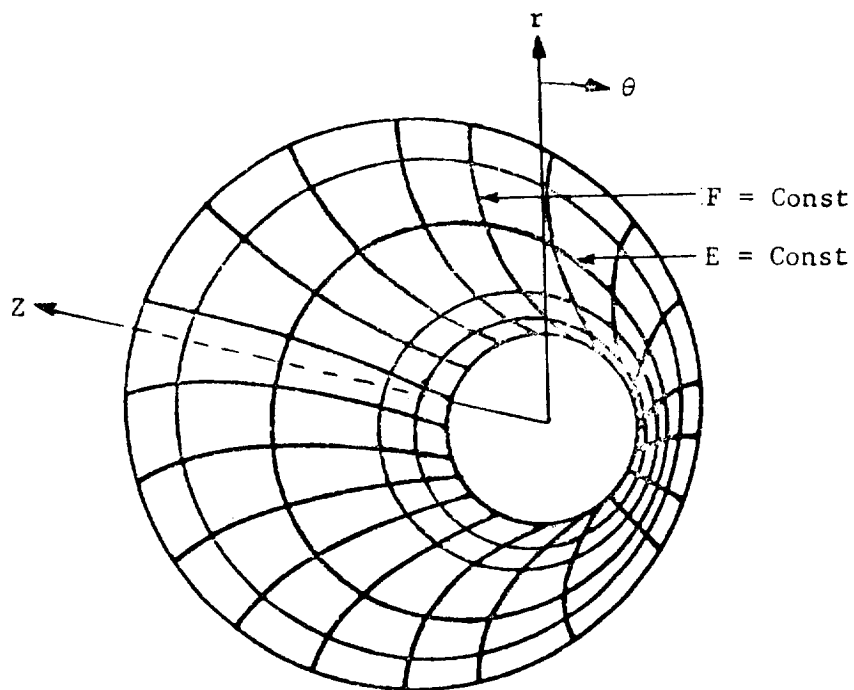
Figure 3.4   E,F Surface Relative to r, Z and θ Coordinates

34
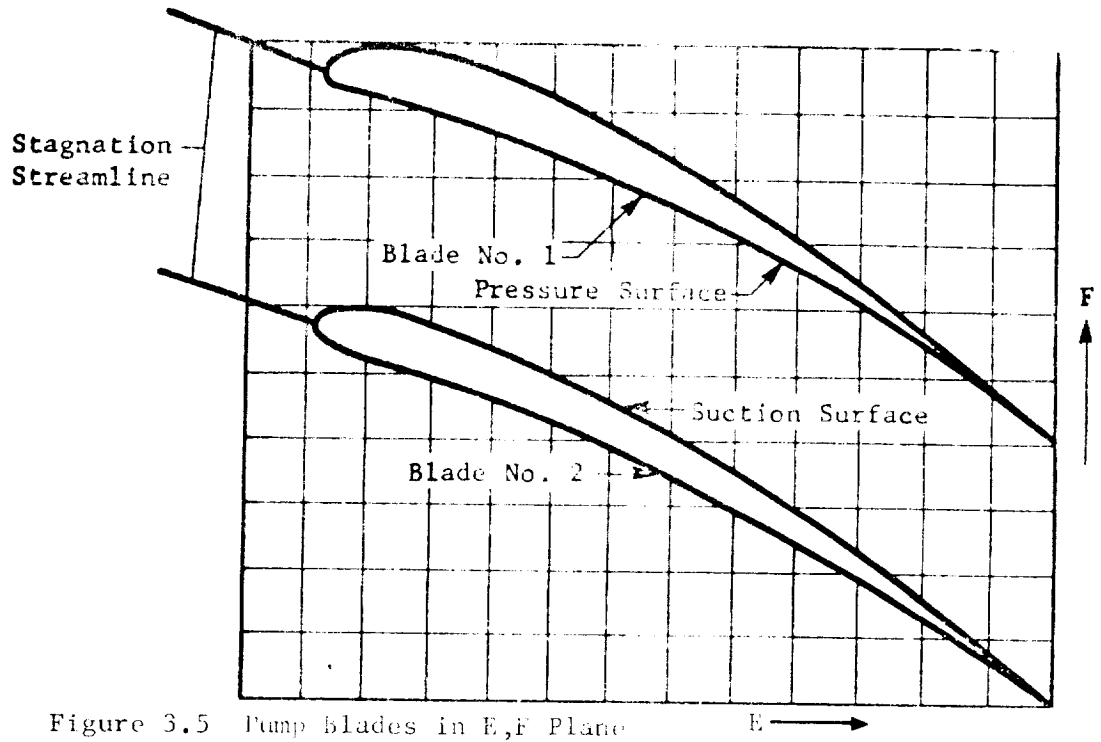
Figure 3.5 Pump Blades in E,F Plane
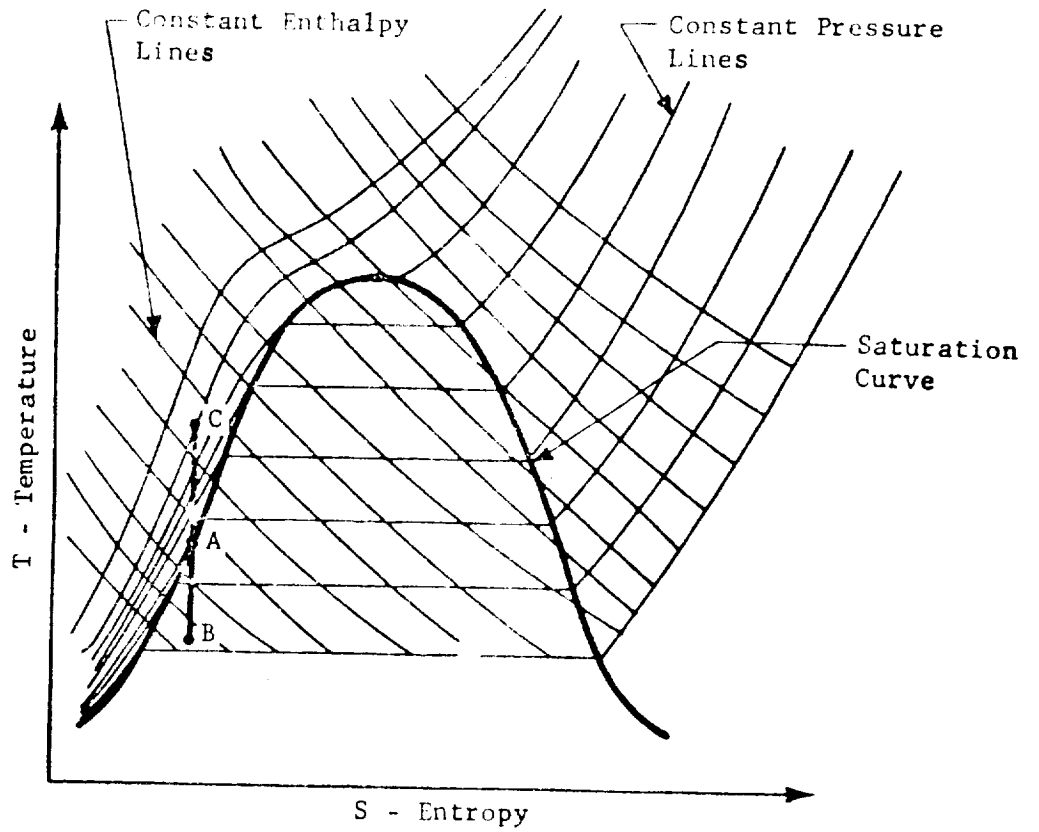
Figure 3.6 Pump Fluid Property Diagram
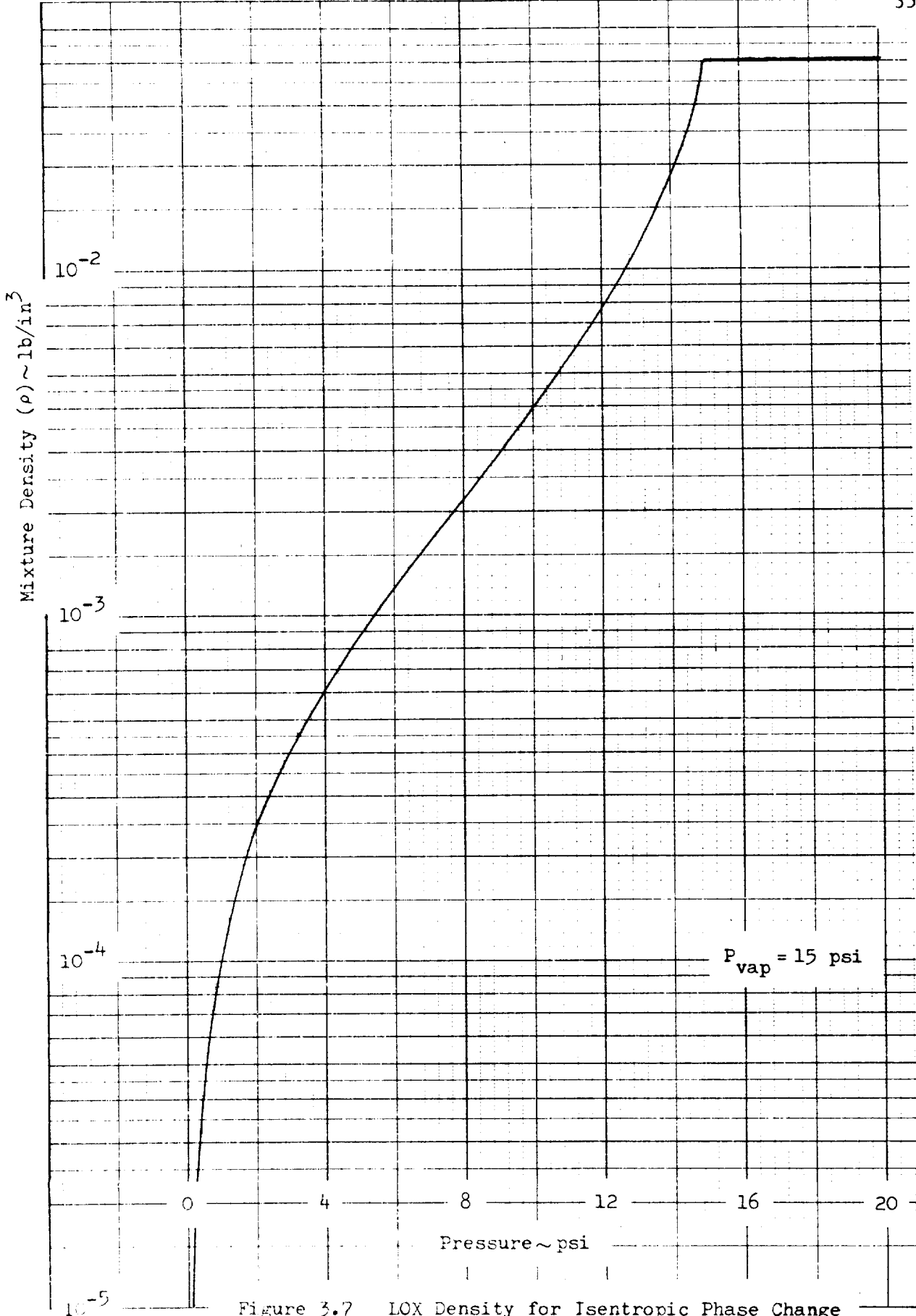
Figure 3.7   LOX Density for Isentropic Phase Change

36

(This page intentionally left blank)

4. Empirical Cavitation Data

4.   EMPIRICAL CAVITATION DATA

4.1   Test Data Analysis

4.1.1   Objectives - The objectives of the test data analysis
are:

a.   Determine the true cavitation compliance from
     all available test data on as many different
     turbopump configurations as possible;

b.   Considering turbopump and propellant parameters
     which influence cavitation, attempt to present
     all the test data in a nondimensional correlated
     form;

c.   Provide test results of specific turbopump con-
     figurations for verification of the analytical
     model.

Completion of the first objective will provide all currently
available turbopump cavitation data in a single document.
An empirical evaluation of the data, in terms of nondimensional
parameters, is a parallel approach to the purely analytical
turbopump cavitation model. The pump configurations selected
for verification of the analytical model should meet the
following requirements:

a.   Accurate determination of cavitation compliance
     from test data;

b.   Controlled and known test conditions;

c.   The turbopump should be typical of those of
     interest in POGO analysis;

d. The turbopump should be consistent with the
    assumptions of the analytical model.

Considering these requirements, the J-2 LOX and F-1 LOX turbo-
pumps were originally selected for model verification. In
addition, the H-1 LOX and LR87 oxidizer pumps were selected
for less detailed study. These selections were based on both
compatibility with the analytical model and confidence in
existing test data, as discussed in the following sections.

4.1.2 Data Sources - Table 4.1 shows all the different
turbopump configurations for which cavitation data is known
to exist. In all of these cases, cavitation data was derived
from tests whose objectives were to determine the natural
frequencies of the propulsion feed system for use in POGO
analysis. Although turbopump cavitation usually has an im-
portant influence on feed system frequency, testing and data
reduction was only concerned with determining an equivalent
cavitation compliance. For determination of feed system
frequency it was not required to separate the true cavitation
compliance from other sources of mechanical compliance in the
vicinity of the turbopump.

Table 4.1 Turbopump Configurations

Vehicle	Stage	Engine	Oxidizer	Fuel
Saturn	S-IB	H-1	LOX	RP-1
Saturn	S-IC	F-1	LOX	RP-1
Saturn	S-II/S-IVB	J-2	LOX	LH_2
Titan	I	LR87	N_2O_4	Aerozine 50*
Titan	II	LR91	N_2O_4	Aerozine 50*
Thor	I	MB-3	LOX	RP-1

    * 50% Hydrazine and 50% UDMH

Test data related to this study comes from one of the following sources:

 a. System tests with flowing propellant and an operating turbopump;

 b. Feed system tests with non-flow propellant in the absence of an operating turbopump;

 c. Feed line component tests on segments whose compliance can not be accurately calculated;

 d. Flight data.

Almost all of the available ground system test data is pulsed; i.e., the system response is measured relative to some known forcing function. The only test results which include the effects of turbopump cavitation are the flow system tests and the flight data. These test results required separation of the cavitation effects from other compliance effects. Some flow system tests have flight feed systems while others have facility feed systems; and some have hot firing engines while others are "bobtailed" (turbopump is driven in normal mode of operation but propellants are not mixed and burned in the main thrust chamber).

4.1.3 Determination of Cavitation Compliance From Natural Frequency - Cavitation compliance cannot be measured directly during a turbopump test and must be determined through use of analysis. A typical procedure for this determination is as follows:

a. Run a flow systems test;

b. Assume an analytical model of the test configuration;

c. Calculate, estimate, or determine from separate tests all model inputs except cavitation compliance;

d. Determine value of cavitation compliance for which model best fits test data.

Since cavitation compliance has its strongest influence on feed system natural frequency (as opposed to gain, damping, etc.) the above procedure is normally reduced to a correlation between test and analytical natural frequencies. These frequencies are a function of the inertance and compliance of the total system. For those unfamiliar with these hydraulic terms an analogy with a spring mass system is given in Figure 4.1. Inertance can be accurately calculated from the geometry of the feed line. The system compliance includes the distributed compressibility of the fluid and the radial flexibility of the suction line, axial flexibility due to a feed line area change, local flexibility of a line joint or bellows, and the compressibility of the cavitation vapor bubbles in the turbo-pump. Only the combined effect of all the system compliances can be determined from a dynamic systems test; thus, the line and fluid compliance must be known before cavitation compliance can be accurately determined. The distributed fluid and line compliance can be calculated fairly accurately. Local flexibilities can be determined from analysis, component tests, and/or system tests without the turbopump operating. Suction line bellows are local flexibilities which often represent a significant portion of the feed system compliance but cannot be determined accurately due to insufficient test data and a lack of analytical methods. A current technology contract (NAS8-25919)

should result in improved analytical methods for determination of all suction line elements. The exact equations relating cavitation compliance to natural frequency are a function of the analytical model used. The more representative the model the more accurate the derived cavitation compliance. Two computer programs which were developed for Titan and Saturn V POGO analysis were modified for general test analysis in this study. These programs consist of: 1) a modal analysis program (Reference 37) for determination of natural frequencies for any distribution of line inertance and compliance; and 2) a transfer function program (unpublished) which utilizes the modal data to generate the transfer function of suction pressure per excitation as a function of excitation frequency. For a lightly damped system with negligible feed line and fluid compliance the cavitation bubble compliance, C_b, can be approximated by

$$C_b = 1/(I\omega_1^2) \tag{4.1}$$

where I is the feed system inertance and ω_1 is the first natural frequency of the feed system. For a uniformly distributed suction line and fluid compliance, which yields an open-closed organ pipe frequency (ω_0), and a lumped duct compliance near the pump inlet (C_d), the cavitation bubble compliance can be approximated by

$$C_b = \frac{1}{I\omega_1^2} \left[\frac{(\omega_1/\omega_0)^2 - 1}{(\omega_1/2\omega_0)^2 - 1} \right] - C_d \tag{4.2}$$

4.1.4 Determination of Natural Frequency From Test Data -

A fairly standard procedure for determining feed system
natural frequency from test data is as follows:

a. Configure a test set up which resembles the
flight feed system as closely as possible;

b. Excite the feed system dynamic response with a
measured forcing function;

c. Generate frequency domain perturbation transfer
function (amplitude ratio and phase) of response
per excitation from the measured results;

d. Natural frequency occurs near frequency of
maximum amplitude ratio and phase shift of 90^{0}.

For most of the test results analyzed herein, the excitation
has been some type of near sinusoidal wave pulsing of suction
flowrate. In this case the pulser frequency has been changed
in steps (or in very slow ramp) and the resulting pressure
oscillations recorded at each frequency increment. This,
together with the measured excitation, yields a perturbative
transfer function of turbopump inlet pressure per excitation.
Another type of excitation which has been successfully used
(Reference 38) is the random noise associated with the engine
combustion process. In this case auto- and/or cross-spectral
analysis is required to determine the frequency domain response
of the system. In most feed system configurations the first
natural frequency is very near the frequency at which the
amplitude ratio is maximum simultaneous with a phase shift of

90° for an appropriate feed system transfer function. In POGO analysis the most important transfer function is turbopump inlet pressure oscillation per turbopump acceleration perturbation $(\partial P_s/\partial g_p)$. Any transfer function which has the same natural frequency as $\partial P_s/\partial g_p$ is an appropriate transfer function. Pulser acceleration and flow acceleration are legitimate excitations whereas transfer functions with respect to pulser pressure can yield significant errors in natural frequency. This effect is shown in the analysis of the J-2 test results. If additional information besides natural frequency (e.g. static gain and damping) are desired from the test results, it is required that a best fit between an analytical and test transfer function be obtained.

4.1.4.1 <u>Test Frequency Correction</u> - In reviewing test data two possible situations were recognized which could cause small errors in the test results. First is the determination of the system natural frequency from a transfer function of suction pressure per pulser pressure $(\partial P_s/\partial P_p)$ in lieu of suction pressure per pulser flow $(\partial P_s/\partial \dot{W}_p)$. Second is the presence of facility lines which do not exist in the flight configuration. Both of these conditions existed on the S-II LOX line tests and each represents an error in frequency determination of about 5% in opposite directions. The effect of using the $\partial P_s/\partial P_p$ transfer function is shown in Appendix C for a simplified system and results in a frequency which is 5% too high. The S-II LOX line test set up had a facility line running from the sump to the facility tank. This line was isolated from the suction line by a large accumulator at the sump; however, the residual effect of the facility line yields a system

natural frequency which is 5% too low. A model of the test and
flight configuration is shown in Figure 4.2. A comparison of
the $\partial P_s/\partial P_p$ transfer function for the test set up with the
correct $\partial P_s/\partial g_p$ transfer function for the flight configuration
is shown in Figure 4.3. Neither of the two possible discre-
pancies are known to exist in any other test data.

4.1.5 Test Results - No attempt has been made to duplicate
previous analysis of pertinent test results. However, in many
cases the analysis had to be extended in order to separate
cavitation compliance from other sources of compliance. Also,
in several instances independent tests on the same configura-
tion produced conflicting results. In these cases, if a review
of both results could not favor one over the other, the discre-
pancy was carried through the analysis and yields a tolerance
on the results. Cavitation compliance is a function of many
propellant and turbopump parameters; however, for a given con-
figuration at a fixed operating point the only significant para-
meter which undergoes a planned variation during tests is turbo-
pump inlet static pressure (P_s). Thus, the cavitation results
presented in the following paragraphs are given as either a
function of P_s or a non-dimensional form of P_s defined by

$$K = \frac{P_s - P_v}{1/2 \; \rho \; V_r^{\;2}} \tag{4.3}$$

where K = cavitation index

P_v = propellant vapor pressure

ρ = propellant mass density

V_r = inducer relative tip velocity

This is a convenient parameter since it has been found that for most turbopump configurations cavitation compliance is a linear function of a constant raised to a power which is proportional to K, i.e., a straight line on semi-log graph paper. Whenever the scatter in the test data allows, this functional relationship will be observed in the presentation of the following test data. The data necessary for calculation of cavitation index is presented in Table 4.2.

4.1.5.1 F-1 LOX Cavitation Compliance

- The F-1 LOX turbopump was tested with a S-IC outboard feed line and an outboard Arrowhead PVC (Pressure-Volume Compensator) duct. The feed line properties were taken from Reference 39. A LOX compressibility of $.135 \times 10^6$ psi ($T = -296°F$) was calculated from velocity of sound data given in Reference 40. The compliance of the main line area change (above the prevalve) was investigated and found to be negligible. The PVC compliance was calculated from component test by Aerrowhead, MSFC and Boeing; and from non-flow system dynamic tests by MSFC and Boeing. These data were then used in a model in which cavitation compliance was varied to match Bobtail (Reference 41) and Single Engine (Reference 42) tests results.

4.1.5.1.1 F-1 LOX PVC Component Test Results

- The total PVC compliance, C_{PVC}, includes the combined effect of the fluid compressibility and radial expansion (C_f) and axial flexibility of the upper and lower annulus area (C_x).

$$C_{PVC} = \frac{dW}{dP} = \frac{d(\rho V)}{dP} = C_x + C_f \qquad (4.4)$$

where
$$C_x = \rho A \frac{dX}{dP} = \rho A^2/K \qquad (4.5)$$

and
$$C_f = \rho \ell \frac{dA}{dP} + A \ell \frac{d\rho}{dP} \qquad (4.6)$$

C_f was calculated to be .011 in^2 and is included as part of the distributed compliance of the feed line model. The results of the component test are summarized in Table 4.3, and discussed below. Figures 4.4 and 4.5 contain unpublished results, supplied by MSFC, of PVC component tests run by Aerrowhead. From Figure 4.4 total PVC compliance can be calculated from dV/dP; however, this result is considerably too large compared with all other data. This can only be explained by the presence of air in the system. Two observations can still be made from these results. 1) dV/dP appears to be nonlinear with respect to pressure, and 2) dV/dP is approximately the same whether or not the PVC ends are restrained (this agrees with an analysis of the areas and spring rates). A more reliable estimate of PVC compliance can be made using Equation (4.5) and the results given in Figure 4.5. This result is independent of the amount of trapped air in the system. Component tests run at MSFC (Reference 43) gave a value of dX/dP of .0056 (2 x .0028 for both the upper and lower annulus) for an Aerrowhead inboard PVC, and .007 for Flexonics outboard PVC. The results were very linear over the pressure range of 40 to 130 psig. The corresponding values of C_x are .060 and .075 in^2 respectively. An equivalent PVC spring rate of K = 34250 lb/in was determined from Boeing component tests on a Aerrowhead outboard PVC (Reference 39), and this was also

fairly linear over the pressure range of 50 to 125 psia. This yields (Equation 4.5) a C_x value of .081 in^2. An analysis of the flexibility of supporting structure used in the Boeing water tests (Reference 39) showed that for the PVC installed in the line C_x could increase to .096 in^2; however, it could never decrease below .081 (a completely rigid mounting of the upper spool and lower flange). Component tests ($\Delta X/\Delta P$) show that the outboard Aerrowhead and Flexonics PVC's have approximately the same compliance while inboard Aerrowhead PVC has about 25% less compliance.

4.1.5.1.2 F-1 LOX PVC Systems Test Results - Analytical feed system natural frequencies as a function of the sum of the cavitation bubble compliance (C_b) and the PVC annulus compliance (C_x) are given in Figure 4.6. Since these two compliances are located fairly close together, the frequencies are practically independent of the distribution between C_b and C_x. The second resonance of a pressure/pulser flow transfer function is shown to be a function of the location of the pulser line. Figure 4.7 gives MSFC dynamic test data with the turbopump isolated from the feedline. Some non-flow tests were run with a Flexonics outboard PVC and some with an Aerrowhead PVC; however, since the component tests indicate they have essentially the same compliance no attempt was made to differentiate between the two. A similar method of obtaining C_x from the Boeing Water Tests (Reference 39) yielded a C_x of .125 in^2 at 80 psia and .086 at 140 psia. This compliance is high enough to suspect that there may be some air trapped in the system, which is always a possibility in non-flow tests.

48

4.1.5.1.3 F-1 LOX Cavitation Compliance - Figure 4.8 shows
MSFC dynamic test results (References 41 and 42) with the
turbopump running. Also shown is the sum of the cavitation
and PVC annulus compliance, C_b and C_x, required to make the
analytical results match the test results. The resulting
cavitation compliance is shown in Figure 4.9 for two different
C_x functions. One is the maximum C_x variation as derived from
a best fit of the MSFC non-flow tests (Figure 4.7). This
variation is much more than can be justified by any component
tests, and also results in a cavitation compliance which shows
less variation with pressure than is expected. The other C_x
function used is a constant value of .081 in^2, as derived from
some of the component tests. Since some of the component tests
indicate some variation in C_x with pressure, a constant value
is probably conservative. The true cavitation compliance should
lie between the limits shown in Figure 4.9.

4.1.5.2 F-1 Fuel Cavitation Compliance - The Rocketdyne
evaluation of fuel pump inlet compliance (Reference 44) from
the F-1 Bobtail Test results (Reference 41) are presented in
Figure 4.10. Also shown are cavitation data derived from feed
system frequencies obtained from the F-1 Bobtail tests and the
S-IC Single Engine Test (Reference 42). The results of this
analysis yield higher values of pump inlet compliance than were
obtained by Rocketdyne. The variation in test frequency data
presented in Figure 4.11 accounts for the lower values of pump
inlet compliance analytically derived from the S-IC Single
Engine Tests. The only differences between the Bobtail and Single
Engine Test are that the Bobtail Test configuration had an out-
board PVC and used discharge pulsing, whereas the Single Engine

Test configuration had an inboard PVC and used suction pulsing. Discharge pulsing should yield the same results as suction pulsing; however, obtaining good reliable feed system frequencies by discharge pulsing usually presents severe data reduction problems. The differences in results are larger than the anticipated differences due to changing PVC ducts. It was concluded that the S-1C Engine Test data was more reliable because it was derived from suction line pulsing, it is more recent data, and it showed less scatter. Since compliance derived from the S-IC Engine Test is less than that derived from the F-1 Bobtail Tests it should contain less PVC duct compliance. Since no PVC duct compliance was available it is assumed that turbopump inlet compliance derived from the F-1 Engine Tests is equal to cavitation compliance.

4.1.5.3 J-2 LOX Cavitation Compliance - Dynamic test data exists for four different J-2 LOX feed systems. They are the S-II inboard test facility feed system, the S-II outboard test facility feed system, the S-IVB test facility feed system, and the Rocketdyne turbopump test facility feed system. These tests were run for a range of turbopump inlet pressures and three different PU (propellant utilization) settings. As expected, the feed system natural frequencies (and thus turbopump cavitation) varied greatly with inlet pressure; however, the effect of PU setting was within the scatter of the data. Thus, for a given inlet pressure, reduced test results from all the different J-2 LOX feed systems should yield the same cavitation compliance. Two independent detailed analyses of test results have been performed. Brown Engineering analyzed the results of the S-II and S-IVB feed system tests (Reference 45) and Rocketdyne analyzed their test facility results

50

(References 46 and 47). Both analyses yield approximately the same predominate resonances when related to common feed systems. This is shown in Figure 4.12 for the S-II and S-IVB flight feed systems (which is somewhat different than the test facility feed systems). Brown Engineering assumed a single compliance turbopump model whereas Rocketdyne derived a turbopump flow impedance transfer function, $G(S)$, from their test data which implies a dual compliance turbopump model. For the same test results (i.e., the same predominate feed system frequency) the two different turbopump models will yield different values of cavitation compliance.

4.1.5.3.1 <u>J-2 LOX Duct Compliance</u> - Also of importance is the amount of fluid and duct compliance present in the suction line. The Brown Engineering analysis derived a lumped compliance from dynamic tests which had the suction line isolated from the pump. Rocketdyne, on the other hand, coupled their test derived turbopump impedance function to flight suction line models and added suction line compliance until the analytical frequencies agreed with flight observed resonances. These results are compared in Table 4.4 and in both cases represent equivalent lumped values at, or near, the turbopump inlet. Both of these approaches are valid and should yield approximately the same results, whereas, the differences shown represent a very significant portion of the total feed system compliance.

4.1.5.3.2 $\underline{J\text{-}2\ LOX\ Turbopump\ Model}$ - The single compliance model (see Figure 4.13a) used in the Brown Engineering analysis has a flow impedance given by

$$G(S)_1 = \frac{P_o}{W_o} = \frac{R}{K_p} \frac{\left[\frac{L}{R} S + 1\right]}{\left[\frac{CL}{K_p} S^2 + \frac{CR}{K_p} S + 1\right]} \qquad (4.7)$$

In this case the resistance, R, and inertance, L, were calculated; and the pump gain, K_p, and the cavitation compliance, C, were derived from test data. This impedance function and Brown Engineering duct compliance shown in Table 4.4 yield cavitation compliances shown in Figure 4.14.

The Rocketdyne analysis fit an impedance function to test data. The form required to give good correlation is given by

$$G(S)_2 = \frac{P_o}{W_o} = \frac{K\left[\left(\frac{S}{\omega_2}\right)^2 + \left(\frac{2\zeta_2}{\omega_2}\right) S + 1\right]}{\left(\frac{S}{\omega_1} + 1\right)\left[\left(\frac{S}{\omega_3}\right)^2 + \left(\frac{2\zeta_3}{\omega_3}\right) S + 1\right]} \qquad (4.8)$$

One possible physical representation which gives this type of response is given in Figure 4.13b. In terms of the physical parameters, the impedance functions become

$$G(S)_2 = \frac{P_o}{W_o} = \frac{R\left[\left(\frac{LC_2R_2}{R}\right)S^2 + \left(\frac{L + R_1R_2R_2}{R}\right) S + 1\right]}{K_p\left[\left(\frac{LC_1C_2R_2}{K_p}\right)S^3 + \frac{C_1}{K_p}\left(L + R_1R_2C_2\right)S^2 + \left(\frac{C_1R}{K_p} + C_2R_2\right)S + 1\right]} \qquad (4.9)$$

Equating coefficients of Equations (4.8) and (4.9) will yield the physical model parameters in terms of the frequency and damping parameters. Table 4.5 gives these results for the latest frequency and damping data given in Reference 47. In this model, C_1 is the main inlet cavitation compliance. It is the most important turbopump parameter in determining the predominate feed system frequency and is independent of pump gain (K_p). To illustrate the effect of the other turbopump parameters consider the case where the impedance beyond the cavitation compliance is very high. Then both of the above **turbopump** models approach an impedance function given by

$$G(S)_3 = \frac{1}{CS}$$

where C is the cavitation compliance. Using Rocketdyne feed system frequencies (Figure 4.12) and duct compliances (Table 4.4) cavitation compliances for both $G(S)_2$ and $G(S)_3$ are shown in Figure 4.15. Although $G(S)_3$ is not a good pump model, the effect of different turbopump models is illustrated.

4.1.5.3.3 <u>J-2 LOX Test Cavitation Compliance</u> - The difference in the Brown Engineering and the Rocketdyne derived cavitation compliance can be attributed to different suction duct compliances and different pump impedance functions. There is considerable test data which indicates that a double compliance model, $G(S)_2$, is a better representation of the turbopump than a single compliance model, $G(S)_1$. From this point of view the Rocketdyne data should be more accurate; however, the Brown Engineering analysis is a more conventional approach which has been used on several other turbopump configurations.

For purposes of this study, both of these results (as shown in
Figure 4.16) are considered to be equally valid. It is thus
assumed that the true inlet cavitation compliance can be any-
where between these limits.

4.1.5.3.4 S-II Flight Data - AS-509 S-II Stage flight data
(Reference 48) were reviewed and the observed LOX feed system
oscillations compared with test results. Two things were
evident from the flight data. First, the observed S-II out-
board feed system contourgram frequency was higher than antici-
pated; and, second, there was an observed frequency change at
engine mixture ratio (EMR) shift. Prior to EMR shift, the
observed outboard frequency was approximately 33% higher than
the predicted value which was based on S-II "bobtail" and
J-2 test results for inlet NPSH in the vicinity of 60 ft.
Furthermore, if the 65 to 75 Hz inboard suction pressure oscil-
lation, observed during and after accumulator fill, represents
a response of the second inboard line ("short stack") mode,
this result is approximately 28% higher than would be analyt-
ically predicted. The following theories have been advanced
by different Saturn V POGO analysts as to the reason for these
apparent frequency discrepancies:

 a. The observed oscillation is not a natural
  frequency of the feed system but a 1/3 sub-
  harmonic of a 90 Hz turbopump self-induced
  oscillation;

b.   the suction line structure is such that the
      propellant rose in the horizontal section does
      not affect the feed system frequency on the
      flight configuration;

c.   For some unknown reason less turbopump cavitation
      exists in the flight vehicle than in the ground
      test.

The true cause remains unresolved; however, if it is due to
reduced cavitation compliance (C_b), the flight results for
both the S-II inboard and outboard feed systems imply that C_b
is at least 70% lower than predicted from test data. This
possible discrepancy must be considered when utilizing the
test results. In the later portion of S-II burn, the engine
mixture ratio (EMR) changed from 5.5 to 4.8. This results in
a predicted decrease in the flow coefficient (ϕ) of 10%. A
reduced flow coefficient results in the turbopump inlet flow
entering the inducer blades with a larger angle of attack.
This should produce increased cavitation compliance and result
in a lower feed system frequency. The observed flight results
were just the opposite. When the EMR changed from 5.5 to 4.8
the S-II outboard LOX contourgram frequency appeared to increase
from 26. to 33. Hz. The reason for this contradiction is unknown.

4.1.5.4 <u>J-2 Fuel Cavitation Compliance</u> - Turbopump cavitation
compliance for the J-2 axial flow fuel pump is shown in Figure
4.17. This data was derived from a Rocketdyne single compli-
ance math model (Reference 46). Since these tests were run at

a Rocketdyne test facility it is assumed that rigid suction lines were used, and thus the results do not contain any pump inlet duct compliance. An analytical model of the S-II outboard feed system was used to determine J-2 fuel pump inlet compliance from a frequency data point (9.5 H_z) supplied by MSFC for Saturn POGO analysis. Although present available data on fuel bellows compliance is incomplete, a value of .004 in^2 was assumed after a review of the J-2 oxidizer configuration and inlet duct compliance test values. The resulting pump inlet compliance derived from this datum falls within the scatter of pump compliance data derived by Rocketdyne as shown in Figure 4.17.

4.1.5.5 <u>H-1 LOX and Fuel Cavitation Compliance</u> - Brown Engineering and Rocketdyne derived values of pump inlet compliance (Reference 49) based on S-IB Bobtail Tests (Reference 50) are shown in Figure 4.18. The mathematical models differed only in the suction line representation while turbopump and discharge line representation were comparable. The characteristic resonant frequencies derived from the test data by Brown Engineering and Rocketdyne also differed since the method employed by each in the interpretation of the test data varied. Both suction line and discharge line pulsing data were available. The use of spectral analysis of the test results by Brown Engineering has shown that discharge line pulsing did not give the correct characteristic frequencies (Reference 51). Lack of data points for the fuel pump inlet compliance in the Brown Engineering analysis is due to the inability of their data reduction procedure to always determine values of feed

system frequencies. Since Rocketdyne did not indicate this to be a problem, their procedure was considered more reliable and will be used exclusively in this analysis. The Bobtail test configuration does not have any suction line bellows located at the pump inlet. Since there are small line bellows located at several points in the fuel and oxidizer lines, it is assumed that their compliance is accounted for in the distributed compliance of the suction lines. Thus, for the H-1 feed systems, the derived pump inlet compliance shown in Figure 4.18 is assumed to result exclusively from turbopump cavitation.

4.1.5.6 MB-3 LOX and Fuel Cavitation Compliance - MB-3 cavitation compliance data was obtained from an Aerospace Corporation evaluation of feed system frequencies on the THOR vehicle (Reference 52). These data are shown in Figure 4.19 as a function of cavitation index (K). They are presented in this report for reference only, as MB-3 turbopump geometry and operating parameters were not available to permit evaluation of the data.

4.1.5.7 LR87 and LR91 Oxidizer and Fuel Cavitation Compliance - Cavitation compliance of the Titan Stage I and II turbopumps is shown in Figure 4.20. This data was determined by combined Martin Marietta Corporation and Aerospace Corporation analysis of pulsed and/or non-pulsed hot firing engine tests, bobtailed turbopump tests, suction line non-flow tests, and flight data. The final results have evolved over several evaluations (particularly in the case of the LR87 data) and no concise documentation exists. The Martin results, presented here, agree closely (except for a density scale factor) with the

Aerospace results given in Reference 31. The LR87 oxidizer
feed system contains the largest amount of non-cavitation
compliance. In this case the suction line distributed com-
pliance was calculated and compared with non-flow test results
(unpublished results of Martin Marietta Corporation tests). These
results indicated that the line bellows located near the pump
inlet contain very little compliance. This is assumed to be
true for the other Titan lines which use similar line bellows.

4.1.6 <u>General Test Data Assessment</u> - The preceding cavitation
compliance test data generally have large uncertainties associ-
ated with the results. In most cases this can be related to the
fact that the objective of these tests was to determine feed
system frequency, not cavitation compliance. In several cases the
results even show large dispersions in feed system frequency for
a given test series and unexplained disagreement between results
of different tests of the same feed system. Assuming the feed
system frequency is accurately known the following error sources
exist for determining cavitation compliance.

      a. Unknown feed line compliance;

      b. Frequency insensitive to cavitation compliance,
          conversely cavitation compliance is very sensitive
          to frequency dispersions;

      c. Unknown turbopump model (test data will not fit
          a physical model).

In addition to dispersions in the results there are unknowns
associated with parameters which affect the amount of cavitation
which occurs. Some of these unknown factors are:

a. Velocity distribution at the turbopump inlet;

b. Propellant back flow into the suction line;

c. Propellant preswirl at the inlet;

d. Amount of absorbed gas in the propellant;

e. Exact propellant temperature at the turbopump inlet;

f. Effect of PU (Propellant Utilization) recirculation flow.

The accumulated effect of all the unknowns must be carefully considered when judging the merits of either an empirical or analytical prediction technique.

4.2 Empirical Data Evaluation

4.2.1 Influential Parameters - In order to evaluate all the different turbopump cavitation compliance test data one has to postulate as to what are the important variables, and attempt to group these into non-dimensional parameters which will yield the same cavitation compliance for all existing turbopump configurations. If this could be accomplished with some degree of success, it could provide a method for predicting the amount of cavitation compliance that will occur on a new turbopump design. The turbopump operating and geometry parameters, and propellant variables which could affect the amount of turbopump cavitation are:

P_s = pump inlet static pressure

$\dot{W}$ = propellant flow rate

H_i = inducer head rise

N = inducer speed

α_i = inducer angle of attack

n_i = number of inducer blades

D_i = inducer tip diameter

D_h = inducer hub diameter

ℓ_i = inducer tip radial clearance

P_v = propellant vapor pressure

ρ = propellant density

h = propellant latent heat of vaporization

The ideal method of assessing the effect of these variables is to conduct cavitation tests where only one parameter is varied at a time. The available test results are for different turbopump configurations (all geometry parameters changed together), each run with a single propellant, at normal operating conditions (usually only inlet pressure is varied). This approach does not give specific empirical dependence of cavitation compliance on parameters other than P_s. The other parameters do vary for different turbopump configurations, but the effects cannot be separated. Thus, only a qualitative empirical evaluation of the results can be performed. This is accomplished by comparing non-dimensional cavitation compliance against non-dimensional turbopump and propellant parameters.

4.2.2 <u>Non-Dimensional Parameters</u> - Ideally there exists a non-dimensional combination of parameters which uniquely describes a cavitation parameter as a function of operating and configuration parameters for all conditions and configurations. The most generally used non-dimensional cavitation parameter is cavitation index, K (Equation 4.3), which combines P_s, P_v, and V_r. The data required to compute cavitation index is given in Table 4.2 for several turbopump configurations. All of the available cavitation compliance data is shown in Figure 4.21 vs cavitation index. When two sources of equally valid

data exist, an average of the two values was assumed for comparison with other data. Although all of this data exhibits the same trend and lies within an order of magnitude band, the variation is much too large to eliminate the need for obtaining cavitation test data on a new turbopump configuration. Turbopump size can be easily accounted for by non-dimensionalizing cavitation compliance (C_b) with respect to size variables. $C_b/n_i D_i{}^2$ vs K is shown in Figure 4.22. This in general narrows the band of data except for the LR-91 oxidizer data. The inducer leading edge angle of attack, assuming no propellant preswirl at the pump inlet, can be calculated by

$$\alpha_i = \beta_i - \tan^{-1}\emptyset \qquad (4.4)$$

where β_i is the inducer blade angle and $\emptyset$ is the flow coefficient. Comparing the values of α_i given in Table 4.2 with the cavitation data given in Figure 4.21 and 4.22 shows no particular correlation. This may be partly due to the fact that all of the LR series turbopumps have cambered inducers which operate at near zero leading edge angle of attacks. All the other turbopumps have flat inducer blades which require a leading edge angle of attack to generate a pressure rise. Thus, α_i is not a good universal cavitation measurement parameter. A turbopump performance parameter, pump specific speed (SS), defined in non-dimensional form as

$$SS = 8136 \left[1 - \frac{D_h{}^2}{D_i{}^2} \right]^{\frac{1}{2}} \emptyset^{\frac{1}{2}} \bigg/ \left[K \right]^{3/4}$$

(Reference 31), was considered as a means for correlating cavitation compliance. Figure 4.23 shows non-dimensional cavitation compliance (related to inducer inlet area $D_i^2 - D_h^2$) as a function of 1/SS. Comparison of Figures 4.22 and 4.23 shows that 1/SS is not significantly better than K. Thor(MB-3) data is not shown because the necessary geometry parameters were not known. Information on other influential parameters given in the preceding paragraph was not obtained for enough turbo-pump configurations to permit non-dimensional evaluation of their affect. However, it is doubtful if the existing spread in data shown in Figures 4.22 and 4.23 can be significantly reduced. Simple non-dimensional **parameters cannot account for such** important affects as blade shape, flow separation, and propellant phase change. The non-dimensional data presented here could be used to predict an order of magnitude cavitation compliance on a new turbopump configuration.

4.2.3 <u>Effect of Inlet Pressure</u> - It is of interest to note what the functional relationship is between inlet pressure (P_s) and cavitation compliance (C_b) as observed from the test data. Assuming that

$$C_b = Constant/P_s^n$$

then

$$n = - \frac{P_s}{C_b} \frac{\partial C_b}{\partial P_s} = - \frac{(K + P_v/q)}{C_b} \frac{\partial C_b}{\partial K}$$

where $K = (P_s - P_v)/q$

and $q = \rho V_r^2/2g$

Measuring average values of K, C_b, and $\partial C_b/\partial K$ from the test results (Figure 4.21), values of "n" were calculated (see Table 4.6). The results show that for the Aerojet turbopumps, "n" fall in the range of 2 to 4. For several other turbopumps, "n" falls in the range of .5 to 1. Due to scatter in the test data, there is a fairly large tolerance associated with $\partial C_b/\partial K$; however, if the trend is correct, these results imply that cavitation compliance, in different turbopumps, is proportional to different powers of P_s. This indicates that an analytical derivation of cavitation compliance, in terms of average flow field parameters, cannot yield good agreement with test results for all configurations. The work of F. Ghahremani (Reference 31) indicates that blade cavitation is inversely proportional to P_s^2, while backflow cavitation is inversely proportional to P_s^3. For the Aerojet turbopumps, this formulation should show good slope agreement (which it does) with test results; however, poor slope agreement could result for some of the other pumps. Current studies are being performed under Contract NAS8-27731 to evaluate this approach with respect to additional turbopump configurations (Reference 56).

Table 4.2

Turbopump Data

	TITAN STAGE I		TITAN STAGE II		SATURN S-IC		SATURN S-II/S-IVB		SATURN S-IB	
Vehicle Stage	OXID	FUEL	OXID	FUEL	OXID	FUEL	OXID	FUEL	OXID	FUEL
Engine Identification	LR-87		LR-91		F1		J2		H1	
Mixture Ratio	1.917		1.67		2.22		4.95		2.41	
Propellant	N_2O_4	A-50	N_2O_4	A-50	LOX	RP-1	LOX	LH_2	LOX	RP-1
Density (ρ) lb/in^3	.0525	.033	.0525	.033	.041	.029	.041	.00255	.041	.029
Suction Line Area in^2	37.2	27.2	27.1	12.2	227	226	49.6	49.6	42.3	26.3
Pump Dimensional Parameters										
Diameter-Inducer Eye (D_i) in	7.10	6.64	5.10	3.80	15.75	15.71	6.75	7.80	7.60	6.12
Diameter-Inducer Hub (D_h) in	2.15	2.24	1.73	0.84	3.51	6.61	1.375	2.93	2.0	2.00
Area Inducer Inlet in^2	36.0	30.7	18.0	10.8	185.0	159.6	34.3	41.0	42.3	26.3
Design Clearance (ℓ) in	.045	.045	.045	.045						
Number of Inducer Blades (n)	3	3	3	3	3	4	3	4	4	4
Diameter of Impeller tip in	9.42	10.75	8.75	4.93	19.50	23.42	10.20	Axial	11.0	13.75
Blade Angle (β) deg. at tip	5.7	5.7	5.7	5.7	9.0	8.6	9.9	7.0	11.3	10.4
Pump Performance Parameters										
Pump Speed (N) RPM	8350	9175	8366	23576	5550	5550	8050	25800	6750	6750
Inducer Tip Velocity (V_i) ft/sec	258	266	186	390	381	380	237	876	224	180
Propellant Velocity (U) ft/sec	23.0	22.4	17.2	27.3	41.4	30.6	22.9	62.3	24.7	26.6
Relative Velocity^2 (V_r^2) ft^2/sec^2	67093.	71258.	34892.	152845.	146875.	145336.	56693.	771257.	50787.	32943.
Flow Rate (W) lb/sec	522.55	272.57	195.05	116.9	3765.	1697.	386.	78.	514.4	243.
Flow Coefficient (ϕ= U/Vi)	.089	.084	.093	.070	.109	.081	.097	.071	.110	.1475
Inducer Tip Angle of Attack (α_i) deg.	0.6	0.9	0.4	1.7	3.6	4.0	5.1	3.7	6.5	3.1

Table 4.3

PVC Annulus Compliance $(C_x \sim in^2)$

Test Conductor	Source	Press=80psia	Press=140psia
(Aerrowhead Inboard PVC)			
Aerrowhead	$\Delta X/\Delta P$	.073	.046
MSFC	$\Delta X/\Delta P$	.060	.060
MSFC	①	.062	.060
(Aerrowhead Outboard PVC)			
Aerrowhead	$\Delta X/\Delta P$	.085	.060
Boeing	$\Delta X/\Delta P$	.081	.081
Boeing	②	.096	.096
Boeing	① ③	.125	.086
MSFC	①	.068	.025
(Flexonics Outboard PVC)			
MSFC	$\Delta X/\Delta P$	.075	.075

① Match to no flow dynamic test results.
② $\Delta X/\Delta P$ results plus mounting flexibility.
③ Possibility of air in the system.

Table 4.4

J-2 LOX Suction Duct and Fluid Compliance

| Feed System | Compliance (in^2) | |
	Brown Eng* (Reference 45)	Rocketdyne** (Reference 47)
S-II Inboard	.0112	.0031
S-II Outboard	.0077	.0055
S-IVB	.0055	.0015

*   Located approximately 10" above turbopump inlet

**   Located at turbopump inlet

Table 4.5

J-2 LOX Physical Model Parameters For $G(S)_2$

NPSH	Ps	C_1	$C_2 Kp$	R_1/Kp	R_2/Kp	L/Kp
40	33.7	.0189	.0158	.418	3.47	.016
45	36.2	.0175	.0173	.371	3.18	.014
50	38.1	.0142	.0163	.376	3.29	.014
55	41.1	.0134	.0140	.346	3.22	.014
60	43.6	.0123	.0119	.318	3.15	.015
65	46.0	.0102	.0112	.304	3.23	.014
70	48.4	.00813	.0105	.327	3.22	.014

Table 4.6

Suction Pressure Power

Turbopump Configuration	C_b	Average Test Parameters			
		k	$\partial C_b/\partial k$	P_v/q	n
LR87 Fuel	.019	.08	−.54	.004	2.37
LR87 Ox	.014	.07	−.37	.018	2.33
LR91 Ox	.027	.10	−.90	.035	4.44
F-1 Fuel	.088	.06	−.94	.000	.64
F-1 Ox	.095	.07	−.95	.013	.83
J-2 Fuel	.019	.036	−.40	.041	1.62
J-2 Ox	.011	.044	−.30	.035	2.10
H-1 Fuel	.012	.26	−.023	.000	.49
H-1 Ox	.014	.13	−.075	.039	.92
MB-3 Fuel	.0023	.21	−.011	.000	1.01
MB-3 Ox	.027	.048	−.60	.02	1.50

$$W = \rho Ax$$
$$mg_c = \rho A \ell \qquad \Bigg\} \quad (1)$$
$$F = PA$$

spring-mass system

fluid system

$$(m S^2 + dS + k) x = F \qquad (2)$$

$$(IS^2 + RS + \frac{1}{C}) W = P \qquad (3)$$
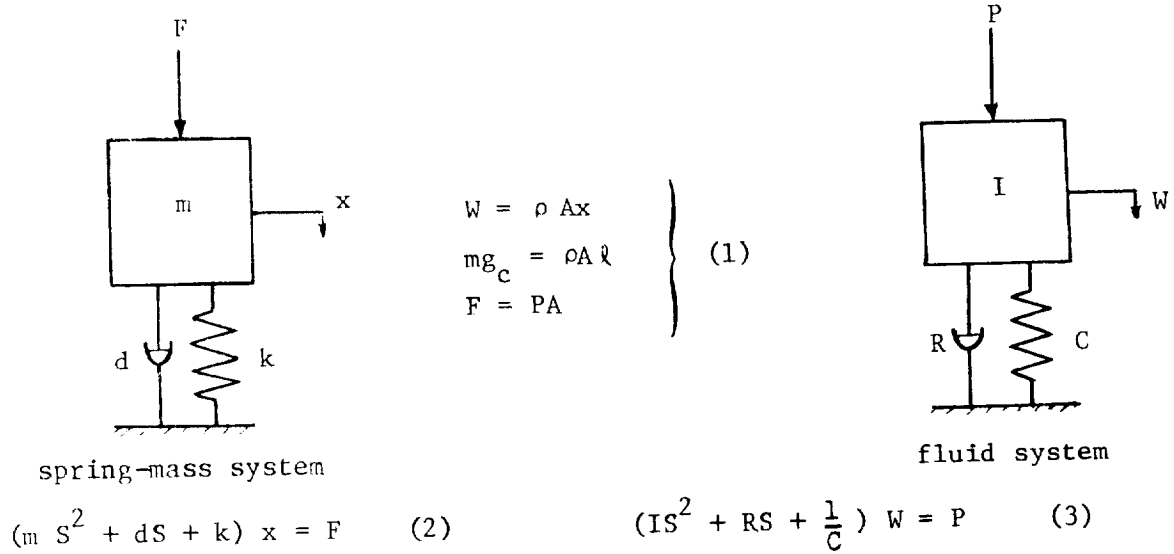
Substitute (1) into (2) or (3) gives:

Inertance, $I = m/\rho A^2 = \ell/Ag_c$

Resistance, $R = d/\rho A^2$

Compliance, $C = \rho A^2/k$

where   A = line area,
        ℓ = line length,
        g_c = gravitational constant,
        ρ = fluid density.

Figure 4.1   Comparison of Spring-Mass and Fluid Systems
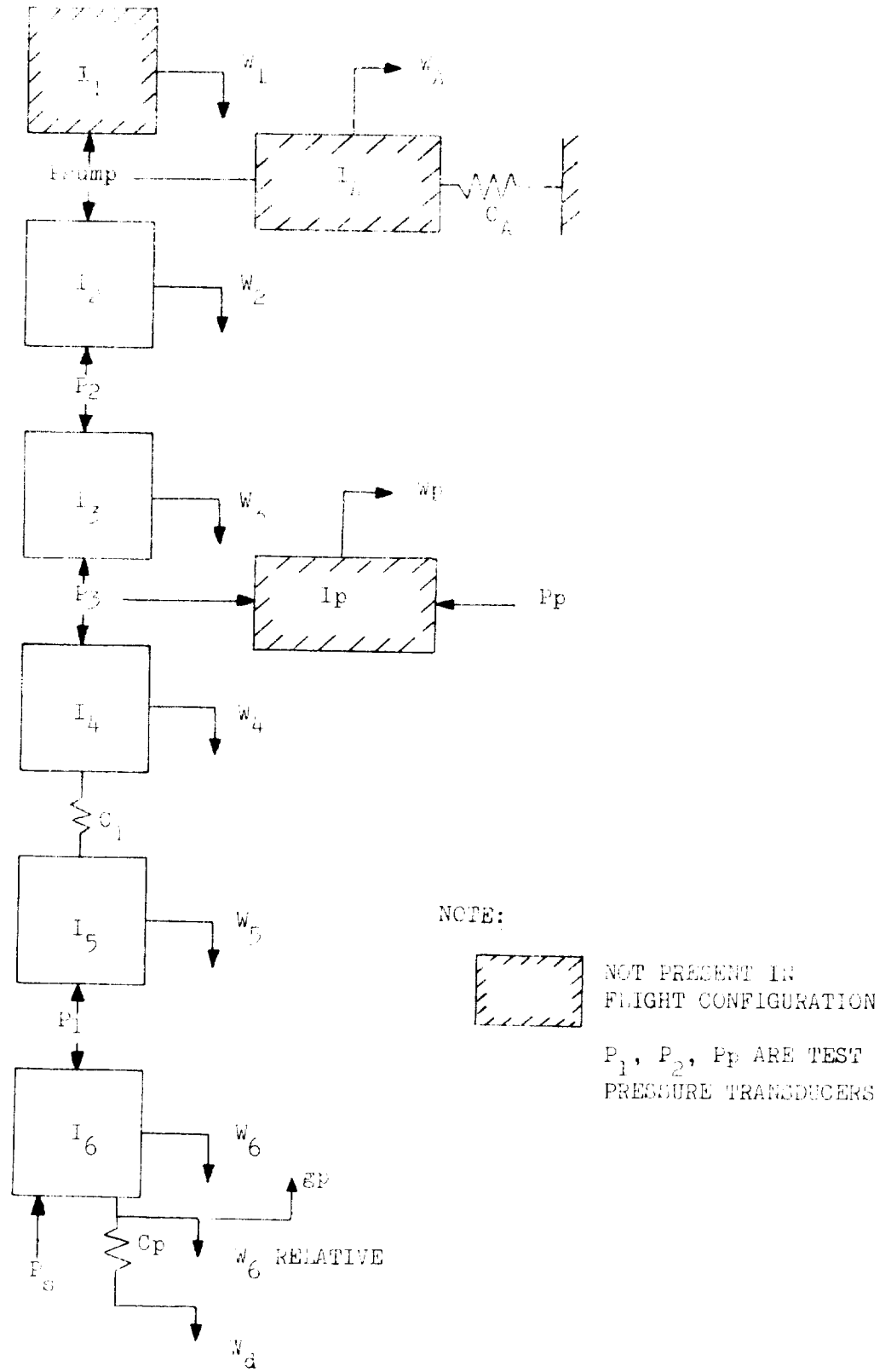
Figure 4.2   Analytical Model of S-II LOX Test Suction Systems
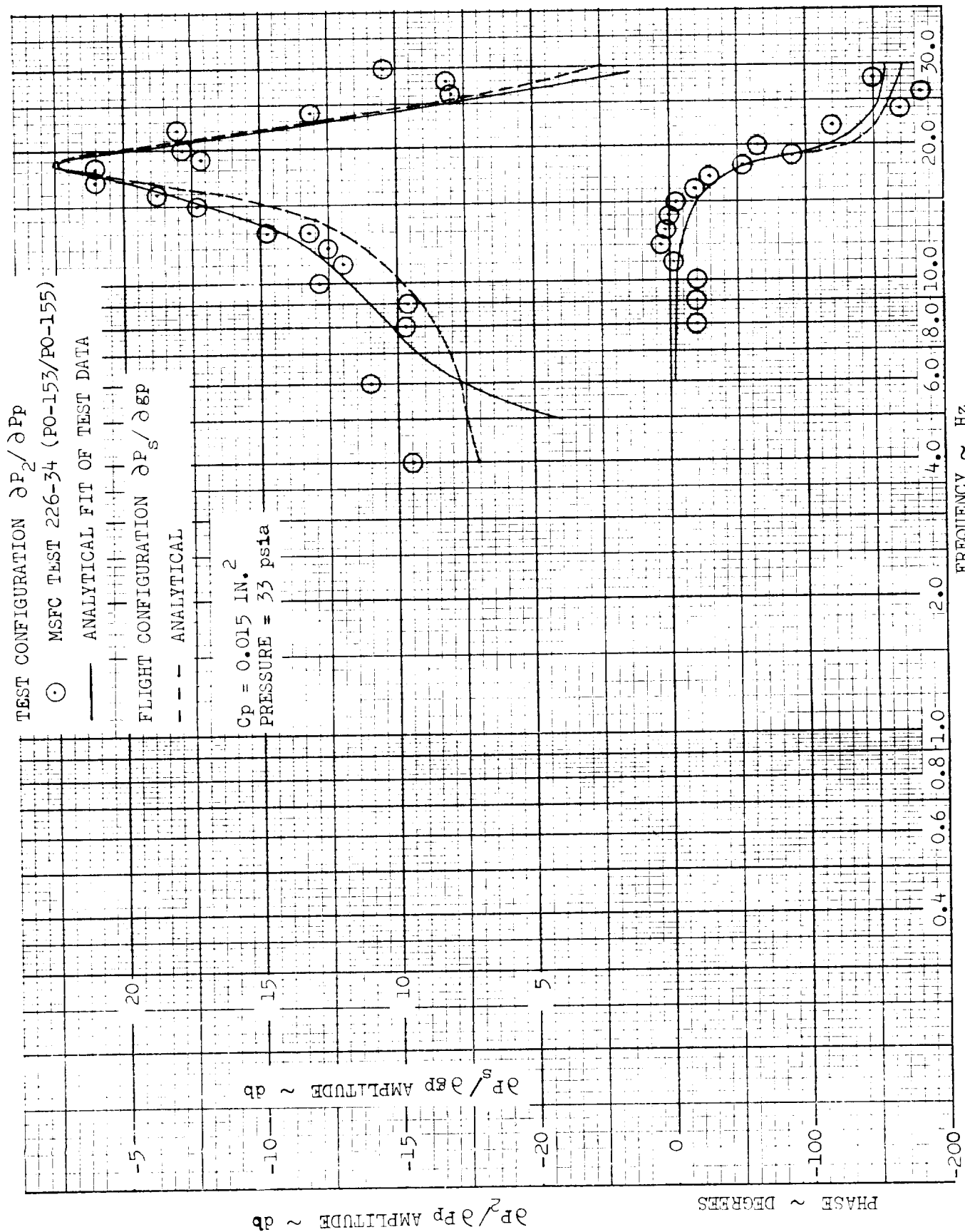
Figure 4.3 S-II LOX Suction Transfer Function
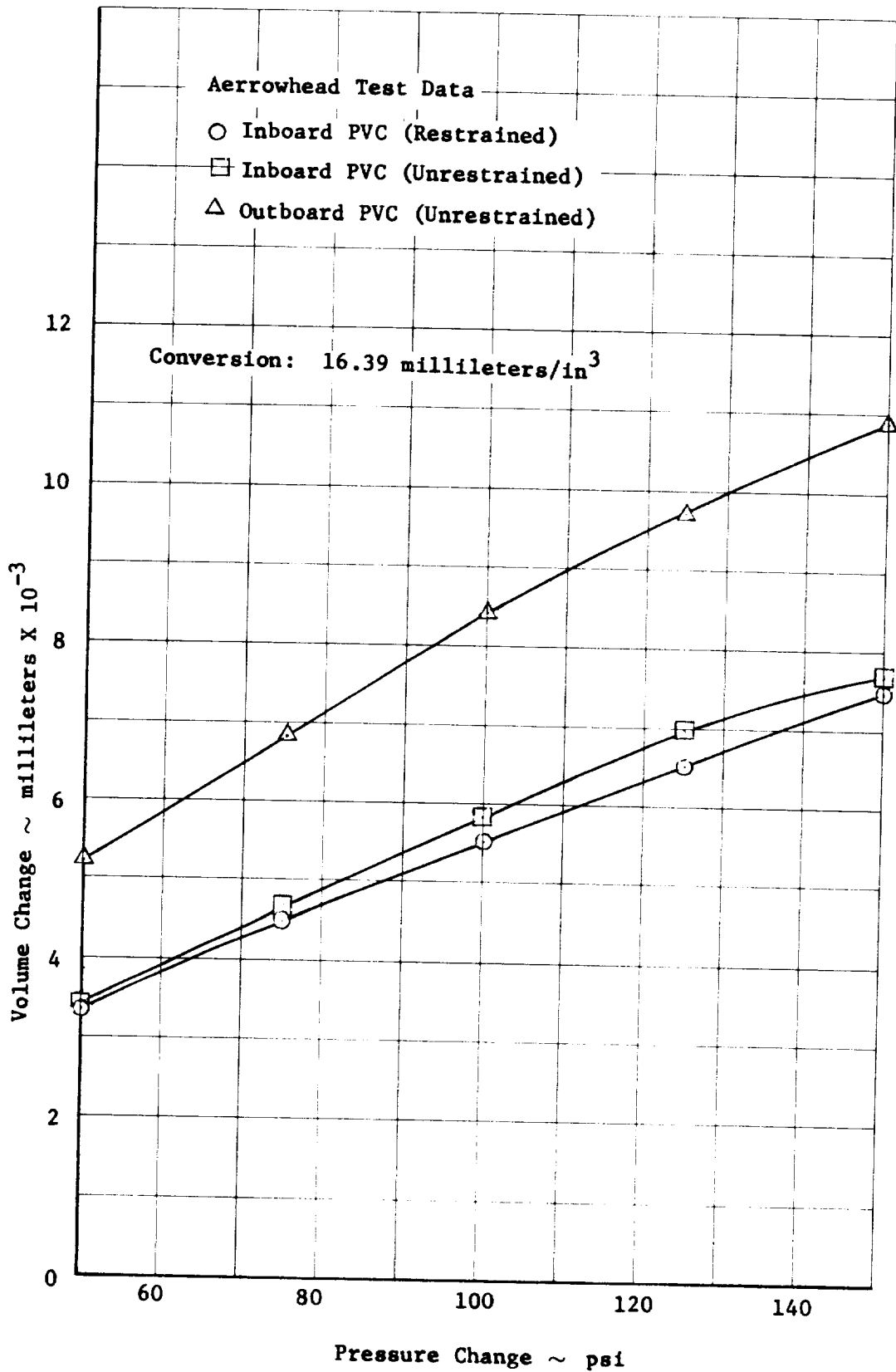
Figure 4.4   S-IC LOX PVC Volume Change With Pressure
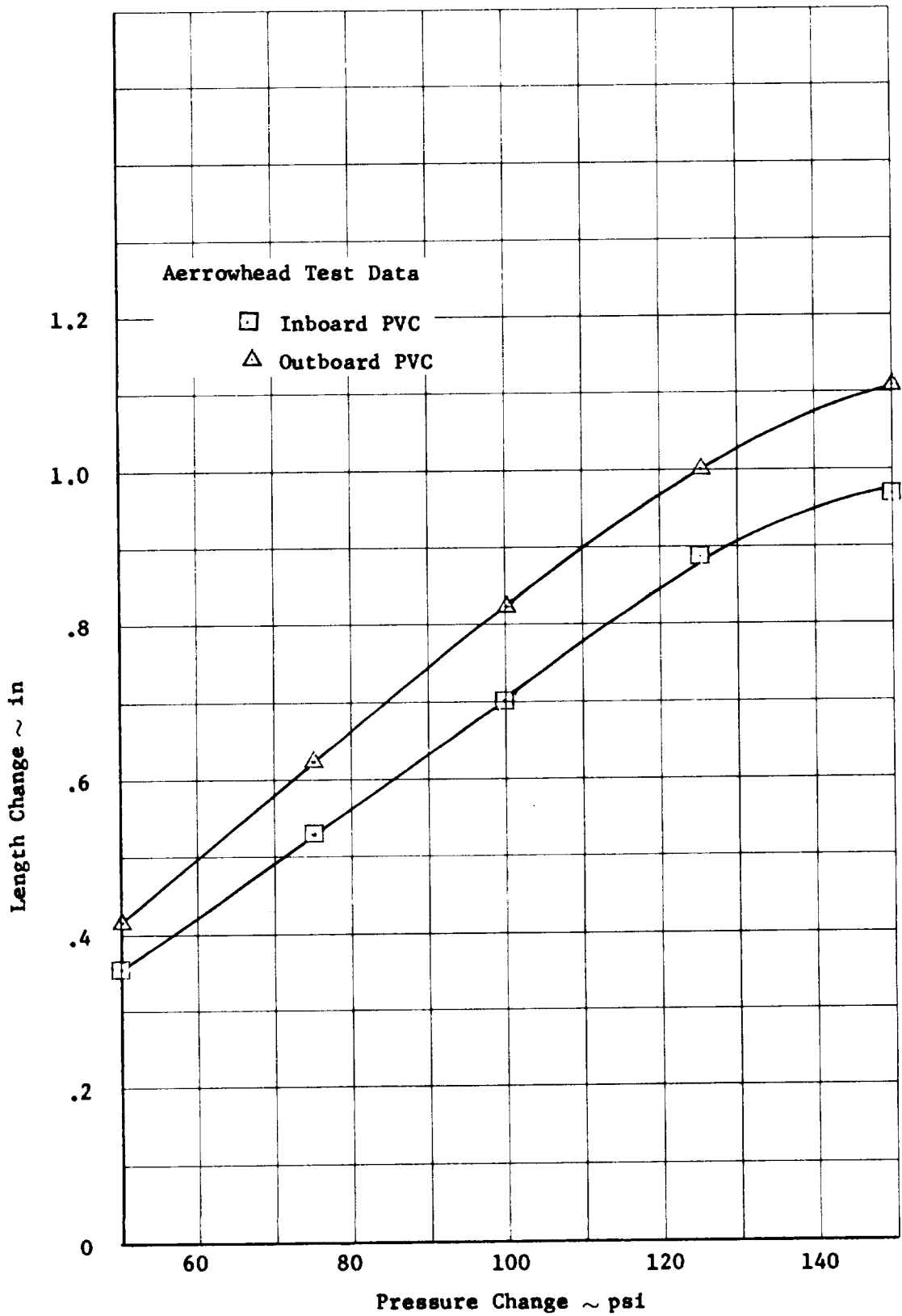
Figure 4.5   S-IC LOX PVC Length Change With Pressure
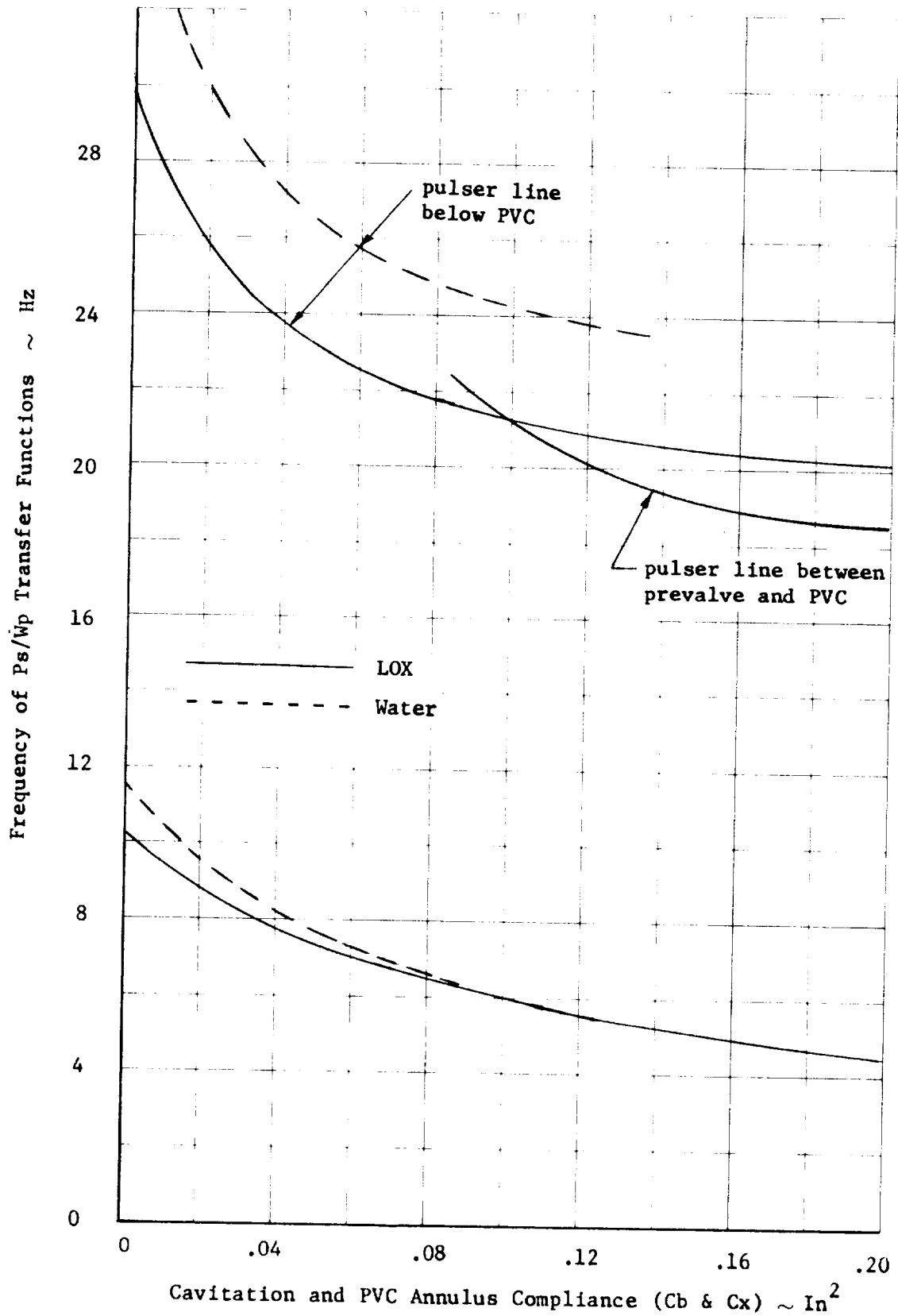
Figure 4.6   S-IC LOX Feed System Frequency Variation
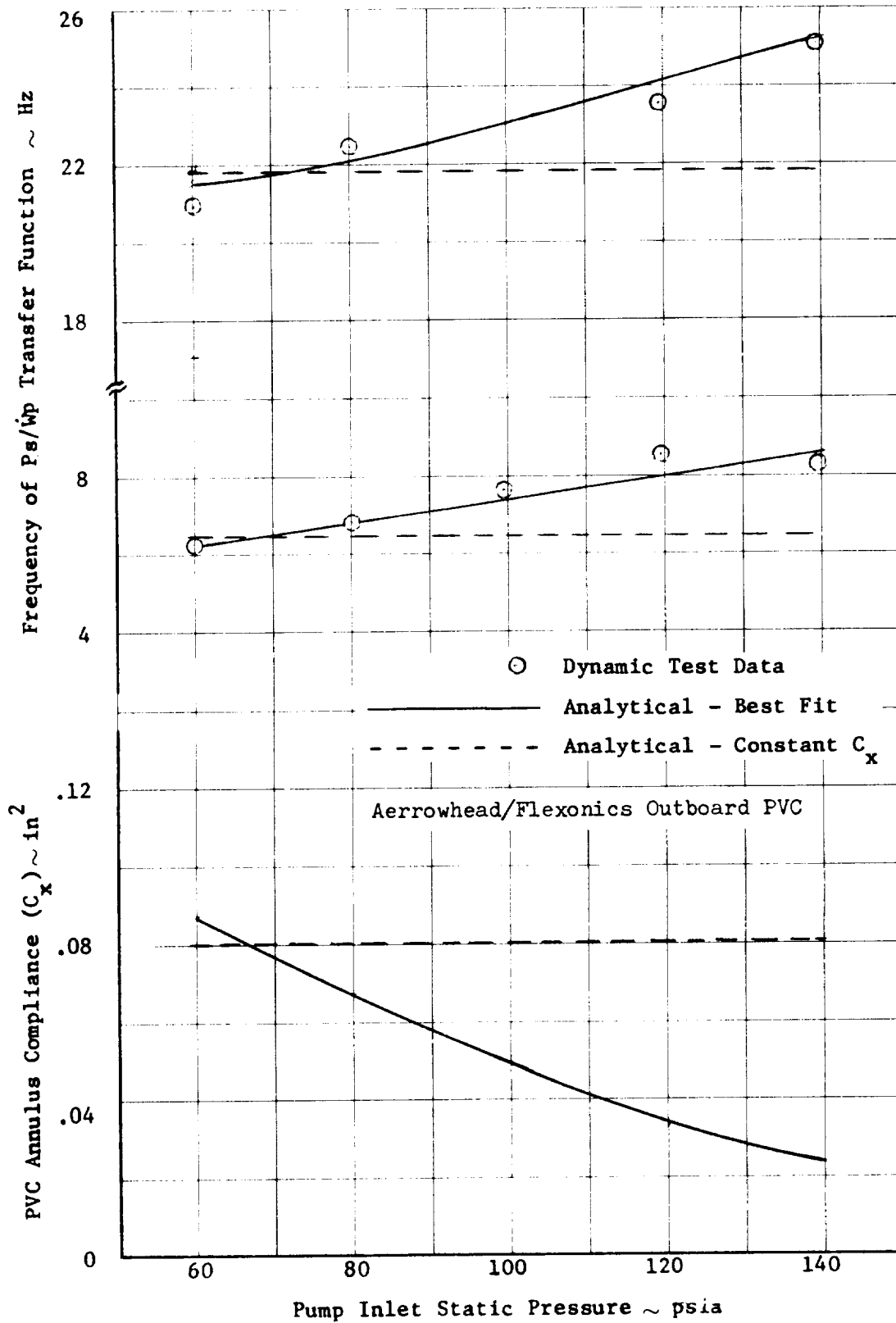
Figure 4.7 S-IC LOX Non-Flow Feed System Data
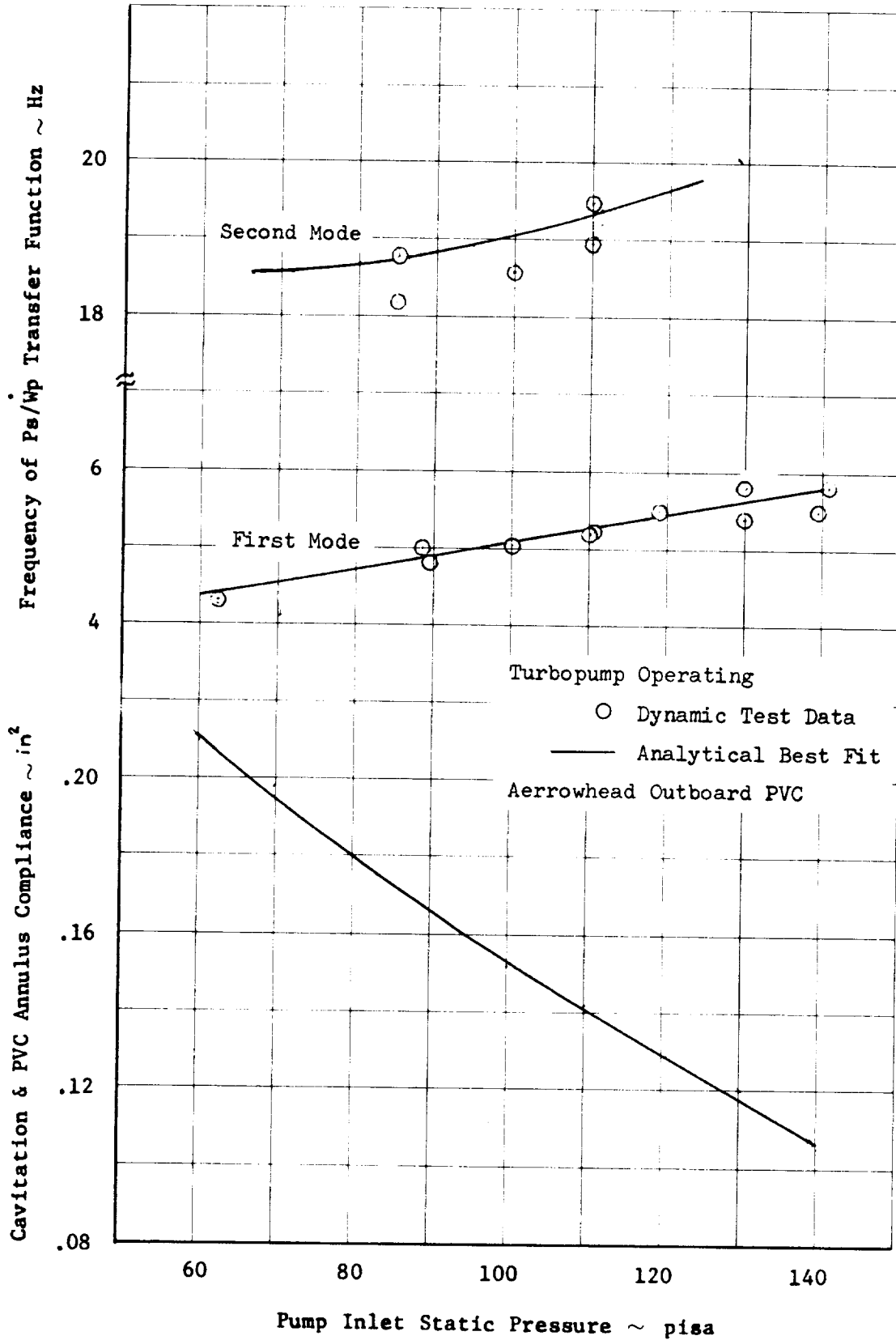
Figure 4.8   S-IC LOX Feed System Data
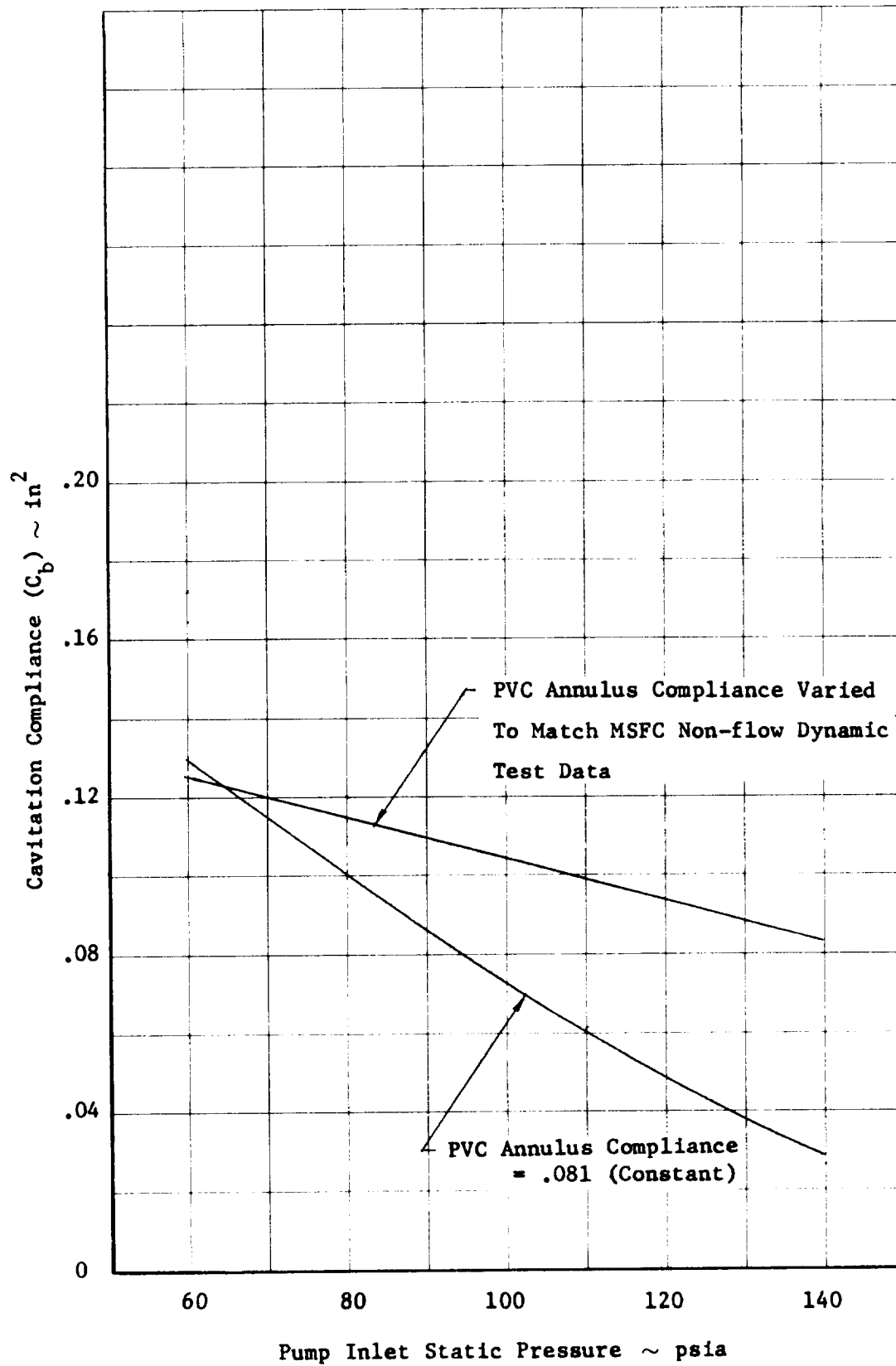
Figure 4.9   F-1 LOX Turbopump Cavitation Compliance
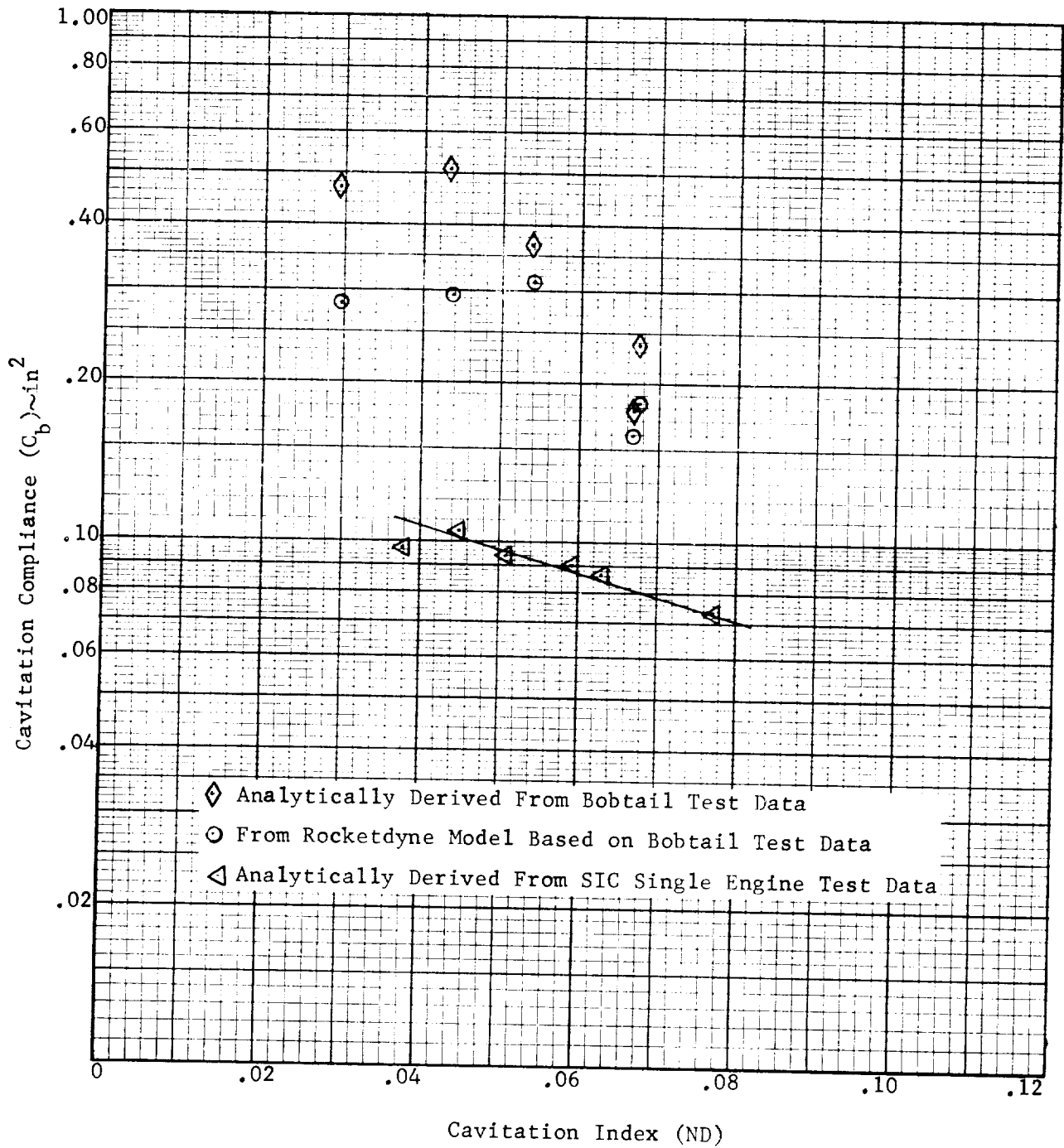
Figure 4.10   F-1 Fuel Turbopump Cavitation Compliance
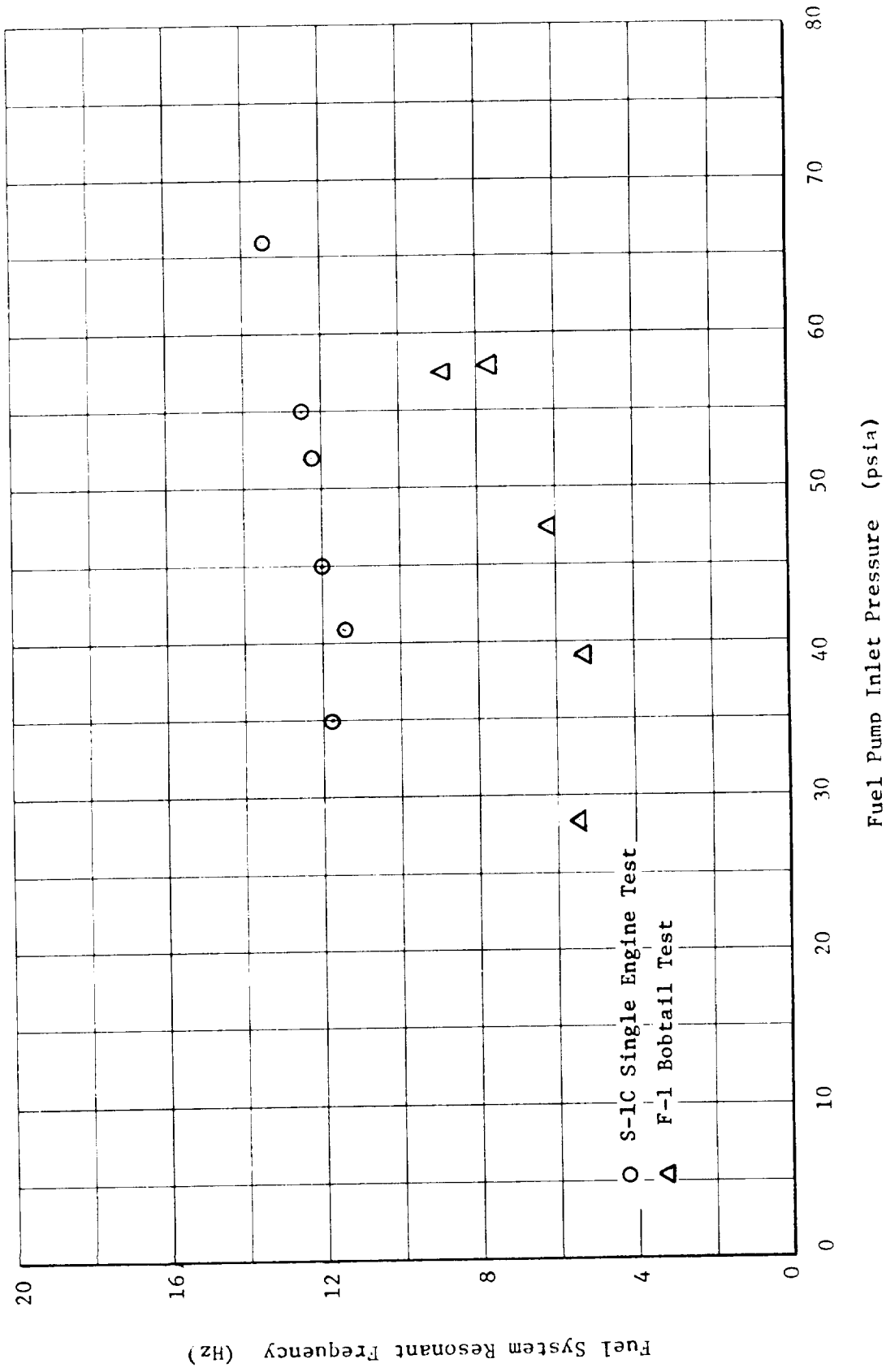
Figure 4.11 F-1 Fuel Feed System Frequency Data
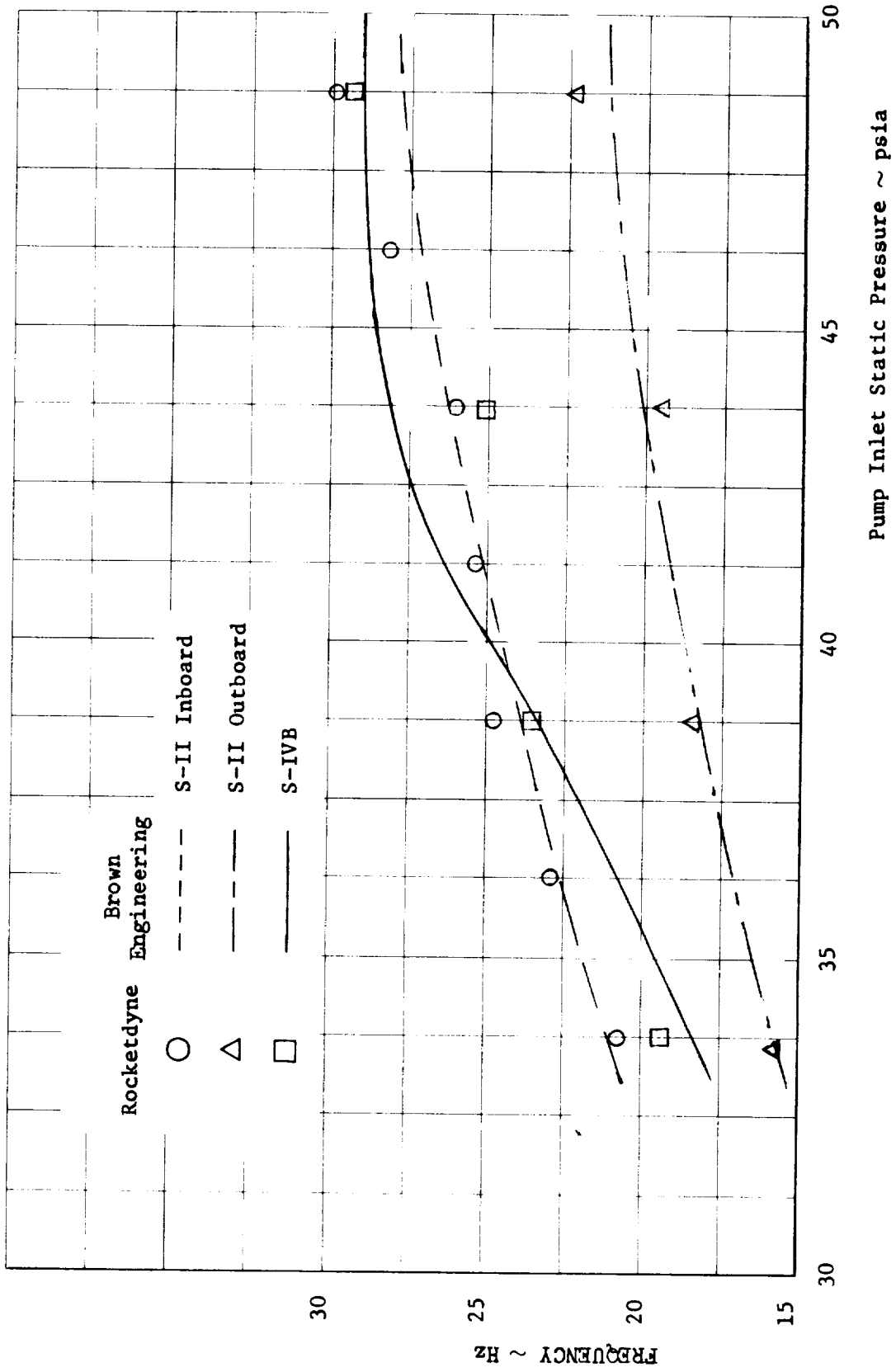
Figure 4.12 J-2 LOX Feed System Resonance
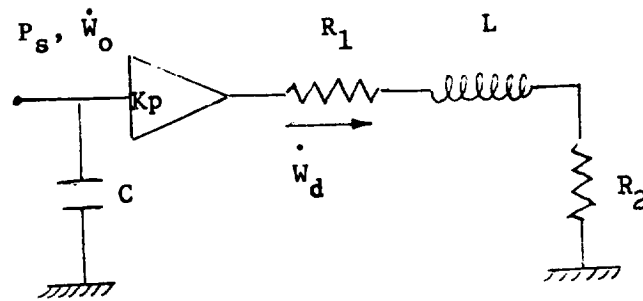
a. Single Compliance Model
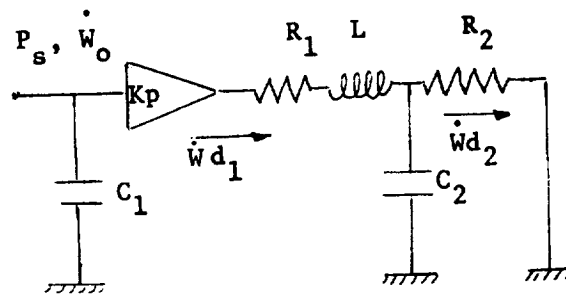
b. Double Compliance Model

Figure 4.13   J-2 LOX Analytical Turbopump Models
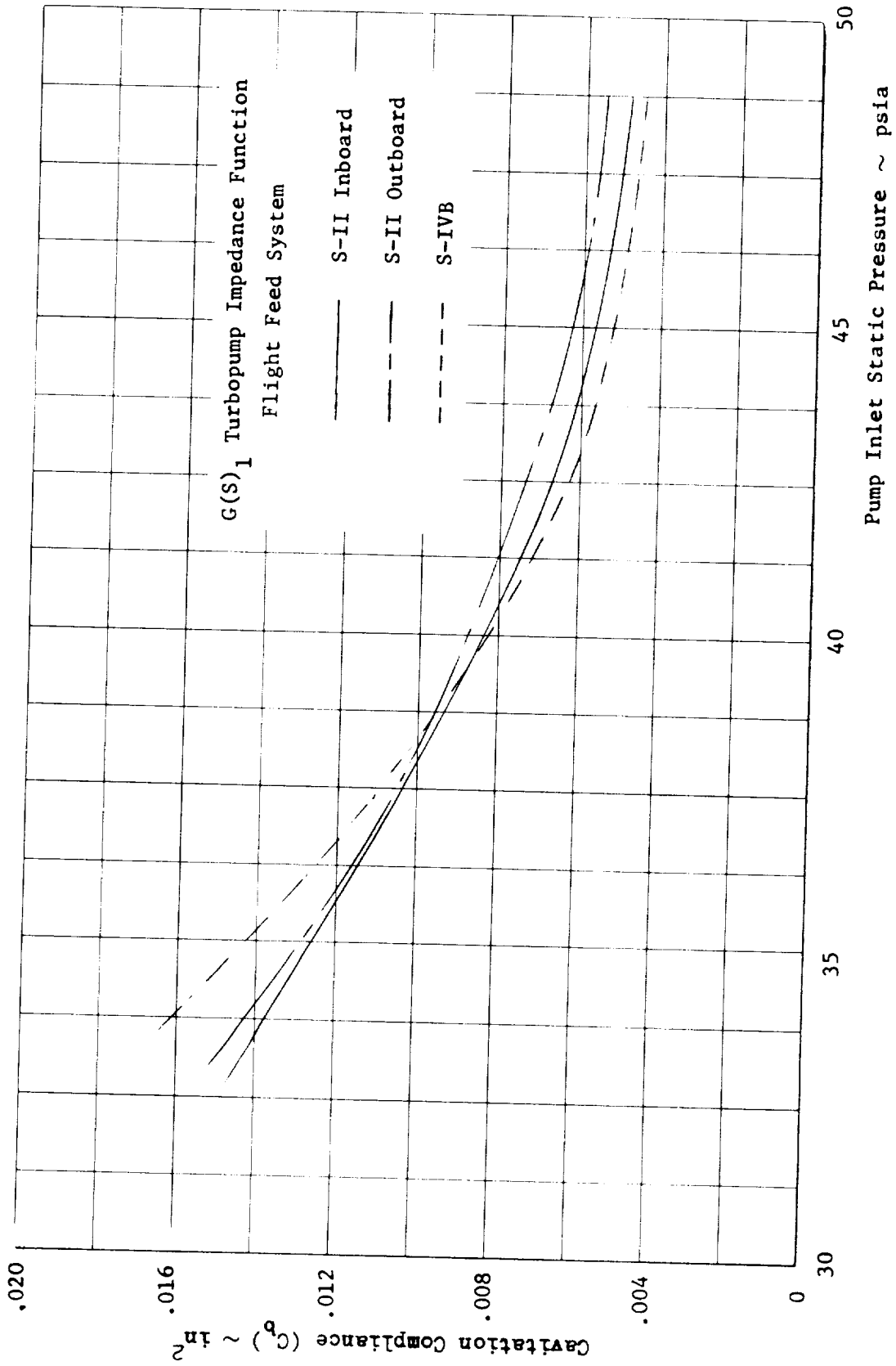
Figure 4.14   J-2 LOX Cavitation Compliance Derived by Brown Engineering
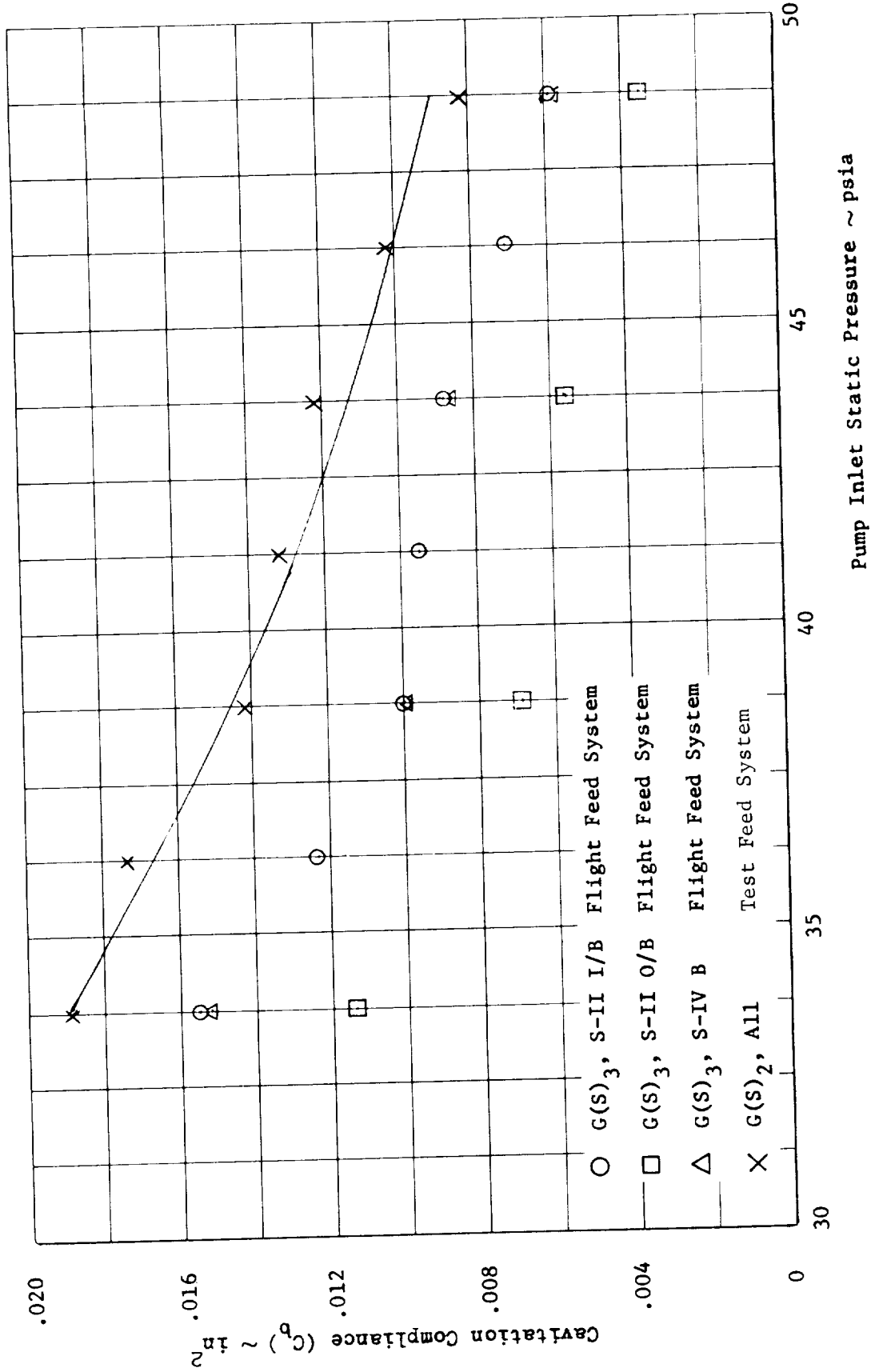
Figure 4.15   Effect of J-2 LOX Turbopump Model on Cavitation Compliance
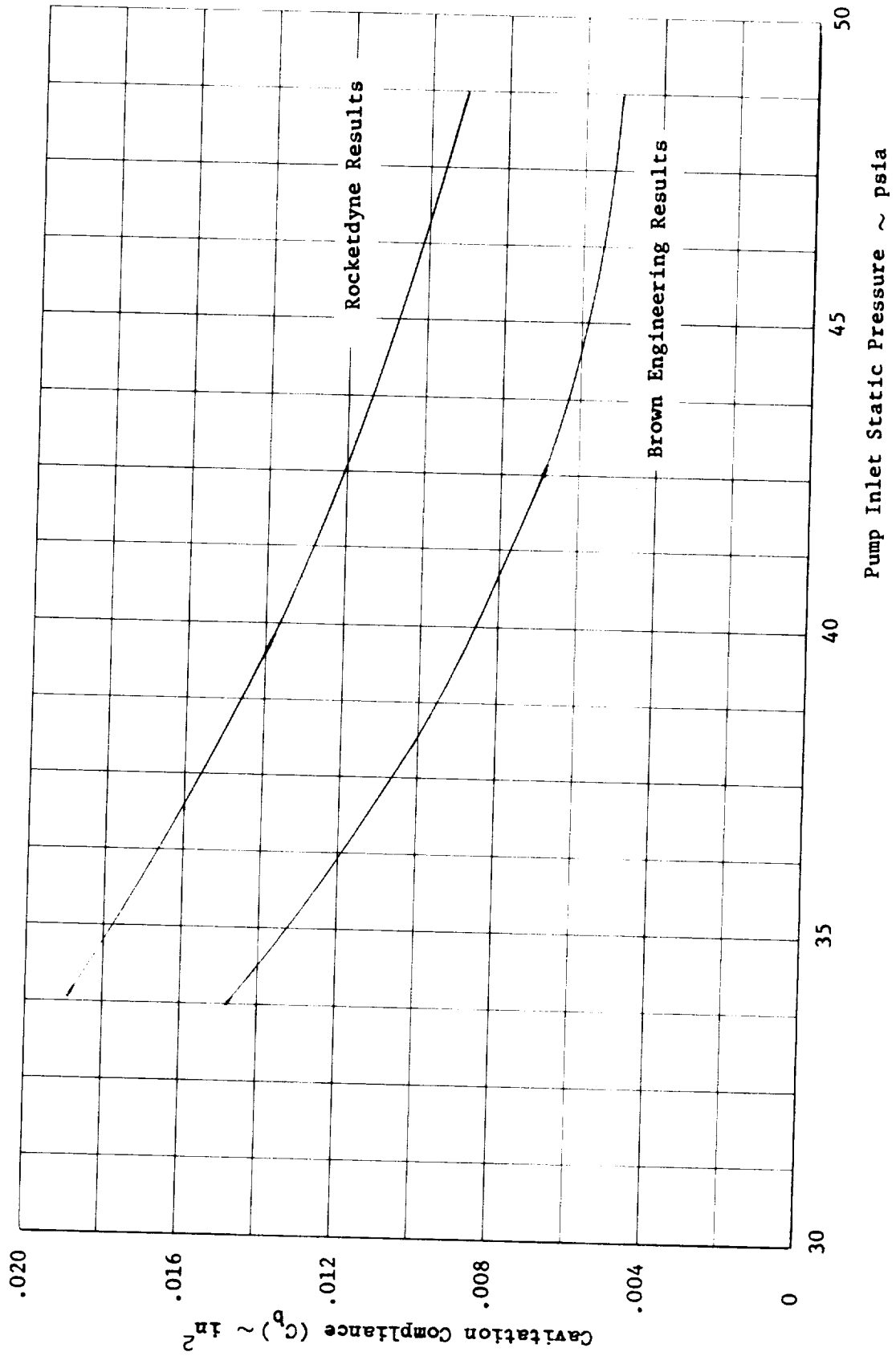
Figure 4.16 J-2 LOX Cavitation Compliance
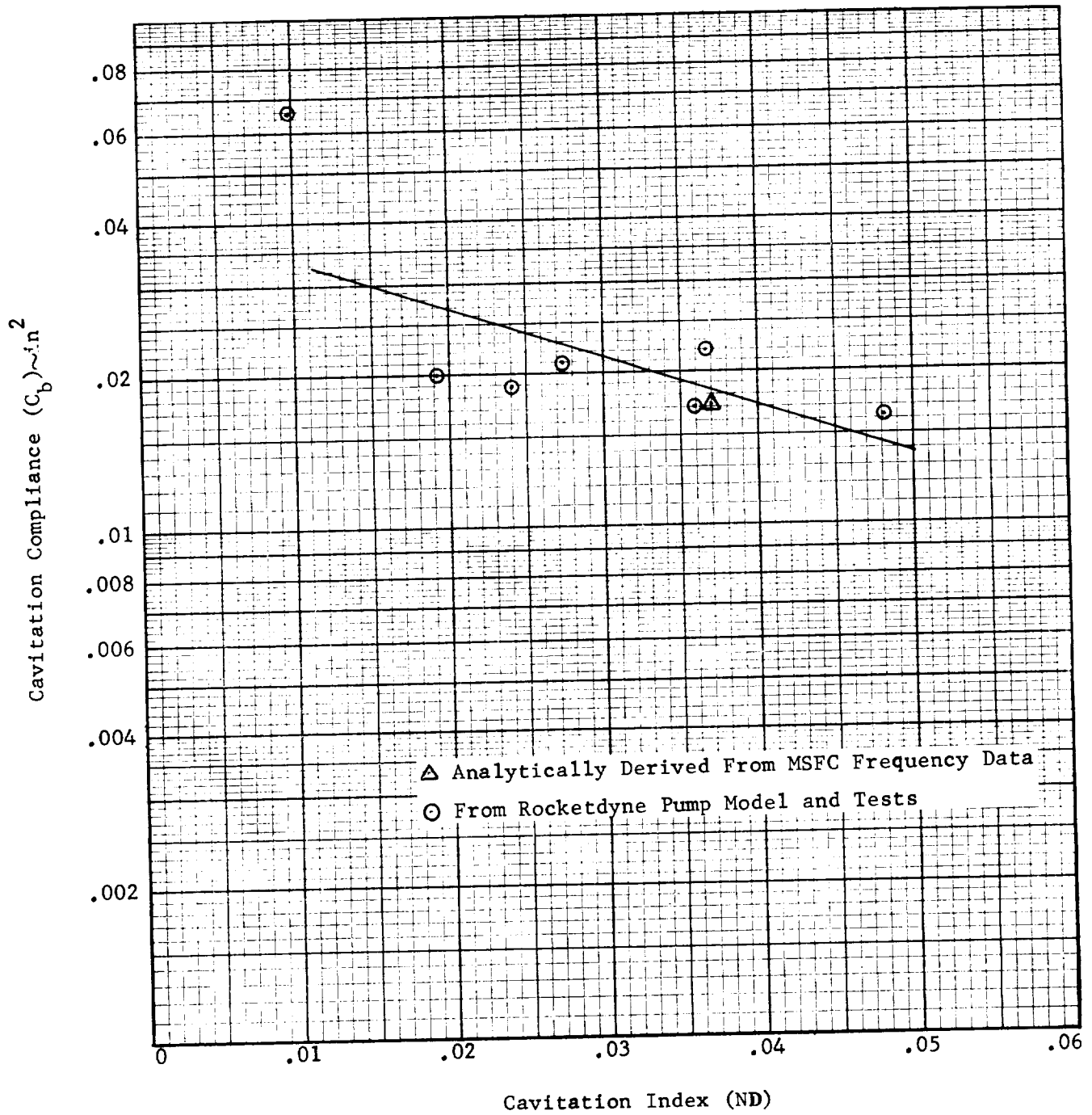
Figure 4.17   J-2 Fuel Turbopump Cavitation Compliance

84
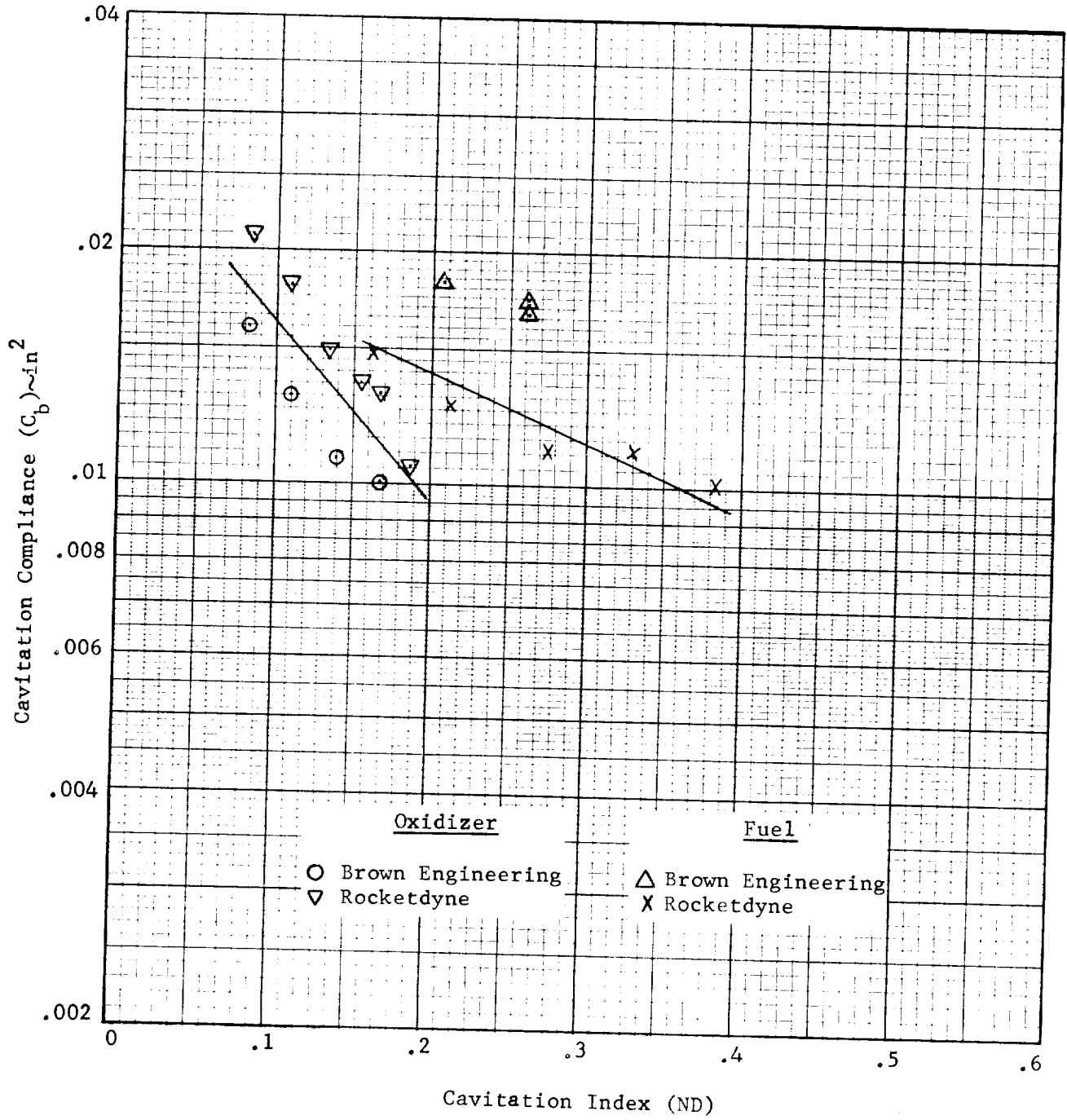
Figure 4.18   H-1 Oxidizer and Fuel Turbopump Cavitation Compliance
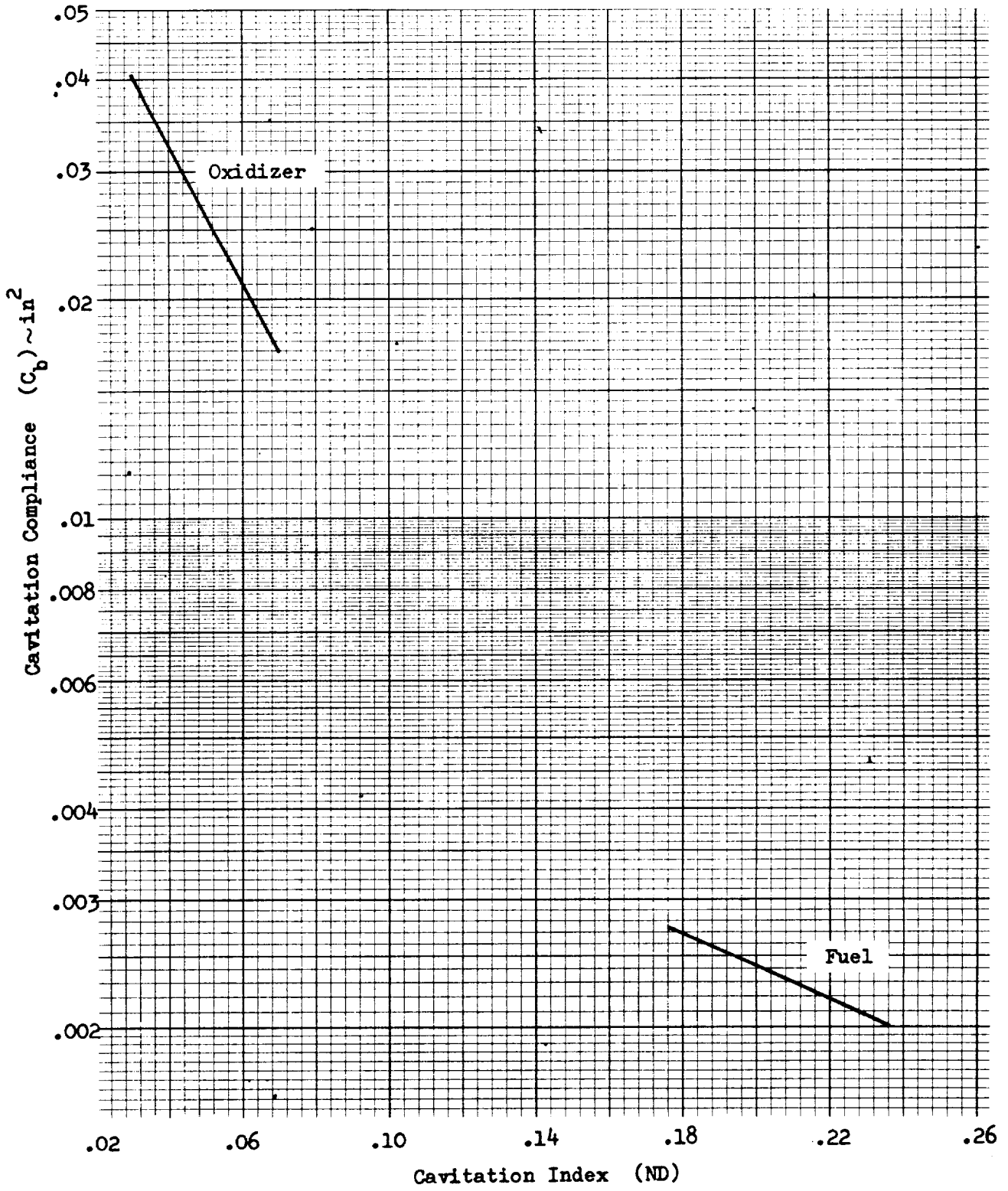
Figure 4.19   MB-3 Cavitation Compliance
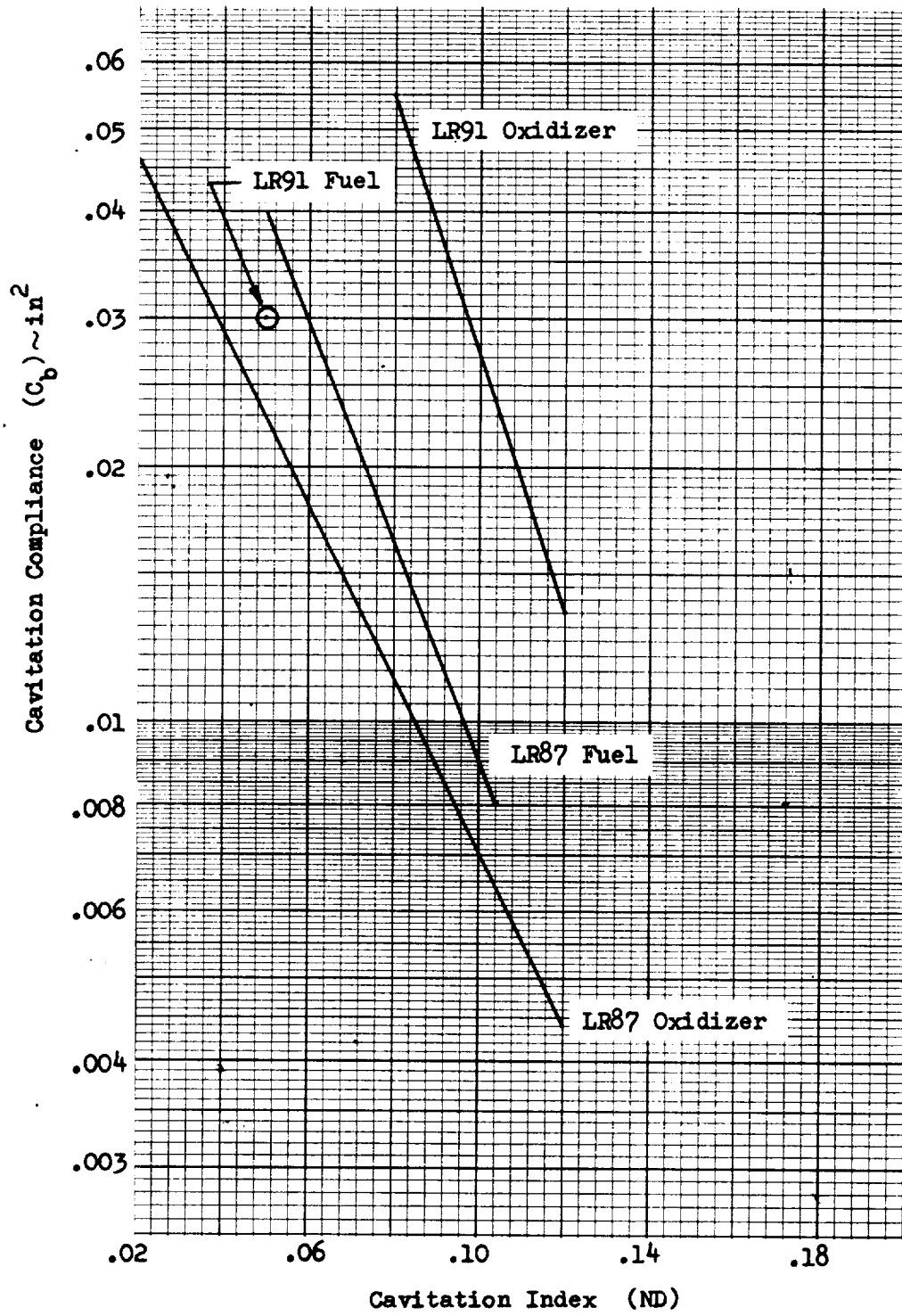
Figure 4.20   Titan Turbopump Cavitation Compliance
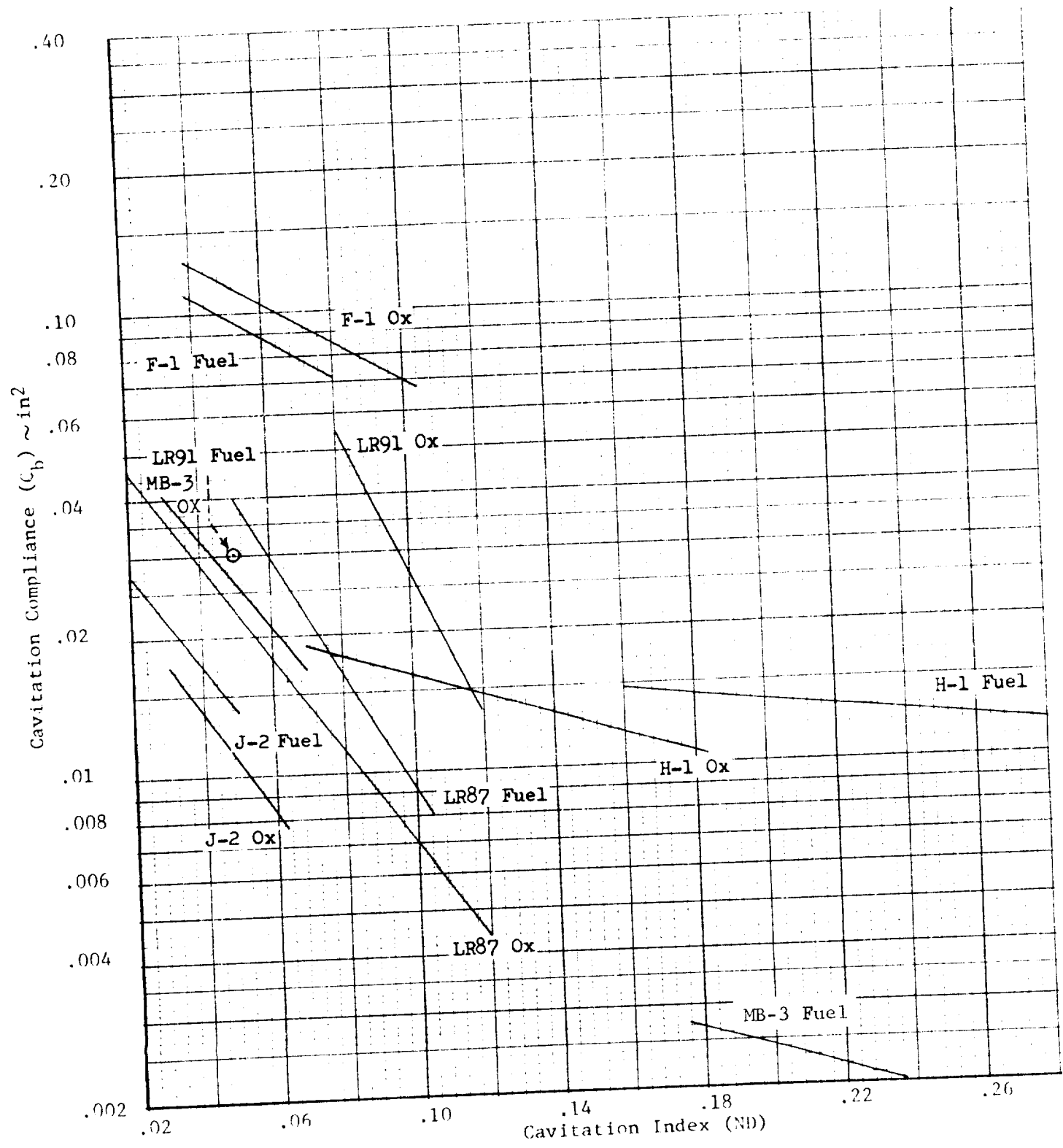
Figure 4.21   Oxidizer and Fuel Turbopump Cavitation Compliance

88
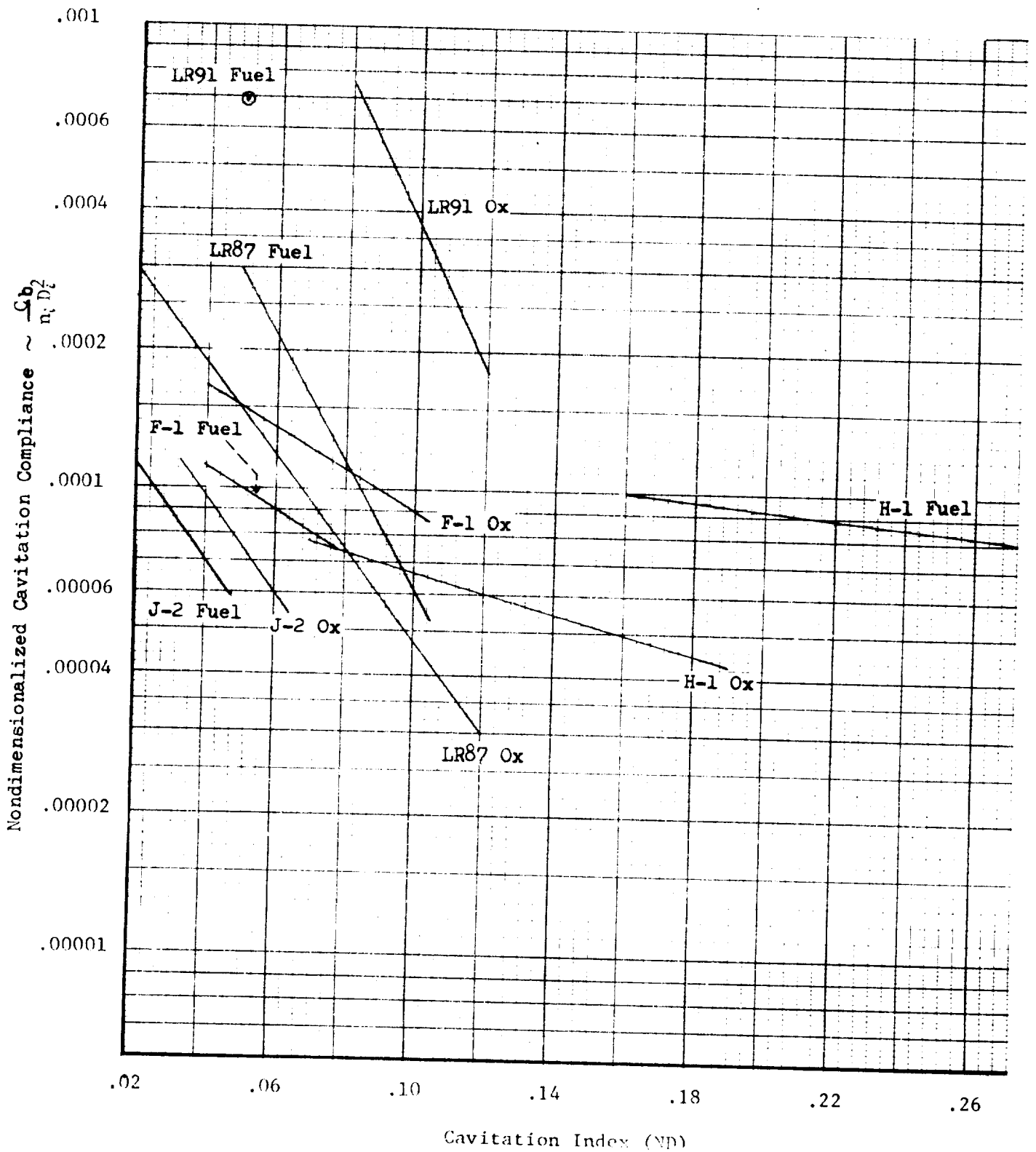
Figure 4.22   Nondimensionalized Turbopump Cavitation Compliance

$$SS = 8136 \left[1- \frac{D_h^2}{D_i^2} \right]^{1/2} \phi^{1/2} / [K]^{3/4}$$
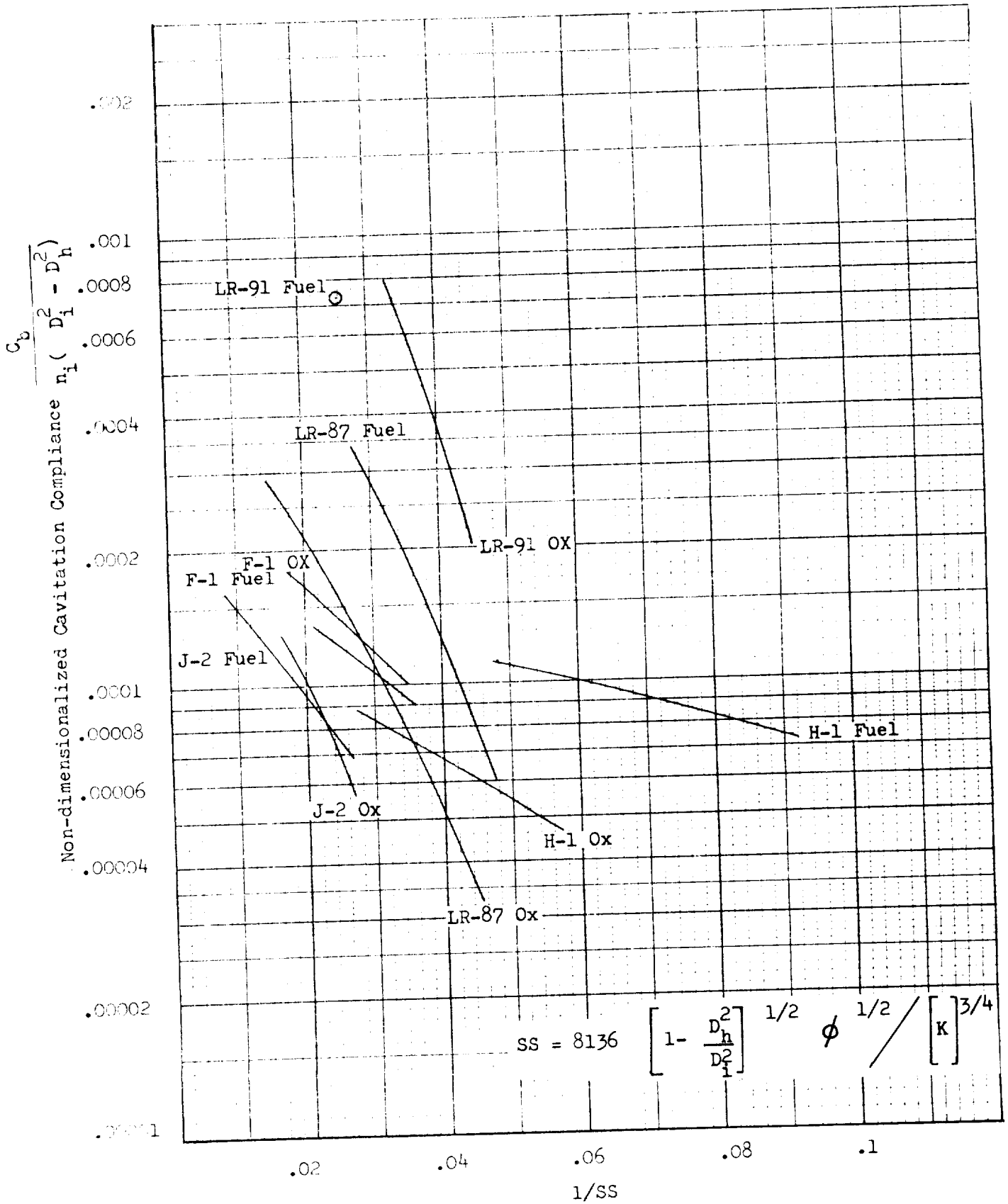
Figure 4.23   Nondimensionalized Turbopump Cavitation Compliance

(This page intentionally left blank)

5. Empirical-Analytical Correlation

5. EMPIRICAL - ANALYTICAL CORRELATION

5.1 Analytical Results - The turbopump cavitation model
described in Section 3. was used to analyze the J-2 LOX, F-1
LOX, H-1 LOX, and LR87 oxidizer turbopumps. These four con-
figurations were selected because they are typical of those of
interest in the determination of cavitation compliance for POGO
analysis. Also, considerable test data exists for these con-
figurations and their geometry and operation are in reasonable
agreement with the assumptions of the analytical model. Be-
cause of the large pressure rise which occurs through the in-
ducers (for example, 100 psi through the J-2 inducer and 300
psi through the F-1 inducer) it is assumed that any mismatch
between the inducer exit flow and the impeller blades is not
sufficient to produce a significant amount of cavitation in
the impeller. For this reason only the inducers were analyzed.

5.1.1 Blade Section Analysis - The complete analysis of
an inducer requires that the computer model be run for different
streamsheets corresponding to different blade cross sections at
different inducer radii. These results are then interpolated
and integrated to yield the total cavitation compliance for all
the inducer blades from the hub to the tip. Initial analyses
performed for the J-2 and F-1 inducers employed the blade
sectional data as tabulated on the inducer design drawings
(Figures 5.1 and 5.2, respectively). This data defines the blade
geometry for a constant distance off the inducer hub, and is
normally only given for a few blade sections. The turbopump
cavitation compliance program was thus restricted by both the
limited amount of input data and the fact that the data supplied
for a given blade section was associated with a constant distance
off the inducer hub, and not a fixed percent of the distance
between the hub and the feedline wall. The results of these

analyses indicated significantly different behavior of the cavitation phenomenon between the hub and blade tip, and did not agree favorably with test data. Recent analyses performed for all four inducers have utilized a different form of input blade geometrical data. A computer program was written to interpolate the supplied data and calculate blade geometrical data for five blade sections located at 10%, 30%, 50%, 70%, and 90% of the blade span. Details of this computer program are given in Appendix F. This simulation improvement resulted in an order of magnitude reduction in predicted cavitation.

5.1.1.1 Figures 5.5 through 5.8 show the blade sectional data derived from the inducer design drawings (Figures 5.1 through 5.4) for the J-2 LOX, F-1 LOX, H-1 LOX, and LR87 oxidizer turbopumps. It is noted that this data has been normalized to the trailing edge. Figures 5.9 through 5.12 show the results of interpolating this data to five blade sections, each at a constant percent of blade span. As shown by these figures, $\Delta Z/\Delta\theta$ is constant and independent of r for the J-2, F-1, and H-1 inducers. These inducers are a constant pitch helical screw design and are symmetrical about the chord. In contrast, the LR87 inducer is a twisted flat plate cambered in the vicinity of the leading edge.

5.1.2 Calculation Procedure - Because most of the inducers analyzed exhibit a linear relationship between blade coordinates Z and θ, the most suitable transformation from the inducer coordinates (r, θ, Z) to the streamsheet coordinates (E, Z) is simply

$$E = Z \qquad\qquad (5.1)$$

$$F = \theta \qquad\qquad (5.2)$$

This transformation is used in lieu of the logarithmic spiral transformation, Equations (3.10), which is more suitable for the impeller portions of a turbopump. For channel flow the streamsheet width varies as a function of Z and is defined by

$$b(Z) = b(Z_o)(r_t(Z) - r_h(Z))/C \qquad (5.3)$$

where: r_t = the blade tip radius

r_h = the hub radius

$b(Z_o)$ = selected streamsheet width at Z_o

$C = (r_t(Z_o) - r_h(Z_o))$

The feedline axial velocity, U, can have any radial distribution provided that continuity is satisfied, i.e.,

$$\dot{W} = 2 \pi \rho_\ell \int_{r_h}^{r_t} U \, r \, dr \qquad (5.4)$$

where ρ_ℓ is the inlet fluid density. For a uniform inlet fluid velocity distribution the flow in a streamsheet annulus is given by

$$\dot{W}_{ss} = 2 \pi \, r(Z_o) \, b(Z_o) \, \rho_\ell \, U \qquad (5.5)$$

For this analysis, a constant value of $b(Z_o)$ was used for all streamsheets in each inducer, causing $\dot{W}_{ss}$ to vary as a function of radius. Other local angles such as the blade angle, β, the inlet flow angle, $\emptyset$, and the angle of attack relative to the upstream undistrubed flow, α, are defined by

$$\beta = \tan^{-1} \left(\frac{1}{r} \frac{\Delta Z}{\Delta \Theta} \right) \tag{5.6}$$

$$\phi = \tan^{-1} \left(\frac{1}{r} \frac{U}{\omega} \right) \tag{5.7}$$

$$\alpha = \beta - \phi \tag{5.8}$$

In the (E, F) coordinate system the blade angle is $\Delta Z/\Delta \Theta$ and the flow angle is U/ω , both of which tend to be independent of the radius or of which streamsheet is under consideration. All of these parameters are given in Table 5.1. Each pump inducer was analyzed for two inlet flow angles, U/ω, and a range of inlet pressures, P_s, for the streamsheets described above. Each calculation produced a description of the flow field in the particular streamsheet in terms of the streamfunction, ψ, pressure field, P, and the weight of propellant in the streamsheet, W_{ss}. Figure 5.13 shows a computer output plot of the streamlines in a J-2 LOX inducer streamsheet which corresponds to a 30% blade section. For the purpose of calculating cavitation compliance the prime model output is W_{ss}, which is computed by

$$W_{ss} = \sum_i \rho_i \; A_i \; b_i \tag{5.9}$$

where ρ_i = density of the two phase fluid at grid point i

A_i = area between grid points

b_i = streamsheet width at grid point i

From Equation (1.2) the cavitation compliance in a streamsheet

between two blades is given by

$$C_{ss} = \frac{\Delta W_{ss}}{\Delta P_s} \qquad (5.10)$$

An example of C_{ss} derived from computer output is shown in Table 5.2. The total turbopump cavitation compliance for N blades is given by

$$C_b = N \int_{r_h}^{r_t} \frac{\partial C_{ss}}{\partial r} \, dr \qquad (5.11)$$

where

$$\frac{\partial C_{ss}}{\partial r} = \frac{C_{ss}}{b} \qquad (5.12)$$

Since most of the cavitation occurs near the inlet; $b = b(Z_o)$ which was chosen to be the same at each radius section. Equation (5.11) thus becomes

$$C_b = \frac{N}{b(Z_o)} \int_{r_h}^{r_t} C_{ss} \, dr \qquad (5.13)$$

5.1.3 **J-2 Results** - Analytical values of W_{ss} were obtained from the computer model for inlet pressures from 32 to 50 psia, values of U/ω (inlet flow direction) of .33 and .20, and five blade sections. The resulting streamsheet compliance is shown in Figure 5.14 for five inlet pressures and the nominal flow direction of U/ω = .33. These results are relatively well be-

haved and exhibit the expected trend with variations in inlet pressure. Also, the variation along the blade appears to be reasonable in view of the following factors:

a. For constant streamsheet inlet thickness the tip streamsheet has a larger fluid flow (Equation 5.5);

b. The blades are thinner at the tip which results in a sharper leading edge;

c. The blades are thinner at the tip which also results in less venturi effect between the blades;

d. The angle of attack at the tip is lower than at the hub (Equations 5.6, 5.7, and 5.8).

The first two factors would tend to produce higher streamsheet compliance at the tip than at the hub while the last two factors have the opposite effect. The graphical integration of these results (Figure 5.14), along with similar results for an inlet flow direction of U/ω = .20, according to Equation (5.13) give the following values of cavitation compliance.

U/ω (in/rad)	.33	.20	Inlet Press (psia)
Cavitation Compliance $\sim$ in^2	.0044	.0063	33.
	.0033	.0053	36.
	.0023	.0039	40.
	.0012	.0023	44.
	.0005	.0014	48.

5.1.3.1 The sensitivity to inlet flow direction requires consideration of the factors involved. The actual analytical inlet flow direction is determined from the slope of the computed streamlines upstream of the blades. The upstream boundary conditions are then automatically adjusted until the computed slope matches the desired slope calculated with respect to the

undisturbed flow. Computation of the potential flow solution at different distances into the suction line (Figure 5.18) showed that propogation of blade disturbances extend approximately one inch upstream. This was found to be true for all the inducers analyzed. The pressure field upstream of this point remains essentially constant ($\pm$1 psi). An additional error source, not included in the model, is fluid prerotation produced by fluid viscosity (Figure 5.19). As stated previously, all flow was assumed to be inviscid. An upper bound of viscous produced prerotation of 67% of the turbopump speed ($\omega_r = 2/3\omega$) was assumed for analytical evaluation. This yielded a new inlet flow direction of $U/(\omega+\omega_r)$, or 60% of the nominal U/ω computed without considering prerotation. This effect is not intended to be representative of actual prerotation values, but is only used to demonstrate the influence on cavitation results.

5.1.4 <u>F-1 Results</u> - Analytical values of streamsheet fluid weight, W_{ss}, were obtained from the computer model for inlet pressures from 60 to 140 psia, U/ω values of .86 and .52, and five blade sections. For the nominal value of inlet flow direction ($U/\omega = .86$), computed without consideration for viscous induced prerotation, the model predicted no cavitation at any of the blade sections for the range of inlet pressures considered. That is, the minimum pressure predicted by the potential flow solution was always greater than the LOX vapor pressure. Reducing the flow direction to 60% of nominal to account for neglected prerotation resulted in small amounts of blade cavitation for inlet pressures below 100 psia. As shown in Figure 5.15 cavitation was observed at the 30%, 50%, and 70% blade sections. Reasons for variations at different blade sections are the same as discussed in Paragraph 5.1.3. Initial predictions, based only on the two blade sections

defined on the drawing (Figure 5.2), assumed that the amount
of cavitation increased toward the blade tip. These results
indicate that was a bad assumption. Local conditions can
produce cavitation at a mid section, while for the same inlet
conditions none occurs at either the hub or the blade tip.
Applying Equation (5.13) to the results in Figure 5.15, and to
the computed results for $U/\omega = .86$, gives the following values
of cavitation compliance.

U/ω (in/rad)	.86	.52	Inlet Press. (psia)
Cavitation $\sim in^2$ Compliance	0	.0020	65
	0	.0009	75
	0	.0005	85
	0	.0002	95
	0	0	105

5.1.5 **H-1 Results** - Analytical values of streamsheet
fluid weight, W_{ss}, were computed for inlet pressures from 40
to 90 psia, U/ω values of .42 and .25, and five blade sections.
The results showed that essentially no cavitation was predicted
for the nominal flow direction of $U/\omega = .42$, and very little
cavitation for the flow direction reduced to account for
possible viscous pre-rotation effects. Figure 5.16 shows the
minimum pressure obtained in the H-1 LOX inducer which occurs
at a grid point near the blade leading edge of the 30% section.
For non-cavitating conditions the pressure increment between
the inlet static pressure and the minimum pressure grid point
is essentially constant for fixed flow conditions. This is
reasonable since compressibility effects should be minimal if
there is no cavitation vapor present. Figure 5.16 shows that

cavitation starts at an inlet pressure of 46 psia for nominal U/ω and 59 psia for U/ω reduced to 60% of nominal. However, even for pressures below these values, so few grid points reach vapor pressure that no significant cavitation is produced. At blade sections other than the 30% sections no cavitation was predicted.

5.1.6 LR87 Oxidizer Results – The computer model generated values of streamsheet fluid weight, W_{ss}, for inlet pressures from 40 to 90 psia, U/ω values of .32 (nominal) and .19, and five blade sections. The results showed no measurable change in W_{ss} implying no blade cavitation. For the nominal inlet flow direction the potential flow solution predicts that the minimum pressure grid point is only 17 psi below the inlet pressure (Figure 5.17). This means that the inlet pressure would have to be reduced to 31 psia before the minimum pressure reaches the vapor pressure resulting in cavitation. This computed pressure reduction from the inlet to the minimum pressure point is considerably less for the LR87 than the other inducers.

These values, along with some of the influential parameters, are shown in Table 5.3 for comparison. Not all of the parameters are in the right direction (lower angle of attack, thinner blade, and lower dynamic pressure); however, the combination could justify the smaller pressure increment for the LR87. For the inlet flow direction reduced by 60% (U/ω = .19) to simulate a worst case viscous pre-rotation, the minimum pressure point is 36 psi lower than the inlet pressure (Figure 5.17). In this case cavitation just begins for an inlet pressure of 49 psia. For the lowest pressure case analyzed, 40 psia, no significant cavitation had developed.

5.2 <u>Comparison With Test Data</u> - The first task performed in the comparison of the analytical and test results was to compare the predicted inducer pressure rise with available test data. Figure 5.20 shows J-2 LOX inducer head rise test data (Reference 53) using water as the test fluid. This indicates a head rise of 172 ft (75 psi for water) for the nominal operating flow rate of 2540 gal/min (U/ω = .33 in/rad). Figure 5.21 shows the corresponding pressure profiles predicted by the computer model at the 50% blade section for an inlet pressure of 100 psia (230 ft NPSH). This shows a predicted pressure rise of greater than 60 psi, and it could easily be 75 psi depending on where the measurement is taken. The model predicts slightly greater pressure rises at a hub blade section (10%) and slightly less pressure rises at a tip blade section (90%). In the actual case, radial mixing will occur and tend to give a uniform pressure rise (in the radial direction) through the inducer. Thus the 50% blade section is felt to be most representative even though the pressure measurement is assumed to be taken on the pump housing nearest to a tip blade section. The J-2 LOX inducer head rise test data was the only pressure data available for comparison with analytical predictions. This single point comparison tends to confirm the overall accuracy of the potential flow equations used to compute pressures through the inducer blades. Analytical-empirical correlation of the cavitation compliance is obviously not as good as the pressure correlation since little or no cavitation was predicted in three out of the four inducers analyzed. On the other hand, test data (Figure 4.21) indicates that a significant amount of cavitation occurs in all turbopumps. Figures 5.22 and 5.23 present a comparison between test data and the cavitation compliance predicted by the analytical model for the J-2 and F-1 LOX inducers, respectively. Since no cavitation was predicted for either the H-1 or LR87 inducers, comparative plots are not presented. Plots of test data for these inducers were presented in Figures 4.18 and 4.20, respectively.

No model assumptions have been identified which could account
for the lack of correlation observed. Reasonable variations in
inlet flow direction to simulate viscous prerotation tended to
improve predictions but failed to yield adequate correlation.
Also, since no cavitation was predicted in some inducers, the
analytical results can not be simply scaled to agree with test
data. The entire results of this analysis indicate that some
other mechanism besides blade cavitation contributes significantly
to total turbopump compliance. Other mechanisms presented
(Section 2.) as having potential significance are: blade tip
clearance flow, circulation flow within the turbopump, and
circulation flow back into the feedline.

5.2.1 Since the effect of cavitation compliance on feed
system natural frequency is of prime interest, it is important
to determine how uncertainties in one propagate into uncertain-
ties in the other. The first feed system natural frequency,
ω_1, can be defined by

$$\omega_1 = \sqrt{\frac{1}{I\,(C_b + C_\ell)}}$$

(5.14)

where   I = suction line fluid inertance

C_b = cavitation compliance

C_ℓ = equivalent total suction line and fluid compliance
     (except pump cavitation) related to the pump inlet.

Differentiating Equation (5.14) yields

$$\frac{d\omega_1}{\omega_1} = -\frac{C_b}{2(C_\ell + C_b)}\frac{dC_b}{C_b}$$

(5.15)

which shows that the percentage change in ω_1 is at most 1/2
the percentage change in C_b, and may be much less if C_ℓ is
large relative to C_b. For the S-II/J-2 LOX feed system, C_ℓ
is .003 to .005 in.^{2} (Rocketdyne results, Table 4.4). Using

these values of C_ℓ and test values of C_b in Equation (5.15), it
may be concluded that for a maximum uncertainty of 10% in S-II
feed system natural frequency cavitation compliance must be known
to within 25%. A similar evaluation on the other systems of
concern results in the following required accuracies in cavi-
tation compliance for a 10% accuracy in frequency: 70% for
S-IC/F-1 LOX; 25% for S-IB/H-1 LOX; and 35% for Titan/LR87 Ox.
As previously stated, an objective of the cavitation model
development is that it be capable of predicting feed system
frequency to within a 10% accuracy. The results predicted by
the current model clearly do not meet this objective. Although
additional refinements and extensions to the existing model
framework could be recommended, it is felt that none of them
have a high probability of resulting in adequate correlation
with test data.

Table 5.1 Inducer Streamsheet Parameters

Inducer	J-2 LOX	F-1 LOX	H-1 LOX	LR-870X
No. of Blades	3	3	4	3
Flow Rate ($\dot{W}$) lb/sec	386.	3765.	514.	522.
Pump Speed (ω) rad/sec	841.	581.	706.	874.
Inlet Velocity (U) in/sec	275.	497.	294.	276.
U/ω in	.33	.86	.42	.32
Chord $\Delta Z/\Delta\theta$ in	.59	1.25	.76	Fig. 5.12
Inlet Thickness ($b(Z_o)$) in	.323	.331	.317	.294
Tip Radius (r_t) in	3.375	7.875	3.80	3.55
Tip Blade Angle (β) deg	9.0	9.9	11.3	5.7
Tip Flow Angle ($\emptyset$) deg	5.6	6.2	6.3	5.2
Tip Angle of Attack (α) deg	3.4	3.7	5.0	0.5

Table 5.2 Streamsheet Cavitation Compliance
J-2 LOX Inducer, 50% Section, U/ω = .33

P_s	W_{ss}	ΔW_{ss}	ΔP	C_{ss}
50	.17938			
48		.00015	4	.00004
46	.17923			
44		.00026	4	.00007
42	.17897			
40		.00042	4	.00011
38	.17855			
36		.00056	4	.00014
34	.17799			
33		.00038	2	.00019
32	.17761			

Table 5.3 Factors Affecting Minimum Inducer Pressure

Inducer	α_{tip} (deg)	α_{hub} (deg)	Blade Thickness[1] (% of channel)	$1/2\rho V_r^2$ (psi)	$P_s - P_{min}$[2] (psi)
J-2 LOX	3.4	15.1	32	433.	(3)
F-1 LOX	3.7	9.4	18	1120.	59
H-1 LOX	5.0	14.5	26	388.	30
LR87 Ox	.5	8.9	19	655.	17

(1) At the 50% blade section

(2) Nominal inlet flow direction

(3) P_{min} = vapor pressure

BLADE SURFACE COORDINATES ALL
R & φ VALUES ARE GAGE DIMENSIONS
REFER TO MD-MISC-48-270 FOR ADDITIONAL
INFORMATION

φ	$R_1=.500$		$R_2=1.250$		$R_3=2.000$	
	$Y_1 \pm.0100$	$Y_2 \pm.0100$	$Y_1 \pm.0100$	$Y_2 \pm.0100$	$Y_1 \pm.0100$	$Y_2 \pm.0100$
20°	.0668	.1179	—	—		
30°	.1042	.2873				
40°	.1477	.4441				
45°			.1469	.2118		
50°	.1984	.5885	.1613	.2980		
55°			.1787	.3793		
60°	.2572	.7208	.1995	.4559	—	—
65°			.2239	.5277		
70°	.3255	.8411	.2521	.5948	.2395	.3000
75°			.2644	.6572	.2625	.3755
80°	.4042	.9495	.3212	.7149	.2889	.4462
85°			.3627	.7679	.3192	.5122
90°	.4940	1.0485	.4096	.8173	.3558	.5733
95°	.5461	1.0979	.4620	.8665	.3932	.6296
100°	.5984	1.1474	.5146	.9160	.4373	.6811
105°	.6508	1.1971	.5671	.9656	.4900	.7307
120°	.8083	1.3474	.7254	1.1155	.6484	.8806
135°	.9668	1.4992	.8844	1.2671	.8076	1.0321
150°	1.1262	1.6527	1.0444	1.4204	.9678	1.1853
165°	1.2867	1.8079	1.2054	1.5754	1.1289	1.3402
180°	1.4485	1.9648	1.3677	1.7321	1.2913	1.4968
195°	1.6116	2.1234	1.5312	1.8905	1.4550	1.6553
210°	1.7763	2.2839	1.6963	2.0508	1.6202	1.8155
225°	1.9427	2.4463	1.8630	2.2130	1.7870	1.9776
240°	2.1108	2.6106	2.0315	2.3771	1.9555	2.1417
255°	2.2807	2.7763	2.2017	2.5432	2.1259	2.3077
265°	2.3995	2.8765	2.3163	2.6551	2.2405	2.4196
270°			2.3737	2.7113	2.2981	2.4759
275°	2.5358	2.9625	2.4338	2.7649	2.3559	2.5324
280°			2.4996	2.8123	2.4143	2.5889
285°	2.6917	3.0342	2.5713	2.8554	2.4771	2.6421
290°			2.6490	2.8935	2.5447	2.6912
295°	2.8691	3.0916	2.7329	2.9266	2.6171	2.7360
300°			2.8231	2.9548	2.6942	2.7767
305°	3.0702	3.1348	2.9197	2.9780	2.7760	2.8131

.12 R (TYP) 3 PLACES

.160 (TYP) 6 PLACES

.080

D₁ 6 SLOTS EQUALLY SPACED WITHIN .010 FILLET R.020 SLOTS MAY BE ROTATED AT RANDOM

A ⑤
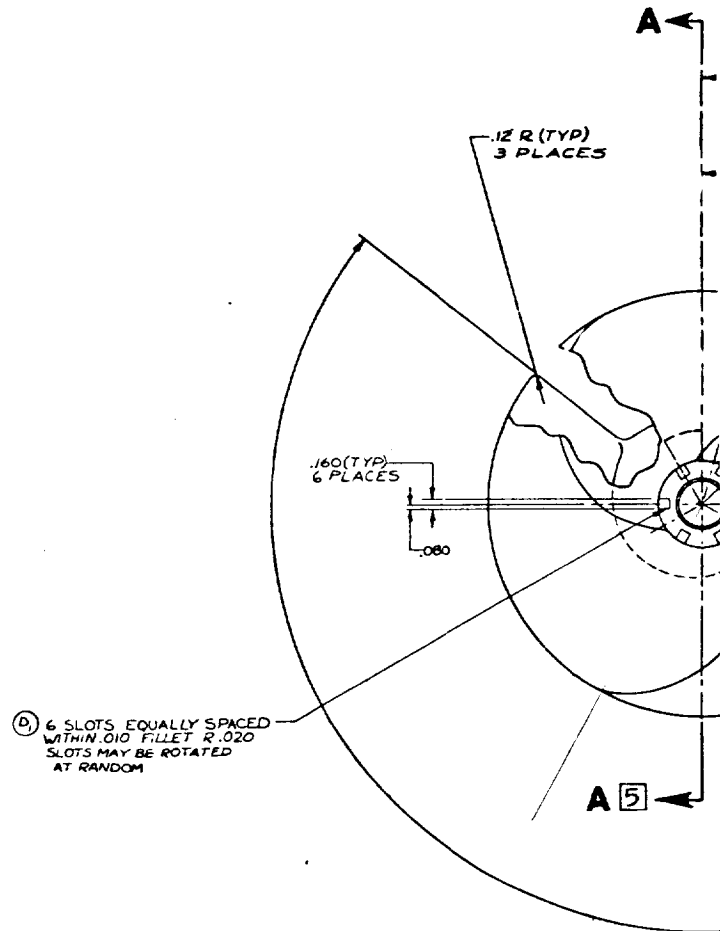
LEADING EDGE TRIM COORDINATES
FAIR SMOOTHLY BETWEEN
COORDINATE POINTS

ANGLE φ BASE	R ±.03
0°	.600 (REF)
15°	1.182
30°	1.644
45°	2.128
60°	2.620
75°	3.090
90°	3.348

Figure 5.1 J-2 LOX Ir

—.005 MAX

1.75
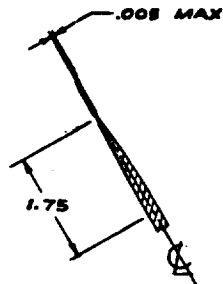
SECTION **B-B** 6
TYPICAL FAIRING SYMMETRICAL
ABOUT ℄ ALL LEADING AND
TRAILING EDGES

φ

R

B

B 6

308° 30' ± 3° 0'

3 BLADES EQUALLY SPACED
WITHIN 0° 15'

3.875 ±.005
2.23
.060 ——— 1.500
.830
.310 ±.005
.060
.7502 +.0020 DIA
LENGTH OF DIM CODED (A) .56
.090(TYP) 6 PLACES
380 R (TYP) 6 PLACES
.7502 ±.0020 DIA .740(TYP) 6 PLACES
.28 R
.19 R
.080 R
6.750±.000 C.A −.005
1.375 DIA
R2
R3
R1
.30
CHAM.030×45°
6°
11-51'
Y1
Y2
.150 3.250 ±.005

SECTION **A-A** 7

iducer

Z

Z₁

2.580

2.080

16°

6°

.500

.300±.000 / .010

2.9830 +.0010/-.008 DIA
BEFORE PLATING
(16) 2.9778 ± DIA
AFTER PLATING

3.9838 +.000/-.0003 DIA
BEFORE PLATING
(3)(4) 3.9778 ± DIA
AFTER PLATING

.030

D

R₁

J ⑩

F ⑥

M DIA

⑤ 2.900 DIA

CHAMFER
.040 × 45°

15°

3.100
DIA

2.080
DIA

⑩

45°

15 12

18°

H ⑨

60°

.060

.09R

AL

.080

3.5000 DIA
GAGE   3.7500 P.D.
(REF)

4.020
DIA.

5.9821
BEFORE
(14) 5.9376
AFTER

6.
CA

INTERNAL SPLINE
PER DATA CHART NO. 1

GROOVE MAY BE PARTIALLY
REMOVED FOR BALANCING

BLADE SURFACE COORDINATES R≤φ
VALUES ARE GAGE DIMENSIONS. REFER TO
MD·MISC·40·596 FOR ADDITIONAL INFORMATION

63/ ALL BLADE
SURFACES

63/

SURFACE E

⑦

4.440±.005

.500±.005

3.000

4.580

1.550

6.700±.005

7.700

Φ°	R₁=.7500		R₂=4.5000	
	Z₁±.010	Z₂±.010	Z₁±.010	Z₂±.010
15°	.6293	.6953		
20°	.6906	.8514		
25°	.7549	1.0031		
30°	.8324	1.1502		
35°	.8923	1.2927		
40°	.9678	1.4307		
45°	1.0460	1.5640		
50°	1.1283	1.6927		
55°	1.2148	1.8166		
60°	1.3058	1.9359		
65°	1.4015	2.0505		
70°	1.5022	2.1602	1.6228	1.8376
75°	1.6081	2.2680	1.7866	1.9973
80°	1.7168	2.3760	1.9489	2.1462
85°	1.8257	2.4843	2.0285	2.2841
90°	1.9350	2.5930	2.1181	2.4110
95°	2.0445	2.7019	2.1896	2.5269
100°	2.1543	2.8111	2.3289	2.6344
105°	2.2643	2.9206	2.4397	2.7462
120°	2.5963	3.2508	2.7693	3.0773
135°	2.9359	3.5838	3.1037	3.4111
150°	3.2882	3.9197	3.4407	3.7476
165°	3.6083	4.2585	3.7797	4.0870
180°	3.9573	4.6000	4.1220	4.4293
195°	4.2972	4.9407	4.4473	4.7746
210°	4.6463	5.2926	4.8158	5.1231
225°	4.5986	5.6439	5.1676	5.4749
240°	5.3543	5.9985	5.5228	5.8300
255°	5.7135	6.3569	5.8846	6.1888
270°	6.0765	6.7190	6.2461	6.5514
285°	6.4435	7.0855	6.6108	6.9180
300°	6.8147	7.4545	6.9817	7.2890
305°	6.9933	7.5701	7.1043	7.4136
310°	7.0811	7.6779	7.2320	7.5379
315°	7.2286	7.7778	7.3694	7.6508
320°	7.3869	7.8699	7.5118	7.7493

⑧
1
2
3
4
5
6
7
8
9
10
11
12
13
14
15
16
17
18
19

SECTION A-A ⑤

Figure 5.2

NOTE: ONE SPACE ON SPLINE NOT CUT (8)

.020±.005 R
(14) OPTIONAL

.020±.005
.030 2 PLACES
(14) OPTIONAL 2 PLACES
30° 2 PLACES
(2) .18 MIN
(2) .25 R MIN
(A₁₂)
.010±.010 R
CHAM .005±.010 x 45°
2 PLACES
(5) 5.200±.005 DIA
(2) .18 MIN
(5) 4.700±.000 DIA
.060±.010
(2) .25 MAX
FULL R (12) OPTIONAL
.060

TAIL F (8)
SCALE 4/1

18°

(4)(3)(6)

A

Z (10)

6.00±.50 R
3 PLACES

(M)

3.625 MINOR DIA
(REF)

Z

(9)

(A)

(2)

(11)

35°±10°
3 PLACES

(11) TYP
3 PLACES

A (8)

57 DIA

1000 DIA
LATING
1000 DIA
LATING
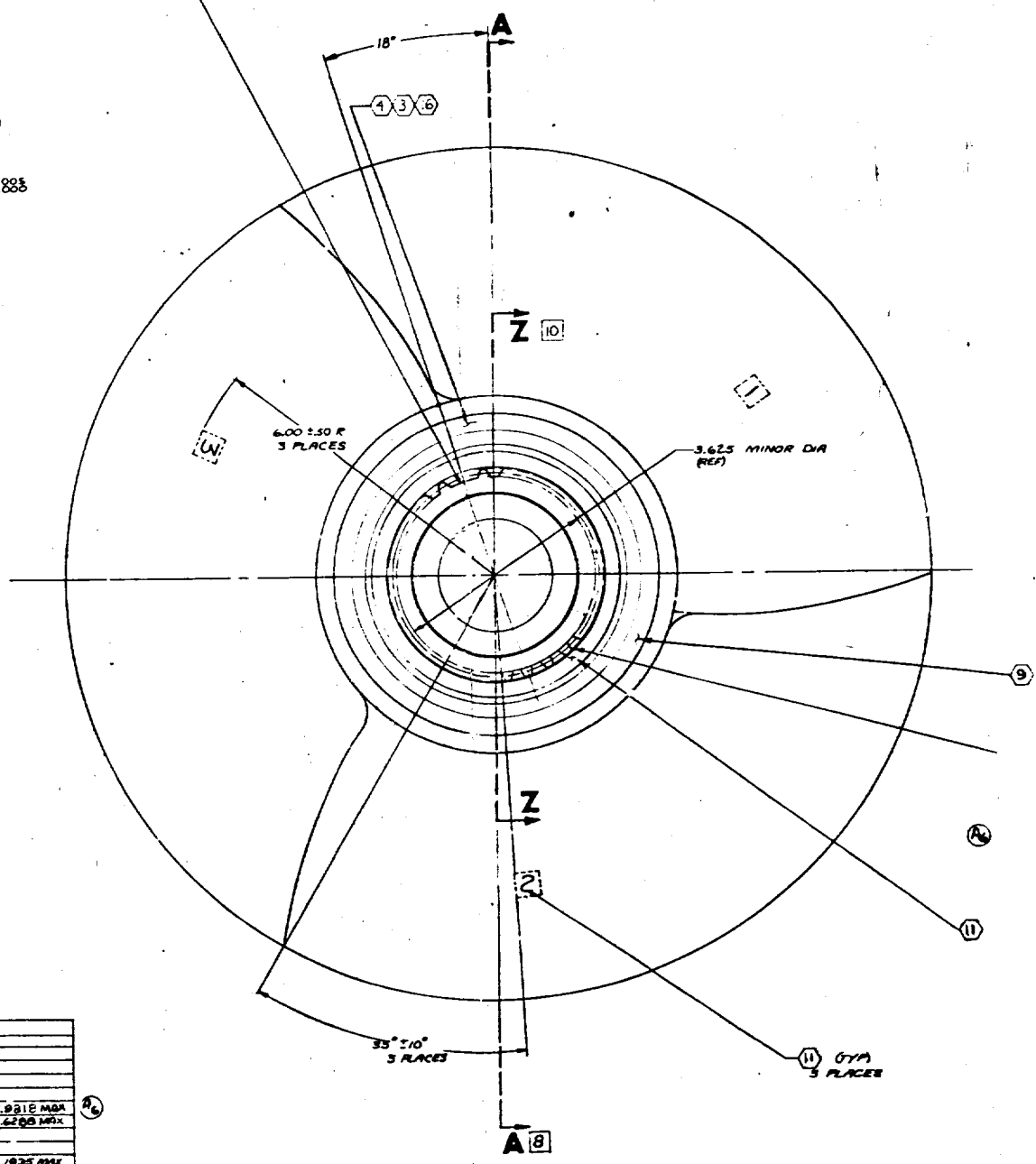
LEADING & TRAILING EDGE
TRIM COORDINATES

Ø°	R_L	R_T
15°	2.654	
30°	3.665	
45°	4.684	
60°	5.711	
75°	6.687	
80°	6.971	
85°	7.212	
90°	7.420	
95°	7.596	
100°	7.727	
105°	7.810	
337°		7.614
335°		6.166
340°		4.350
342°57′		3.300 REF

SPLINE DATA CHART NO. 1		
NO. TEETH	30	
DIAMETRAL PITCH	8/16	
PRESSURE ANGLE	30°00′	
PITCH DIA	3.7500 REF	
BASE DIA	3.24759	
MAJOR DIA	3.9750 MIN	3.9818 MAX
MINOR DIA	3.6250 MIN	3.6288 MAX
FORM DIA	3.6250	
FILLET RADIUS	.033 MIN	
CIRCULAR TOOTH SPACE	.1960 MIN	.1935 MAX
MEASURING PIN DIA	.18000	
DIMENSION BETWEEN 2 PINS	3.5529 MIN	3.5555 MAX
OUT OF ROUNDNESS-PITCH DIA	.0013 MAX	
LEAD ERROR	.0006 MAX	
CLASS OF FIT	CLASS A MODIFIED	
TYPE OF FIT	SIDE FIT-FILLET ROOT	
TOOTH TO TOOTH SPACING ERROR	.0004 MAX	
ACCUMULATED PITCH ERROR-NON ADJ	.0015 MAX	
PROFILE ERROR	.0006 MAX	

(A₆)

F-1 LOX Inducer
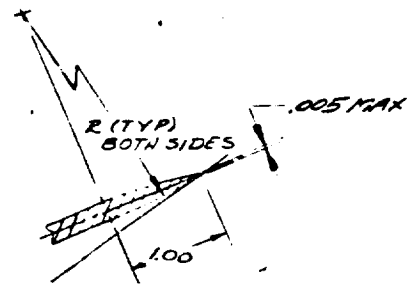
SECTION **C·C**

TYPICAL FAIRING FOR LEADING
AND TRAILING EDGES OF ALL
BLADES
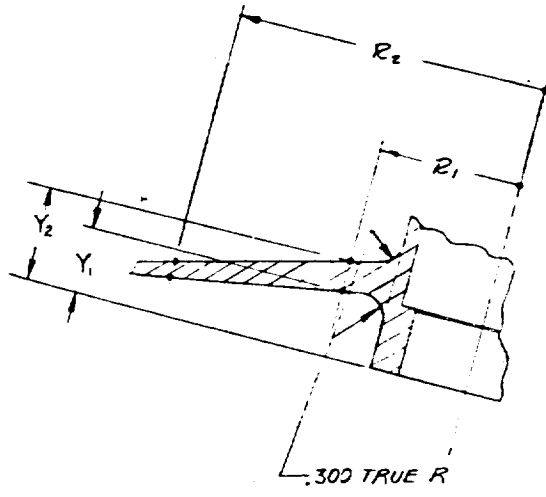
.300 R TRUE (TYP)
ALL LEADING &
TRAILING EDGES

.300 TRUE R

SECTION **B·B**
(TYP) 4 BLADES

185°30'
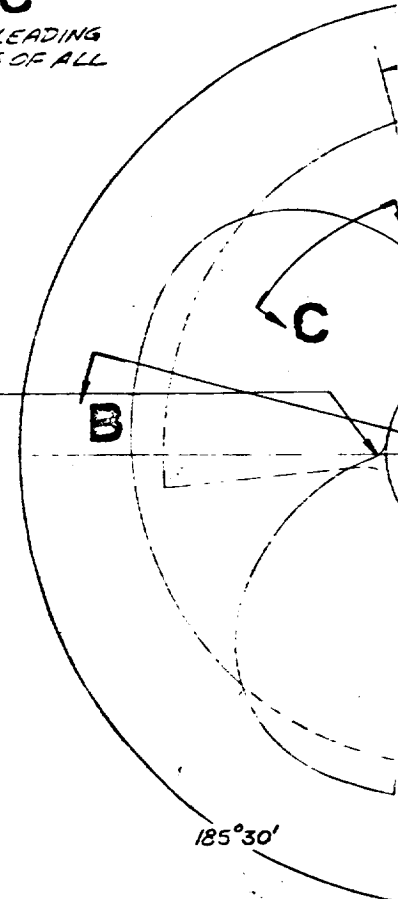
— BLADE SURFACE COORDINATES —
FOR ADDITIONAL INFORMATION REFER TO
MD-MISC-48-250. R_1, R_2 & ϕ ARE GAGE DIM'S

ϕ	$R_1 = 1.5000$		$R_2 = 3.2000$		R_L
	$Y \pm .0050$	$Y_2 \pm .0050$	$Y \pm .0050$	$Y \pm .0050$	
5°					
10°	.0100	.0346			
15°	.0433	.1342			1.892
20°	.0808	.2264			
25°	.1228	.3117			
30°	.1654	.3906			2.796
35°	.2208	.4635			
40°	.2770	.5307	.0200	.0639	
45°	.3425	.5965	.0590	.1526	3.470
50°			.1082	.2301	
60°	.5334	.7894	.2330	.3624	3.722
75°	.7253	.9820	.4252	.5547	
90°	.9305	1.1784	.6209	.7505	
105°	1.1210	1.3808	.8221	.9520	
120°	1.3297	1.5924	1.0320	1.1622	
135°	1.5506	1.8177	1.2546	1.3854	
150°	1.7874	2.0597	1.4935	1.6250	
155°	1.8658	2.1394	1.5785	1.7100	
165°	1.9560	2.2200	1.6635	1.7950	
165°	2.0534	2.2947	1.7487	1.8810	
170°	2.1587	2.3635	1.8325	1.9706	
175°	2.2725	2.4270	1.9319	2.0507	
180°	2.3957	2.4853	2.0439	2.1195	

Figure 5.3 H-1 LOX Inducer

4 BLADES EQUALLY SPACED
WITHIN 0°15'

A

0°

ϕ

.0940 ±.0005

.1885 +.0020 -.0000

C

R_L

.010 MAX R

1.530 +.005 -.000

B

ROTATION

A

2.650

13°56'(REF)

12°

7.600 +.000 -.005 DIA

6.525 +.005 -.005 DIA

2.500 DIA

.700

.020 R (MAX)

1.730 DIA

1.438 +.001 -.000 DIA

3

CHAM .030 x 45°

0 2

A2

4 6

3
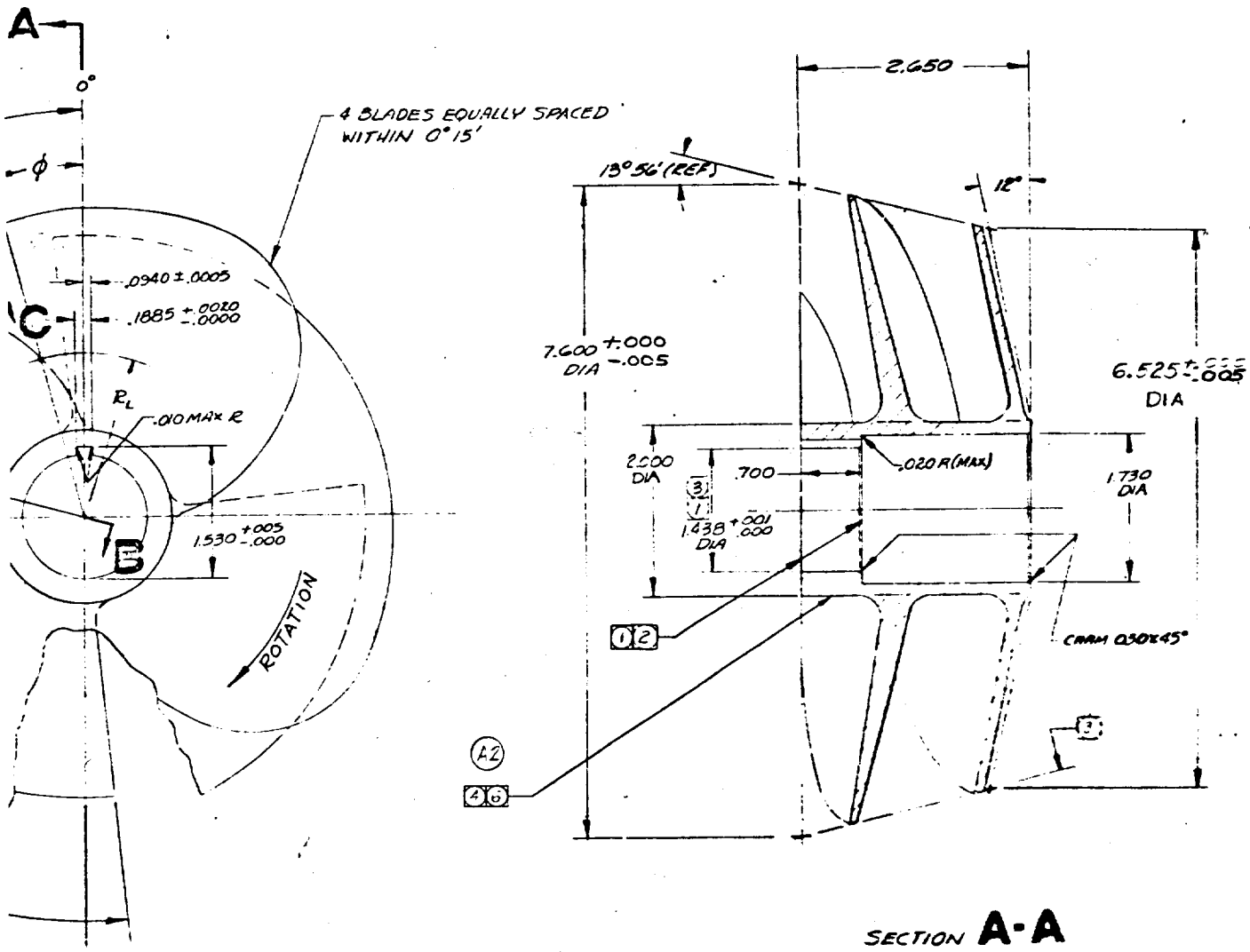
SECTION **A-A**

12. PLAN MACHINING PER RA0103-006
11. PENETRANT INSPECT PER MIL-I-6866(RA0115-116 TYPE III A)
10. REHEAT TREAT AFTER ROUGH MACHINING TO T-6
   CONDITION PER RA0111-010
9. SERIALIZE BY ELECTROCHEMICAL ETCH PER RA0104-007
   COMPLETE TRACEABILITY REQUIRED
8. KEY SLOT MAY BE ROTATED AT RANDOM
   WITH RESPECT TO BLADES
7. FOR IN PLANT HANDLING PROTECT BLADES
   BY PACKAGING PER RX 23060
6. CHROMIC ACID ANODIZE PER MIL-A-8625
   TYPE I (RA0109-021 TYPE I)
5. IDENTIFY BY ELECTROCHEMICAL ETCH PER RA0104-008
4. CONCENTRIC WITHIN .002 T.I.R.
3. PARALLEL WITHIN .001 TOTAL
   (HUB SURFACE ONLY)
2. NORMAL WITHIN .001 TOTAL
   (HUB SURFACE ONLY)
1. MACHINE PER RA0103-002

<u>NOTE: UNLESS OTHERWISE SPECIFIED</u>

DIMENSIONS PRIOR TO FINISH	DATE	SUP.
TOLERANCES EXCEPT AS NOTED	DRWN	MAT'L
.XXX=±.010, .XX=±.01, ANGLES=±30'		
125 MACH. SURF. ROUGHNESS EXCEPT AS NOTED (PER MIL-STD-10)		
HEAT TREAT PER		MATL MAKE FROM
7		451220 DIE FORGING
FINISH 6		

AXIS OF ROTATION
OF θ

.175
.174

NEAR SIDE OF
VANES IN TOP VIEW

.3750 DIA CUTTER
.3745

.241
.240

AXIS OF ROTATION
OF α OR α'

VANE
THICKNESS
AT TIP

.241
.240

.3750 DIA CUTTER
.3745

VANE THICKNESS AT HUB
NEGLECTING FILLET RADII

θ=0° FOR
VANE SHO

.175
.174

θ=13°45' REF
SEE TAB BLK

CUTTER LOCATION FOR VANES
NO SCALE

θ=0°
REF

.50 R TRUE
6 PLACES

SEE

40°
REF

2°0' TOL ZONE
BETWEEN 'W' θ=0°
REF & 'V' θ=78° REF
LOCATED AS SHOWN

A

θ = 78° REF
SEE TAB BLK

1.00 R
TRUE
3 PLCS

θ = 47° REF
SEE TAB BLK

D

H

H   K

R REF 9 VANES
SEE TAB BLK

D

θ=0°
FOR FULL VANE
SHOWN REF

A

5° REF

9 VANES REF
SEE TAB BLK

TOP VIEW

φ REF
SEE T

BLOCK 1

TABULATION OF VALUES FOR STREAMLINING OF FULL VANES

THICKNESS ALONG LEADING EDGE (VIEW D-D)

'θ' BSC	'R' BSC	'T' BSC
6°0'	1.075	(IN FILLET)
13°45'	1.265	.060
18°30'	1.400	
23°15'	1.600	
31°30'	1.800	
37°15'	2.000	
42°45'	2.200	
48°15'	2.400	
53°30'	2.600	
58°45'	2.800	
64°0'	3.000	
69°15'	3.200	
74°15'	3.400	

THICKNESS ALONG TIP CONTOUR (VIEW H-H)

"φ" BSC	"S" BSC
7°0'	.073
12°0'	.083
17°0'	.093
22°0'	.104
27°0'	.115
32°0'	.126
37°0'	.137
42°0'	.149
47°0'	NORMAL VANE THICKNESS
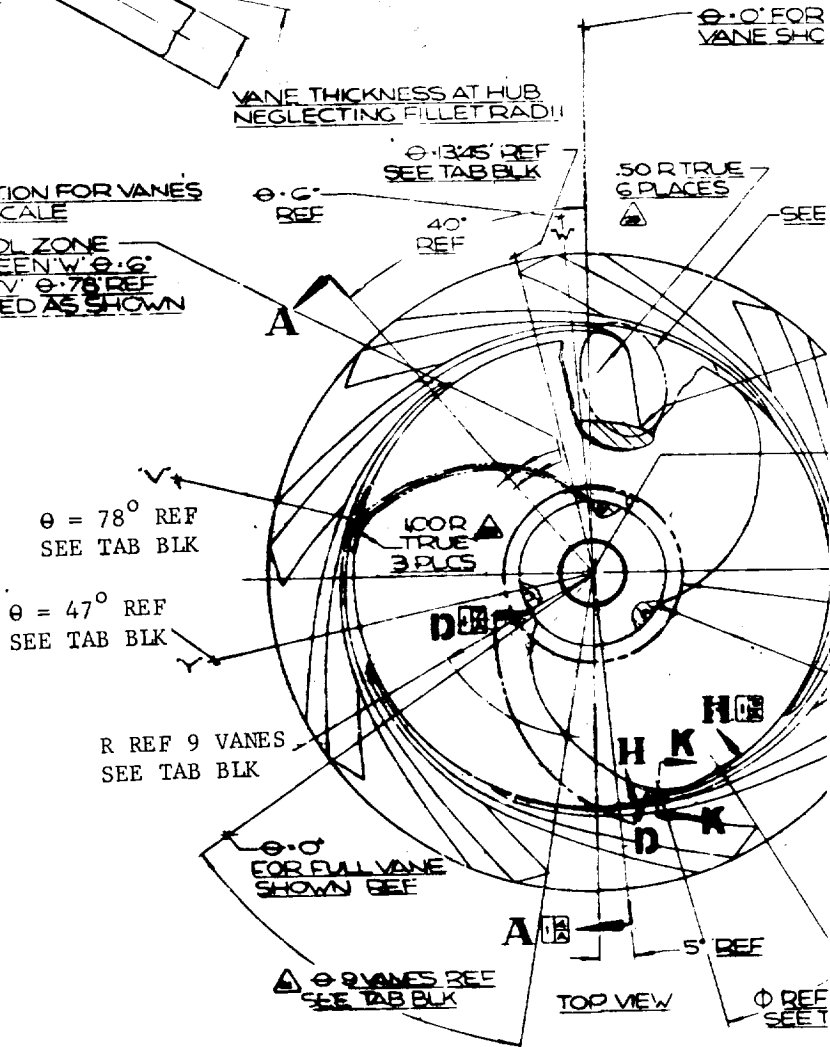
SECTION K-K
TYP SECTION OF
LEADING EDGE OF
FULL & PARTIAL VANES
THRU HUB & TIP RADII
SCALE: NONE

FULL R AT LEAD
EDGE BLENDIN
FLAT AT TIP & I
.19 R REF AT HU

Figure

.002
.001

FULL
WN REF △

TOLERANCE ZONE
IN AREA OF 4.011
RADIUS BASIC

DETAIL L ▣
SCALE: 1/1

DETAIL J ▣

SEE DETAIL L ▣

⊥ A .0009

5.980 REF

4.885

⊥ A .003

1.092
1.097

4.011 R
BASIC

⊥ A .002

.995

.08

63

⊥ A .008

.19 R TRUE △
6 PLACES △

.19 R TRUE
18 PLACES

.06 R

1.265 R REF
SEE TAB BLK

7.100
7.090
DIA

1.900
DIA

3.50
DIA

9.630
DIA

SEE DETAIL F ▣

9.640
DIA

1.075 REF HUB R
BETWEEN VANES

.5DR

.19 R TRUE △
3 PLACES

9.205
DIA

7.480
7.470

FULL R
0.020

7.475
BSC

12°30'
REF

1.00 AT INTER-
SECTION OF SURF

α REF
α' REF

.842 AT INTER-
SECTION OF SURF

9 VANES
TAB BLK

.230
BSC

4.890
4.880

SECTION A-A ▣

ING
IG TO
JTO FILLET R
B

18. ALL DIM ARE FINAL & APPLY AT 68°F ONLY.

5.4 LR87 Oxidizer Inducer
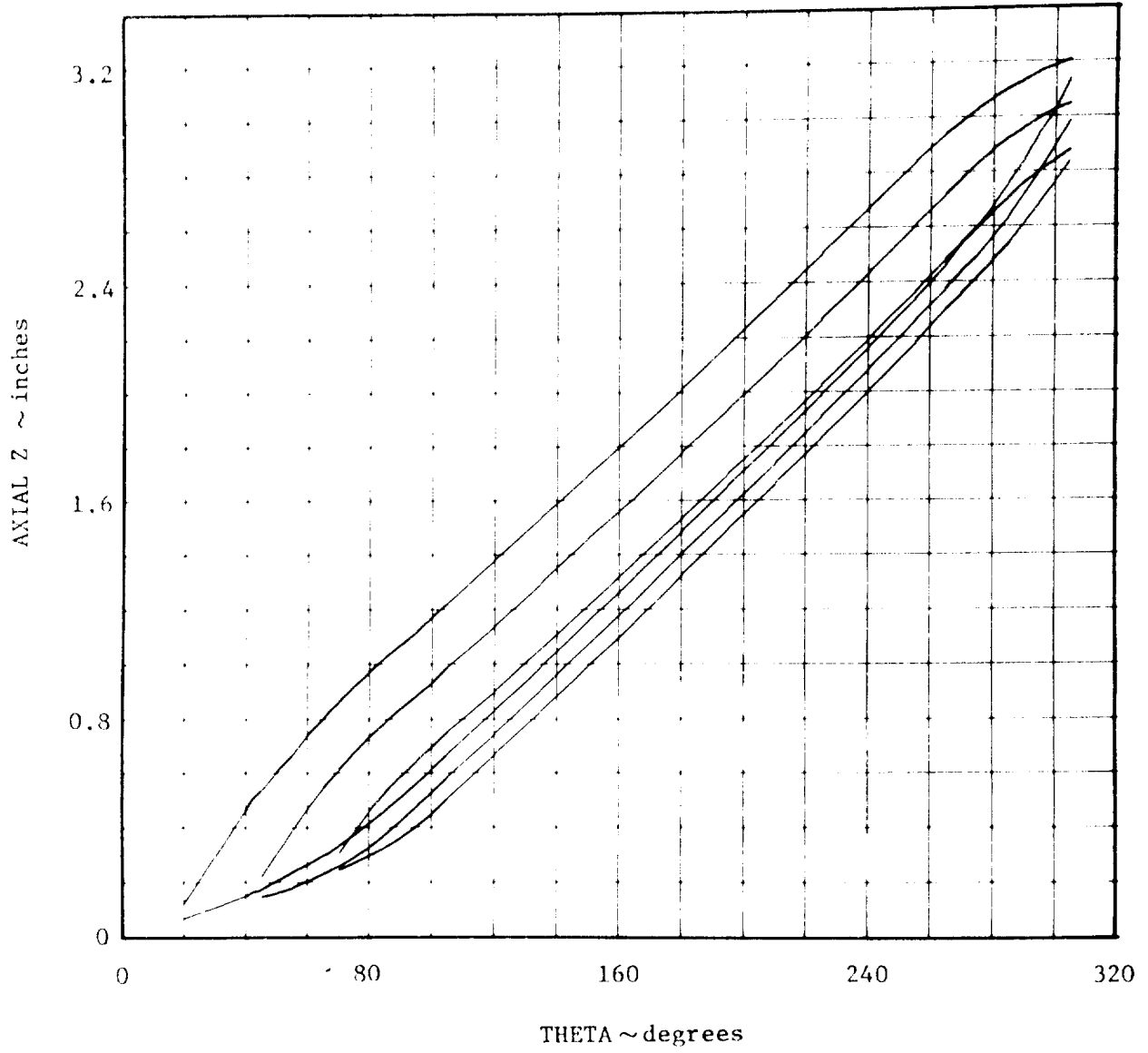
Figure 5.5   J-2 LOX Inducer Blade Sections
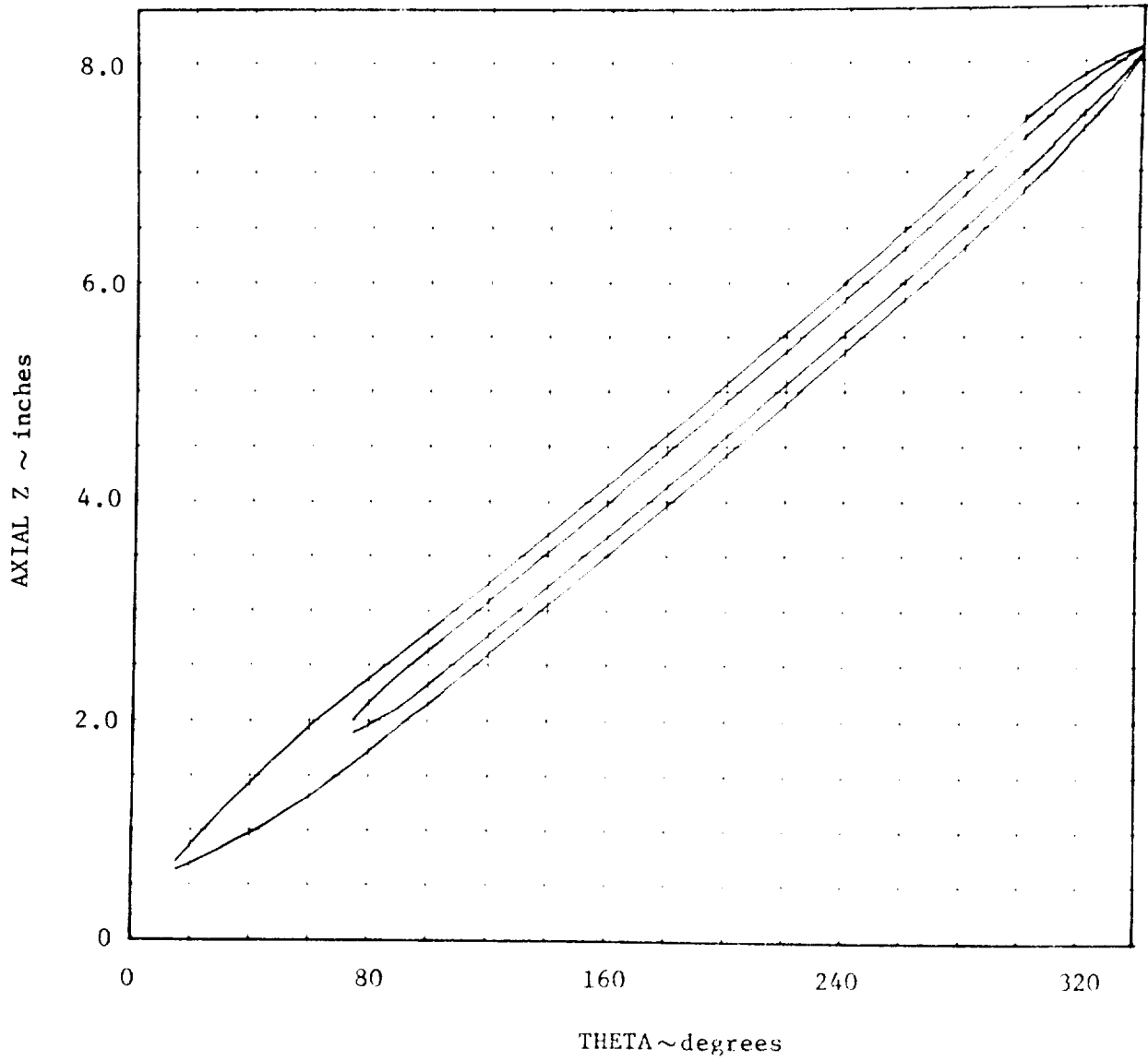
Figure 5.6   F-1 LOX Inducer Blade Sections
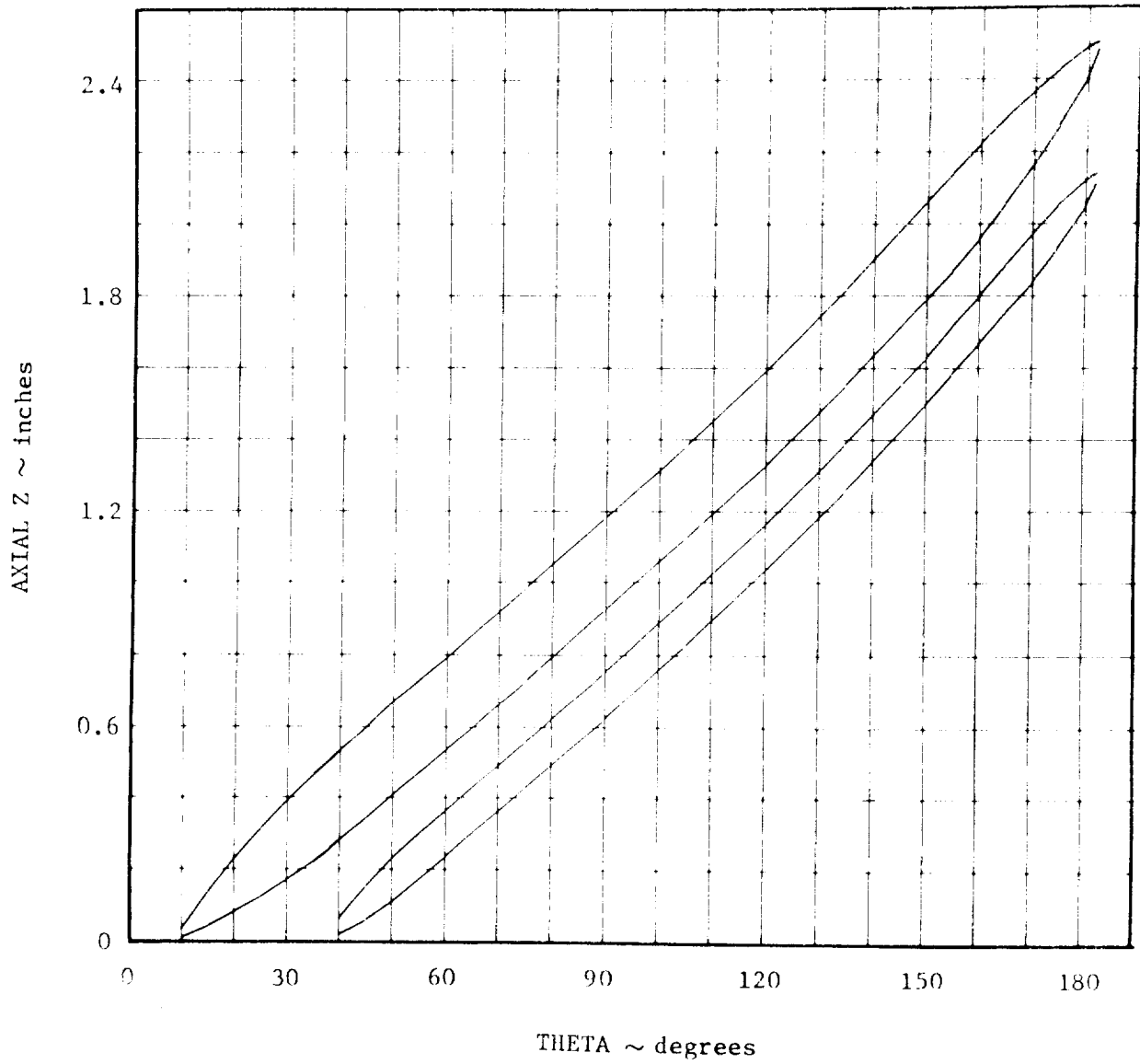
Figure 5.7 H-1 LOX Inducer Blade Sections
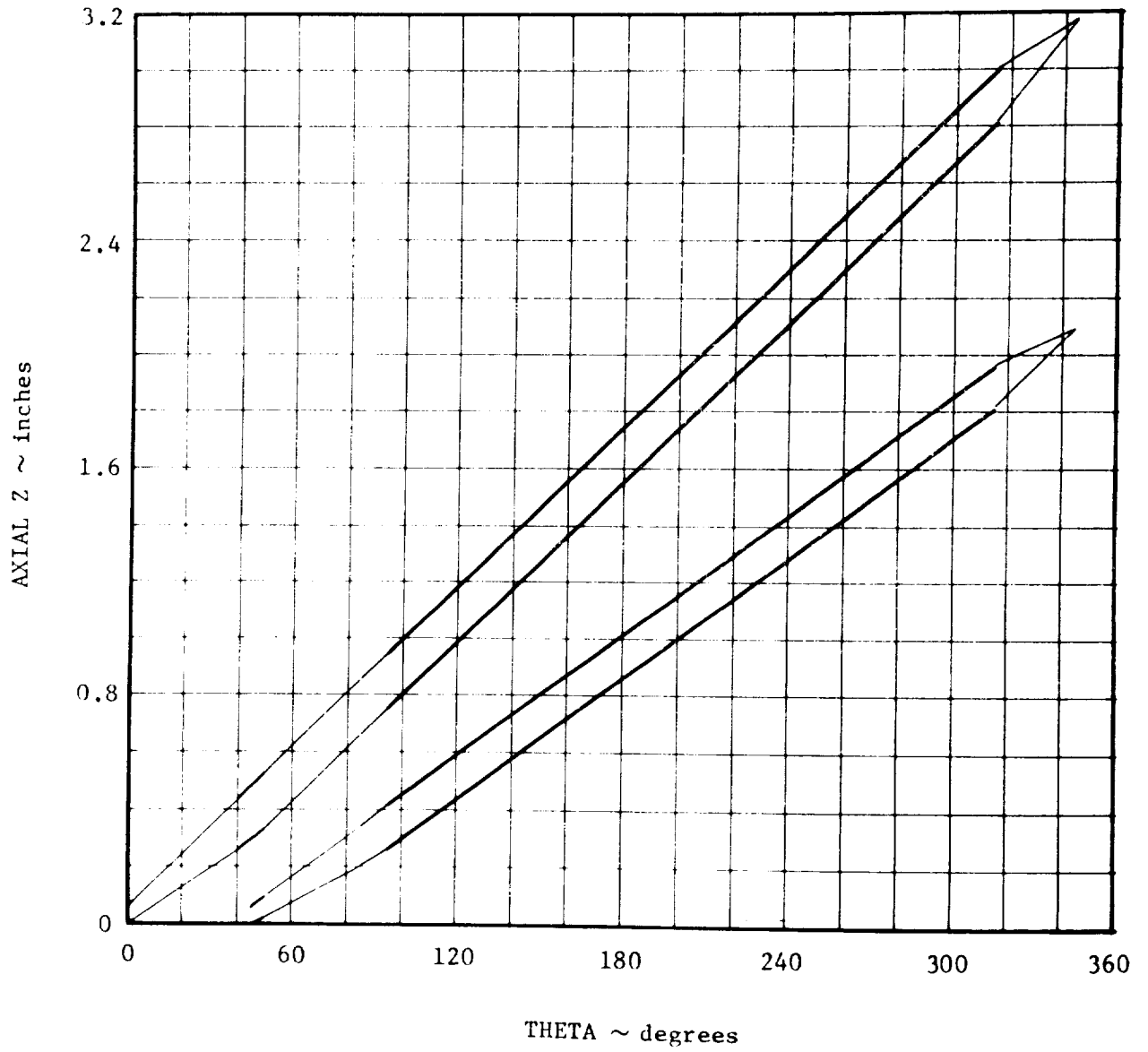
Figure 5.8 LR87 Oxidizer Inducer Blade Sections
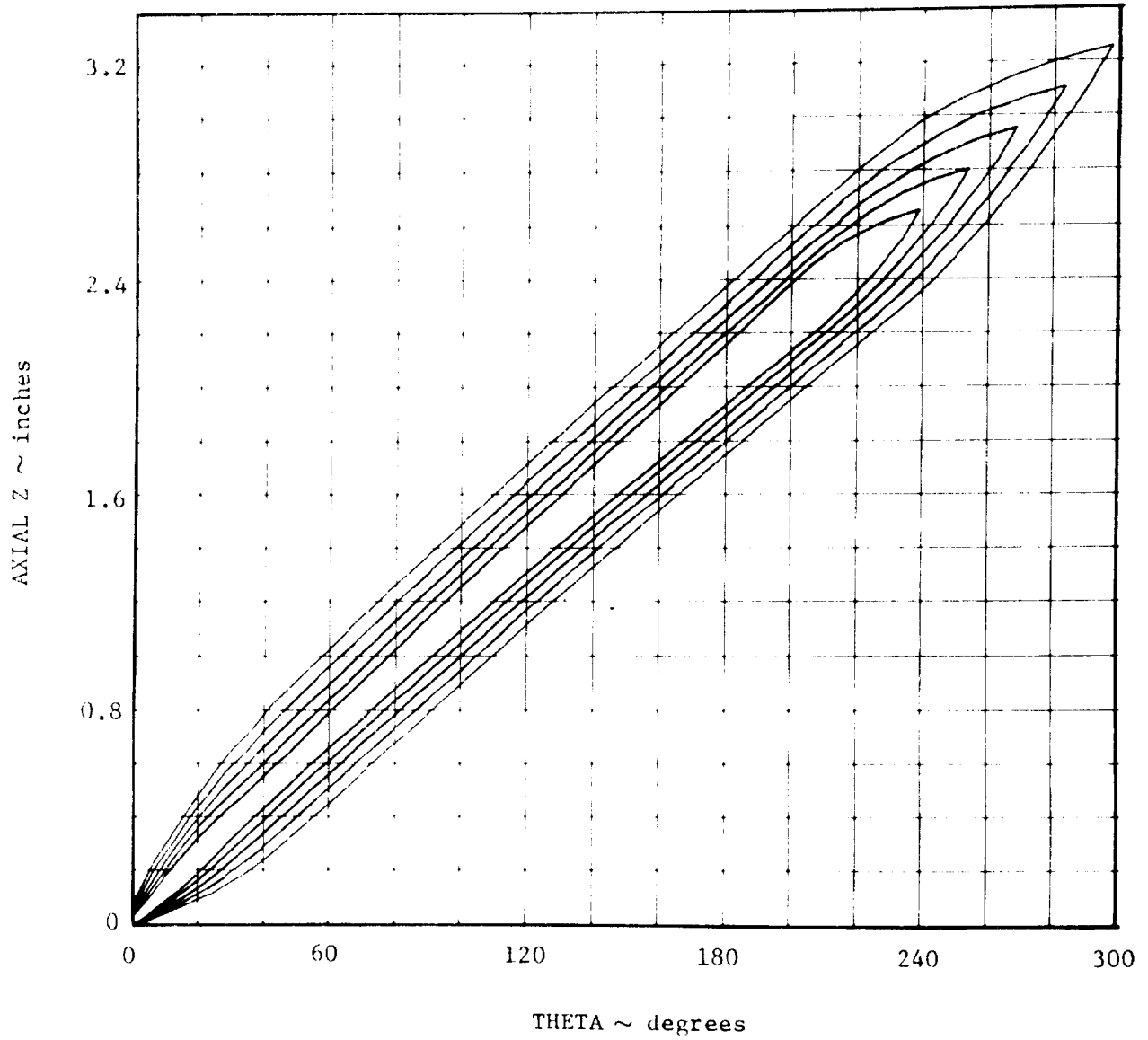
Figure 5.9 J-2 LOX Inducer Interpolated Blade Sections
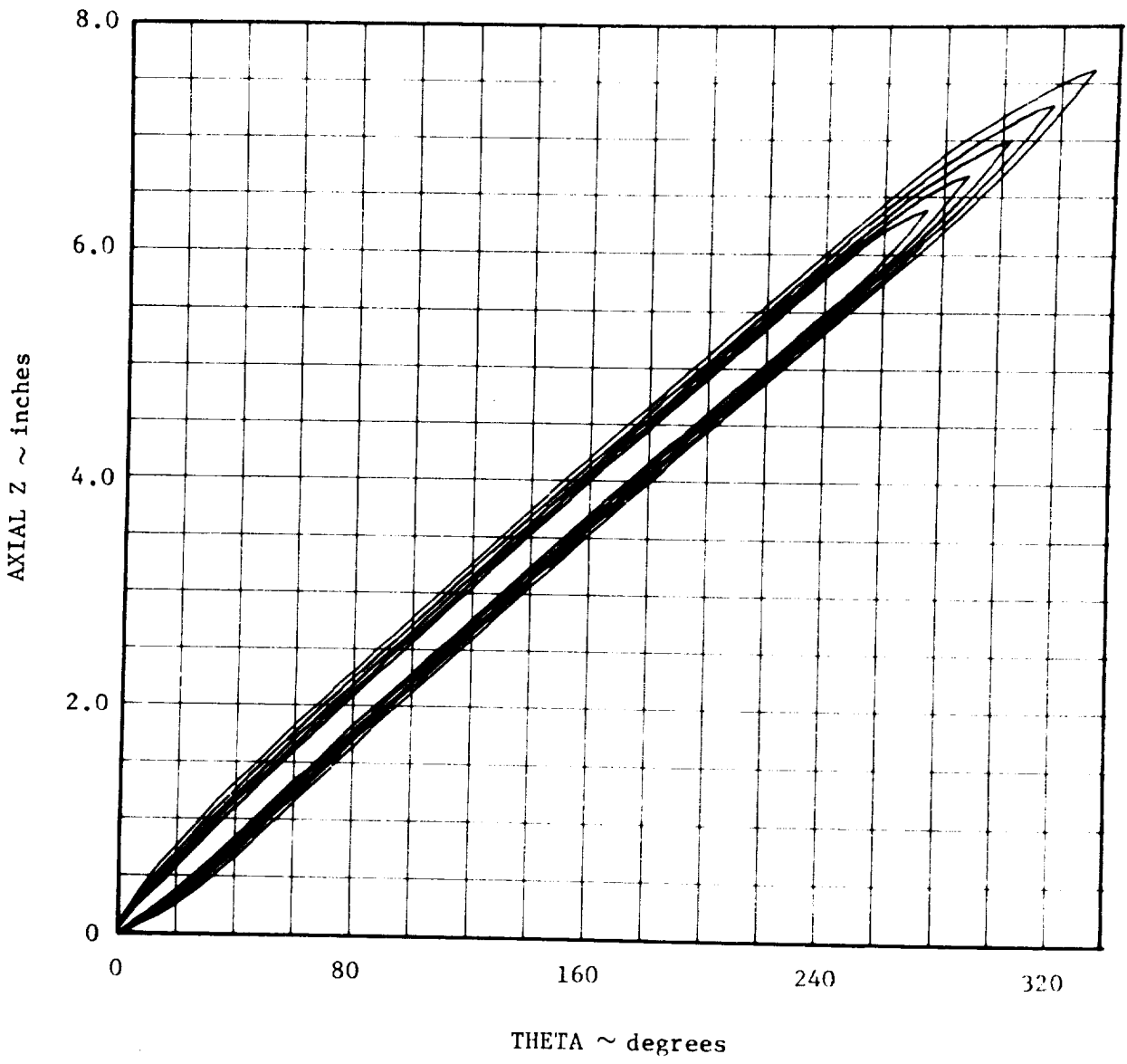
Figure 5.10 F-1 LOX Inducer Interpolated Blade Sections
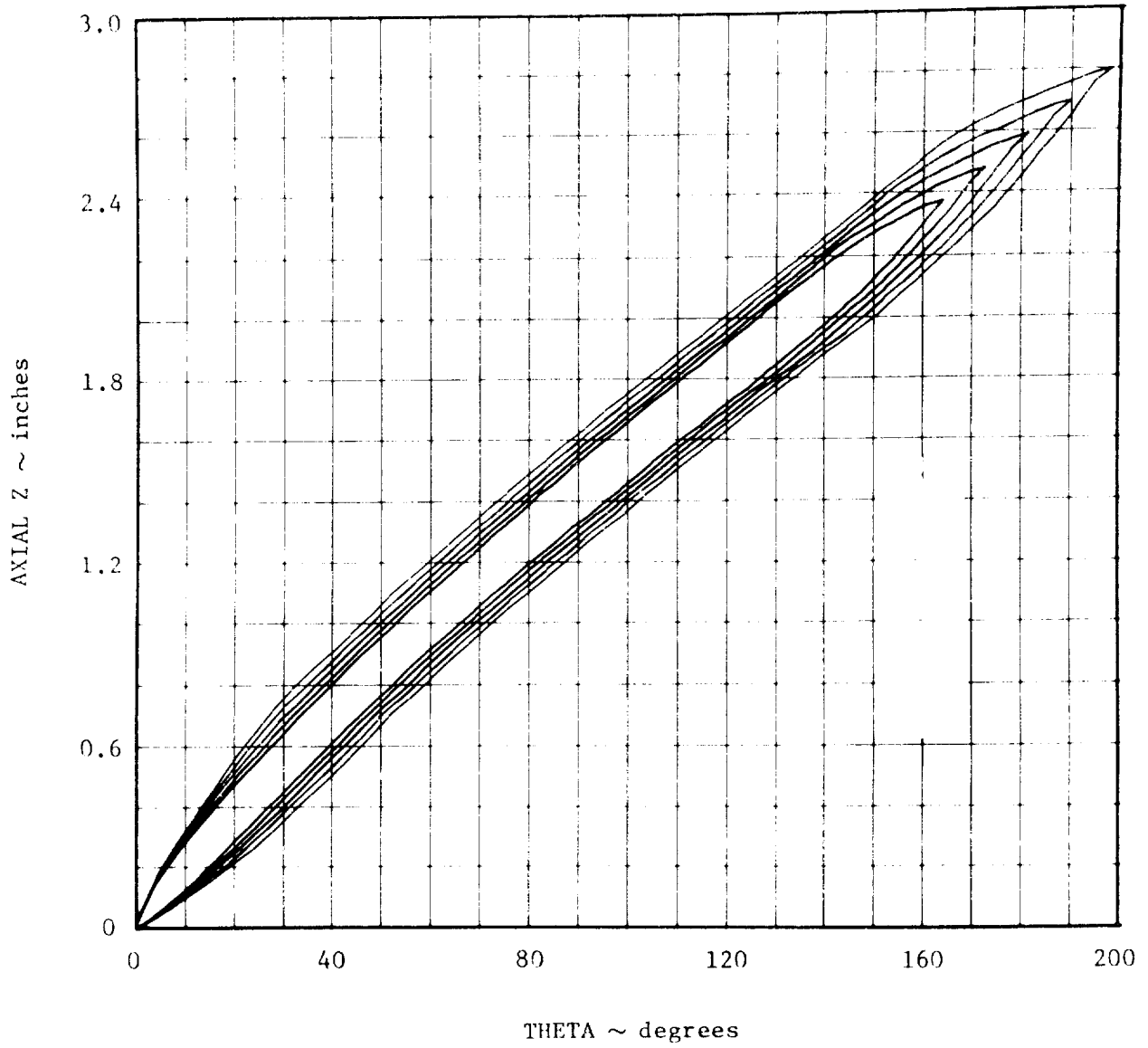
Figure 5.11   H-1 LOX Inducer Interpolated Blade Sections
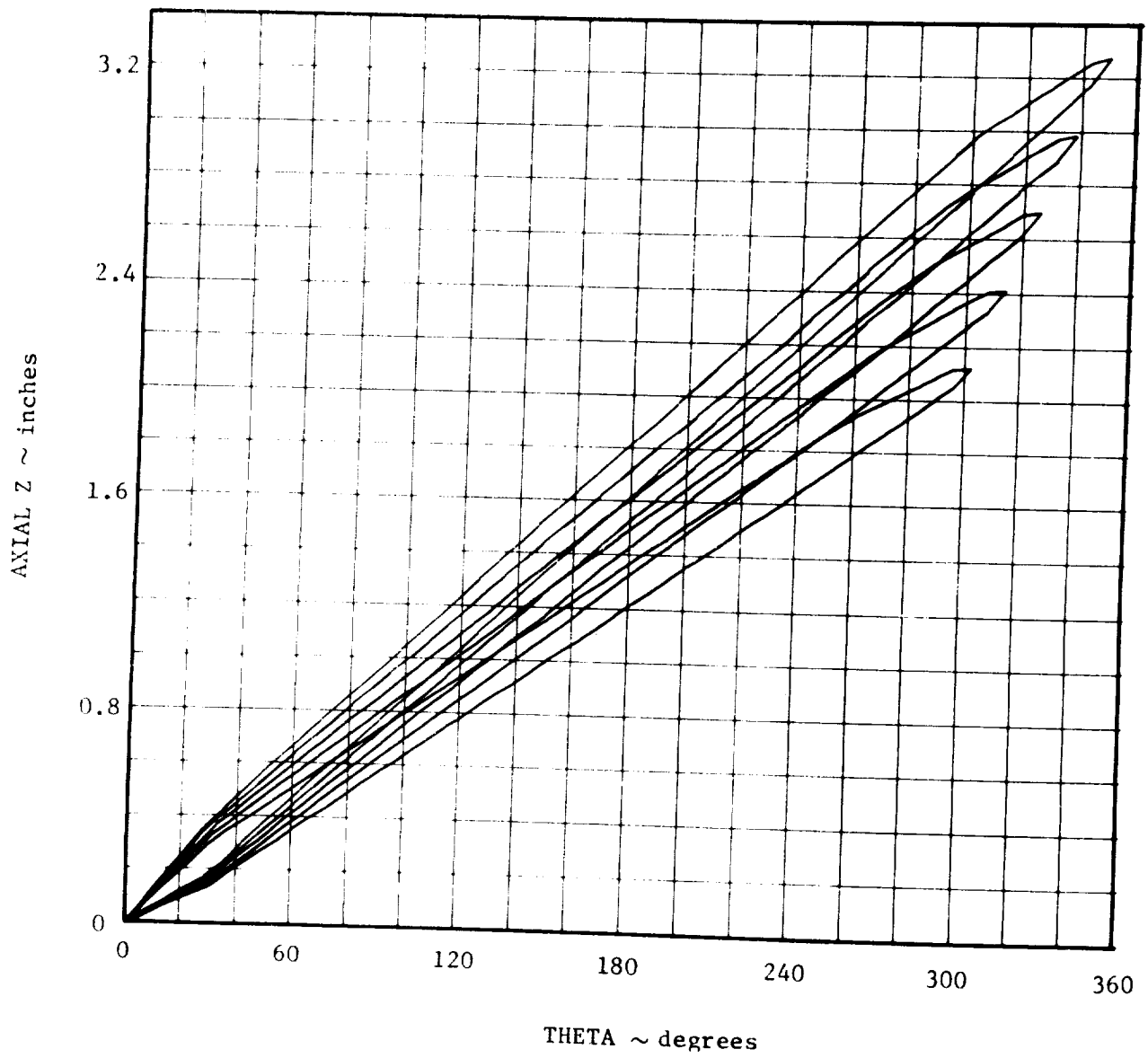
Figure 5.12   LR87 Oxidizer Inducer Interpolated Blade Sections
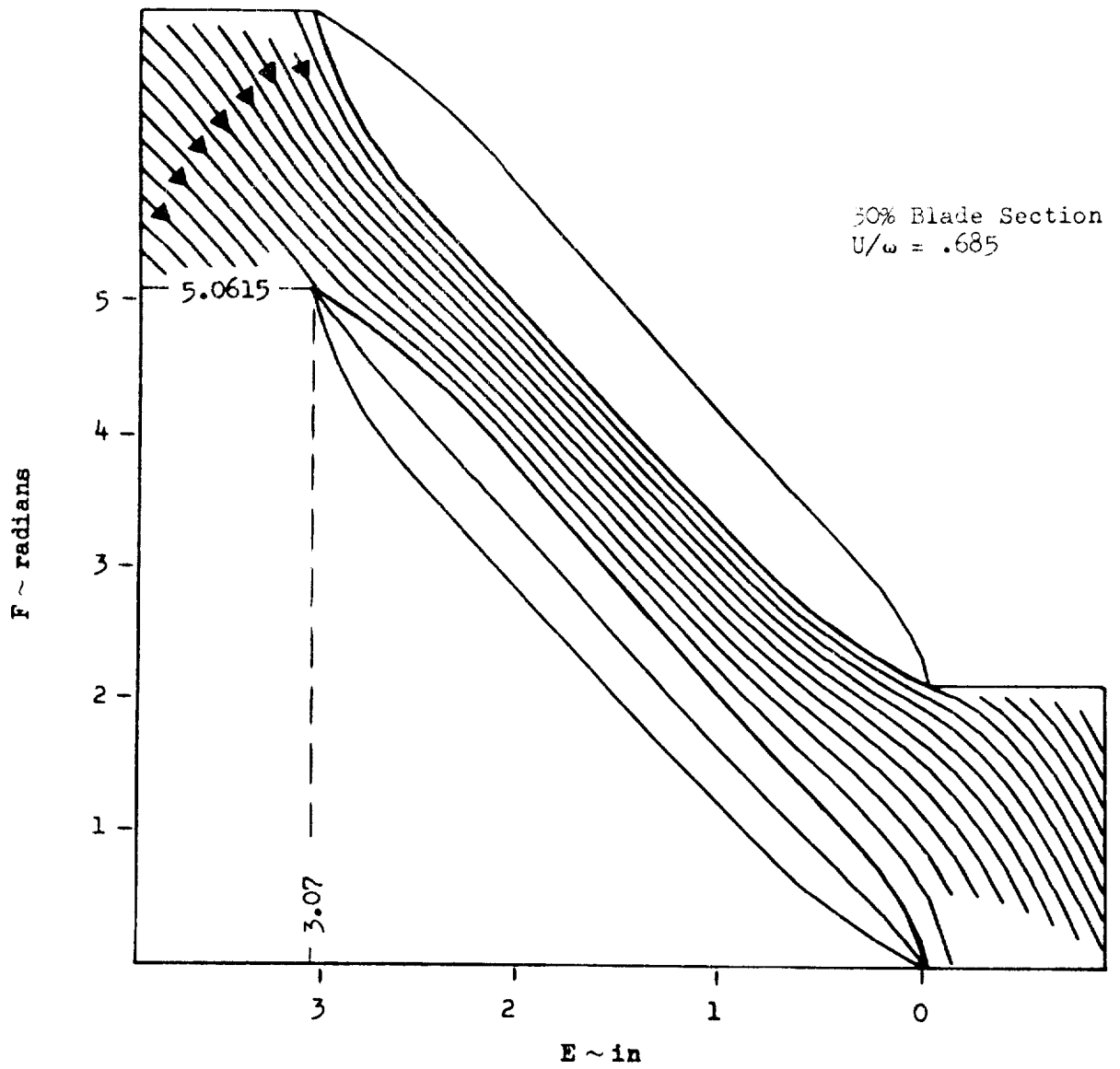
Figure 5.13   J-2 LOX Inducer Streamlines
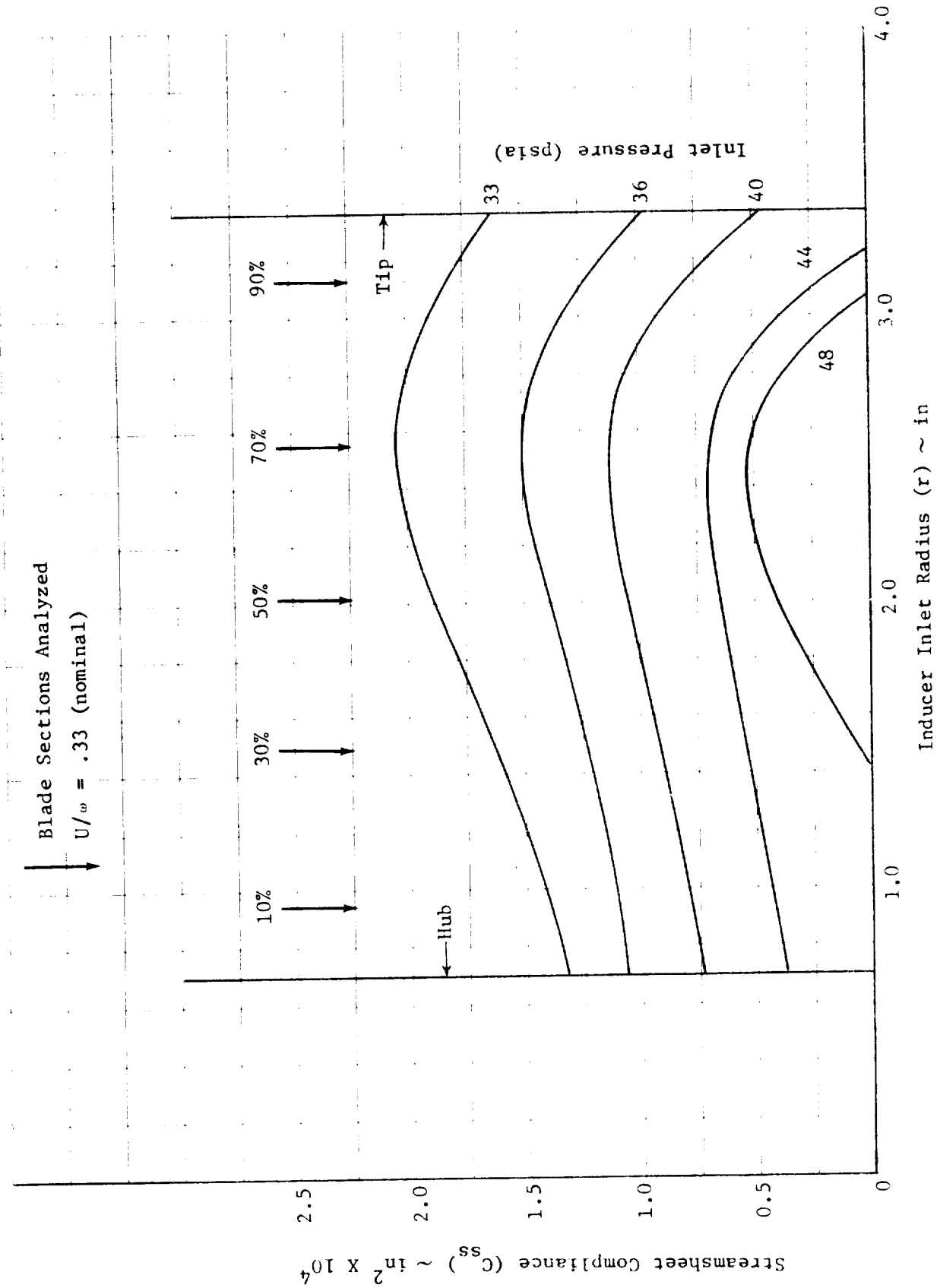
Figure 5.14   J-2 LOX Inducer Streamsheet Compliance
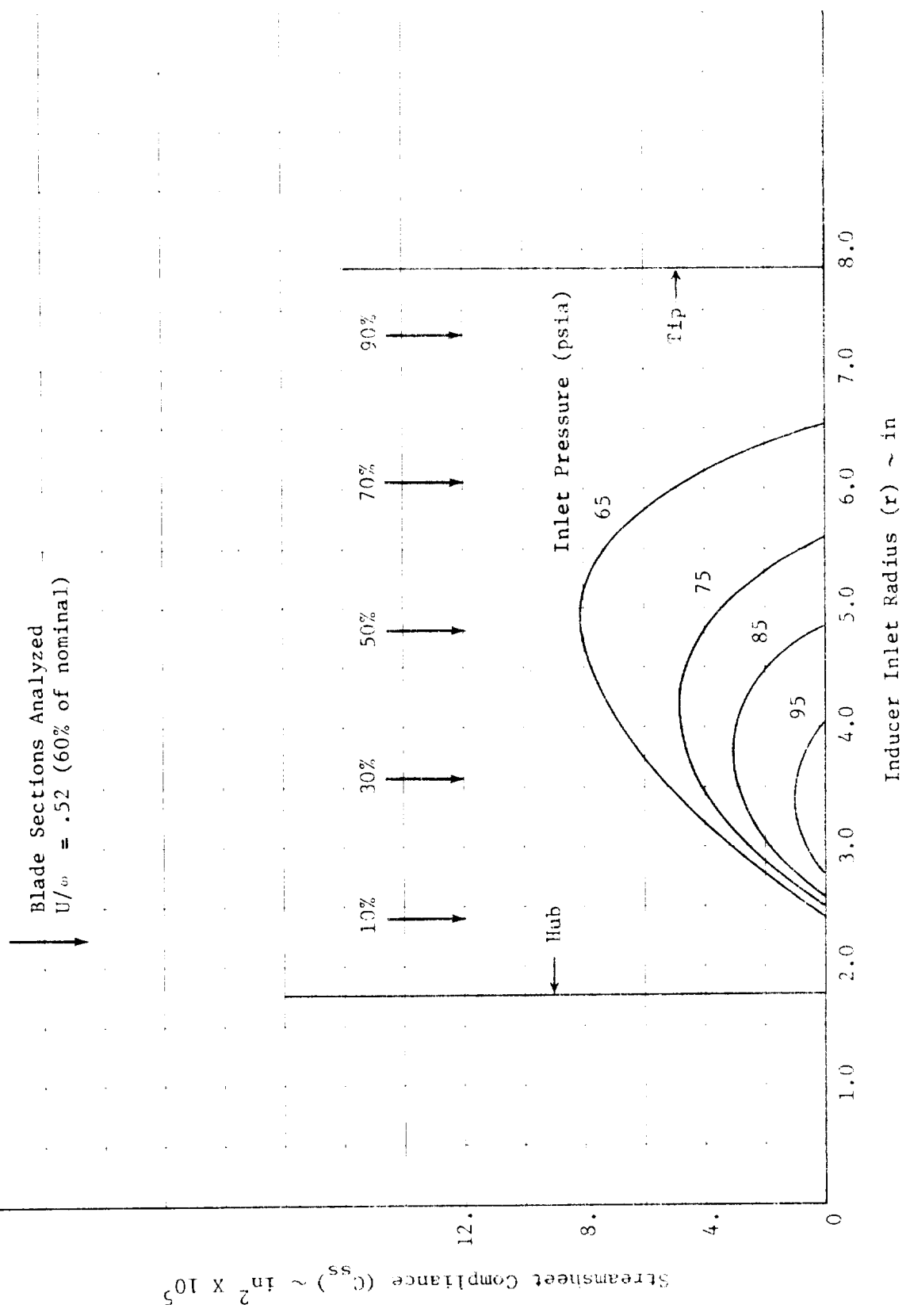
Figure 5.15 F-1 LOX Inducer Streamsheet Compliance
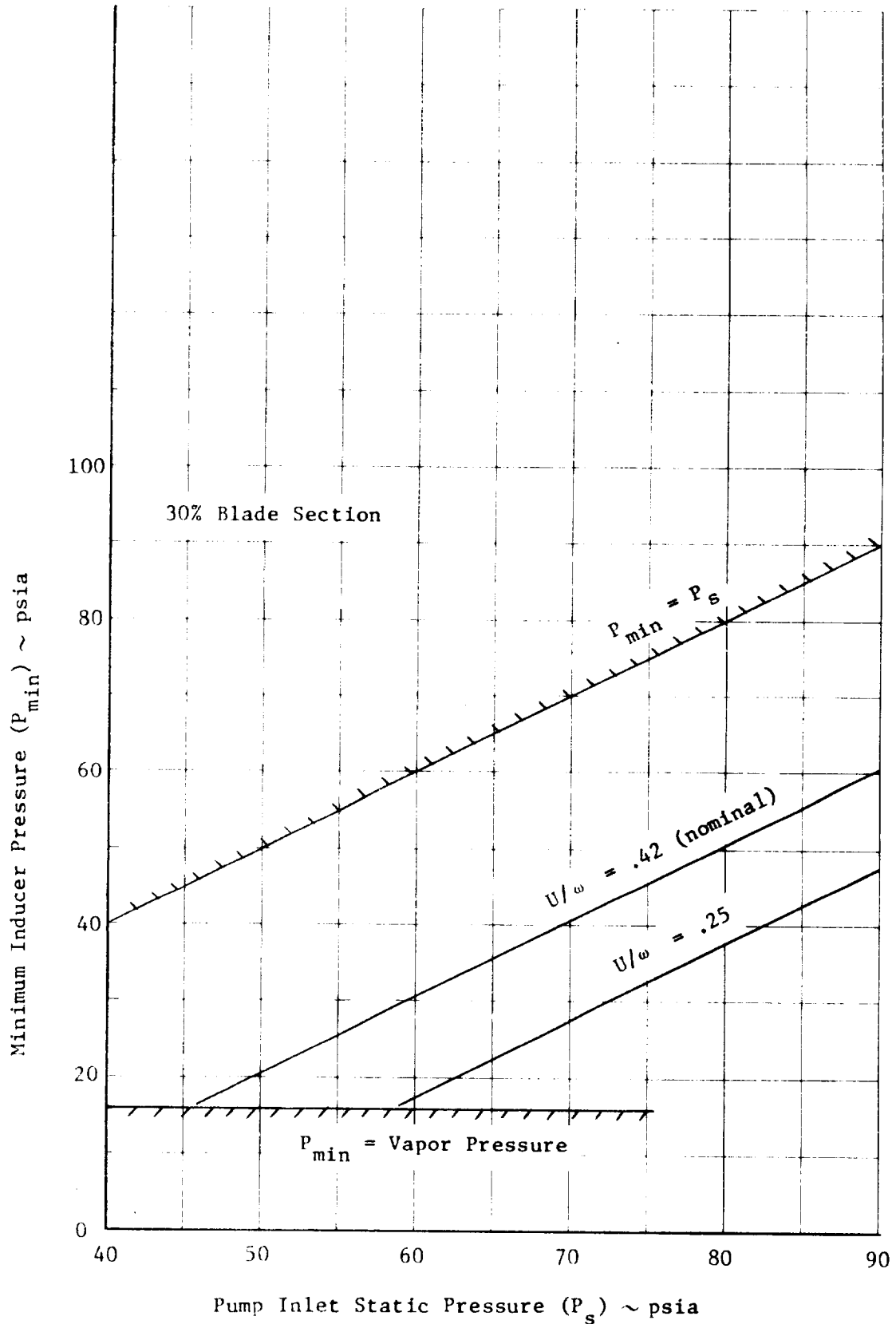
Figure 5.16 H-1 LOX Minimum Predicted Inducer Pressure
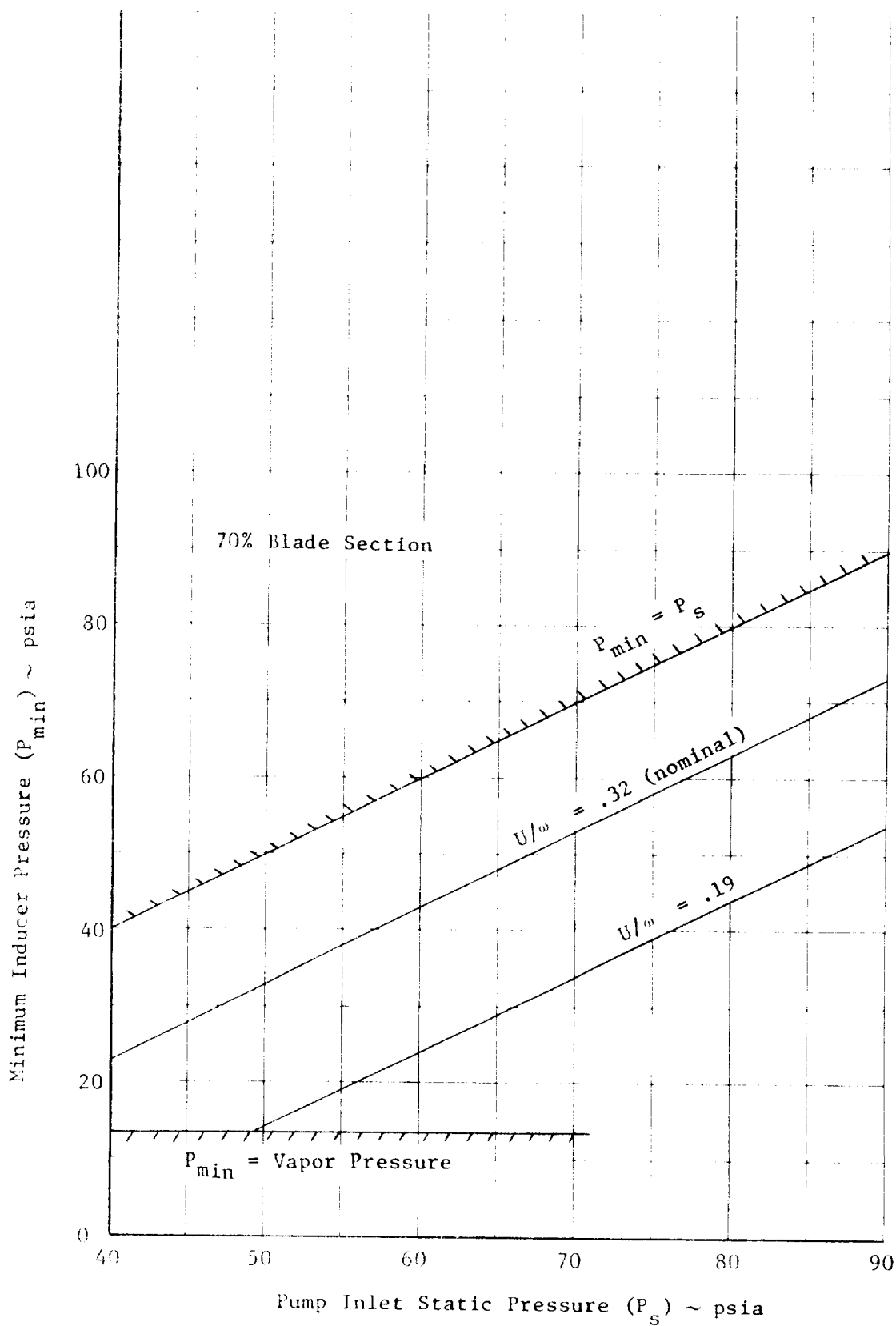
Figure 5.17 LR37 Oxidizer Minimum Predicted Inducer Pressure

126

J-2 LOX INDUCER
50% BLADE SECTION
U/ω = .33 in/rad
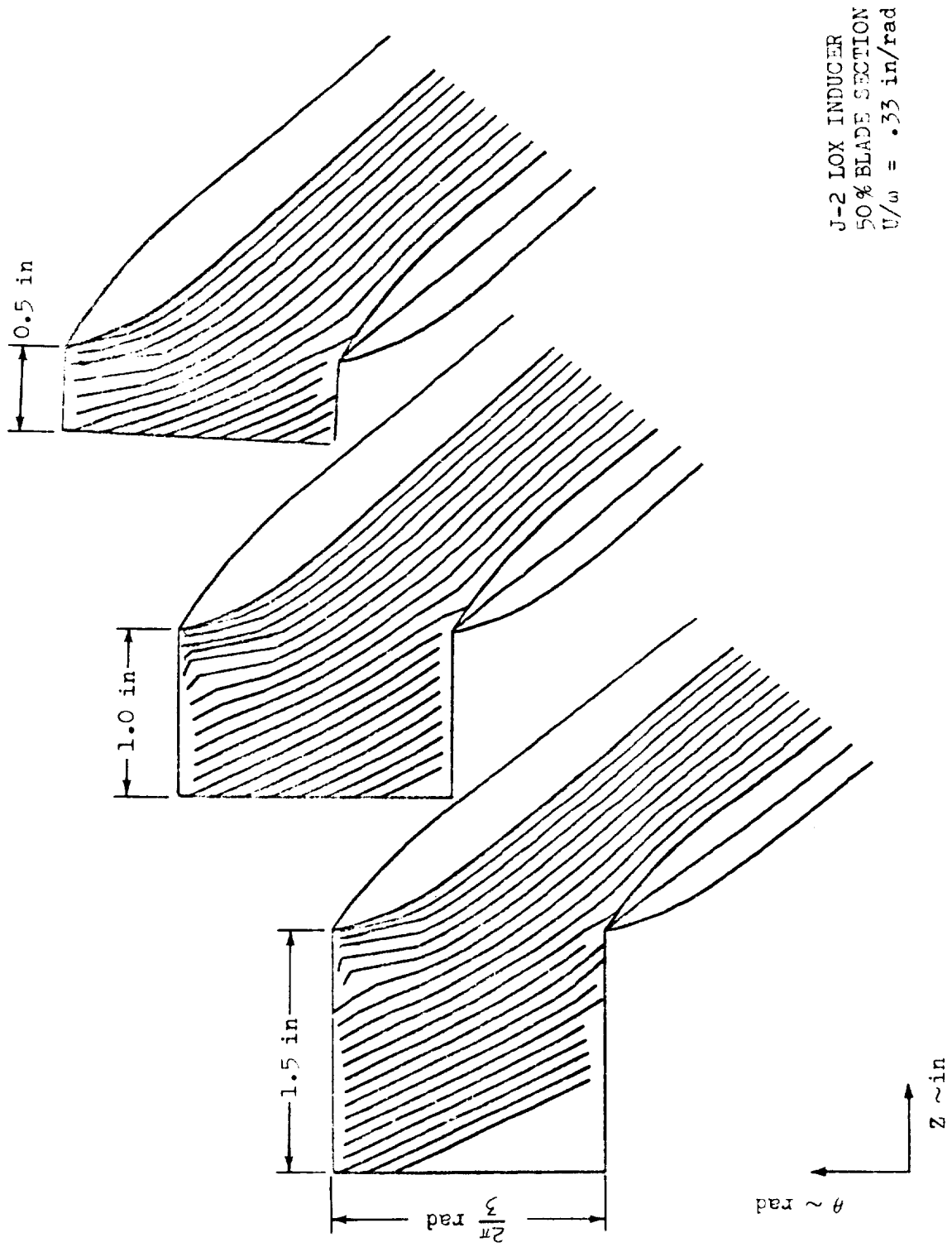
Figure 5.18   Effect of Inlet Boundary Conditions
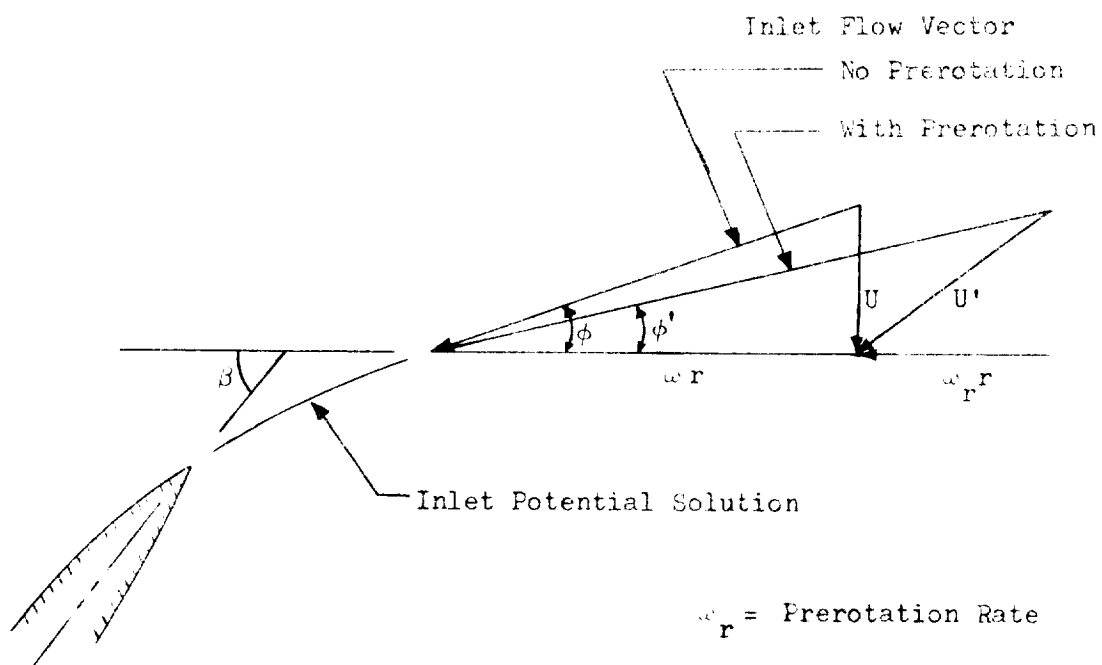
Figure 5.19 Effect of Prerotation on Inlet Flow Vector
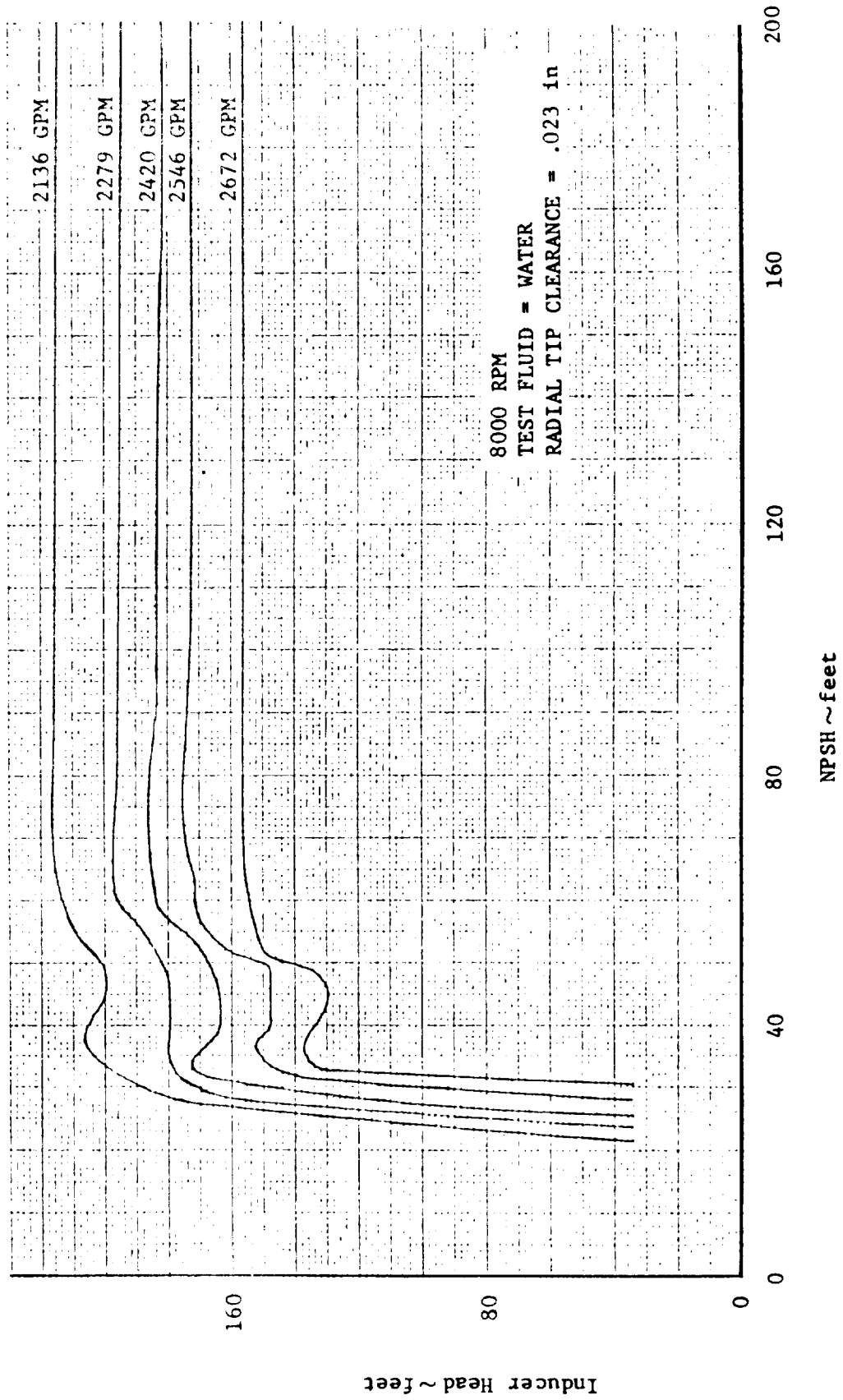
Figure 5.20   J-2 LOX Inducer Suction Performance
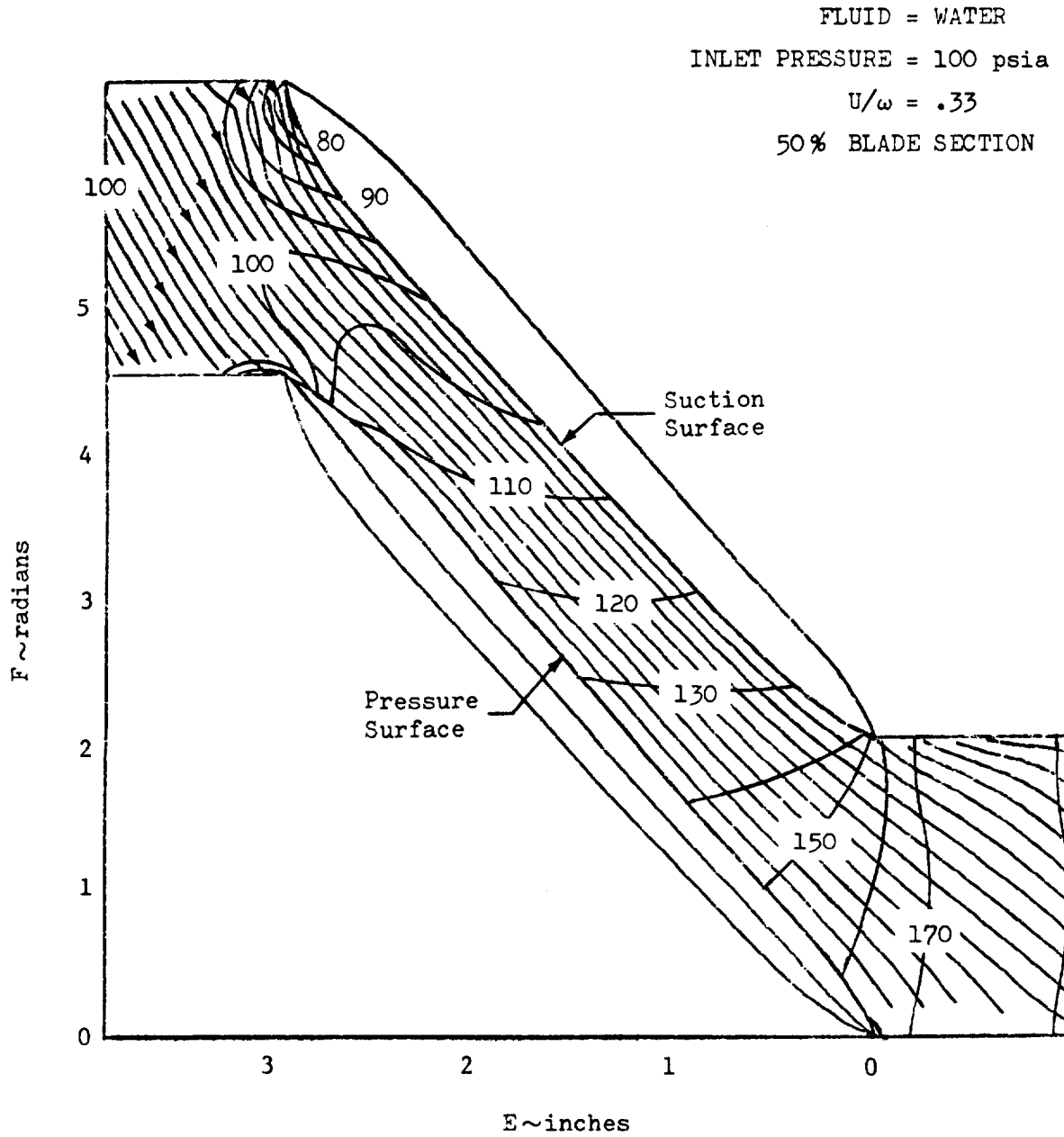
Figure 5.21   J-2 Inducer Pressure Profiles
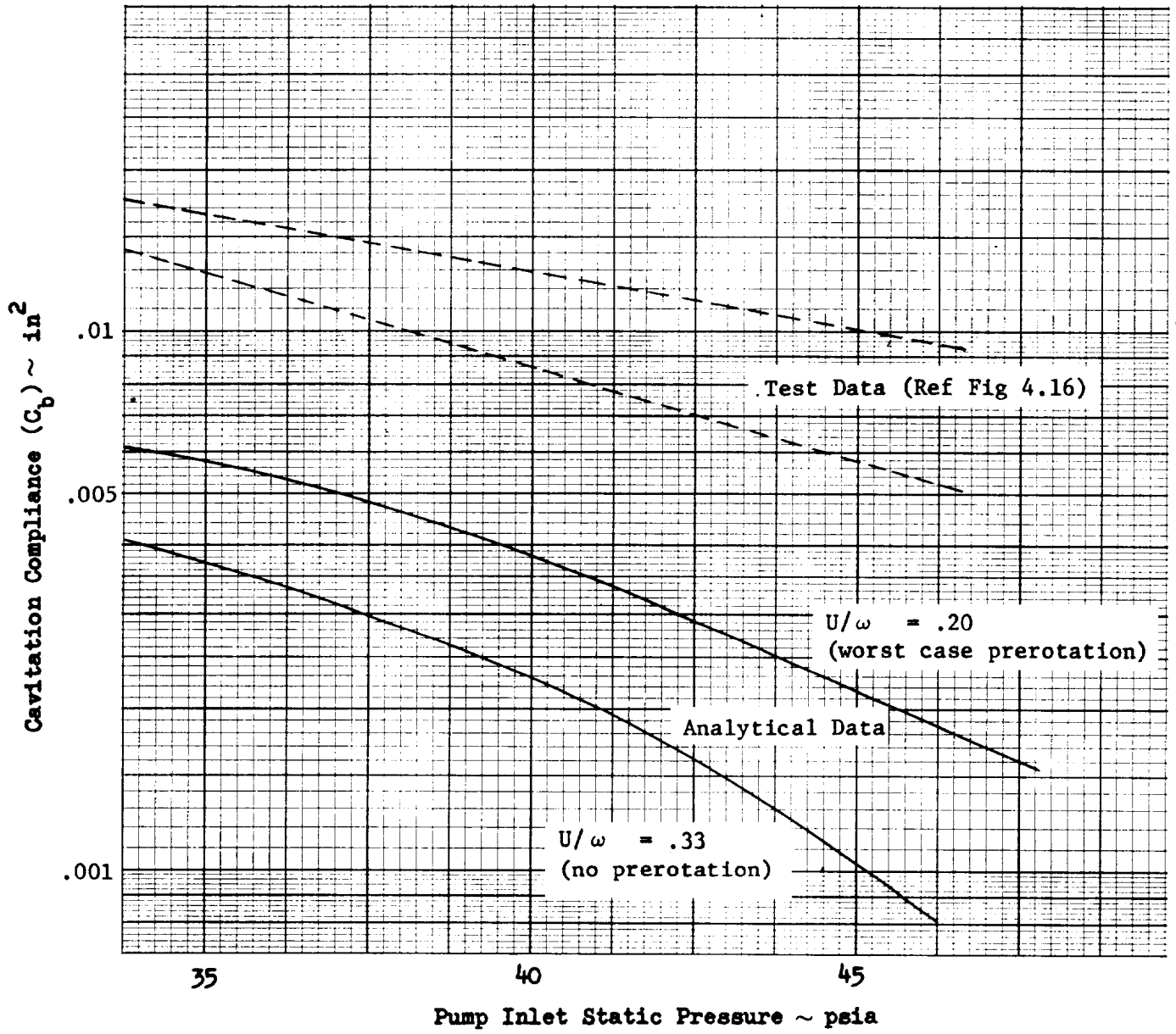
Figure 5.22   J-2 Lox Analytical-Empirical Comparison
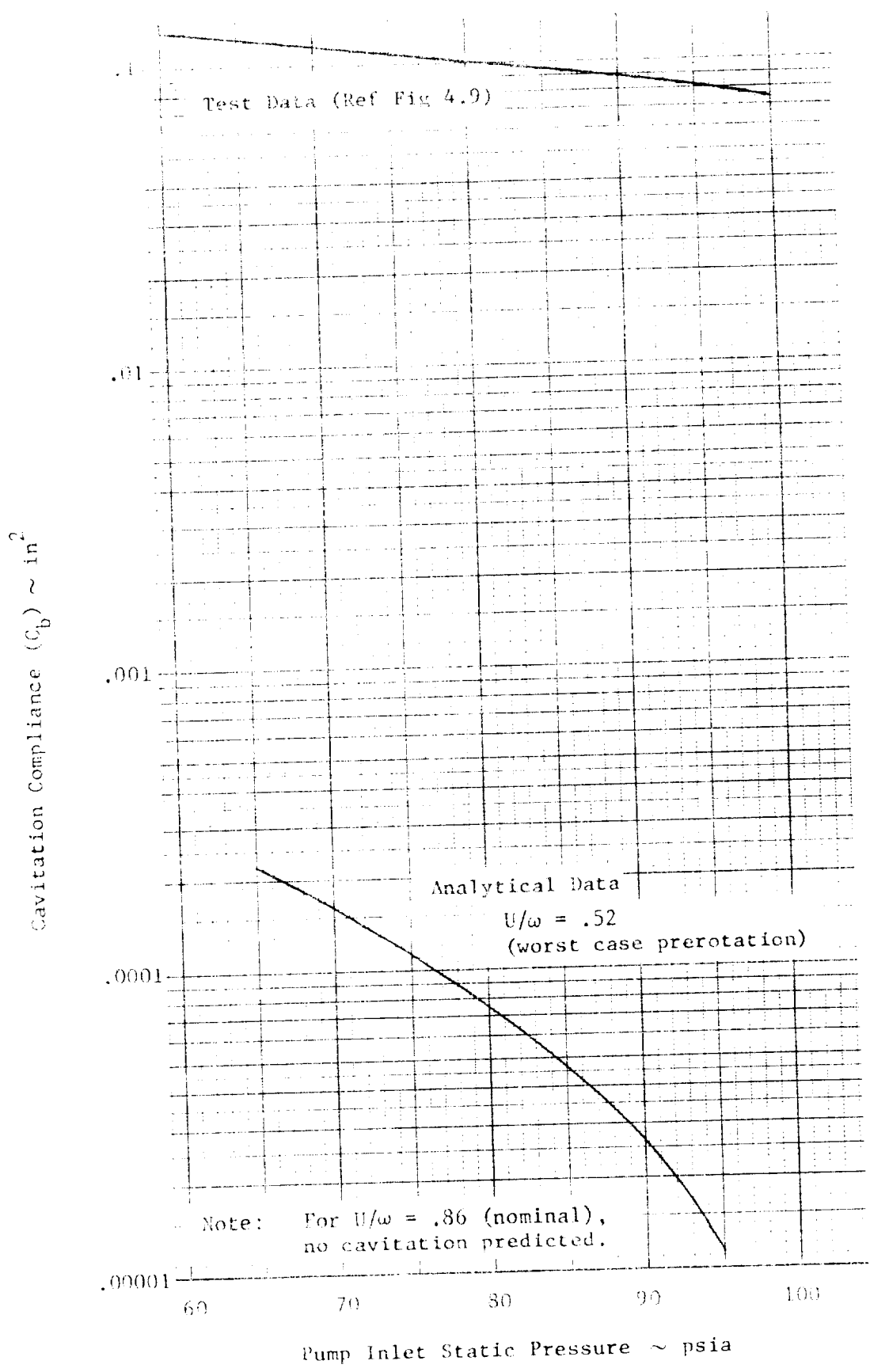
Figure 5.23   F-1 LOX Analytical-Empirical Comparison

(This page intentionally left blank)

6. Conclusions and Recommendations

6. CONCLUSIONS AND RECOMMENDATIONS

The following conclusions and recommendations are based on the analysis of available test data, the turbopump cavitation model development, the analysis of the model results, and the correlation between test data and model predictions.

a. Large uncertainties exist in most cavitation compliance values derived from test data. This is because the objective of the tests was to determine natural frequency, and cavitation compliance must usually be derived from an assumed relationship.

b. Cavitation compliance test results for all available turbopump configurations do not correlate with any simple nondimensional combination of turbopumps and fluid parameters.

c. Compliance derived from a phase change process is a function of the local flow conditions and, unlike compressibility of a gas, is not necessarily directly proportional to the vapor volume.

d. The turbopump pressure field, derived from a potential solution, will not predict a large enough blade surface cavitation region to yield agreement with test results.

e. Mechanisms other than blade cavitation contribute the major amount of total turbopump compliance.

f. Turbopump pulse tests, using accurate inlet and outlet dynamic flow meters, should be conducted for the purpose of investigating cavitation compliance. These tests should vary the following parameters

one at a time: test fluid, dissolved gas, operating conditions (pressure, speed, and flow), tip clearance, natural frequency and oscillation amplitude (effect of nonequilibrium phase changes), etc.

g. Precise analytical simulation of the cavitation process can not be obtained until a dedicated test program (item f.) is performed.

7. References

7. REFERENCES

1. E. Avdlad: Prevention of Coupled Structure - Propulsion Instability (POGO). NASA Space Vehicle Design Criteria. NASA SP-8055. National Aeronautics and Space Administration, October, 1970.

2. R. L. Goldman and G. C. Reis: A Method for Determining the POGO Stability of Large Launch Vehicles. Technical Report No. TR 69-7C. Martin Marietta Corporation (RIAS), Baltimore, Maryland, June, 1969.

3. R. D. Vaage and R. A. Zehnle: Linear Equation Development System Coupled Longitudinal Oscillations (POGO). TM 0472/20-68. Martin Marietta Corporation, Denver, Colorado, May, 1968.

4. F. E. Bikle, L. E. Fidler and J. B. Rohrs: A Study of System Coupled Instability Analysis Techniques. Technical Report AFRPL-TR-66-143. Air Force Rocket Propulsion Laboratory, Edwards Air Force Base, California, July, 1966.

5. F. E. Bikle, L. E. Fidler and T. C. Hendricks: System Coupled Dynamic Instability Amplitude Limiting Analysis and Evaluation Final Report. Technical Report AFRPL-TR-68-41. Air Force Rocket Propulsion Laboratory, Edwards Air Force Base, California, March, 1968.

6. A. L. Worlund, et al: "The Reduction of POGO Effects by Gas Injection." AIAA Second Propulsion Joint Conference, Colorado Springs, Colorado, June, 1966.

7. R. L. Rich: "Saturn V POGO and a Solution." AIAA Structural Dynamics and Aeroelasticity Specialist Conference, New Orleans, Louisiana, April, 1969.

8. F. G. Hammit: Impact and Cavitation Erosion and Material Mechanical Properties. Report No. 03371-1-T. Cavitation and Multiphase Flow Lab, Michigan University, Ann Arbor, Michigan, November, 1969.

9. Frederick G. Hammitt: Collapsing Bubble Damage to Solids. AROD-6310:10-E. Cavitation and Multiphase Flow Lab, Michigan University, Ann Arbor, Michigan, 1969.

136

10. Frederick G. Hammitt and David M. Ericson, Jr.: <u>Scale Effects Including Gas Content Upon Cavitation in a Flowing System</u>. Technical Report 01357-11-T. Cavitation and Multiphase Flow Lab, Michigan University, Ann Arbor, Michigan, May, 1969.

11. Frank R. Schiebe: <u>The Influence of Gas Nuclei Size Distribution on Transient Cavitation Near Inception</u>. Report No. 107. St. Anthony Falls Hydraulic Lab, Minnesota University, Minneapolis, Minnesota, May, 1969.

12. L. H. Bernd: <u>Study of the Surface Films of Gas Nuclei (As Related to Cavitation and Tensile Strength in Water)</u>. Report TIS64GL143. Advanced Technology Laboratories, General Electric Co., September, 1964.

13. M. D. Rosenberg: <u>Gaseous-Type Cavitation in Liquids</u>. Technical Memorandum 26. Acoustics Research Laboratory, Harvard University, Cambridge, Massachusetts, August, 1953.

14. D. M. Ericson, Jr.: <u>Observations and Analyses of Cavitating Flow in Venturi Systems</u>. NASA-CR-106115. Dept. of Mechanical Engineering, Michigan University, Ann Arbor, Michigan, July, 1969.

15. M. S. Plesset and P. S. Epstein: "The Stability of Gas Bubbles in Liquid-Gas Solution." <u>Journal of Chemical Physics</u>. Vol. 18, No. 11, November, 1950.

16. M. S. Plesset and S. A. Zwick: "A Nonsteady Heat Diffusion Problem With Spherical Symmetry." <u>Journal of Applied Physics</u>, Vol. 23, No. 1, January, 1952.

17. M. S. Plesset and S. A. Zwick: "The Growth of Vapor Bubbles in Superheated Liquids." <u>Journal of Applied Physics</u>, Vol. 25, No. 1, April, 1954.

18. L. A. Skinner and S. G. Bankoff: "Dynamics of Vapor Bubbles in Spherically Symmetric Temperature Fields of General Variation." <u>The Physics of Fluids</u>, Vol. 7, No. 1, January, 1964.

19. H. K. Forster and N. Zuber: "Growth of a Vapor Bubble in a Superheated Liquid." <u>Journal of Applied Physics</u>, Vol. 25, No. 1, April, 1954.

20. A. J. Stepanoff: "Cavitation in Centrifugal Pumps with Liquids Other Than Water." _Journal of Engineering for Power_, January, 1961.

21. A. J. Stepanoff: "Cavitation Properties of Liquids." _Journal of Engineering for Power_. Paper 63-AHGT-22.

22. J. K. Jakobsen: "On the Mechanism of Head Breakdown in Cavitating Inducers." _Journal of Basic Engineering_, Paper 63-AHGT-29.

23. L. B. Stripling and A. J. Acosta: "Cavitation in Turbopumps." _Journal of Basic Engineering_, Part 1, September, 1962.

24. L. B. Stripling: "Cavitation in Turbopumps." _Journal of Basic Engineering_, Part 2, September, 1962.

25. R. B. Wade: _Flow Past a Partially Cavitating Cascade of Flat Plate Hydrofoils_. Report E-79-4. California Institute of Technology, Pasadena, California, January, 1963.

26. R. E. Davis, L. L. Coons and D. D. Scheer: "Internal Streamline Flow Analysis for Turbopump Inducers Under Cavitating and Noncavitation Conditions." AIAA Paper No. 70-629, June, 1970.

27. M. S. Plesset: "The Dynamics of Cavitation Bubbles." _Journal of Applied Mechanics_, September, 1949.

28. M. S. Plesset: _Bubble Dynamics_. Report 85-23. California Institute of Technology, Pasadena, California, February, 1963.

29. F. R. Gilmore: _The Growth or Collapse of a Spherical Bubble in a Viscous Compressible Fluid_. Report 26-4. Hydrodynamics Laboratory, California Institute of Technology, Pasadena, California, April, 1952.

30. C. Hunter: "On the Collapse of an Empty Cavity in Water." _Fluid Mechanics_, Vol. 8, August, 1960.

31. F. Ghahremani: _Turbopump Cavitation Compliance_. Report TOR-0059(6531-01)-2, The Aerospace Corporation, El Segundo, California, September, 1970.

138

32. R. F. Soltis and M. J. Miller: Visual Observations of Flow Through a Radial-Bladed Centrifugal Impeller. NASA TN D-4282. National Aeronautics and Space Administration, Washington, D. C.

33. S. M. Futral, Jr., and D. E. Holeski: Experimental Results of Varying the Blade-Shroud Clearance in a 6.02 Inch Radial-Inflow Turbine. NASA TN D-5513. National Aeronautics and Space Administration, Washington, D. C., January, 1970.

34. L. W. Norquist, et al: "Development of Close-Coupled Accumulators for Suppressing Missile Longitudinal Oscillations (POGO)." Paper No. 69-547, AIAA Fifth Propulsion Joint Specialists Conference (Colorado Springs, Colorado), June 9-13, 1969.

35. L. A. Weber: Thermodynamics and Related Properties of Oxygen From the Triple Point to 300°K at Pressures to 330 Atmospheres. NBS Report 9710A. National Bureau of Standards, Boulder, Colorado, August, 1968.

36. R. V. Southwell: Relaxation Methods in Theoretical Physics. Oxford University Press, London, England, 1952.

37. R. Zehnle and J. Knapp: POGO Linear Stability Analysis Techniques and Computer Programs. TM 0472-10-70-03. Martin Marietta Corporation, Denver, Colorado, April, 1970.

38. R. G. Wagner and S. Rubin: Detection of Titan POGO Characteristics by Analysis of Random Data. Report No. TR-0066(5305)-3. Aerospace Corporation, El Segundo, California, February, 1970.

39. LOX Suction Duct Dynamic Evaluation, D13339, Summary of Test Results. D5-14061. The Boeing Company, Southeast Division, Launch Vehicle Branch, May, 1970.

40. A Compendium of the Properties of Materials at Low Temperatures. WADD-TR-60-56. National Bureau of Standards, Cryogenic Engineering Laboratory, Boulder, Colorado, December, 1961.

41. B. K. Aldrich: *S-IC Propellant Feed System POGO Study*. Internal Note - Test 3-67. Fluid Mechanics Test Section, Marshall Space Flight Center Test Laboratory, Alabama, January, 1967.

42. J. C. Pearson: *S-IC Single Engine POGO Tests*. Memorandum S&E-ASTN-TSF-#28-70. Marshall Space Flight Center, Alabama, May, 1970.

43. *S-IC LOX Inboard and Outboard PVC Pressure Testing*. Memorandum R-TEST-CT-69-68. Marshall Space Flight Center, Alabama, October, 1968.

44. *Engine System Transfer Functions for Support of S-V Vehicle Longitudinal Stability (POGO) Analysis Program*. R-6929. Rocketdyne, North American Rockwell, Canoga Park, California, March, 1967.

45. G. L. Murphy: *Summary Report - POGO Suppression Analysis of the S-II and S-IVB LOX Feed Systems*. ASD-ASTN-1040. Brown Engineering Company, Huntsville, Alabama, November, 1969.

46. *Investigation of 17 Hertz Closed-Loop Instability on S-II Stage of Saturn V*. R-7970. Rocketdyne, North American Rockwell, Canoga Park, California, August, 1969.

47. "Current J-2 Engine Transfer Functions and LOX Pump Termination Impedance, G(S)." Letter S&E-ASTN-A-70-113. NASA, Marshall Space Flight Center, Alabama, September, 1970.

48. "Saturn V POGO Working Group Meeting Presentation (Boeing)." Marshall Space Flight Center, Alabama, February 18, 1971.

49. *Comparison Between Brown's and Rocketdyne's Pump Cavitation Compliance Results for H-1 Fuel and LOX Bobtail Test Stand Runs*. Memorandum TD-D1-PTF-021-50. Brown Engineering Company, Huntsville, Alabama, March 1, 1967.

50. *S-IB Propellant Feed System "POGO" Study*. Internal Note-Test-15-67. Marshall Space Flight Center, Alabama, 1967.

51. R. D. Hill: *Frequency Response of Propellant Feed Lines and Turbopump by Pulsing Either Below the Pump or Above the Pump on the Bobtail Test Stand*. Brown Engineering Company, Huntsville, Alabama, June, 1968.

52. ATM66(6182-03)-866-2433, 3-22, Aerospace Corporation, El Segundo, California, March 25, 1966 (Unpublished).

53. F. C. O'Hern: "J-2 Oxidizer Inducer Performance", Internal Letter No. D/596/115, North American Rockwell, 29 January 1971.

54. Chung-Hua Wu: A General Theory of Three Dimensional Flow in Subsonic and Supersonic Turbomachines of Axial, Radial, and Mixed Flow Types. NACA TN 2604. National Advisory Committee for Aeronautics, January, 1952.

55. "CDC 280 Software Package" Appendix A, Report M-69-27, Martin Marietta Corporation, Denver, Colorado.

56. F. Ghahremani: "Empirical Evaluation of Pump Inlet Compliance" - Monthly Status Reports (September 1971 through March 1972). Aerospace Corporation, El Segundo, California.

Appendixes

APPENDIX A

Equations of Motion in Impeller Meridional Plane

For a (r,θ,z) coordinate system (Figure A.1), the equations of relative motion for a turbopump impeller rotating with angular velocity ω about z (Reference 53) are:

$$\rho\left[\frac{\partial V_r}{\partial t} + V_r \frac{\partial V_r}{\partial r} + \frac{V_\theta}{r} \frac{\partial V_r}{\partial \theta} + V_z \frac{\partial V_r}{\partial z} - \frac{(V_\theta + \omega r)^2}{r}\right]$$

$$= -\frac{\partial P}{\partial r} - \left[\frac{1}{r}\frac{\partial}{\partial r}(r \cdot \tau_{rr}) + \frac{1}{r}\frac{\partial \tau_{r\theta}}{\partial \theta} - \frac{1}{r}\tau_{\theta\theta} + \frac{\partial \tau_{rz}}{\partial z}\right] + \rho g_r \qquad (A.1)$$

$$\rho\left(\frac{\partial V_\theta}{\partial t} + V_r \frac{\partial V_\theta}{\partial r} + \frac{V_\theta}{r}\frac{\partial V_\theta}{\partial \theta} + V_z \frac{\partial V_\theta}{\partial z} + \frac{V_R V_\theta}{r} + 2\omega V_r\right)$$

$$= -\frac{1}{r}\frac{\partial P}{\partial \theta} - \left[\frac{1}{r^2}\frac{\partial}{\partial r}\left(r^2 \tau_{r\theta} + \frac{1}{r}\frac{\partial \tau_{\theta\theta}}{\partial \theta} + \frac{\partial \tau_{\theta z}}{\partial z}\right)\right] + \rho g_\theta \qquad (A.2)$$

$$\rho\left(\frac{\partial V_z}{\partial t} + V_r \frac{\partial V_z}{\partial r} + \frac{V_\theta}{r}\frac{\partial V_z}{\partial \theta} + V_z \frac{\partial V_z}{\partial z}\right)$$

$$= -\frac{\partial P}{\partial z} - \left[\frac{1}{r}\frac{\partial}{\partial r}(r\tau_{rz}) + \frac{1}{r}\frac{\partial \tau_{\theta z}}{\partial \theta} + \frac{\partial \tau_{zz}}{\partial z}\right] + \rho g_z \qquad (A.3)$$

where $\rho \cdot V_\theta^2 / r$ is the centrifugal force. It gives the effective force in the r direction due to fluid motion in the θ direction. The term $\rho \cdot V_r \cdot V_\theta / r$ is the coriolis force. It is the effective force in the θ direction when there is flow in both the r and θ directions. For steady inviscid flow in the absence of gravity equations (A.1) through (A.3) can be written

$$\frac{dV_r}{dt} - \frac{(V_\theta + \omega r)^2}{r} = -\frac{1}{\rho}\frac{\partial P}{\partial r} = V_r \frac{\partial V_r}{\partial r} + \frac{V_\theta}{r}\frac{\partial V_r}{\partial \theta} + V_z \frac{\partial V_r}{\partial z} - \frac{(V_\theta + \omega r)^2}{r} \quad (A.4)$$

142
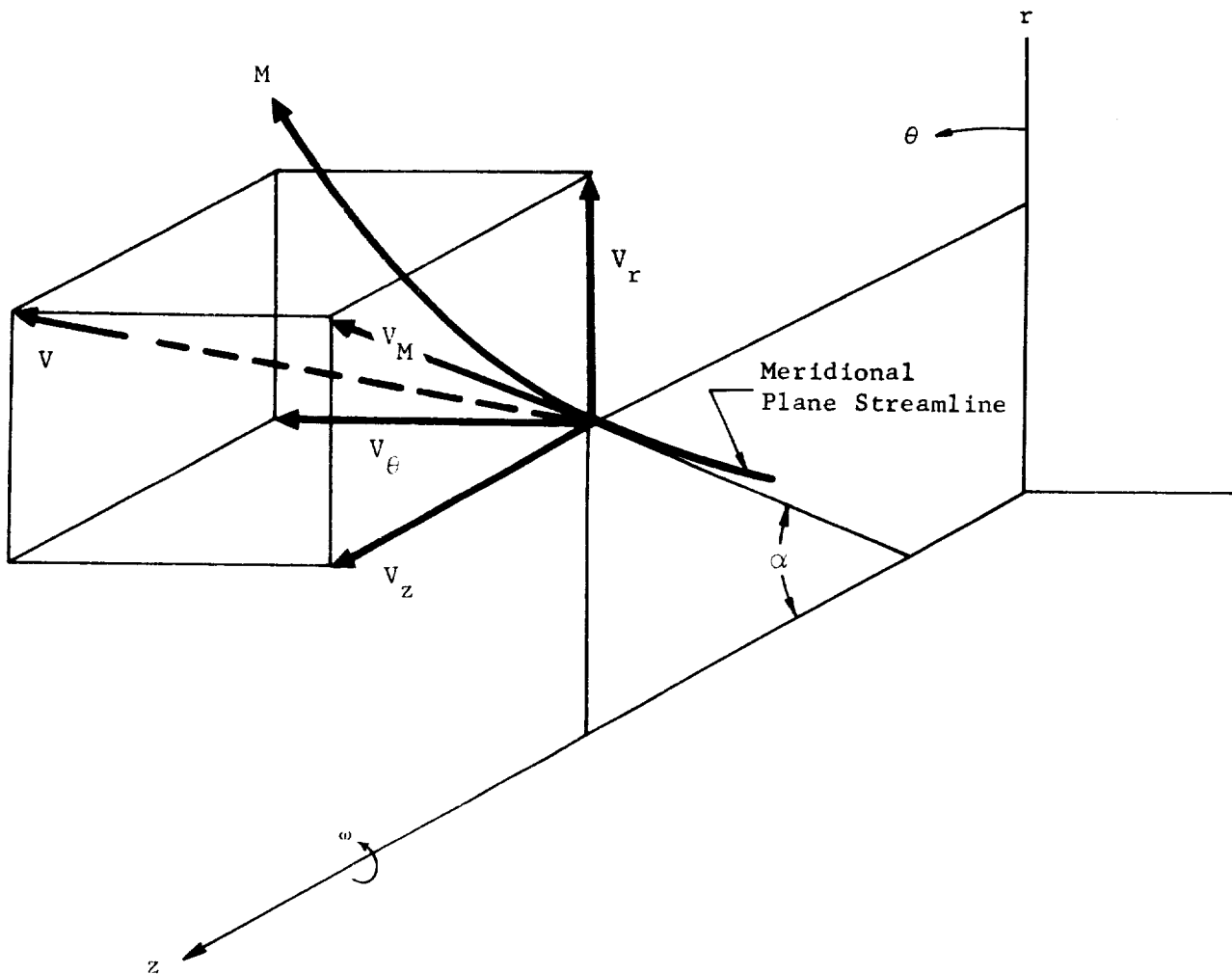
Figure A.1   Fluid Element Coordinates

$$\frac{dV_\theta}{dt} + \frac{V_r V_\theta}{r} + 2\omega V_r = - \frac{1}{\rho r}\frac{\partial P}{\partial \theta}$$

$$= V_r \frac{\partial V_\theta}{\partial r} + \frac{V_\theta}{r}\frac{\partial V_\theta}{\partial \theta} + V_z \frac{\partial V_\theta}{\partial z} + \frac{V_r V_\theta}{r} + 2\omega V_r \qquad (A.5)$$

$$\frac{dV_z}{dt} = -\frac{1}{\rho}\frac{\partial P}{\partial z} = V_r \frac{\partial V_z}{\partial r} + \frac{V_\theta}{r}\frac{\partial V_z}{\partial \theta} + V_z \frac{\partial V_z}{\partial z} \qquad (A.6)$$

Assuming the vanes of the impeller guide the fluid or that channel flow exists approximately, a stream surface may be constructed half way between blades (Figure A.2). The stream surface S can be described by

$$S = S(r, \theta, z) \qquad (A.7)$$

Solving for θ,

$$\theta = \theta(r, z) \qquad (A.8)$$

The static pressure in a turbopump is generally a function of r, θ and z:

$$P = P(r, \theta, z). \qquad (A.9)$$

On S

$$P^* = P(r, \theta(r,z), z) \qquad (A.10)$$

since θ on the surface is specified by Equation (A.8). The relation between the partial derivatives of static pressure in the three-dimensional field to that on the stream surface "S" is:

$$\frac{\partial P^*}{\partial r} = \frac{\partial P}{\partial r} + \frac{\partial P}{\partial \theta}\frac{\partial \theta}{\partial r} \qquad (A.11)$$

$$\frac{\partial P^*}{\partial z} = \frac{\partial P}{\partial z} + \frac{\partial P}{\partial \theta}\frac{\partial \theta}{\partial z} \qquad (A.12)$$

Substituting Equations (A.11) and (A.12) into (A.4) and (A.6),

$$\frac{dV_r}{dt} - \frac{(V_\theta + r\omega)^2}{r} = -\frac{1}{\rho}\left(\frac{\partial P^*}{\partial r} - r\frac{\partial \theta}{\partial r}\cdot\frac{1}{r}\frac{\partial P}{\partial \theta}\right) \qquad (A.13)$$

144

$$\frac{dV_\theta}{dt} + \frac{V_r V_\theta}{r} + 2\omega V_r = -\frac{1}{\rho r}\frac{\partial P}{\partial \theta} \tag{A.14}$$

$$\frac{dV_z}{dt} = -\frac{1}{\rho}\left(\frac{\partial P^*}{\partial z} - r\frac{\partial \theta}{\partial z} \cdot \frac{1}{r}\frac{\partial P}{\partial \theta}\right) \tag{A.15}$$
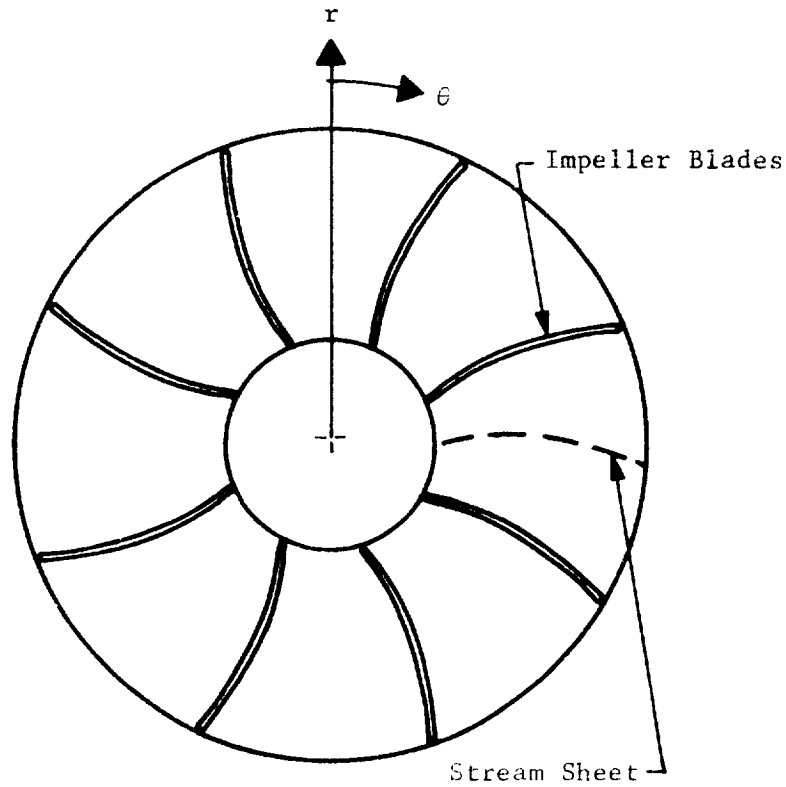
Figure A.2   Axial View of Impeller

The circumferential pressure gradient $\frac{1}{r}\frac{\partial P}{\partial \theta}$ can be eliminated from Equations (A.13) and (A.15) by (A.14)

$$\frac{dV_r}{dt} - \frac{(V_\theta + \omega r)^2}{r} = -\frac{1}{\rho}\left[\frac{\partial P^*}{\partial r} + r^\rho\frac{\partial \theta}{\partial r}\left(\frac{dV_\theta}{dt} + \frac{V_r V_\theta}{r} + 2\omega V_r\right)\right]$$

$$\frac{dV_r}{dt} - \frac{V_\theta'^2}{r} = -\frac{1}{\rho}\left[\frac{\partial P^*}{\partial r} + r^\rho\frac{\partial \theta}{\partial r}\left(\frac{1}{r}\frac{\partial}{\partial t}(rV_\theta')\right)\right] \tag{A.16}$$

where $V_\theta' = V_\theta + \omega r$ and $dr/dt = V_r$.

$$\frac{dV_z}{dt} = -\frac{1}{\rho}\left[\frac{\partial P^*}{\partial z} + r\rho\frac{\partial \theta}{\partial z}\left(\frac{dV_\theta}{dt} + \frac{V_r V_\theta}{r} + \dots V_r\right)\right]$$

$$\frac{dV_z}{dt} = -\frac{1}{\rho}\left[\frac{\partial P^*}{\partial z} + r\rho\frac{\partial \theta}{\partial z}\left(\frac{1}{r}\frac{d}{dt}\left(rV_\theta'\right)\right)\right] \tag{A.17}$$

If the flow is restricted to a streamline on the stream sheet and the streamline is projected on the meridional plane (Figures A.3 and A.4), the tangent to the projected streamline at any point makes an angle α with the impeller axis.
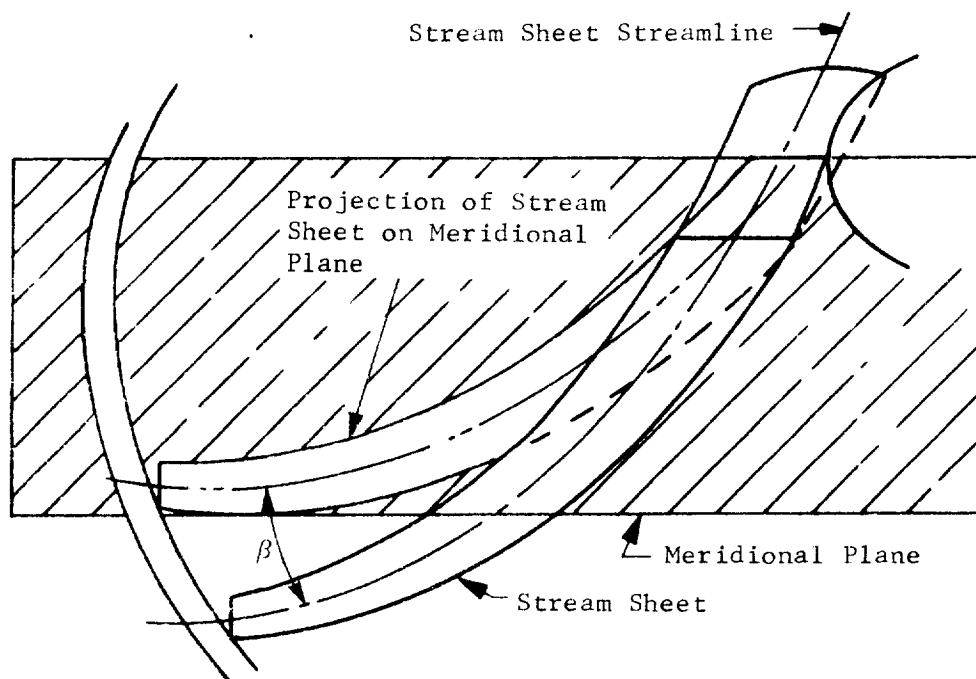
Figure A.3   Projection of Stream Sheet on Meridional Plane
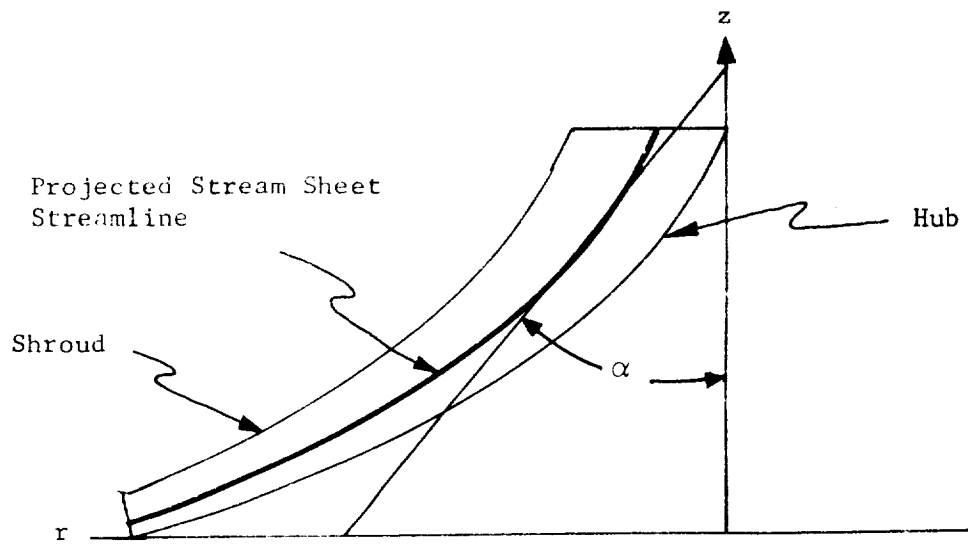
Figure A.4   Meridional Plane of Impeller
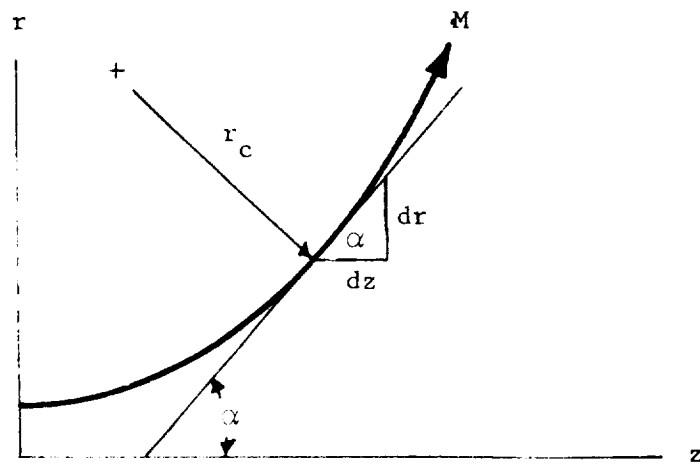
Figure A.5   Meridional Streamline

The velocity components V_r and V_z of the stream sheet streamline lead to a velocity V_M in the meridional plane where:

$$V_m^2 = V_r^2 + V_z^2 \tag{A.18}$$

$$V_r = V_m \sin \alpha \tag{A.19}$$

$$V_z = V_m \cos \alpha \tag{A.20}$$

Differentiating,

$$\frac{dV_r}{dt} = \frac{dV_M}{dt} \sin \alpha + V_M \frac{d\alpha}{dt} \cos \alpha \tag{A.21}$$

$$\frac{dV_z}{dt} = \frac{dV_M}{dt} \cos \alpha - V_M \frac{d\alpha}{dt} \sin \alpha \tag{A.22}$$

α is related to the radius of curvature of the projected streamline by

$$dM = r_c \, d\alpha \tag{A.23}$$

or

$$\frac{1}{r_c} = \frac{d\alpha}{dM} = \frac{\frac{d\alpha}{dt}}{\frac{dM}{dt}} = \frac{1}{V_M} \frac{d\alpha}{dt} \tag{A.24}$$

$$\therefore \frac{d\alpha}{dt} = \frac{V_M}{r_c} \tag{A.25}$$

Combining Equations (A.16) through (A.25),

$$\frac{dV_M}{dt} \cos \alpha - \frac{V_M^2}{r_c} \sin \alpha = - \frac{1}{\rho} \left\{ \frac{\partial P^*}{\partial z} + r\rho \frac{\partial \theta}{\partial z} \left[\frac{1}{r} \frac{d(rV'_\theta)}{dt} \right] \right\} \tag{A.26}$$

$$\frac{dV_M}{dt} \sin \alpha + \frac{V_M^2}{r_c} \cos \alpha = \frac{V_\theta'^2}{r} - \frac{1}{\rho} \left\{ \frac{\partial P^*}{\partial r} + r\rho \frac{\partial \theta}{\partial r} \left[\frac{1}{r} \frac{\partial(rV_\theta')}{\partial r} \right] \right\} \qquad (A.27)$$

$$\frac{dP^*}{dN} = \frac{\partial P^*}{\partial r} \frac{\partial r}{\partial N} + \frac{\partial P^*}{\partial z} \frac{\partial z}{\partial N} \qquad (A.28)$$

$$\frac{\partial r}{\partial N} = \cos \alpha \quad \text{and} \quad \frac{\partial z}{\partial N} = -\sin \alpha \qquad (A.29)$$

$$\therefore \frac{dP^*}{dN} = \frac{\partial P^*}{\partial r} \cos \alpha - \frac{\partial P^*}{\partial z} \sin \alpha \qquad (A.30)$$

where $\frac{d}{dN}$ is the derivative with respect to the normal to the streamline.

Multiplying Equation (A.26) by $\sin \alpha$ and substituting Equation (A.30)

$$\frac{dV_M}{dt} \sin \alpha \cdot \cos \alpha - \frac{(V_M \sin \alpha)^2}{r_c} =$$

$$- \frac{1}{\rho} \left[\frac{\partial P^*}{\partial r} \cos \alpha - \frac{\partial P^*}{\partial N} + r\rho \frac{\partial \theta}{\partial z} \left(\frac{1}{r} \frac{d(rV_\theta')}{dt} \right) \sin \alpha \right] \qquad (A.31)$$

Multiplying Equation (A.27) by $\cos \alpha$

$$\frac{dV_M}{dt} \sin \alpha \cdot \cos \alpha + \frac{(V_M \cos \alpha)^2}{r_c} - \frac{V_\theta'^2}{r} \cos \alpha =$$

$$- \frac{1}{\rho} \left[\frac{\partial P^*}{\partial r} \cos \alpha + r\rho \frac{\partial \theta}{\partial r} \left(\frac{1}{r} \frac{\partial(rV_\theta')}{\partial t} \right) \cos \alpha \right] \qquad (A.32)$$

Subtracting Equation (A.31) from (A.32)

$$\frac{V_M^2}{r_c} - \frac{V_\theta'^2}{r} \cos \alpha = - \frac{1}{\rho} \frac{\partial P^*}{\partial N} + \frac{1}{\rho r} \left(r\rho \frac{\partial \theta}{\partial z} \sin \alpha - r\rho \frac{\partial \theta}{\partial r} \cos \alpha \right) \left(\frac{d(rV_\theta')}{dt} \right) \qquad (A.33)$$

From Figure A.3 the velocity along the stream sheet streamline V is related to the projected velocity V_M and the velocity V_θ' by

$$V_M = V \cos \beta \tag{A.34}$$

$$V_\theta = V \sin \beta \quad \text{or} \quad V_\theta' = V \sin \beta + \omega r \tag{A.35}$$

Equation (A.33) becomes

$$\frac{(V \cos \beta)^2}{r_c} - \frac{(V \sin \beta + \omega r)^2}{r} \cos \sigma = -\frac{1}{\rho} \frac{\partial P}{\partial N} + \left\{ \frac{V \cos \beta}{\omega} \right\} \cdot$$

$$\left[\left(r \rho \frac{\partial \theta}{\partial z} \sin \sigma - r \rho \frac{\partial \theta}{\partial r} \cos \sigma \right) \left(\frac{dV_\theta}{dM} + \frac{V \sin \beta \sin \sigma}{r} + 2 \omega \sin \sigma \right) \right] \tag{A.36}$$

Multiplying Equation (A.4) by $V_r = \dfrac{dr}{dt}$, Equation (A.5) by $V_\theta = r \dfrac{d\theta}{dt}$, and Equation (A.6) by $V_z = \dfrac{dz}{dt}$ yields:

$$V_r \frac{dV_r}{dt} - \frac{V_r \left(V_\theta + \omega r \right)^2}{r} = -\frac{1}{\rho} \frac{\partial P}{\partial t} \tag{A.37}$$

$$V_\theta \frac{dV_\theta}{dt} + \frac{V_r V_\theta^2}{r} + 2\omega V_r V_\theta = -\frac{1}{\rho} \frac{\partial P}{\partial t} \tag{A.38}$$

$$V_z \frac{\partial V_z}{\partial t} = -\frac{1}{\rho} \frac{\partial P}{\partial t} \tag{A.39}$$

Adding the above three equations,

$$V_r \frac{dV_r}{dt} - \frac{V_r \omega^2 r^2}{r} + V_\theta \frac{dV_\theta}{dt} + V_z \frac{dV_z}{dt} = -\frac{3}{\rho} \frac{\partial P}{\partial t} \tag{A.40}$$

$$V^2 = V_r^2 + V_\theta^2 + V_z^2 \tag{A.41}$$

and

$$\frac{dV^2}{dt} = 2V_r \frac{dV_r}{dt} + 2V_\theta \frac{dV_\theta}{dt} + 2V_z \frac{dV_z}{dt} \tag{A.42}$$

$$\therefore \frac{1}{2} \frac{dV^2}{dt} - V_r \omega^2 r = -\frac{3}{\rho} \frac{dP}{dt} \tag{A.43}$$

Integrating Equations (A.42) and (A.43) along a streamline between a station in the pump inlet, i, and a point in the pump

$$\frac{1}{2}\left(V^2 - V_i^2\right) - \frac{\omega^2}{2}\left(r^2 - r_i^2\right) = -3\int_i \frac{dP}{\rho} \tag{A.44}$$

But

$$V'^2 = V_\theta'^2 + V_r^2 + V_z^2 \tag{A.45}$$

$$V_t' = V_\theta + \omega r \tag{A.46}$$

$$\therefore V'^2 = V_\theta^2 + V_r^2 + V_z^2 + 2\omega r V_\theta + \omega^2 r^2 \tag{A.47}$$

$$V'^2 = V^2 + 2\omega r V_\theta + \omega^2 r^2 \tag{A.48}$$

$$V'^2 = V^2 + 2\omega r V_\theta' - \omega^2 r^2 \tag{A.49}$$

and along a streamline Bernoulli's equation is

$$P_t = P + \frac{1}{2}\rho V^2 \tag{A.50}$$

If ω = const: Equation (A.44) can be written

$$\frac{V^2}{2} - \frac{\omega^2 r^2}{2} + \frac{2\omega r V_{\theta_i}}{2} - \frac{3P_{t_i}}{\rho} = -\frac{3P}{\rho} \tag{A.51}$$

Taking the derivative of Equation (A.51) with respect to N

$$V\frac{dV}{dN} - \omega^2 r\frac{dr}{dN} + \omega\frac{d}{dN}\left(rV_{\theta_i}'\right) - \frac{3}{\rho}\frac{\partial P_{t_i}}{\partial N} = -\frac{3}{\rho}\frac{\partial P}{\partial N} \tag{A.52}$$

Substituting Equation (A.52) into Equation (A.36)

$$V \frac{dV}{dN} = \dots r \frac{dr}{dN} - \omega \frac{\partial}{\partial N}\left(r V'_{\theta_i}\right) + \frac{3}{\rho} \frac{\partial P_{t_i}}{\partial N} + \frac{3(V \cos \beta)^2}{r_c} - 3\frac{(V \sin \beta + \omega r)^2}{r} \cos \alpha$$

$$-3\frac{V \cos \beta}{\dots}\left(r\frac{\rho \partial \theta}{\partial z} \sin \alpha - r\frac{\rho \partial \theta}{\partial r} \cos \theta\right)\left(\frac{dV_\theta}{dM} + \frac{V \sin \beta \sin \alpha}{r} + 2\omega \sin \alpha\right) \quad (A.53)$$

Equation (A.53) combined with hub and shroud boundary conditions, inlet conditions, and the continuity equation in the form:

$$\frac{\dot{W}}{N_b} = \int_{N_1}^{N_2} \int_{\theta_s}^{\theta_P} V \cdot r \cdot d\theta \cdot dN \quad (A.54)$$

where: $\dot{W}$ = total pump flow rate

N_1, N_2 = streamline numbers

θ_P = θ on pressure surface of blade

θ_s = θ on suction surface of adjacent blade

N_L = number of blades

provides a solution to the incompressible flow problem in the meridional plane. The solution involves the numerical integration of Equations (A.53) and (A.54) from streamline to streamline in the meridional plane.

APPENDIX B

Growth of a Thermal Cavitation Bubble

A thermal cavitation bubble appears in a turbopump when the local static pressure drops below the vapor pressure of the liquid. The bubble growth begins either on a small gas nucleus lodged in the walls of the fluid container, on dust and colloidal matter suspended in the media, or on a small bubble of contaminant gas free in the fluid. Bubble growth is due to essentially three mechanisms. First, additional contaminant gas can diffuse into the bubble; second the bubble grows because of a decrease in ambient pressure; and third, growth results from a phase change occurring at the bubble wall.

The initial nucleus is composed solely of contaminant gases or a mixture of contaminant gas and liquid vapor. The effect of the initial contaminant gas and the additional contaminant gas that diffuses into the nucleus during its growth is important only during the initial stages of growth. Due to the large surface tension force, the initial growth of the bubble is slow. However, once the bubble radius has increased by an order of magnitude, the presence of the contaminant gases is relatively unimportant.

The flow of fluid surrounding a single bubble can be treated as incompressible and irrotational and, hence, can be described by a potential function, ψ

$$- \frac{\partial \psi}{\partial r} = \dot{r}$$ (B.1)

where r is the radius from the center of the bubble to any point in the fluid and $\dot{r}$ is the velocity of the fluid at that point. The boundary conditions $\dot{r} = \dot{R}$ at $r = R$, where R is the bubble radius, and $\dot{r} = 0$ at $r = \infty$ establish the potential function to be

$$\psi = \frac{R^2 \cdot \dot{R}}{r}$$ (B.2)

Since the fluid is considered incompressible with gravitational effects negligible, the work done by a growing bubble appears only as a change in kinetic energy of the fluid surrounding the bubble. The increment of work done by the bubble in expanding from R to R + ΔR is

$$\Delta W = \Delta P \cdot 4\pi \cdot R^2 \cdot \Delta R \qquad (B.3)$$

where

$$\Delta P = P_R - P_\infty$$

In terms of the rate of change of work with respect to R

$$\frac{dW}{dR} = \left(P_R - P_\infty\right) \cdot 4\pi R^2 \qquad (B.4)$$

The kinetic energy of the fluid between R and r is

$$KE = \tfrac{1}{2} mv^2 = \tfrac{1}{2} \int_R^r 4\pi\rho_L r^2 \dot{r}^2 dr \qquad (B.5)$$

where ρ_L is the mass density of the liquid.

But from Equation (B.2)

$$\dot{r} = -\frac{\partial \varphi}{\partial r} = \frac{R^2 \dot{R}}{r^2} \qquad (B.6)$$

$$\therefore KE = 2\pi\rho_L R^4 \dot{R}^2 \int_R^r \frac{dr}{r^2} \qquad (B.7)$$

or

$$KE = 2\pi\rho_L R^4 \dot{R}^2 \left(\frac{1}{R} - \frac{1}{r}\right) \qquad (B.8)$$

letting $r \to \infty$

$$KE = 2\pi\rho_L R^3 \dot{R}^2 \qquad (B.9)$$

The rate of change of kinetic energy with respect to R is:

$$\frac{d}{dR}\,(KE) = 2\pi\rho_L\,\frac{d}{dR}\left(R^3\dot{R}^2\right) \tag{B.10}$$

Setting Equation (B.4) equal to Equation (B.10)

$$\left(P_R - P_\infty\right)4\pi R^2 = 2\pi\rho_L\,\frac{d}{dR}\left(R^3\dot{R}^2\right) \tag{B.11}$$

But

$$\frac{d}{dR} = \frac{dt}{dR}\cdot\frac{d}{dt} = \frac{1}{\dot{R}}\frac{d}{dt}$$

$$\therefore\;\frac{P_R - P_\infty}{\rho_L} = \frac{1}{2R^2\dot{R}}\frac{d}{dt}\left(R^3\dot{R}^2\right) \tag{B.12}$$

Equation (B.12) therefore, is the equation of motion governing bubble growth. The same results can be obtained starting with the Bernoulli equation

$$\frac{P - P_\infty}{\rho_L} = \tfrac{1}{2}\dot{r}^2 + \frac{\partial\varphi}{\partial t} \tag{B.13}$$

The temperature at the bubble wall will be controlled by the evaporation process. If it is assumed that the pressure in the bubble is uniform and at the vapor pressure, P_v, of the liquid corresponding to the temperature at the bubble wall, then P_R is related to P_v by:

$$P_R = P_v - 2\frac{\sigma}{R} \tag{B.14}$$

where σ is the surface tension of the fluid

$$\therefore\;\frac{1}{2R^2\dot{R}}\frac{d}{dt}\left(R^3\dot{R}^2\right) = \frac{1}{\rho_L}\left(P_v - P_\infty - \frac{2\sigma}{R}\right) \tag{B.15}$$

If the boiling curve of a fluid is linear or nearly so over the region in which bubble growth takes place, the saturation pressure P_s can be related to the saturation temperature T_s by

$$P_s = A \cdot T_s + B \tag{B.16}$$

$P_v - P_\infty$ can be expressed as

$$P_v - P_\infty = A\left(T_R - T_o\right) + A\left(T_o - T_{P_\infty}\right) \tag{B.17}$$

where T_o is the fluid temperature a great distance from the bubble and T_{P_∞} is the saturation temperature corresponding to the time-dependent ambient pressure.

Equation (B.15) then becomes

$$\frac{1}{2R^2\dot{R}} \frac{d}{dt}\left(R^3 \cdot \dot{R}^2\right) = \frac{A}{\rho_L}\left[\left(T_R - T_o\right) + \left(T_o - T_{P_\infty}\right)\right] - \frac{2\sigma}{\rho_L R} \tag{B.18}$$

If it is assumed that the temperature a great distance from the bubble, T_o, remains constant during bubble growth the quantity $T_R - T_o$ can be obtained from the solution to the problem of non-steady heat diffusion with boundary motion of Plesset and Zwick (Reference 16). The equations will not be derived here. However, the final results can be expressed by the following equation:

$$T_R - T_o = -\left(\frac{D}{\pi}\right)^{\frac{1}{2}} \int_0^t \frac{R^2(x) \cdot (\partial T/\partial r)_{r=R(x)}}{\left[\int_x^t R^4(y)dy\right]^{\frac{1}{2}}} dx \tag{B.19}$$

where D is the thermal diffusivity of the fluid and the variable y is associated with a translation of the time axis. The derivative $(\partial T/\partial r)$ is the temperature gradient at the bubble wall. Equation (B.18) is then

$$\frac{1}{2R^2\dot{R}} \frac{d}{dt}\left(R^3\dot{R}^2\right) = \frac{A}{\rho_L}\left(T_o - T_{P_\infty}\right) - \frac{A}{\rho_L}\left(\frac{D}{\pi}\right)^{\frac{1}{2}} \int_0^t \frac{R^2(x) \cdot (\partial T/\partial r)_{r=R(x)}}{\left[\int_x^t R^4(y) \cdot dy\right]^{\frac{1}{2}}} dx - \frac{2\sigma}{\rho_L R} \tag{B.20}$$

The temperature gradient at the bubble wall can be obtained from a mass and heat balance as follows. The heat transfer at the bubble wall per unit time is:

$$\dot{Q} = 4\pi R^2 k \left(\frac{\partial T}{\partial r}\right)_{r=R} \qquad \text{(B.21)}$$

where k is the thermal conductivity.

This heat goes into vaporizing liquid at a rate

$$\frac{dm_L}{dt} = \frac{\dot{Q}}{L} \qquad \text{(B.22)}$$

where L is the latent heat of vaporization.

The rate at which liquid is evaporated is equal to the rate of mass addition to the bubble:

$$\frac{dm_L}{dt} = \frac{dm_v}{dt} \qquad \text{(B.23)}$$

where m_v = mass of vapor

but

$$m_v = (4/3)\pi R^3 \rho_v \qquad \text{(B.24)}$$

and

$$\frac{dm_v}{dt} = (4/3)\pi \frac{d}{dt}\left(R^3 \rho_v\right) = (4/3)\pi \left(3R^2 \cdot \dot{R} \cdot \rho_v + R^3 \dot{\rho}_v\right) \qquad \text{(B.25)}$$

$$\therefore \frac{4\pi R^2 k}{L} \left(\frac{\partial T}{\partial r}\right)_{r=R} = (4/3)\pi \left(3R^2 \cdot \dot{R} \cdot \rho_v + R^3 \dot{\rho}_v\right) \qquad \text{(B.26)}$$

or

$$\left(\frac{\partial T}{\partial r}\right)_{r=R} = \frac{L}{k}\rho_v \cdot \dot{R} + \frac{LR}{3k}\dot{\rho}_v \qquad \text{(B.27)}$$

The growth of a vapor bubble under conditions of variable ambient pressure and variable vapor density is described by a solution to Equations (B.20) and (B.27).

APPENDIX C

Simplified Test Feed System Transfer Functions

A simplified analytical model of the S-II inboard LOX suction line with the by-pass pulser line is shown in Figure C.1. Solution of these equations give the following transfer functions:

$$\frac{\partial Ps}{\partial \dot{W}p} = \frac{-I_1}{\left(1 + 2\zeta\frac{S}{\omega} + \frac{S^2}{\omega^2}\right)} \tag{C.1}$$

$$\frac{\partial Ps}{\partial Pp} = \frac{(I_{1p}/I_p)}{\left(1 + 2\zeta_1\frac{S}{\omega_1} + \frac{S^2}{\omega_1^2}\right)} \tag{C.2}$$

$$\frac{\partial P_1}{\partial Pp} = \frac{\partial Ps}{\partial Pp}\left(1 + \frac{S^2}{\omega_0^2}\right) \tag{C.3}$$

where
$$I = \ell/Agc$$

$$\omega^2 = 1/\left[C\ (I_1 + I_2)\right]$$

$$\omega_1^2 = 1/\left[C\ (I_{1p} + I_2)\right]$$

$$\omega_0^2 = 1/CI_2$$

$$I_{1p} = I_1 I_p/(I_1 + I_p)$$

$$\zeta = 1/2\ \omega\ (I_1 + I_2)\ \frac{\partial \dot{W}d}{\partial Ps}$$

$$\zeta_1 = 1/2\omega_1 (I_{1p} + I_2) \frac{\partial \dot{W}d}{\partial Ps}$$

$$\frac{\partial \dot{W}d}{\partial Ps} = \text{engine flow transfer function}$$

The true system transfer function of suction pressure with respect to pump acceleration is:

$$\frac{\partial Ps}{\partial \ddot{g}p} = \frac{- (I_1 + I_2) \rho \, Agc}{\left(1 + 2\zeta \frac{S}{\omega} + \frac{S^2}{\omega^2}\right)} \tag{C.4}$$

and, therefore, the only test transfer function that has the right dynamics (correct natural frequency) is $\partial Ps/\partial \dot{W}p$. However, since pulser flow acceleration is not easy to measure accurately, frequency can also be determined from $\partial Ps/\partial Pp$ if the proper correction is applied. For the S-II inboard LOX line, the natural resonance of the $\partial Ps/\partial Pp$ transfer function will be approximately 5% too high. This is independent of where the line pressure is measured except as the pressure transducer moves up the line an anti-resonance will approach the resonance from above.

For other test configurations, the $\partial Ps/\partial Pp$ transfer function will give approximately the correct natural frequency provided that the pulser line inertance (from the suction line to the pressure transducer) is large relative to the inertance in the suction line between the tank and pulser line.

Test Setup (S-II LOX L/B)

Model

Equations

7.97" I.D.

2" I.D.

by pass pulser

Pp

12"

Ps

33'

20'

pump cavitation

Wp

Pp

I_p

W_1

I_1

P_1

W_2

I_2

C

Wd

Ps

$$I_1 W_1 S^2 = -P_1$$

$$I_p W_p S^2 = P_1 - P_p$$

$$I_2 W_2 S^2 = P_1 - P_s$$

$$W_2 - W_d = C\,P_s$$

$$W_1 = W_p + W_2$$

Approximate Values

$$I_1 = .00173 \; sec^2/in^2$$

$$I_2 = .00107 \; sec^2/in^2$$

$$I_p = .01 \; sec^2/in^2$$
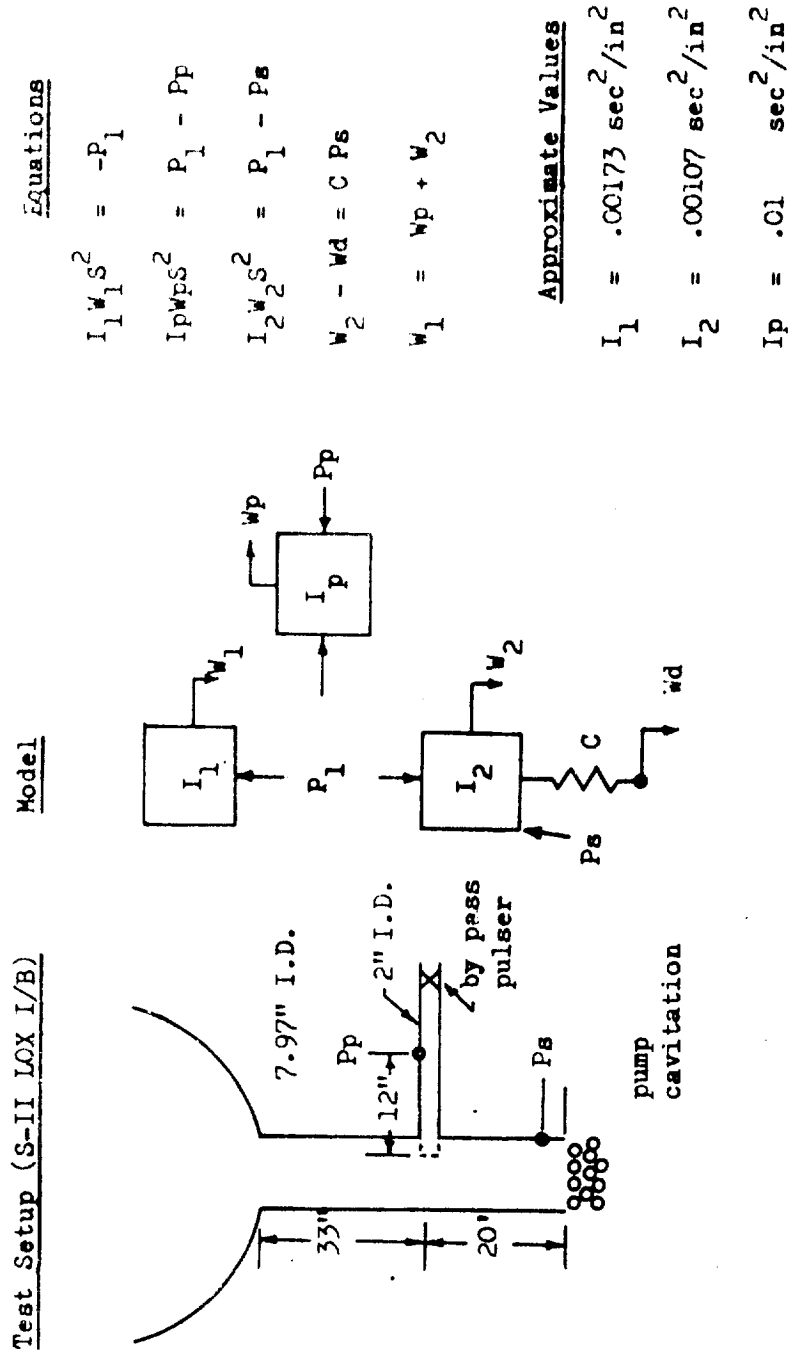
FIGURE C.1 Simplified Suction Line Model for Pulse Test

APPENDIX D

Turbopump Program Users Instructions

The turbopump cavitation flow program has been written in the Fortran IV program language for the CDC 6000 series computer. The program is made up of a main controlling program and seven subroutines. The main program controls the sequence of solution steps and the adjustment of boundary conditions to meet proper inlet and exit flow conditions.

The first subroutine employed (PREP) reads in the input data, sets up the grid system, and establishes initial estimates of the streamfunction at each grid point. Subroutine RELAX is used next to solve the flow and energy equations throughout the field. This solution is accomplished by applying relaxation techniques to a finite difference form of the equations. The first series of relaxation solutions is done with the density throughout the field set equal to the liquid density. This solution is referred to as the incompressible or uncoupled solution. The relaxation solution is then continued with the completely coupled two phase flow equations. Following this solution, boundary conditions are checked, adjusted, and the relaxation solution repeated until the proper inlet and exit conditions are satisfied. The last operation of the program prepares and prints out the output data.

Subroutine TABL is an interpolation subroutine used by the main program and many of the subroutines. Subroutine PREWRT prepares the output data for printing while subroutine SETUP prepares the output data for computer plotting. Subroutines WRTOUT and PLOTT respectively do the writing and plotting of the output.

A flow diagram for the program is given in Figure D.1. With the exception of the plotting capabilities, this program should be compatible with any computer which has a FORTRAN IV compiler. The plotting routines are documented in Reference 55. The routine ALTFILE is required on the CDC 6000 computer so that the TAPE9 buffer area may also be used for TAPE10 through TAPE99.

The problem solution is initiated by plotting the inducer or impeller blade sections (Figures 5.3 and 5.4) and the relationship between density and pressure for equilibrium

phase changes (Figure 3.7). All input variables are defined
in the program listing of subroutine PEER (Appendix E). Input
dimensions and internal program variables are shown in Figures
D.2 through D.4.

Parts of a sample output from the turbopump cavitation flow
program are presented at the end of this Appendix. The first
data printed is the input data. Next is a tabulation of the
iterations required for solution along with the value of the
maximum residual (RESIM) throughout the field for each itera-
tion. Following the last iteration, which corresponds to the
uncoupled solution, the pressure and density is printed out
at each grid point in the system. The next item to be printed
(volume) is the weight of propellant in the streamsheet analyzed.
Finally, for the uncoupled solution the values of the stream-
function, ψ, theta, θ, potential function, ϕ, circumfrential
velocity, V, and meridional velocity, U, are printed for in-
crements along the E axis. At this point the solution is con-
tinued on a coupled basis and the pressure data printed out
for each iteration. After the final iteration of the coupled
solution the pressure field, the weight of fluid in the stream-
sheet, and the streamfunction - velocity fields are printed out.

```
N = 51   L = 51   K = 51   NN = 1   LL = 1   MNM = 51

B =      2.0944   O =      60.0000   RT =        6.7500


RS =    0.          THETS =    0.          ES1 =    0.
RS =     .0300      THETS =     .0937      ES1 =     .0300
RS =     .0650      THETS =     .1874      ES1 =     .0650
RS =     .1050      THETS =     .2812      ES1 =     .1050
RS =     .1480      THETS =     .3749      ES1 =     .1480
RS =     .1970      THETS =     .4686      ES1 =     .1970
RS =     .2500      THETS =     .5624      ES1 =     .2500
RS =     .3050      THETS =     .6561      ES1 =     .3050
RS =     .3630      THETS =     .7498      ES1 =     .3630
RS =     .4210      THETS =     .8436      ES1 =     .4210
RS =     .4810      THETS =     .9373      ES1 =     .4810
RS =     .5390      THETS =    1.0310      ES1 =     .5390
RS =     .5980      THETS =    1.1247      ES1 =     .5980
RS =     .6570      THETS =    1.2184      ES1 =     .6570
RS =     .7150      THETS =    1.3122      ES1 =     .7150
RS =     .7730      THETS =    1.4059      ES1 =     .7730
RS =     .8300      THETS =    1.4996      ES1 =     .8300
RS =     .8880      THETS =    1.5934      ES1 =     .8880
RS =     .9450      THETS =    1.6871      ES1 =     .9450
RS =    1.0020      THETS =    1.7808      ES1 =    1.0020
RS =    1.0590      THETS =    1.8746      ES1 =    1.0590
RS =    1.1160      THETS =    1.9683      ES1 =    1.1160
RS =    1.1720      THETS =    2.0620      ES1 =    1.1720
RS =    1.2280      THETS =    2.1557      ES1 =    1.2280
RS =    1.2840      THETS =    2.2494      ES1 =    1.2840
RS =    1.3390      THETS =    2.3432      ES1 =    1.3390
RS =    1.3950      THETS =    2.4369      ES1 =    1.3950
RS =    1.4500      THETS =    2.5306      ES1 =    1.4500
RS =    1.5050      THETS =    2.6244      ES1 =    1.5050
RS =    1.5600      THETS =    2.7181      ES1 =    1.5600
RS =    1.6150      THETS =    2.8118      ES1 =    1.6150
RS =    1.6690      THETS =    2.9056      ES1 =    1.6690
RS =    1.7230      THETS =    2.9993      ES1 =    1.7230
RS =    1.7770      THETS =    3.0930      ES1 =    1.7770
RS =    1.8310      THETS =    3.1867      ES1 =    1.8310
RS =    1.8840      THETS =    3.2804      ES1 =    1.8840
RS =    1.9380      THETS =    3.3742      ES1 =    1.9380
RS =    1.9910      THETS =    3.4679      ES1 =    1.9910
RS =    2.0430      THETS =    3.5616      ES1 =    2.0430
RS =    2.0960      THETS =    3.6554      ES1 =    2.0960
RS =    2.1490      THETS =    3.7491      ES1 =    2.1490
RS =    2.2060      THETS =    3.8428      ES1 =    2.2060
RS =    2.2640      THETS =    3.9366      ES1 =    2.2640
RS =    2.3240      THETS =    4.0303      ES1 =    2.3240
RS =    2.3890      THETS =    4.1240      ES1 =    2.3890
RS =    2.4560      THETS =    4.2177      ES1 =    2.4560
RS =    2.5290      THETS =    4.3115      ES1 =    2.5290
RS =    2.6090      THETS =    4.4052      ES1 =    2.6090
RS =    2.6920      THETS =    4.4989      ES1 =    2.6920
RS =    2.7800      THETS =    4.5926      ES1 =    2.7800
RS =    2.8880      THETS =    4.6864      ES1 =    2.8880
```

RP =	0.	THETP =	2.0944	EP2 =	0.
RP =	.1530	THETP =	2.1881	EP2 =	.1530
RP =	.2430	THETP =	2.2818	EP2 =	.2430
RP =	.3300	THETP =	2.3756	EP2 =	.3300
RP =	.4090	THETP =	2.4693	EP2 =	.4090
RP =	.4840	THETP =	2.5630	EP2 =	.4840
RP =	.5510	THETP =	2.6568	EP2 =	.5510
RP =	.6180	THETP =	2.7505	EP2 =	.6180
RP =	.6810	THETP =	2.8442	EP2 =	.6810
RP =	.7440	THETP =	2.9379	EP2 =	.7440
RP =	.8050	THETP =	3.0317	EP2 =	.8050
RP =	.8670	THETP =	3.1254	EP2 =	.8670
RP =	.9280	THETP =	3.2191	EP2 =	.9280
RP =	.9890	THETP =	3.3128	EP2 =	.9890
RP =	1.0500	THETP =	3.4066	EP2 =	1.0500
RP =	1.1100	THETP =	3.5003	EP2 =	1.1100
RP =	1.1710	THETP =	3.5940	EP2 =	1.1710
RP =	1.2310	THETP =	3.6878	EP2 =	1.2310
RP =	1.2910	THETP =	3.7815	EP2 =	1.2910
RP =	1.3510	THETP =	3.8752	EP2 =	1.3510
RP =	1.4100	THETP =	3.9689	EP2 =	1.4100
RP =	1.4700	THETP =	4.0627	EP2 =	1.4700
RP =	1.5290	THETP =	4.1564	EP2 =	1.5290
RP =	1.5880	THETP =	4.2501	EP2 =	1.5880
RP =	1.6470	THETP =	4.3438	EP2 =	1.6470
RP =	1.7050	THETP =	4.4376	EP2 =	1.7050
RP =	1.7640	THETP =	4.5313	EP2 =	1.7640
RP =	1.8220	THETP =	4.6250	EP2 =	1.8220
RP =	1.8800	THETP =	4.7188	EP2 =	1.8800
RP =	1.9380	THETP =	4.8125	EP2 =	1.9380
RP =	1.9960	THETP =	4.9062	EP2 =	1.9960
RP =	2.0540	THETP =	4.9999	EP2 =	2.0540
RP =	2.1120	THETP =	5.0937	EP2 =	2.1120
RP =	2.1690	THETP =	5.1874	EP2 =	2.1690
RP =	2.2270	THETP =	5.2811	EP2 =	2.2270
RP =	2.2840	THETP =	5.3748	EP2 =	2.2840
RP =	2.3410	THETP =	5.4686	EP2 =	2.3410
RP =	2.3980	THETP =	5.5623	EP2 =	2.3980
RP =	2.4540	THETP =	5.6560	EP2 =	2.4540
RP =	2.5070	THETP =	5.7498	EP2 =	2.5070
RP =	2.5590	THETP =	5.8435	EP2 =	2.5590
RP =	2.6100	THETP =	5.9372	EP2 =	2.6100
RP =	2.6560	THETP =	6.0309	EP2 =	2.6560
RP =	2.6990	THETP =	6.1247	EP2 =	2.6990
RP =	2.7370	THETP =	6.2184	EP2 =	2.7370
RP =	2.7720	THETP =	6.3121	EP2 =	2.7720
RP =	2.8010	THETP =	6.4058	EP2 =	2.8010
RP =	2.8270	THETP =	6.4996	EP2 =	2.8270
RP =	2.8510	THETP =	6.5933	EP2 =	2.8510
RP =	2.8710	THETP =	6.6870	EP2 =	2.8710
RP =	2.8880	THETP =	6.7808	EP2 =	2.8880

RC =	0.	THETC =	0.	EC1 =	0.
RC =	.0920	THETC =	.0937	EC1 =	.0920
RC =	.1540	THETC =	.1874	EC1 =	.1540
RC =	.2170	THETC =	.2812	EC1 =	.2170
RC =	.2790	THETC =	.3749	EC1 =	.2790
RC =	.3400	THETC =	.4686	EC1 =	.3400
RC =	.4000	THETC =	.5624	EC1 =	.4000
RC =	.4620	THETC =	.6561	EC1 =	.4620
RC =	.5220	THETC =	.7498	EC1 =	.5220
RC =	.5820	THETC =	.8436	EC1 =	.5820
RC =	.6430	THETC =	.9373	EC1 =	.6430
RC =	.7030	THETC =	1.0310	EC1 =	.7030
RC =	.7630	THETC =	1.1247	EC1 =	.7630
RC =	.8230	THETC =	1.2184	EC1 =	.8230
RC =	.8820	THETC =	1.3122	EC1 =	.8820
RC =	.9420	THETC =	1.4059	EC1 =	.9420
RC =	1.0010	THETC =	1.4996	EC1 =	1.0010
RC =	1.0590	THETC =	1.5934	EC1 =	1.0590
RC =	1.1180	THETC =	1.6871	EC1 =	1.1180
RC =	1.1760	THETC =	1.7808	EC1 =	1.1760
RC =	1.2350	THETC =	1.8746	EC1 =	1.2350
RC =	1.2930	THETC =	1.9683	EC1 =	1.2930
RC =	1.3500	THETC =	2.0620	EC1 =	1.3500
RC =	1.4080	THETC =	2.1557	EC1 =	1.4080
RC =	1.4650	THETC =	2.2494	EC1 =	1.4650
RC =	1.5220	THETC =	2.3432	EC1 =	1.5220
RC =	1.5790	THETC =	2.4369	EC1 =	1.5790
RC =	1.6360	THETC =	2.5306	EC1 =	1.6360
RC =	1.6930	THETC =	2.6244	EC1 =	1.6930
RC =	1.7490	THETC =	2.7181	EC1 =	1.7490
RC =	1.8050	THETC =	2.8118	EC1 =	1.8050
RC =	1.8610	THETC =	2.9056	EC1 =	1.8610
RC =	1.9170	THETC =	2.9993	EC1 =	1.9170
RC =	1.9730	THETC =	3.0930	EC1 =	1.9730
RC =	2.0290	THETC =	3.1867	EC1 =	2.0290
RC =	2.0840	THETC =	3.2804	EC1 =	2.0840
RC =	2.1390	THETC =	3.3742	EC1 =	2.1390
RC =	2.1940	THETC =	3.4679	EC1 =	2.1940
RC =	2.2490	THETC =	3.5616	EC1 =	2.2490
RC =	2.3020	THETC =	3.6554	EC1 =	2.3020
RC =	2.3540	THETC =	3.7491	EC1 =	2.3540
RC =	2.4080	THETC =	3.8428	EC1 =	2.4080
RC =	2.4600	THETC =	3.9366	EC1 =	2.4600
RC =	2.5110	THETC =	4.0303	EC1 =	2.5110
RC =	2.5630	THETC =	4.1240	EC1 =	2.5630
RC =	2.6140	THETC =	4.2177	EC1 =	2.6140
RC =	2.6650	THETC =	4.3115	EC1 =	2.6650
RC =	2.7180	THETC =	4.4052	EC1 =	2.7180
RC =	2.7710	THETC =	4.4989	EC1 =	2.7710
RC =	2.8260	THETC =	4.5926	EC1 =	2.8260
RC =	2.8880	THETC =	4.6864	EC1 =	2.8880

```
RD =     2.4920   BD  =      .1818   SIAD =      .1057   ED  =     -1.0830
RD =     2.4780   BD  =      .1846   SIAD =      .1057   ED  =      -.9533
RD =     2.4640   BD  =      .1874   SIAD =      .1057   ED  =      -.8233
RD =     2.4500   BD  =      .1903   SIAD =      .1057   ED  =      -.6933
RD =     2.4370   BD  =      .1931   SIAD =      .1057   ED  =      -.5633
RD =     2.4230   BD  =      .1960   SIAD =      .1057   ED  =      -.4333
RD =     2.4090   BD  =      .1988   SIAD =      .1057   ED  =      -.3033
RD =     2.3950   BD  =      .2017   SIAD =      .1057   ED  =      -.1733
RD =     2.3810   BD  =      .2045   SIAD =      .1057   ED  =      -.0433
RD =     2.3670   BD  =      .2074   SIAD =      .1057   ED  =       .0867
RD =     2.3540   BD  =      .2102   SIAD =      .1057   ED  =       .2167
RD =     2.3400   BD  =      .2130   SIAD =      .1057   ED  =       .3467
RD =     2.3260   BD  =      .2159   SIAD =      .1057   ED  =       .4767
RD =     2.3120   BD  =      .2187   SIAD =      .1057   ED  =       .6067
RD =     2.2980   BD  =      .2216   SIAD =      .1057   ED  =       .7367
RD =     2.2850   BD  =      .2244   SIAD =      .1057   ED  =       .8667
RD =     2.2710   BD  =      .2273   SIAD =      .1057   ED  =       .9967
RD =     2.2570   BD  =      .2301   SIAD =      .1057   ED  =      1.1270
RD =     2.2430   BD  =      .2329   SIAD =      .1057   ED  =      1.2570
RD =     2.2290   BD  =      .2358   SIAD =      .1057   ED  =      1.3870
RD =     2.2150   BD  =      .2386   SIAD =      .1057   ED  =      1.5170
RD =     2.2020   BD  =      .2415   SIAD =      .1057   ED  =      1.6470
RD =     2.1880   BD  =      .2443   SIAD =      .1057   ED  =      1.7770
RD =     2.1740   BD  =      .2472   SIAD =      .1057   ED  =      1.9070
RD =     2.1600   PD  =      .2500   SIAD =      .1057   ED  =      2.0370
RD =     2.1460   BD  =      .2528   SIAD =      .1057   ED  =      2.1670
RD =     2.1330   BD  =      .2557   SIAD =      .1057   ED  =      2.2970
RD =     2.1190   BD  =      .2585   SIAD =      .1057   ED  =      2.4270
RD =     2.1050   BD  =      .2614   SIAJ =      .1057   ED  =      2.5570
RD =     2.0910   BD  =      .2642   SIAD =      .1057   ED  =      2.6870
RD =     2.0770   BD  =      .2671   SIAD =      .1057   ED  =      2.8170
RD =     2.0630   BD  =      .2699   SIAD =      .1057   ED  =      2.9470
RD =     2.0500   BD  =      .2727   SIAD =      .1057   ED  =      3.0770
RD =     2.0360   BD  =      .2756   SIAD =      .1057   ED  =      3.2070
RD =     2.0220   BD  =      .2784   SIAD =      .1057   ED  =      3.3370
RD =     2.0080   BD  =      .2813   SIAJ =      .1057   ED  =      3.4670
RD =     1.9940   BD  =      .2841   SIAD =      .1057   ED  =      3.5970
RD =     1.9810   BD  =      .2870   SIAD =      .1057   ED  =      3.7270
RD =     1.9670   BD  =      .2898   SIAD =      .1057   ED  =      3.8570
RD =     1.9530   BD  =      .2926   SIAD =      .1057   ED  =      3.9870
RD =     1.9390   BD  =      .2955   SIAD =      .1057   ED  =      4.1170
RD =     1.9250   BD  =      .2983   SIAD =      .1057   ED  =      4.2470
RD =     1.9120   BD  =      .3012   SIAD =      .1057   ED  =      4.3770
RD =     1.8980   BD  =      .3040   SIAD =      .1057   ED  =      4.5070
RD =     1.8840   BD  =      .3069   SIAD =      .1057   ED  =      4.6370
RD =     1.8700   BD  =      .3097   SIAD =      .1057   ED  =      4.7670
RD =     1.8560   BD  =      .3126   SIAD =      .1057   ED  =      4.8970
RD =     1.8420   BD  =      .3154   SIAD =      .1057   ED  =      5.0270
RD =     1.8290   BD  =      .3182   SIAD =      .1057   ED  =      5.1570
RD =     1.8150   BD  =      .3211   SIAD =      .1057   ED  =      5.2870
RD =     1.8010   BD  =      .3239   SIAD =      .1057   ED  =      5.4170
```

166

```
KKL = 27   INPUF =   0    BN =      3.0000  WW =     842.0000

VTHIN =  1000.0000   VNOIN =   274.8000  PS  =    15.0000
RHOT =      .0000  HT =    0.     PT =      .0150
RHOT =      .0000  HT =    0.     PT =      .0300
RHOT =      .0000  HT =    0.     PT =      .0740
RHOT =      .0000  HT =    0.     PT =    ..1320
RHOT =      .0000  HT =    0.     PT =      .2650
RHOT =      .0001  HT =    0.     PT =      .4700
RHOT =      .0001  HT =    0.     PT =      .8090
RHOT =      .0002  HT =    0.     PT =     1.3380
RHOT =      .0003  HT =    0.     PT =     2.1020
RHOT =      .0005  HT =    0.     PT =     3.1900
RHOT =      .0008  HT =    0.     PT =     4.7040
RHOT =      .0015  HT =    0.     PT =     6.7330
RHOT =      .0032  HT =    0.     PT =     9.3930
RHOT =      .0105  HT =    0.     PT =    12.8120
RHOT =      .0409  HT =    0.     PT =    17.1260
RHOT =      .0409  HT =    0.     PT =    25.0000
RHOT =      .0409  HT =    0.     PT =    30.0000
RHOT =      .0409  HT =    0.     PT =    36.0000
RHOT =      .0409  HT =    0.     PT =    57.0000
RHOT =      .0409  HT =    0.     PT =   100.0000
RHOT =      .0409  HT =    0.     PT =   150.0000
RHOT =      .0409  HT =    0.     PT =   175.0000
RHOT =      .0409  HT =    0.     PT =   200.0000
RHOT =      .0409  HT =    0.     PT =   300.0000
RHOT =      .0409  HT =    0.     PT =   500.0000
RHOT =      .0409  HT =    0.     PT =   700.0000
RHOT =      .0409  HT =    0.     PT =  1000.0000
```

```
BEGIN MAIN PROGRAM   INCREMENT THETA AND THEN E
STEP NO. ONE COMPLETE   INCREMENT E AND THEN THETA
ITERATION NUMBER =    1       RESIM =     11.5183
ITERATION NUMBER =    2       RESIM =      2.6713
ITERATION NUMBER =    3       RESIM =       .9615
ITERATION NUMBER =    4       RESIM =       .6371
ITERATION NUMBER =    5       RESIM =       .4649
ITERATION NUMBER =    6       RESIM =       .3882
ITERATION NUMBER =    7       RESIM =       .3439
ITERATION NUMBER =    8       RESIM =       .3052
ITERATION NUMBER =    9       RESIM =       .2712
ITERATION NUMBER =   10       RESIM =       .2415
ITERATION NUMBER =   11       RESIM =       .2154
ITERATION NUMBER =   12       RESIM =       .1925
             VTHTA =      440.59
ITERATION NUMBER =   13       RESIM =       .2308
ITERATION NUMBER =   14       RESIM =       .2106
ITERATION NUMBER =   15       RESIM =       .1729
             VTHT2 =      477.00
ITERATION NUMBER =   16       RESIM =      1.9332
ITERATION NUMBER =   17       RESIM =      1.2643
ITERATION NUMBER =   18       RESIM =       .8813
ITERATION NUMBER =   19       RESIM =       .6690
ITERATION NUMBER =   20       RESIM =       .5466
ITERATION NUMBER =   21       RESIM =       .4789
ITERATION NUMBER =   22       RESIM =       .4181
ITERATION NUMBER =   23       RESIM =       .3659
ITERATION NUMBER =   24       RESIM =       .3219
ITERATION NUMBER =   25       RESIM =       .2852
ITERATION NUMBER =   26       RESIM =       .2607
ITERATION NUMBER =   27       RESIM =       .2377
ITERATION NUMBER =   28       RESIM =       .2166
ITERATION NUMBER =   29       RESIM =       .1974
ITERATION NUMBER =   30       RESIM =       .1801
             VTHT2 =      683.58
ITERATION NUMBER =   31       RESIM =      1.4799
ITERATION NUMBER =   32       RESIM =       .9777
ITERATION NUMBER =   33       RESIM =       .6876
ITERATION NUMBER =   34       RESIM =       .5268
ITERATION NUMBER =   35       RESIM =       .4431
ITERATION NUMBER =   36       RESIM =       .3907
ITERATION NUMBER =   37       RESIM =       .3433
ITERATION NUMBER =   38       RESIM =       .3025
ITERATION NUMBER =   39       RESIM =       .2680
ITERATION NUMBER =   40       RESIM =       .2430
ITERATION NUMBER =   41       RESIM =       .2230
ITERATION NUMBER =   42       RESIM =       .2043
ITERATION NUMBER =   43       RESIM =       .1871
```

```
P =     4.6675702E+01     IN =     55     JC =     23     RHO =     4.1000000E-02
P =    -3.4023753E+02     IN =     50     JC =     24     RHO =     4.1000000E-02
P =    -3.4023753E+02     IN =     50     JC =     24     RHO =     4.1000000E-02
P =    -3.4023753E+02     IN =     50     JC =     24     RHO =     6.0000000E-06
P =     3.0468643E+01     IN =     51     JC =     24     RHO =     4.1000000E-02
P =     3.0468643E+01     IN =     51     JC =     24     RHO =     4.1000000E-02
P =     6.4769333E+01     IN =     52     JC =     24     RHO =     4.1000000E-02
P =     6.1914359E+01     IN =     53     JC =     24     RHO =     4.1000000E-02
P =     5.5674399E+01     IN =     54     JC =     24     RHO =     4.1000000E-02
P =     5.2196954E+01     IN =     55     JC =     24     RHO =     4.1000000E-02
P =     5.2196954E+01     IN =     55     JC =     24     RHO =     4.1000000E-02
P =    -3.6635503E+02     IN =     50     JC =     25     RHO =     4.1000000E-02
P =    -3.6635503E+02     IN =     50     JC =     25     RHO =     4.1000000E-02
P =    -3.6635503E+02     IN =     50     JC =     25     RHO =     6.0000000E-06
P =     7.1561888E+01     IN =     51     JC =     25     RHO =     4.1000000E-02
P =     8.8397838E+01     IN =     52     JC =     25     RHO =     4.1000000E-02
P =     7.2384835E+01     IN =     53     JC =     25     RHO =     4.1000000E-02
P =     6.0701382E+01     IN =     54     JC =     25     RHO =     4.1000000E-02
P =     5.5440809E+01     IN =     55     JC =     25     RHO =     4.1000000E-02
P =     5.5440809E+01     IN =     55     JC =     25     RHO =     4.1000000E-02
P =    -1.0906847E+03     IN =     50     JC =     26     RHO =     4.1000000E-02
P =    -1.0906847E+03     IN =     50     JC =     26     RHO =     4.1000000E-02
P =    -1.0906847E+03     IN =     50     JC =     26     RHO =     6.0000000E-06
P =     1.4466197E+01     IN =     51     JC =     26     RHO =     4.1000000E-02
P =     1.4466197E+01     IN =     51     JC =     26     RHO =     4.1000000E-02
P =     1.4466197E+01     IN =     51     JC =     26     RHO =     2.2156833E-02
P =     7.5372255E+01     IN =     52     JC =     26     RHO =     4.1000000E-02
P =     6.7070811E+01     IN =     53     JC =     26     RHO =     4.1000000E-02
P =     5.8513096E+01     IN =     54     JC =     26     RHO =     4.1000000E-02
P =     5.4855696E+01     IN =     55     JC =     26     RHO =     4.1000000E-02
P =     5.4855696E+01     IN =     55     JC =     26     RHO =     4.1000000E-02
P =    -1.3379538E+03     IN =     50     JC =     27     RHO =     4.1000000E-02
P =    -1.3379538E+03     IN =     50     JC =     27     RHO =     4.1000000E-02
P =    -1.3379538E+03     IN =     50     JC =     27     RHO =     6.0000000E-06
P =    -7.7274892E+01     IN =     51     JC =     27     RHO =     4.1000000E-02
P =    -7.7274892E+01     IN =     51     JC =     27     RHO =     4.1000000E-02
P =    -7.7274892E+01     IN =     51     JC =     27     RHO =     6.0000000E-06
P =     3.2876837E+01     IN =     52     JC =     27     RHO =     4.1000000E-02
P =     3.2876837E+01     IN =     52     JC =     27     RHO =     4.1000000E-02
P =     4.8862768E+01     IN =     53     JC =     27     RHO =     4.1000000E-02
P =     4.8862768E+01     IN =     53     JC =     27     RHO =     4.1000000E-02
P =     5.0418879E+01     IN =     54     JC =     27     RHO =     4.1000000E-02
P =     5.0983057E+01     IN =     55     JC =     27     RHO =     4.1000000E-02
P =     5.0983057E+01     IN =     55     JC =     27     RHO =     4.1000000E-02
ITERATION NUMBER =     44          RESIM =          0.
```

+++++++   VOLUME =   1.55393E-01
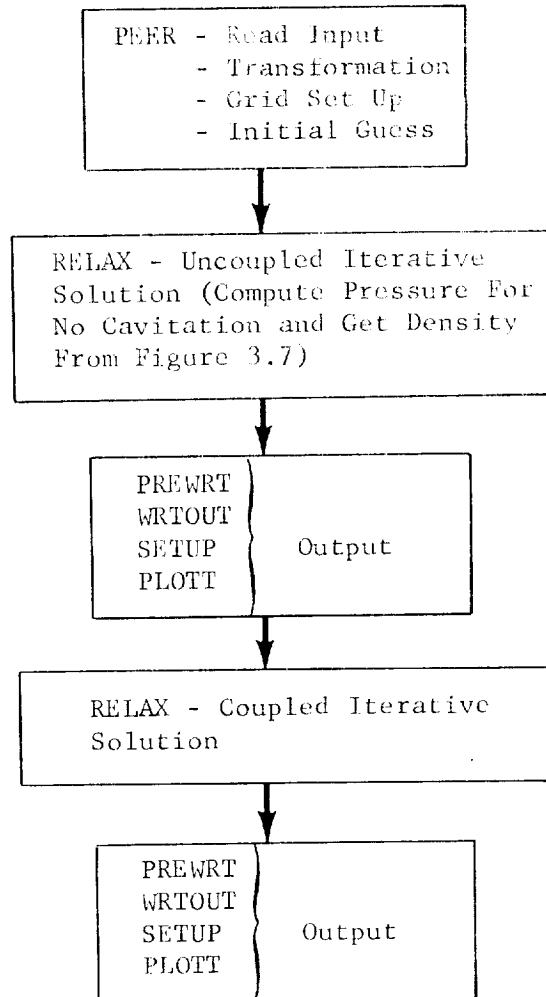
Figure D.1 Turbopump Program Computation Sequence
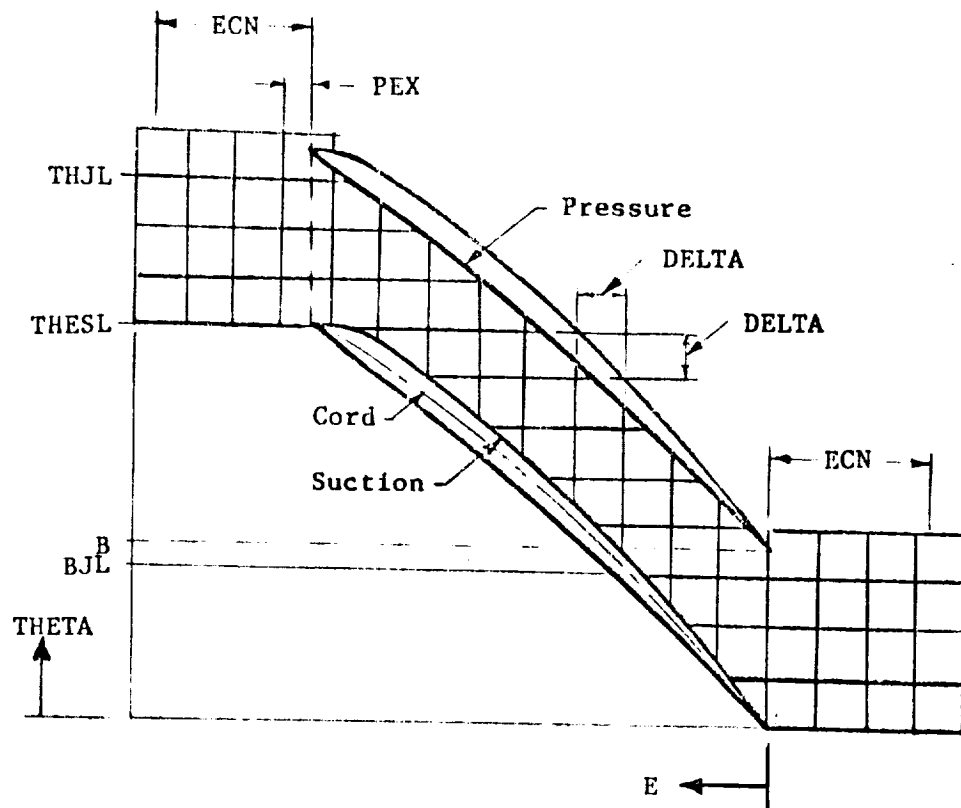
Figure D.2   THETA, E Dimensions

171
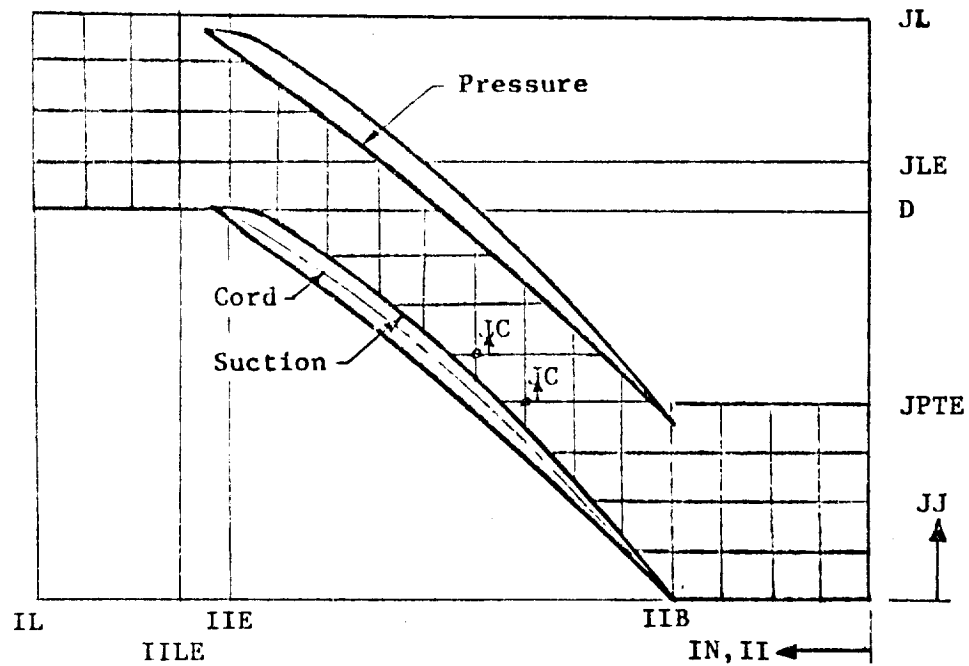
Figure D.3   Grid Increment Number
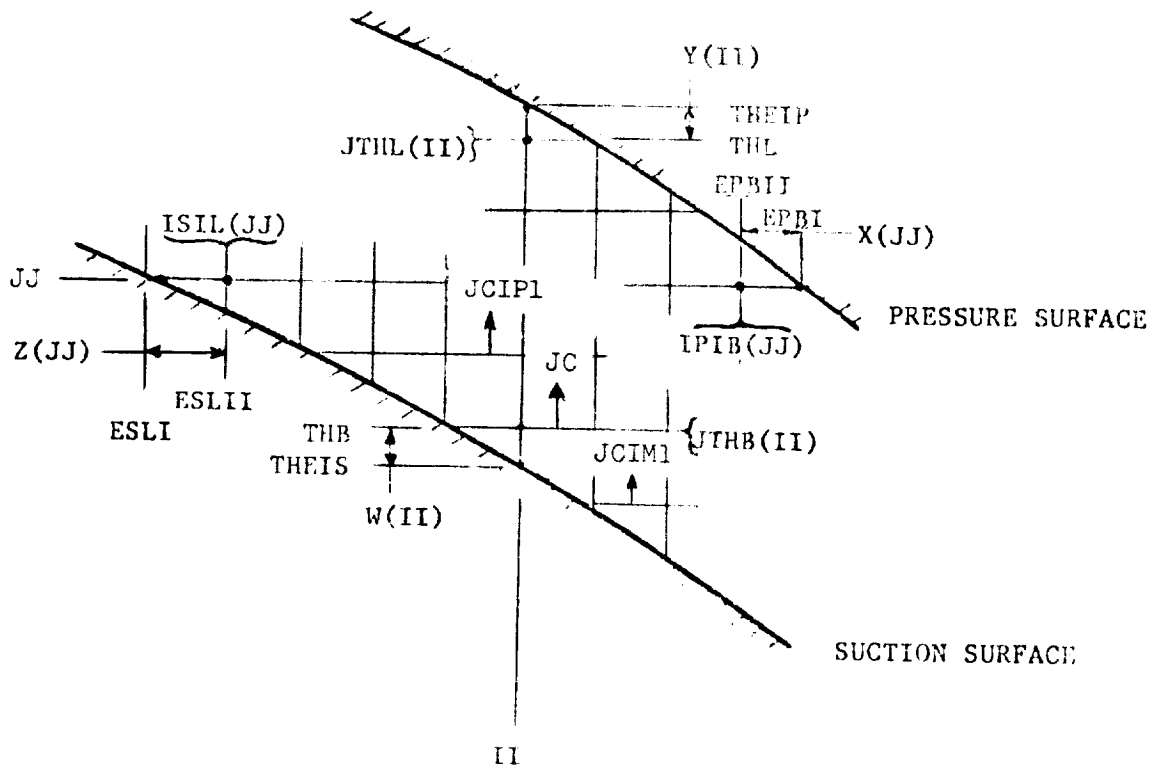
Figure D.4   Grid Increment For Extrapolation to Blade Surfaces

APPENDIX E

Turbopump Program Listing

```
      PROGRAM MAIN ( INPUT, OUTPUT, TAPE5 = INPUT, TAPE6 = OUTPUT,
     *             TAPE9, FILMPL )
C
C         COMPRESSIBLE - INCOMPRESSIBLE FLOW TURBO PUMF PROGRAM
C
      COMMON    ISIL(150), IPIB(150), W(150), X(150), Y(150), Z(150),
     *          JTHL(150), JTHB(150), PSI(100,100),
     *          RS(100), RP(100), ES1(100), RC(100),
     *          ED(150), RD(150), BD(150), SIAD(150), MNM, IL, JL, IIB,
     *          IIE, B, DELTA, RESIM, OPSIP, KK, DEX, ACC, JLE, BN,
     *          PSIPR, RHO(100,100), G, WDOT, WW, KKL, RHOIN, POIN, HOIN,
     *          RCIN, VTHIN, VMOIN, PS, RR(150), BZ(150), SIA(150), RT,
     *          INPUF, RRL,ITRIP,POEL,JOPL
C
C         ZERO OUT ARRAYS
      ITRIP=0
      DO 100 JJ = 1, 150
      W(JJ)     = 0.
      Y(JJ)     = 0.
  100 CONTINUE
C
      DO 150 II = 1, 150
      X(II)     = 0.
      Z(II)     = 0.
  150 CONTINUE
C
      DO 250 JJ = 1, 100
      DO 200 II = 1, 100
      PSI(II,JJ) = 0.
  200 CONTINUE
  250 CONTINUE
C
C         CALL PEER TO READ INPUT DATA AND SET UP GRID
C
      G           = 386.4
  300 CALL PEER
      ER          = PSIPR/ 70.
      ACC         = ER
C
C         OBTAIN FIRST RELAXATION
C
      CALL RELAX
C
      DEPSI=-PSIPR/50.
      ILMI=IL-1
      VTHTA=(PSI(ILMI,1)-PSI(IL,1))/DELTA
      VTHTA=VTHTA/(RHOIN*BZ(IL)*RR(IL))
      WRITE(6,399) VTHTA
  399 FORMAT(10X,* VTHTA = * F10.2)
  400 IF(ABS(VTHTA-WW).LT.15.0) GO TO 900
      JTB=JTHB(IL)
      JTL=JTHL(IL)
      JJ=0
      DO 800 JN=JTB,JTL
      JJ=JJ+1
```

```
      PSI(IL,JJ)=PSI(IL,JJ)+DEPSI
 800  CONTINUE
      CALL RELAX
      ILMI=IL-1
      VTHT2=(PSI(ILMI,1)-PSI(IL,1))/DELTA
      VTHT2=VTHT2/(RHOIN*BZ(IL)*RR(IL))
      WRITE(6,899) VTHT2
 899  FORMAT(10X,* VTHT2 = *,F10.2)
      DVTHD=(VTHT2-VTHTA)/DEPSI
      DEPSI=(WW-VTHT2)/DVTHD
      VTHTA=VTHT2
      GO TO 400
C         WRITE OUT FIRST RELAXATION
C
 900  ITRIP=1
      DO 1000 JDELP=1,JDPL
      POIN=PCIN-PDEL
      WRITE(6,989) POIN
 989  FORMAT(10X,* POIN = *F10.3)
      CALL RELAX
      CALL PREWRT
      CALL WRTOUT
1000  CONTINUE
      GO TO 300
      END
```

```
      SUBROUTINE TABL ( AI, BD, CI, DD, M, J, K )
C
C.  MONO-VARIANT TABLE LOOK UP ROUTINE
C.      EXTRAPOLATICN = LINEAR BASED ON FIRST OR LAST TWO POINTS
C.      INTERPOLATICN = LINEAR, QUADRATIC, OR CUBIC
C
C.  SUBROUTINE ARGUMENTS
C.      AI = GIVEN INDEPENDENT VARIABLE
C.      BD = DESIRED DEPENDENT VARIABLE
C.      CI = SET OF INDEPENDENT VARIABLES
C.      DD = SET OF DEPENDENT VARIABLES
C.      M  = ORDER OF INTERPOLATION (1,2,3)
C.      J  = FIRST POINT IN TABLE (USUALLY 1)
C.      K  = LAST POINT IN TABLE
C
      DIMENSION      CI(1), DD(1)
C
 8001 FORMAT ( * UNSUCCESFUL TABLE LCCK UP * )
C
C.  IS AI INSIDE RANGE OF TABLE
C
      IF ( AI .GT. CI(K) )                    GO TO 100
      IF ( AI .LT. CI(J) )                    GO TO 200
      GO TO 300
C
C.  EXTRAPOLATE IF AI OUTSIDE TABLE RANGE
C
  100 BD          = DD(K) + ( DD(K) - DD(K-1) ) * ( AI - CI(K) ) / (CI(K)
     *              - CI(K-1) )
      GO TO 1700
  200 BD          = DD(J) + ( DD(J+1) - DD(J) ) * ( AI - CI(J) ) /
     *              ( CI(J+1) - CI(J) )
      GO TO 1700
C
C.  DOES AI = POINT IN TABLE
C
  300 DO 400 IN = J, K
      I         = IN
      IF ( ( ABS ( AI - CI(I) ) ) .LT. 0.00001 )  GO TO 500
  400 CONTINUE
      GC TO 600
  500 BD        = DD(I)
      GO TO 1700
C
C.  LOCATE POSITION IN TABLE
C
  600 DO 700 IO = J, K
      I         = IO
      IF ( CI(I) .GT. AI )                    GO TO 800
  700 CONTINUE
      WRITE (6,8001)
      CALL EXIT
C
  800 GO TO ( 900, 1000, 1300 ),  M
C
```

```
C.   LINEAR INTERPOLATION
C
  900 Y1          = DD(I-1)
      Y2          = DD(I)
      X1          = CI(I-1)
      X2          = CI(I)
      DEX         = X2 - X1
      DY1         = Y2 - Y1
      BD          = Y1 + ( AI - X1 ) * DY1 / DEX
         GO TO 1700
C
C.   QUADRATIC INTERPOLATION
C
 1000 IF ( I .EQ. K )                          GO TO 1100
      Y1          = DD(I-1)
      Y2          = DD(I)
      Y3          = DD(I+1)
      X1          = CI(I-1)
      X2          = CI(I)
      X3          = CI(I+1)
         GO TO 1200
 1100 Y1          = DD(I-2)
      Y2          = DD(I-1)
      Y3          = DD(I)
      X1          = CI(I-2)
      X2          = CI(I-1)
      X3          = CI(I)
 1200 B1          = Y1 * ( AI - X2 ) * ( AI - X3 ) / ( ( X1 - X2 ) *
     *              ( X1 - X3 ) )
      B2          = Y2 * ( AI - X1 ) * ( AI - X3 ) / ( ( X2 - X1 ) *
     *              ( X2 - X3 ) )
      B3          = Y3 * ( AI - X1 ) * ( AI - X2 ) / ( ( X3 - X1 ) *
     *              ( X3 - X2 ) )
      BD          = B1 + B2 + B3
         GO TO 1700
C
C.   CUBIC INTERPOLATION
C
 1300 IF ( I .EQ. K )                          GO TO 1400
      IF ( ( I - 1 ) .EQ. J )                  GO TO 1500
      Y1          = DD(I-2)
      Y2          = DD(I-1)
      Y3          = DD(I)
      Y4          = DD(I+1)
      X1          = CI(I-2)
      X2          = CI(I-1)
      X3          = CI(I)
      X4          = CI(I+1)
         GO TO 1600
C
 1400 Y1          = DD(I-3)
      Y2          = DD(I-2)
      Y3          = DD(I-1)
      Y4          = DD(I)
      X1          = CI(I-3)
```

```
        X2              = CI(I-2)
        X3              = CI(I-1)
        X4              = CI(I)
         GC TC 1600
C
  1500 Y1              = CO(I-1)
        Y2              = OD(I)
        Y3              = JJ(I+1)
        Y4              = DD(I+2)
        X1              = CI(I-1)
        X2              = CI(I)
        X3              = CI(I+1)
        X4              = CI(I+2)
C
  1600 80              = Y1 * ( AI - X2 ) * ( AI - X3 ) * ( AI - X4 ) / (
       *                 ( X1 - X2 ) * ( X1 - X3 ) * ( X1 - X4 ) )
       *                + Y2 * ( AI - X1 ) * ( AI - X3 ) * ( AI - X4 ) / (
       *                 ( X2 - X1 ) * ( X2 - X3 ) * ( X2 - X4 ) )
       *                + Y3 * ( AI - X1 ) * ( AI - X2 ) * ( AI - X4 ) / (
       *                 ( X3 - X1 ) * ( X3 - X2 ) * ( X3 - X4 ) )
       *                + Y4 * ( AI - X1 ) * ( AI - X2 ) * ( AI - X3 ) / (
       *                 ( X4 - X1 ) * ( X4 - X2 ) * ( X4 - X3 ) )
  1700 RETURN
        END
```

```
      SUBROUTINE PEER
C
C.    INPUT AND SETUP ROUTINE
C.       SETUP INCLUDES INITIALIZATION, TRANSFORMATION, GRID SET UP, AND
C.       FIRST GUESS AT STREAM FUNCTION AND DENSITY VALUES
C
C.    INPUT DEFINITION
C.       N         = NO. OF INPUT BLADE COORDINATES (SUCTION SURFACE)
C.       L         = NO. OF INPUT BLADE COORDINATES (PRESSURE SURFACE)
C.       K         = NO. OF INPUT BLADE COORDINATES (CORD LINE)
C.       NN        = NOT USED
C.       LL        = NOT USED
C.       MNM       = NO. OF INPUT STREAM TUBE COORDINATES
C.       B         = ANGLE BETWEEN BLADES (RAD) = 6.28/BN
C.       D         = NO. OF F (THETA) GRID INCREMENTS FROM TRAILING TO
C.                   LEADING EDGE OF BLADE
C.       RT        = BLADE TIP RADIUS (IN)
C.       ENC       = LENGTH OF FLOW FIELD INFRONT AND BEHINE BLADE (IN)
C.       RP(I)     = R OR Z COORDINATE OF PRESSURE SURFACE (I=1,L) (IN)
C.       RS(I)     = R OR Z COORDINATE OF SUCTION SURFACE   (I=1,N) (IN)
C.       RC(I)     = R OR Z COORDINATE OF CORD LINE         (I=1,K) (IN)
C.       THETS(I)  = THETA   COORDINATE OF SUCTION SURFACE  (I=1,N) (DEG)
C.       THETP(I)  = THETA   COORDINATE OF PRESSURE SURFACE (I=1,L) (DEG)
C.       THETC(I)  = THETA   COORDINATE OF CORD LINE        (I=1,K) (DEG)
C.       RO(I)     = RADIUS COORD. OF STREAM TUBE CENTER LINE(I=1,MNM)(IN)
C.       BO(I)     = WIDTH  COORD. OF STREAM TUBE RADIAL DIR.(I=1,MNM)(IN)
C.       SLAO(I)   = SIN(A) COORD. OF STREAM TUBE CENTER LINE(I=1,MNM)(ND)
C.                   A = ANGLE BETWEEN IMPELLER C.L. AND STREAM TUBE C.
C.       EO(I)     = AXIAL  COORD. OF STREAM TUBE CENTER LINE(I=1,MNM)(IN)
C.        NOTE **** ALL BLADE AND STREAM TUBE COORDINATE DATA STARTS AT
C.                  AT BLADE TRAILING EDGE AND GOES +VE IN UPSTREAM DIR.
C.       KKL       = NO. OF POINTS IN RHO-H-P TABLE
C.                   CONDITIONS OR INTERIOR POINTS DEPENDING ON FLAG (INPUF
C.       INPUF     = FLAG FOR DIFFERENT INLET AND EXIT BOUNDARY CONDITIONS
C.                 = 0 FOR STREAM LINES PARALLEL TO BLADE CORD LINE
C.                 = 1 EQUIVALENT TO 2 AT INLET AND 0 AT EXIT
C.                 = 2 INPUT STREAM FUNCTION AT ALL GRID POINTS
C.                 = 3 INPUT BOTTOM STREAM FUNCTION VALUE
C.                 = 4 EQUIVALENT TO
C.       BN        = NO. OF IMPELLER BLADES
C.       WW        = PUMP SPEED (RAD/SEC)
C.       WDOT      = FLOW RATE IN STREAM TUBE ANULUS (LB/SEC)
C.       ROHIN     = PROPELLANT DENSITY AT INLET (LB/IN**3)
C.       PCIN      = STATIC PRESSURE AT INLET (LB/IN**2)
C.       HOIN      = ENTHALPY AT INLET (FT/SEC)
C.       VTHIN     = CIRCUMFERENTIAL FLUID VELOCITY AT INLET (IN/SEC)
C.       VMOIN     = PROPELLANT LINE VELOCITY AT INLET (IN/SEC)
C.       PS        = PROPELLANT VAPOR PRESSURE (LB/IN**2)
C.       RCIN      = RADIUS OF CENTER OF STREAM TUBE ANULUS AT INLET (IN)
C.                 = RO(MNM)
C.       RHOT(I)   = PROP. DENSITY  VALUES NEAR SATURATION (I=1,KKL)(LB/IN3
C.       HT(I)     = PROP. ENTHALPY VALUES REF. TO HOIN    (I=1,KKL)(FT/SEC
C.       PT(I)     = PROP. PRESSURE VALUES NEAR SATURATION (I=1,KKL)(LB/IN2
C.       PSI(I,J)  = STREAM FUNCTION VALUES AT GRID POINTS, BOUNDARY
C.                   CONDITIONS OR INTERIOR POINTS DEPENDING ON FLAG(INPUF)
```

```
C
 7997 FORMAT(8A10)
 7998 FORMAT(1H1,10X,8A10)
 7999 FORMAT(10X,8A10)
 8000 FORMAT(6I5,5F10.4)
 8001 FORMAT(4E10.3)
 8002 FORMAT(3E10.3)
 8003 FORMAT(3I5,/,(10E8.3))
 8004 FORMAT(10F8.3)
 8009 FORMAT(1X5HRS = F10.4,10H   THETS = F10.4,8H   ES1 = F10.4)
 8010 FORMAT(1X5HRP = F10.4,10H   THETP = F10.4,8H   EP2 = F10.4)
 8012 FORMAT(1X5HRC = F10.4,10H   THETC = F10.4,8H   EC1 = F10.4)
 8011 FORMAT(5HON = I2,7H   L = I2,7H   K = I2,8H   NN = I2,8H   LL = ,
     1 I2,8H   NNM = ,I2,//5H B = F10.4,7H   D = F10.4,8H   RT = F10.4,
     2 8H  ENC = ,F10.4,8H  PNC = ,F10.4 //)
 8013 FORMAT(1X 5HRJ = F10.4,10H   BJ   = F10.4,10H   SIAJ = F10.4,
     *          10H   EJ   = F10.4 )
 8014 FORMAT(1X8HDELTA = F10.4,9H THESL = F10.4,5H E = F10.4,8H THJL = F
     110.4,6H JL = I4,6H IL = I4,7H IIB = I4/7H IIE = I4,7H JLE = I4)
 8015 FORMAT(8E10.4)
 8016 FORMAT(1X8H  KKL = ,I2,10H   INPUF = ,I2,8H    BN = ,F10.4,7H   WW =
     1 F10.4,9H  WDOT = ,F10.4,10H  RHOIN = ,F10.4,9H  POIN = ,F10.4,9H
     2 HOIN = ,F10.4,//,11H    VTHIN = ,F10.4,10H  VMOIN = ,F10.4,7H  PS
     3 = ,F10.4,9H  ROIN = ,F10.4,10H  PSINU = ,F10.4,10H   PSIND = ,
     4 F10.4)
 8017 FORMAT(1X9H  RHOT = ,F10.4,7H  HT = ,F10.4,7H  PT = ,F10.4)
 8018 FORMAT(//)
 8019 FORMAT(1X46HBEGIN MAIN PROGRAM  INCREMENT THETA AND THEN E)
 8020 FORMAT(1X49HSTEP NO. ONE COMPLETE  INCREMENT E AND THEN THETA)
 8030 FORMAT(1X5HII = I4,7H  JN = I4/6H  W = F10.4,6H  X = F10.4,
     16H  Y = F10.4,6H  Z = F10.4)
 8035 FORMAT(1X5HJJ = I4,9H  IPIB = I4,9H  ISIL = I4/9H  ESLI = F10.4,
     1 9H  ESLII= F10.4,9H  EPBI = F10.4,10H  EPBII = F10.4)
 8040 FORMAT(1X5HJJ = I4,9H  IPIB = I4,9H  ISIL = I4/9H  ESLI = F10.4,
     110H  ESLII = F10.4)
C
      COMMON    /ABC/
     *          RHOT(100), HT(100), PT(100)
      COMMON    /CBA/
     *          ENC
      COMMON    /NOG/
     *          NNOG, LNOG, KNOG, ILNOG, THETMIN, THETMAX, EMIN,
     *          EMAX, ICNT(99), THETS(100), THETC(100), THETP(100),
     *          EC1(100), EP2(100), ESS1(100), KNT1, KNT2
      COMMON    ISIL(150), IPIB(150), W(150), X(150), Y(150), Z(150),
     *          JTHL(150), JTHB(150), PSI(100,100),
     *          RS(100), RP(100), ES1(100), RC(100),
     *          EJ(150), RJ(150), BJ(150), SIAJ(150), MNM, IL, JL, IIB,
     *          IIE, B, DELTA, RESIM, DPSIP, KK, DEX, ACC, JLE, BN,
     *          PSIPR, RHO(100,100), G, WDOT, WW, KKL, RHOIN, POIN, HOIN,
     *          ROIN, VTHIN, VMOIN, PS, RR(150), BZ(150), SIA(150), RT,
     *          INPUF, RRL,ITRIP,PDEL,JJPL
C
C         READ INPUT DATA
C
```

```
      READ(5,7997) I1,I2,I3,I4,I5,I6,I7,I8
      IF (EOF,5) 50,60
 50   CALL EXIT
 60   WRITE(6,7998)I1,I2,I3,I4,I5,I6,I7,I8
      READ(5,7997) I1,I2,I3,I4,I5,I6,I7,I8
      WRITE(6,7999)I1,I2,I3,I4,I5,I6,I7,I8
      READ (5,8000)     N, L, K, NN, LL, MNM, B, D, RT, ENC, BNC
      WRITE (6,8011)     N, L, K, NN, LL, MNM, B, D, RT, ENC, BNC
      READ (5,8004)     (RP(I),I=1,L)
      READ (5,8004)     (RS(I),I=1,N)
      READ (5,8004)     (RC(I),I=1,K)
      READ (5,8004)     (THETS(I),I=1,N)
      READ (5,8004)     (THETP(I),I=1,L)
      READ (5,8004)     (THETC(I),I=1,K)
C
      READ (5,8001)     (RD(I),BD(I),SIAD(I),ED(I),I=1,MNM)
      READ (5,8003)     KKL, INPUF,JOPL, BN, WW, WDOT, RHOIN, POIN,
     *                  HOIN,VTHIN, VMOIN, PS, ROIN, PSINU, PSIND,PDEL
      READ (5,8002)     (RHOT(I),HT(I),PT(I),I=1,KKL)
C
C.  TRANSFORM FROM R,THETA PLANE TO E,THETA PLANE
C.      FOR THIS CASE BOTH ARE LINEAR TRANSFORMATIONS
C
      DO  100 I = 1, N
      ES1(I)      = RS(I)
      THETS(I)    = THETS(I) / 57.2958
 100  CONTINUE
      DO  200 I = 1, L
      EP2(I)      = RP(I)
      THETP(I)    = THETP(I) / 57.2958
 200  CONTINUE
      DO  300 I = 1, K
      EC1(I)      = RC(I)
      THETC(I)    = THETC(I) / 57.2958
 300  CONTINUE
C
C.      OVER RIDE BD INPUT
C
      CALL TABL ( ES1(N), RRL, ED, RD, 1, 1, MNM )
      DELTA       = THETC(K) / D
C
C          WRITE OUT INPUT DATA AND VALUES CALCULATED FROM INPUT
C
      WRITE (6,8009)     ((RS(I),THETS(I),ES1(I)),I=1,N)
      WRITE (6,8018)
      WRITE (6,8010)     ((RP(I),THETP(I),EP2(I)),I=1,L)
      WRITE (6,8018)
      WRITE (6,8012)     ((RC(I),THETC(I),EC1(I)),I=1,K)
      WRITE (6,8018)
      WRITE (6,8013)     ((RD(I),BD(I),SIAD(I),ED(I)),I=1,MNM)
      WRITE (6,8018)
      WRITE (6,8016)     KKL, INPUF, BN, WW, WDOT, RHOIN, PCIN, HOIN,
     *                  VTHIN, VMOIN, PS, ROIN, PSINU, PSIND
      WRITE (6,8017)     (RHOT(I),HT(I),PT(I),I=1,KKL)
C
```

```
      THESL        = 0 * DELTA
      JL           = IFIX ( THETP(L) / DELTA ) + 1
      THJL         = FLOAT ( JL - 1 ) * DELTA
      E            = - FLOAT ( IFIX ( ENC / DELTA ) + 1 ) * DELTA
      IL           = IFIX ( ( EC1(K) + ENC ) / DELTA ) + IFIX ( BNC /
     *               DELTA ) + 1
      NNOG         = N
      LNOG         = L
      KNOG         = K
      ILNOG        = IL
      THETHIN      = AMIN1 ( THETS(1), THETP(1), THETC(1) )
      THETMAX      = AMAX1 ( THETS(N), THETP(L), THETC(K) )
      PSIPR        = WDOT / BN
      DELPS        = PSIPR * DELTA / B
C
      DO 500 IJK= 1, N
      ESS1(IJK) = ES1(IJK)
  500 CONTINUE
C
      IIB          = IFIX ( ENC / DELTA ) + 1
      IIE          = IFIX ( EC1(K) / DELTA ) + IFIX ( ENC / DELTA ) + 1
      RESIM        = 0.
      DPSIP        = PSIPR / 20.
      JPTE         = IFIX ( B / DELTA ) + 1
      JLE          = IFIX(D) + 1
      PEX          = ( FLOAT ( IFIX ( EC1(K) / DELTA ) ) * DELTA ) +
     *               DELTA - EC1(K)
      IILE         = IIE + 1
      IF ( PEX .EQ. 0. )                       GO TO 600
       GC TO 700
C
  600 PEX          = DELTA
  700 DEX          = PEX / DELTA
      IF ( THJL .EQ. THETP(L) )               GO TO 800
       GO TO 900
C
  800 JL           = JL - 1
      THJL         = THJL - DELTA
  900 THETA        = -DELTA
      WRITE (6,8014)     DELTA, THESL, E, THJL, JL, IL, IIB, IIE, JLE
      WRITE (6,8019)
C
C.    INCREMENT THETA AND CALCULATE E DIMENSION BETWEEN GRID POINTS AND
C.    BLADE SURFACES
C
      DO 2100 JJ= 1, JL
      THETA        = THETA + DELTA
      IF ( ABS ( 1. - ( THETA / THESL ) ) - .0001 ) 1300, 1300, 1000
 1000 IF ( THETA .GT. THESL )                 GO TO 1300
C
C.       E INCREMENT NEXT TO SUCTION SURFACE = Z(JJ)
C
 1100 CALL TABL ( THETA, ESLI, THETS, ES1, 2, 1, N )
      ISIL(JJ)     = IFIX ( ESLI / DELTA ) + IFIX ( ENC / DELTA ) + 1
      ESLII        = FLOAT ( IFIX ( ESLI / DELTA ) ) * DELTA
```

```
      IF ( ESLII .EQ. ESLI )                    GO TO 1200
      GO TO 1400
C
 1200 ISIL(JJ)  = ISIL(JJ) - 1
      ESLII     = ESLII - DELTA
      GO TO 1400
C
 1300 ISIL(JJ)  = IL - 1
      ESLII     = 0.
      ESLI      = DELTA
C
 1400 IF ( THETA .GT. 8 )                       GO TO 1500
      IPIB(JJ)  = 2
      GO TO 1600
C
C.    E INCREMENT NEXT TO PRESSURE SURFACE = X(JJ)
C
 1500 CALL TABL ( THETA, EPBI, THETP, EP2, 2, 1, L )
      IPIB(JJ)  = IFIX ( EPBI / DELTA ) + IFIX ( ENC / DELTA ) + 2
      EPBII     = ( FLOAT ( IFIX ( EPBI / DELTA ) + 1 ) ) * DELTA
 1600 IPB       = IPIB(JJ)
      ISL       = ISIL(JJ)
      X(JJ)     = 1.
      Z(JJ)     = 1.
      DO 2000 IN= IPB, ISL
      IF ( IN .EQ. ISIL(JJ) )                   GO TO 1700
      GO TO 1800
C
 1700 Z(JJ)     = ( ESLI - ESLII ) / DELTA
      GO TO 2000
 1800 IF ( ( THETA .GT. 8 ) .AND. ( IN .EQ. IPIB(JJ) ) ) GO TO 1900
      GO TO 2000
C
 1900 X(JJ)     = ( EPBII - EPBI ) / DELTA
 2000 CONTINUE
 2100 CONTINUE
      WRITE (6,8020)
C
C.  INCREMENT E AND 1) LOOK UP STREAM TUBE DIMENSIONS, 2) CALCULATE THET
C.  DIMENSION BETWEEN GRID PCINTS AND BLADE SURFACES, AND 3) PROVIDE
C.  FIRST GUESS OF STREAM FUNCTION AND DENSITY AT GRID POINTS
C
      DO 3800 II=1, IL
      W(II)     = 1.
      Y(II)     = 1.
      E         = E + DELTA
      CALL TABL ( E, RRR, ED, RD, 1, 1, MNM )
      RR(II)    = RRR
      CALL TABL ( E, BZZ, ED, BD, 1, 1, MNM )
      BZ(II)    = BZZ
C     BZ(II)    = (BD(MNM)/(RRR**2.))*(RD(MNM)**2.)
C
      CALL TABL ( E, SIDD, ED, SIAD, 1, 1, MNM )
      SIA(II)   = SIDD
      IF( E .GT. 0. )                           GO TO 2800
```

```
C
C.        REGION DOWN STREAM OF BLADES
C
      THETA        = -DELTA
C
C.        EXTRAPOLATE BACK ALONG BLADE CORD LINE
C
      CALL TABL ( E, THEC, EC1, THETC, 1, 1, K )
      JTHL(II)  = IFIX ( B / DELTA ) + 1
      BJL       = FLOAT ( JTHL(II) - 1 ) * DELTA
      JTHB(II)  = 1
      IF ( BJL .EQ. B )                       GO TO 2200
      GO TO 2300
C
 2200 JTHL(II)  = JTHL(II) - 1
      BJL       = B - DELTA
 2300 IF ( ( ABS(E) ) .LT. 0.0001 )          GO TO 2400
      GO TO 2500
C
 2400 THETA     = 0.
      JTHB(II)  = 2
 2500 JTB       = JTHB(II)
      JTL       = JTHL(II)
      JJ        = 0
C
      DO 2700 JN=JTB, JTL
      JJ        = JJ + 1
      THETA     = THETA + DELTA
      PSI(II,JJ)= ( THETA - THEC ) * PSIPR / B
      RHO(II,JJ)= RHOIN
      IF ( JN .EQ. JTHL(II) )                GO TO 2600
      GO TO 2700
C
 2600 Y(II)     = ( B - BJL ) / DELTA
 2700 CONTINUE
      GO TO 3800
C
 2800 IF ( E .GT. EC1(K) )                   GO TO 3500
C
C.        REGION BEWEEN BLADES
C
      CALL TABL ( E, THEIS, ES1, THETS, 2, 1, N )
C
C.        THETA INCREMENT NEXT TO PRESSURE SURFACE = Y(II)
C
      CALL TABL ( E, THEIP, EP2, THETP, 2, 1, L )
      JTHL(II)  = IFIX ( THEIF / DELTA ) + 1
      THL       = FLOAT ( JTHL(II) - 1 ) * DELTA
      IF ( THL .EQ. THEIP )                  GO TO 2900
      GO TO 3000
C
 2900 THL       = THL - DELTA
      JTHL(II)  = JTHL(II) - 1
C
C.        THETA INCREMENT NEXT TO SUCTION SURFACE = W(II)
```

```
C
 3000 JTHB(II)   = IFIX ( THEIS / DELTA ) + 2
      THB        = FLOAT ( JTHB(II) - 1 ) * DELTA
      THETA      = THB - DELTA
      DELTH      = THEIP - THEIS
      JTB        = JTHB(II)
      JTL        = JTHL(II)
      JJ         = 0
C
      DO 3400 JN= JTB, JTL
      JJ         = JJ + 1
      THETA      = THETA + DELTA
      PSI(II,JJ)= ( THETA - THEIS ) * PSIPR / DELTH
      RHO(II,JJ)= RHOIN
      IF ( JN .EQ. JTHB(II) )               GO TO 3100
       GO TO 3200
C
 3100 W(II)      = ( THB - THEIS ) / DELTA
 3200 IF ( JN .EQ. JTHL(II) )               GO TO 3300
       GO TO 3400
C
 3300 Y(II)      = ( THEIP - THL ) / DELTA
 3400 CONTINUE
       GO TO 3800
C
C.    REGION UP STREAM OF BLADES
C
 3500 JTHL(II)   = JL
C
C.       EXTRAPOLATE FORWARD ALONG BLADE CORD LINE
C
      CALL TABL ( E, THEC, EC1, THETC, 1, 1, K )
C     J2 BLADE AND INLET FLOW SLOPE
      DTDE = 1.7
      DWDU = 3.0
      DELD = DWDU - DTDE
      IF ( E.LT.(EC1(K) + .5)) THEC = THEC + 1.*DELD*(E - EC1(K))**2
      IF ( E.GE.(EC1(K)+.5)) THEC = THEC +.25*DELD + DELD*(E -EC1(K)-.5)
      JTHB(II)   = IFIX (D) + 1
      THETA      = ( D - 1. ) * DELTA
      JTB        = JTHB(II)
      JTL        = JTHL(II)
      JJ         = 0
C
      DO 3700 JN= JTB, JTL
      JJ         = JJ + 1
      THETA      = THETA + DELTA
      PSI(II,JJ)= ( THETA - THEC ) * PSIPR / B
      RHO(II,JJ)= RHOIN
      IF ( JN .EQ. JTHL(II) )               GO TO 3600
       GO TO 3700
C
 3600 Y(II)      = ( THETP(L) - THJL ) / DELTA
 3700 CONTINUE
      JLIM       = JTL - JTB + 1
```

```
      IF ( INPUF .EQ. 1 ) READ (5,8015) ( PSI(II,JJ), JJ = 1, JLIM )
 3800 CONTINUE
C
      IF ( INPUF .GT. 1 .AND. INPUF .LT. 4 )      GO TO 4000
 3900 IF ( INPUF .GE. 3 )                         GO TO 4200
      GO TO 4400
 4000 PSIUP     = PSINU
C
      DO 4100 JJ= 1, JLIM
      PSIUP     = PSIUP + JELPS
      PSI(IL,JJ)= PSIUP
 4100 CONTINUE
      GO TO 3900
C
 4200 PSIDN     = PSIND
      DO 4300 JJ= 1, JPTE
      PSIDN     = PSIDN + DELPS
      PSI(1,JJ) = PSIDN
 4300 CONTINUE
C
 4400 DO 4600 I = 1, 110
      DO 4500 J = 1, 55
      RHO(I,J)  = RHOIN
 4500 CONTINUE
 4600 CONTINUE
C
      RETURN
      END
```

```
      SUBROUTINE RELAX
C
C          RELAXATION SUBROUTINE
C
 8001 FORMAT ( 20H ITERATION NUMBER = , I4, 14H      RESIM = , F10.4 )
 8002 FORMAT ( * P = *, E15.7, *    IN = *, I4, *   JC = *, I4, *     RHO
     * I = *, E15.7,*     PCAL = *, E12.5 )
 8003 FORMAT ( *     RHOCM = *, E12.5, *       P = *, E12.5, * \ IN = *, I5,
     *         *         JC = *, I5 )
C
      COMMON    /PLT/
     *          R(100,100), RESID(100)
      COMMON    ISIL(150), IPIB(150), W(150), X(150), Y(150), Z(150),
     *          JTHL(150), JTHB(150), PSI(100,100),
     *          RS(100), RP(100), ES1(100), RC(100),
     *          ED(150), RD(150), BD(150), SIAD(150), MNM, IL, JL, IIB,
     *          IIE, B, DELTA, RESIM, DPSIP, KK, DEX, ACC, JLE, BN,
     *          PSIPR, RHO(100,100), G, WDOT, WW, KKL, RHOIN, POIN, HOIN,
     *          ROIN, VTHIN, VMOIN, PS, RR(150), BZ(150), SIA(150), RT,
     *          INPUF, RRL,ITRIP,PDEL,JDPL
      COMMON    /ABC/
     *          RHOT(100), HT(100), PT(100)
      DATA      NUM    /0/
C
C          ARITHMETIC STATEMENT FUNCTIONS FOR INTERPOLATION
C
      AA(DEX)    = ( ( DEX / 3. ) + ( 0.5 * DEX ** 2 ) + ( ( DEX ** 3 )
     *          / 6. ) ) * ( -1. )
      BB(DEX)    = ( ( 3. * DEX / 2. ) + ( 2. * DEX ** 2 ) + ( ( DEX **
     *          3 ) / 2. ) )
      CC(DEX)    = ( 3. * DEX + ( ( 5. * DEX ** 2. ) / 2. ) + ( ( DEX
     *          ** 3. ) / 2. ) ) * ( -1. )
      DD(DEX)    = ( 1. + ( 11. * DEX / 6. ) + ( DEX ** 2. ) + ( ( DEX
     *          ** 3. ) / 6. ))
C
      RESI2 = 10000.
      ILM1 = IL - 1
      CKK        = 1.
      CCC        = 1.
  100 DPSI1      = ( -11. * PSI(IL,1) + 18. * PSI(IL-1,1) -9.
     *          * PSI(IL-2,1) + 2. * PSI(IL-3,1) ) / DELTA
      VTHC       = - CCC * DPSI1 / ( RHO(IL,1) * BZ(IL) * RR(IL) * 6. )
      DENO = 1./(RHOIN*BZ(IL)*RR(IL))**2.
      BOIN       = DENO * ( ( ( D1+ D2) / DELTA ) ** 2 + ( ( E1+ E2)
     *          / DELTA ) ** 2 )
C
      DO 3400 JJ= 1, JL
      IPB        = IPIB(JJ)
      ISL        = ISIL(JJ)
      II         = 0
C
      DO 3300 IN= IPB, ISL
      II         = II + 1
      JC         = JJ - JTHB(IN) + 1
      JCIP1      = JJ - JTHB(IN+1) + 1
```

```
      JCIM1       = JJ - JTHB(IN-1) + 1
C
      IF ( ( IN .LT. IIB ) .OR. ( IN .GT. IIE ) )    GC TO 1100
  200 IF ( JJ .EQ. JTHB(IN) )                GO TO 300
      GO TO 500
C
  300 PSIJ        = 0.
      RHIJ        = RHO(IN,JC) * ( 1. + W(IN) ) - RHO(IN,JC+1) * W(IN)
      IF ( IN .EQ. ISIL(JJ) )                GO TO 400
      GO TO 2100
C
  400 PSII        = 0.
      RHII        = RHO(IN,JC) * ( 1. + Z(JJ) ) - RHO(IN-1,JCIM1) * Z(JJ)
      BIJ         = BZ(IN)
      BII         = ( 1. - Z(JJ) ) * BZ(IN) + Z(JJ) * BZ(IN+1)
      GO TO 2200
C
  500 IF ( IN .EQ. IPIB(JJ) )                GO TO 600
      GO TO 700
C
  600 PSI(IN-1,JCIM1)= PSIPR
      BII         = BZ(IN+1)
      BIJ         = BZ(IN)
      RHO(IN-1,JCIM1)= ( 1. + X(JJ) ) * RHO(IN,JC) - X(JJ) *
     *               RHO(IN+1,JCIP1)
      PSIJ        = PSI(IN,JC-1)
      RHIJ        = RHO(IN,JC-1)
      PSII        = PSI(IN+1,JCIP1)
      RHII        = RHO(IN+1,JCIP1)
      IF ( IN .GT. IIE )                     GO TO 2100
C
  700 IF ( JJ .EQ. JTHL(IN) )                GO TO 800
      GO TO 900
  800 PSI(IN,JC+1)= PSIPR
      RHO(IN,JC+1)= RHO(IN,JC) * ( 1. + Y(IN) ) - RHO(IN,JC-1) * Y(IN)
  900 IF ( IN .EQ. ISIL(JJ) )                GO TO 1000
      IF ( IN .EQ. IPIB(JJ) )                GO TO 2200
      GO TO 2000
C
 1000 IF ( IN .GT. IIE )                     GO TO 2000
      PSII        = 0.
      BII         = ( 1. - Z(JJ) ) * BZ(IN) + Z(JJ) * BZ(IN+1)
      BIJ         = BZ(IN)
      RHII        = RHO(IN,JC) * ( 1. + Z(JJ) ) - RHO(IN-1,JCIM1) * Z(JJ)
      RHIJ        = RHO(IN,JC) * ( 1. + W(IN) ) - RHO(IN,JC+1) * W(IN)
      PSIJ        = FSI(IN,JC-1)
      GO TO 2300
C
 1100 IF ( JJ .EQ. JTHB(IN) )                GO TO 1200
      GO TO 1600
 1200 JJL         = JTHL(IN) - JTHB(IN) + 1
      PSIJ        = PSI(IN,JJL) - PSIPR
      RHIJ        = RHO(IN,JJL)
      W(IN)       = Y(1)
      IF ( IN .LT. IIB )                     GO TO 1300
```

```
      GC TO 1400
C
 1300 DEX       = 1.0
      PSIJ      = 4. * PSI(IN,JC+1) - 6. * PSI(IN,JC+2) + 4. *
     *            PSI(IN,JC+3) - PSI(IN,JC+4)
      RHIJ      = 4. * RHO(IN,JC+1) - 6. * RHO(IN,JC+2) + 4. *
     *            RHO(IN,JC+3) - RHO(IN,JC+4)
 1400 IF ( ( IN .EQ. ISL ) .AND. ( IN .LT. IIB ) )    GO TO 1500
      GO TO 2100
C
 1500 PSII      = 0.
      RHII      = RHO(IN,JC) * ( 1. + Z(JJ) ) - RHO(IN-1,JCIM1) * Z(JJ)
      BII       = ( 1. - Z(JJ) ) * BZ(IN) + Z(JJ) * BZ(IN+1)
      BIJ       = BZ(IN)
      GO TO 2200
 1600 IF ( JJ .EQ. JTHL(IN) )             GO TO 1700
      GO TO 2000
C
 1700 PSI(IN,JC+1)= PSI(IN,1) + PSIPR
      RHO(IN,JC+1)= RHO(IN,1)
      IF ( IN .LT. IIB )                  GO TO 1800
      GO TO 1900
C
 1800 DEX       = Y(1)
      PSI(IN,JC+1)= AA(DEX) * PSI(IN,JC-3) + BB(DEX) * PSI(IN,
     *            JC-2) + CC(DEX) * PSI(IN,JC-1) + DD(DEX) * PSI(
     *            IN,JC)
      RHO(IN,JC+1)= AA(DEX) * RHO(IN,JC-3) + BB(DEX) * RHO(IN,JC-2) +
     *            CC(DEX) * RHO(IN,JC-1) + DD(DEX) * RHO(IN,JC)
C
 1900 IF ( ( IN .EQ. IPIB(JJ) ) .AND. ( IN .GT. IIE ) )    GO TO 200
 2000 PSIJ      = PSI(IN,JC-1)
      RHIJ      = RHO(IN,JC-1)
 2100 PSII      = PSI(IN+1,JCIP1)
      BII       = BZ(IN+1)
      BIJ       = BZ(IN)
      RHII      = RHO(IN+1,JCIP1)
C
 2200 WWW       = 1.0
      XXX       = 1.0
      YYY       = 1.0
      ZZZ       = 1.0
      IF ( JJ .EQ. JTHL(IN) )        YYY = Y(IN)
      IF ( JJ .EQ. JTHB(IN) )        WWW = W(IN)
      IF ( IN .EQ. IPIB(JJ) )        XXX = X(JJ)
      IF ( IN .EQ. ISIL(JJ) )        ZZZ = Z(JJ)
C
      D1        = ZZZ * ( PSI(IN-1,JCIM1) - PSI(IN,JC) ) /
     *            ( XXX * ( XXX + ZZZ ) )
      D2        = XXX * ( PSI(IN,JC) - PSII ) / ( ZZZ * ( XXX +
     *            ZZZ ) )
      E1        = YYY * ( PSIJ - PSI(IN,JC) ) / ( WWW * ( YYY +
     *            WWW ) )
      E2        = WWW * ( PSI(IN,JC) - PSI(IN,JC+1) ) /
     *            ( YYY * ( YYY + WWW ) )
```

```
C
C       IF((IN.EQ.ISL).AND.(ISL.EQ.ILM1).AND.(JC.EQ.3)) GO TO 2210
C       GO TO 2220
C2210  BOIN = DENO*(((D1+D2)/DELTA)**2+((E1+E2)/DELTA)**2)
 2220  IF ( ITRIP .EQ. 0 )                        GO TO 2600
       WRSQ        = ( WH * RR(IN) ) ** 2
       DENO        = 1. / ( RHOIN * BZ(IN) * RR(IN)) ** 2.
       IF(IN.LT.IIE) GO TO 2300
       COIN = BOIN - ((RR(IN)*WH)**2.)
       GO TO 2400
C
 2300  COIN        = BOIN - ( ( RRL * WH ) ** 2. )
 2400  DOIN        = COIN + ( POIN * 2. * G / RHOIN )
       P           = RHOIN * ( DENO * ( ( ( D1 + D2 ) / DELTA ) ** 2 +
      *              ( ( E1 + E2 ) / DELTA ) ** 2 ) - WRSQ - DOIN ) * ( -1.
      *              ) / ( 2. * G )
       WRITE(6,8002)P,IN,JC,RHO(IN,JC)
       IF((IN.EQ.ISL).AND.(ISL.EQ.ILM1))GO TO 2510
       IF(P.LT.POIN) GO TO 2510
       GO TO 2500
 2510  WRITE(6,8002)P,IN,JC,RHO(IN,JC)
C
 2500  IF ( P .LT. PS )                           GO TO 2700
       GO TO 3300
 2600  RHIJ        = AMAX1 ( RHIJ, 0.000006 )
       RHO(IN,JC+1)= AMAX1 ( RHO(IN,JC+1), 0.000006 )
       RHII        = AMAX1 ( RHII, 0.000006 )
       RHO(IN-1,JCIM1)= AMAX1 ( RHO(IN-1,JCIM1), 0.000006 )
C
       A1          = ( 2. * ( RR(IN) ** 2 ) * WH * BZ(IN) * RHO(IN,JC)
      *              * SIA(IN) ) * DELTA * DELTA
       C1          = ZZZ * ( ALOG ( RHO(IN-1,JCIM1) * BIJ ) - ALOG ( RHO(IN
      *              ,JC) * BZ(IN) ) ) / ( XXX * ( XXX + ZZZ ) )
       C2          = XXX * ( ALOG ( RHO(IN,JC) * BZ(IN) ) - ALOG ( RHII *
      *              BII ) ) / ( ZZZ * ( XXX + ZZZ ) )
       R1          = ( PSI(IN-1,JCIM1) - PSI(IN,JC) ) / ( XXX * (
      *              XXX + ZZZ ) )
       R2          = ( PSI(IN,JC) - PSII ) / ( ZZZ * ( ZZZ + XXX ) )
       R3          = ( PSI(IN,JC+1) - PSI(IN,JC) ) / ( YYY * ( YYY +
      *              WWW ) )
       R4          = ( PSI(IN,JC) - PSIJ ) / ( WWW * ( WWW + YYY ) )
       C3          = WWW * ( ALOG (RHIJ) - ALOG ( RHO(IN,JC) ) ) / ( YYY *
      *              ( YYY + WWW ) )
       C4          = YYY * ( ALOG (RHO(IN,JC) ) - ALOG ( RHO(IN,JC+1) ) ) /
      *              ( WWW * ( YYY + WWW ) )
C
       R(IN,JC)    = - ( A1 + ( D1 + D2 ) * ( C1 + C2 ) * CCC - 2. * ( ( R1
      *              - R2 ) * CCC + ( R3 - R4 ) * CKK ) + ( E1 + E2 ) * (
      *              C3 + C4 ) * CKK )
C
       IF ( ITRIP .EQ. 0 )                        GO TO 3300
       IF(P.GT.POIN ) GO TO 3300
C      WRITE (6,8002)      P, IN, JC, RHO(IN,JC)
       GO TO 3300
C
```

```
2700 CALL TABL ( P, RHIP, PT, RHOT, 1, 1, KKL )
     IF (RHIP.LT..000006) RHIP=.000006
     WRITE(6,8002) P,IN,JC,RHIP
     RHO(IN,JC) = RHIP
     GO TO 3300
     GO TO 2710
**************** RELAX
2720 IF (ABS((RHIP/RHO(IN,JC))-1.0).LT..001) GO TO 2710
     RHO(IN,JC)=.5*(RHO(IN,JC)+RHIP)
     RHOCM=RHO(IN,JC)
     DENO=1./(RHOCM*BZ(IN)*RR(IN))**2
     P           = RHOCM * ( DENO * ( ( ( D1 + D2 ) / DELTA ) ** 2 + ( (
    *               E1 + E2 ) / DELTA ) ** 2 ) - WRSQ - DOIN ) * ( -1. )
    *               / ( 2. * G )
     GO TO 2700
2705 WRITE(6,8002) P,IN,JC,RHIP
     GO TO 2600
2710 WRITE(6,8002) P,IN,JC,RHO(IN,JC)
     GO TO 2600
     IF ( RHIP .LE. 0. )                      RHIP = 0.000006
C
**************** RELAX
2800 RHOCM      = RHIP
     IF ( ITRIP .EQ. 1 )                      RHO(IN,JC) = RHOCM
     WRITE (6,8003)      RHOCM, P, IN, JC
     IF ( ITRIP . EQ. 1 )                     GO TO 3300
C
     DENO       = 1. / ( RHOCM * BZ(IN) * RR(IN) ) ** 2.
     PCAL       = RHOCM * ( DENO * ( ( ( D1 + D2 ) / DELTA ) ** 2 + ( (
    *               E1 + E2 ) / DELTA ) ** 2 ) - WRSQ - DOIN ) * ( -1. )
    *               / ( 2. * G )
     IF ( ITRIP .EQ. 0 )                      GO TO 2900
     WRITE (6,8002)      P, IN, JC,   RHO(IN,JC), PCAL
C
2900 IF ( ( ABS ( PCAL / P ) - 1. ) .LT. 0.0001 )    GO TO 3100
     IF ( PCAL .LT. PSAV )                    GO TO 3000
     RHO(IN,JC) = RHOCM
     GO TO 3100
3000 RHO(IN,JC) = RHOIN - 0.05 * ( RHO(IN,JC) - RHOCM )
     IF ( RHO(IN,JC) .LT. 0.00002 )           RHO(IN,JC) = RHOIN
     GO TO 2600
C
3100 IF ( RHOCM .LE. 0. )                     RHOCM = 0.000006
3200 RHO(IN,JC) = RHOCM
     GO TO 2600
3300 CONTINUE
3400 CONTINUE
     IF(ITRIP.NE.0) GO TO 4800
3500 DO 4300 JJ= 1, JL
     IPB        = IPIB(JJ)
     ISL        = ISIL(JJ)
     II         = 0
C
     DO 4200 IN= IPB, ISL
     II         = II + 1
```

```
      WWW        = 1.0
      XXX        = 1.0
      YYY        = 1.0
      ZZZ        = 1.0
      IF ( JJ .EQ. JTHL(IN) )                 YYY = Y(IN)
      IF ( JJ .EQ. JTHB(IN) )                 WWW = W(IN)
      IF ( IN .EQ. IPIB(JJ) )                 XXX = X(JJ)
      IF ( IN .EQ. ISIL(JJ) )                 ZZZ = Z(JJ)
C
      JC         = JJ - JTHB(IN) + 1
      JCIP1      = JJ - JTHB(IN+1) + 1
      JCIM1      = JJ - JTHB(IN-1) + 1
      DPSI       = R(IN,JC) / ( ( 1. / WWW ) + ( 1. / XXX ) + ( 1. / YYY
     *            ) + ( 1. / ZZZ ) )
      R(IN,JC)   = 0.
      PSI(IN,JC)= PSI(IN,JC) + DPSI
C
      IF ( ( IN .LT. IIB ) .OR. ( IN .GT. IIE ) )   GO TO 3600
      IF ( ( JJ .EQ. JTHB(IN) ) .AND. ( IN .EQ. ISIL(JJ) ) ) GO TO 4100
      IF ( JJ .EQ. JTHB(IN) )                 GO TO 4000
      IF ( IN .EQ. ISIL(JJ) )                 GO TO 4100
      GO TO 3900
C
 3600 IF ( JTHB(IN) .EQ. JJ )                 GO TO 3700
      IF ( JTHL(IN) .EQ. JJ )                 GO TO 3800
      GO TO 3900
 3700 JJL        = JTHL(IN) - JTHB(IN) + 1
      JB         = JTHL(IN)
      R(IN,JJL) = R(IN,JJL) + DPSI * ( 1. / YYY )
      IF ( IN .EQ. ISIL(JJ) )                 GO TO 4100
      GO TO 4000
C
 3800 JJB        = JTHB(II)
      R(IN,1)    = R(IN,1) + DPSI
      R(IN,JC-1)=R(IN,JC-1)+DPSI*(1./WWW)
      GO TO 4000
C
 3900 R(IN,JC-1)= R(IN,JC-1) + DPSI * ( 1. / WWW )
 4000 R(IN+1,JCIP1)= R(IN+1,JCIP1) + DPSI * ( 1. / ZZZ )
 4100 R(IN,JC+1)= R(IN,JC+1) + DPSI * ( 1. / YYY )
      R(IN-1,JCIM1)= R(IN-1,JCIM1) + DPSI * ( 1. / XXX )
 4200 CONTINUE
 4300 CONTINUE
C
      ILM1       = IL - 1
      DO 4500 II= 2, ILM1
      RESID(II) = 0.
      JJ         = 0
      JTB        = JTHB(II)
      JTL        = JTHL(II)
C
      DO 4400 JN= JTB, JTL
      JJ         = JJ + 1
      IF ( ( ABS (R(II,JJ) ) ) .GT. RESID(II) )   RESID(II)=ABS(R(II,JJ))
 4400 CONTINUE
```

```
 4500 CONTINUE
C
      DO 4600 II= 2, ILM1
      IF ( RESID(II) .GT. RESIM )           RESIM = RESID(II)
 4600 CONTINUE
      IF(RESIM.GT.RESI2)      STOP
      RESI2=2.0*RESIM
      IF ( RESIM .GT. ACC )                 GO TO 4700
      GO TO 4800
C
 4700 NUM        = NUM + 1
      WRITE (6,8001)      NUM, RESIM
      RESIM      = 0.
      IF(NUM.EQ.50)    GO TO 4710
      GO TO 100
 4710 CALL PREWRT
      CALL WRTOUT
       GC TO 100
C
 4800 NUM        = NUM + 1
      WRITE (6,8001)      NUM, RESIM
      RESIM      = 0.
      RETURN
      END
```

```
      SUBROUTINE PREWRT
C
C            ROUTINE TO CALCULATE DPSIDD, DPSIDU, AND PHI VALUES BEFORE
C            GOING INTO WRTOUT
C
 8001 FORMAT ( ////* *******  VOLUME = *, E12.5 )
C
      COMMON      ISIL(150), IPIB(150), W(150), X(150), Y(150), Z(150),
     *            JTHL(150), JTHB(150), PSI(100,100),
     *            RS(100), RP(100), ES1(100), RC(100),
     *            ED(150), RD(150), BD(150), SIAD(150), MNM, IL, JL, IIB,
     *            IIE, B, DELTA, RESIM, DPSIP, KK, DEX, ACC, JLE, BN,
     *            PSIPR, RHO(100,100), G, WDOT, WW, KKL, RHOIN, POIN, HOIN,
     *            ROIN, VTHIN, VPOIN, PS, RR(150), BZ(150), SIA(150), RT,
     *            INPUF, RRL,ITRIP,PDEL,JDPL
      COMMON / CBA /
     *            ENC
      COMMON      /NDG/
     *            NNDG, LNDG, KNDG, ILNDG, THETMIN, THETMAX, EMIN,
     *            EMAX, ICNT(99), THETS(100), THETC(100), THETP(100),
     *            EC1(100), EP2(100), ESS1(100), KNT1, KNT2
C
      HDELTA      = DELTA * 0.5
      SUM         = 0.
      ILL         = IL - 1
      E           = -( FLOAT ( IFIX ( ENC / DELTA ) ) * DELTA ) - DELTA
C
      DO 3000 II= 1, ILL
      E           = E + DELTA
      JTB         = JTHB(II)
      JTL         = JTHL(II)
      JJ          = 0
C
      DO 2900 JN= JTB, JTL
      JJ          = JJ + 1
C
 2100 COSA        = COS ( ASIN ( SIA(II) ) )
      THETA       = FLOAT (JN-1) * DELTA
      IF ( II .LE. IIB )                    GO TO 2200
      IF ( JN .EG. JTB )                    GO TO 2400
      IF ( JN .EQ. JTL )                    GO TO 2600
C
      VOLUME      = DELTA / COSA * DELTA * RR(II) * BZ(II)
      GO TO 2800
C
 2200 DELT        = DELTA
      DELE        = DELTA
      IF ( II .EQ. 1 )                      DELE = HDELTA
      IF ( JN .EQ. JTL )                    DELT = HDELTA + DELTA * Y(1)
      IF ( JN .EQ. 1 )                      DELT = HDELTA
      VOLUME      = DELE / COSA * RR(II) * DELT * BZ(II)
      GO TO 2800
C
 2300 DELE        = DELTA
      IF ( II .EQ. ISIL(1) )                DELE = HDELTA + DELTA * Z(1)
```

```
      VOLUME     = DELE / COSA * RR(II) * HDELTA * BZ(II)
      GO TO 2800
C
 2400 IF ( II .GT. IIE )                     GO TO 2500
      EU1        = E + HDELTA
      EL1        = E - HDELTA
      CALL TABL ( EU1, THETU1, ESS1, THETS, 2, 1, NNDG )
      CALL TABL ( EL1, THETL1, ESS1, THETS, 2, 1, NNDG )
C
      THETU2     = THETA + HDELTA
      THETL2     = THETA - HDELTA
      CALL TABL ( THETU2, EU2, THETS, ESS1, 2, 1, NNDG )
      CALL TABL ( THETL2, EL2, THETS, ESS1, 2, 1, NNDG )
C
      EULC       = AMIN1 ( EU1, EU2 )
      THETLC     = AMIN1 ( THETU1, THETU2 )
      EHGT       = ( EULC - EL1 ) / COSA
      TLNGTH     = (( THETU2 - THETLC ) + ( THETU2 - THETL1 )) / 2.0
      VOLUME     = EHGT * RR(II) * BZ(II) * TLNGTH
      GO TO 2800
C
 2500 VOLUME     = DELTA / COSA * RR(II) * HDELTA * BZ(II)
      GO TO 2800
C
 2600 IF ( II .GT. IIE )                     GO TO 2700
      EU1        = E + HDELTA
      EL1        = E - HDELTA
      CALL TABL ( EU1, THETU1, EP2, THETP, 2, 1, LNDG )
      CALL TABL ( EL1, THETL1, EP2, THETP, 2, 1, LNDG )
C
      THETU2     = THETA + HDELTA
      THETL2     = THETA - HDELTA
      CALL TABL ( THETU2, EU2, THETP, EP2, 2, 1, LNDG )
      CALL TABL ( THETL2, EL2, THETP, EP2, 2, 1, LNDG )
C
      EULC       = AMAX1 ( EL1, EL2 )
      THETLC     = AMAX1 ( THETL1, THETL2 )
      EHGT       = ( EU1 - EULC ) / COSA
      TLNGTH     = (( THETU1 - THETL2 ) + ( THETLC - THETL2 )) / 2.0
      VOLUME     = EHGT * RR(II) * TLNGTH * BZ(II)
      GO TO 2800
C
 2700 DELT       = HDELTA + DELTA * Y(II)
      VOLUME     = DELTA / COSA * RR(II) * DELT * BZ(II)
C
 2800 VOLUME     = VOLUME * RHO(II,JJ)
      SUM        = SUM + VOLUME
 2900 CONTINUE
 3000 CONTINUE
      WRITE (6,8001)          SUM
      RETURN
      END
```

```
      SUBROUTINE WRTOUT
C
C          ROUTINE TO PROCESS AND PRINT OUTPUT
C
 8001 FORMAT ( 5H E = ,F10.4,7H    I = ,I4,7H    R = ,F10.4,7H    B = ,F10.
     *4,9H    SIA = ,F10.4)
 8002 FORMAT(1X6HPSI = F10.4,10H   THETA = F10.4,8H   PHI = F10.4,6H   V =
     *F10.4,6H   U = F10.4)
 8003 FORMAT( * IJK IS GREATER THAN 25 * )
C
      COMMON       ISIL(150), IPIB(150), W(150), X(150), Y(150), Z(150),
     *             JTHL(150), JTHB(150), PSI(100,100),
     *             RS(100), RP(100), ES1(100), RC(100),
     *             ED(150), RD(150), BD(150), SIAD(150), MNM, IL, JL, IIB,
     *             IIE, B, DELTA, RESIM, OPSIP, KK, DEX, ACC, JLE, BN,
     *             PSIPR, RHO(100,100), G, WDOT, WW, KKL, RHOIN, POIN, HOIN,
     *             RCIN, VTHIN, VMOIN, PS, RR(150), BZ(150), SIA(150), RT,
     *             INPUF, RRL,ITRIP,PDEL,JOPL
     COMMON       /PLT/
     *             THTA(100)
      COMMON       /CBA/
     *             ENC
      COMMON       /NDG/
     *             NNDG, LNDG, KNDG, ILNDG, THETMIN, THETMAX, EMIN,
     *             EMAX, ICNT(99), THETS(100), THETC(100), THETP(100),
     *             EC1(100), EP2(100), ESS1(100), KNT1, KNT2
C
C          ARITHMETIC STATEMENT FUNCTIONS FOR INTERPOLATION
C
      AA(DEX)     = ( ( DEX / 3. ) + ( 0.5 * DEX ** 2 ) + ( ( DEX ** 3 ) /
     *             6. ) ) * ( -1. )
      BB(DEX)     = ( ( 3. * DEX / 2. ) + ( 2. * DEX ** 2 ) + ( ( DEX ** 3
     *             ) / 2. ) )
      CC(DEX)     = ( 3. * DEX + ( ( 5. * DEX ** 2. ) / 2. ) + ( ( DEX **
     *             3. ) / 2. ) ) * ( -1. )
      DD(DEX)     = ( 1. + ( 11. * DEX / 6. ) + ( DEX ** 2. ) + ( ( DEX **
     *             3. ) / 6. ) )
C
      E           = -( FLOAT ( IFIX ( ENC / DELTA ) ) * DELTA ) - DELTA
      EMIN        = E + DELTA
      ECC1        = EC1(KNDG)
      THETCC      = THETC(KNDG)
      THETPP      = THETP(LNDG)
C
      IJKNDG      = 160
      SIMIN       = -1.05 * PSIPR
      KNT1        = 0
      KNT2        = 0
      LFILE       = 9
      ILL         = IL - 1
C
      DO  700 II= 1, ILL
      E           = E + DELTA
      CALL TABL ( E, RPRNT, ED, RD, 3, 1, MNM )
      CALL TABL ( E, BPRNT, ED, BD, 3, 1, MNM )
```

```
      CALL TABL ( E, SIAPRT, EO, SIAO, 3, 1, MNN )
C
      KKK        = 0
      LLL        = 0
      JTB        = JTHB(II)
      JTL        = JTHL(II)
      JJ         = 0
      MM         = 0
C
      DO  500 JN= JTB, JTL
      IC         = II - IPIB(JN) + 1
      JJ         = JJ + 1
      MM         = MM + 1
      IF ( ( II .LT. IIB ) .OR. ( II .GT. IIE ) )        GO TO 300
      IF ( JN .EQ. JTB )                        GO TO 100
      GO TO 300
C
  100 THTA(MM)   = ( ( FLOAT(JN-1) ) - W(II) ) * DELTA
      DEX        = W(II)
      RC(MM)     = AA(DEX) * PSI(II,JJ+3) + BB(DEX) * PSI(II,JJ+2) +
     *             CC(DEX) * PSI(II,JJ+1) + DD(DEX) * PSI(II,JJ)
      MM         = MM + 1
      GO TO 300
C
  200 MM         = MM + 1
      THTA(MM)   = ( ( FLOAT(JN-1) ) + Y(II) ) * DELTA
      DEX        = Y(II)
      RC(MM)     = AA(DEX) * PSI(II,JJ-3) + BB(DEX) * PSI(II,JJ-2) +
     *             CC(DEX) * PSI(II,JJ-1) + DD(DEX) * PSI(II,JJ)
      GO TO 400
C
  300 THTA(MM)   = ( FLOAT(JN-1) ) * DELTA
      RC(MM)     = PSI(II,JJ)
      IF ( JN .EQ. JTL )                        GO TO 200
  400 K          = MM
  500 CONTINUE
C
      PSIP       = SIMIN
      JJK        = 0
C
      DO 600 IJK= 1, IJKNDG
      PSIP       = PSIP + DPSIP
      IF ( PSIP .LT. -0.0001 .AND. E .LT. ECC1 )        GO TO 600
      IF ( FSIP .GT. PSIPR .AND. E .GT. 0. )            GO TO 700
C
      CALL TABL ( PSIP, THETA, RC, THTA, 3, 1, K )
      IF ( THETA .LT. 0. .OR. THETA .GT. THETPP )       GO TO 600
      IF ( E .GE. ECC1 .AND. THETA .LT. THETCC )        GO TO 600
      IF ( E .LE. ESS1(1) .AND. THETA .GT. THETP(1) )   GO TO 600
C
      IF ( MOD(IJK,2) .EQ. 0 )                   GO TO 600
C
      IFILE      = IFIX ( ( PSIP + PSIPR ) / ( DPSIP * 2.0 ) + 9.25 )
      ICNT(IFILE) = ICNT(IFILE) + 1
      IF ( IFILE .EQ. 44 )                   IFILE = 2
```

```
      CALL ALTFILE ( LFILE, IFILE, NOUM )
      LFILE      = IFILE
      WRITE (IFILE)       E, THETA, PSIP
  600 CONTINUE
  700 CONTINUE
C
      CALL ALTFILE (LFILE, 9, NOUM )
      EMAX      = E
      CALL PLOTT
      KK        = 1
      RETURN
      END
```

```
      SUBROUTINE PLOTT
C
C        SUBROUTINE TO PLOT OUTPUT DATA
C
      COMMON    /PLT/
     *          E(200), THETA(200), PSI(200)
      COMMON    /NDG/
     *          NNDG, LNDG, KNDG, ILNDG, THETMIN, THETMAX, EMIN,
     *          EMAX, ICNT(99), THETS(100), THETC(100), THETP(100),
     *          EC1(100), EP2(100), ES1(100), KNT1, KNT2
C
      DATA      KNTO / 0 /
      IF ( KNTO .NE. 0 )                        GO TO 100
      CALL INIT280
      KNTO      = 1
  100 CONTINUE
C
      EMIN      = AMIN1 ( EMIN, ES1(1), EP2(1), EC1(1) )
      EMAX      = AMAX1 ( EMAX, ES1(NNDG), EP2(LNDG), EC1(KNDG) )
      THETPP    = THETP(1)
      CALL SETUP
C
      DO  200 I = 1, NNDG
      E(I)      = THETS(I) + THETPP
  200 E(I+100)  = EMAX - ( ES1(I) - EMIN )
      DO  300 I = 1, LNDG
      THETA(I)  = THETP(I) - THETPP
  300 THETA(I+100) = EMAX - ( EP2(I) - EMIN )
      DO  400 I = 1, KNDG
  400 PSI(I)    = EMAX - ( EC1(I) - EMIN )
C
      DO  500 I = 1, 2
      CALL LINES ( E(101), THETS(1), NNDG )
      CALL LINES ( THETA(101), THETP(1), LNDG )
      CALL LINES ( PSI(1), THETC(1), KNDG )
      CALL LINES ( E(101), E(1), NNDG )
      CALL LINES ( THETA(101), THETA(1), LNDG )
      CALL LINE ( E(101), THETPP, EMAX, THETPP )
      CALL LINE ( EMAX, THETP, EMAX, THETMIN )
      CALL LINE ( EMIN, THETP(LNDG), THETA(LNDG+100), THETP(LNDG) )
      CALL LINE ( EMIN, THETC(KNDG), PSI(KNDG), THETC(KNDG) )
  500 CONTINUE
C
      LFILE     = 9
      DO  800 I = 9, 99
      IJK       = ICNT(I)
      ICNT(I)   = 0
      IF ( IJK .EQ. 0 )                         GO TO 800
      II        = I
      IF ( I .EQ. 44 )                          II = 2
      CALL ALTFILE ( LFILE, II, NDUM )
      LFILE     = II
      REWIND II
      IF ( IJK .EQ. 1 )                         GO TO 800
C
```

```
      DO  600 J = 1, IJK
      READ (II)      E(J),  THETA(J), PSI(J)
      E(J)        = EMAX - ( E(J) - EMIN )
  600 CONTINUE
      REWIND II
C
      DO  700 J = 1, 2
      CALL LINES ( E(1), THETA(1), IJK )
  700 CONTINUE
C
  800 CONTINUE
      CALL ALTFILE ( LFILE, 9, NDUM )
      CALL FRAME
      RETURN
      END
```

```
      SUBROUTINE SETUP
C
C         SUBROUTINE TO SETUP GRID FOR PLOTS
C
      COMMON    /NDG/
     *          NNDG, LNDG, KNDG, ILNDG, THETMIN, THETMAX, EMIN,
     *          EMAX, ICNT(99), THETS(100), THETC(100), THETP(100),
     *          EC1(100), EP2(100), ES1(100), KNT1, KNT2
C
      CALL CHAROPT ( 0, 0, 1, 0, 0 )
      CALL LINEOPT ( 0, 1 )
      CALL ABSBEAM ( .15, .993 )
      CALL ABSVECT ( .15, .214 )
      CALL ABSVECT ( .930, .214 )
C
      CALL LINEOPT ( 0, 0 )
      CALL MAP ( EMIN, EMAX, THETMIN, THETMAX, .15, .930, .214, .993 )
      DO  100 K = 1, 2
      CALL ABSBEAM ( .5, .15 )
      CALL SYMBOL   ( 3HE$. )
      CALL ABSBEAM ( .05, .6 )
      CALL SYMBOL   ( 3HF$. )
      CALL ABSBEAM ( .4, .08 )
  100 CALL SYMBOL   ( 27HCOORDINATES IN E, F PLANES. )
      RETURN
      END
```

APPENDIX F

Input Data Interpolation Program

For all of the turbopump inducers analyzed in this study, blade geometrical data was derived from inducer design drawings. This data is normally tabulated on the drawing for only a few blade sections at a constant distance off the inducer hub. A computer program was written to provide input data for additional blade sections located at a constant percent of blade span. Figure F.1 illustrates this procedure. Sections R_1 and R_2 represent typical blade sections for which blade geometrical data is supplied. This data is linearized to yield associated geometry for blade sections at 10%, 30%, 50%, 70%, and 90% of the blade span, shown as dashed lines in this figure.

Figures F.2 through F.6 show a typical sequence of data manipulation for the J-2 LOX inducer. Figure F.2 is a plot of the tabulated data given on the inducer design drawing (Figure 5.1). This data is normalized to the blade leading edge (Figure F.3), non-dimensionalized (Figure F.4), and linearly interpolated (Figure F.5) to yield the required input data for the five blade sections (Figure F.6). The final form of the data is then punched on computer cards for input to the turbopump cavitation compliance program.

The following pages of this appendix present a listing of the input data interpolation program. The liberal use of comment cards makes the program operation self-explanatory. Sample input/output listings are also provided.

```
      PROGRAM BLADE2(INPUT,OUTPUT,TAPE5=INPUT,TAPE6=OUTPUT,FILMPL,PUNCH)BD2    2
C.        PROGRAM TO INTERPOLATE BLADE INPUT DATA FOR TWO SECTIONS       BD2    4
      DATA STOP/6HSTOP/                                                  BD2    6
      DIMENSION TITL1(8), TITL2(8), X(50), Y11(50), Y12(50), Y21(50), Y2BD2    8
     12(50), Y1DUM(50), Y2DUM(50), Y3DUM(50), Y4DUM(50), X1(50), X2(50),BD2   10
     2 TEY(5), XLEDG(5), XSS(5,51), YLEDG(5), XT(51), YT11(51), YT12(51)BD2   12
     3, YT21(51), YT22(51), TEP(5,50), RSTREAM(3), XLSQ(3), YLSQ(3), RADBD2   14
     4(3), YR1(3), YR2(3), Y1(5,51), Y2(5,51), YCC(51), TPAC(51), AX(51)BD2   16
     5, RX(51), RO(51), BO(51), YZER1(51), YSLP1(51), YZER2(51), YSLP2(5BD2   18
     6)                                                                 BD2   20
C.        DEFINITION OF INPUT DATA                                       BD2   22
C.        CARD 1    TITL1 = TITLE COMMON TO ALL CASES     (8A1) FORMAT)  BD2   24
C.        CARD 2    TITL2 = TITLE PECULIAR TO EACH CASE   (8A10 FORMAT)  BD2   26
C.        CARD 3    IPUNCH,INTERP                         (10I5 FORMAT)  BD2   28
C.          IPUNCH= FLAG TO CONTROL PUNCHING OF OUTPUT DATA              BD2   30
C.          INTERP= FLAG TO CONTROL INTERPOLATION OF INPUT DATA          BD2   32
C.        CARD 4    ALF1,ALF2,FSR,HL,HX                   (5F10.4 FORMAT) BD2   34
C.          ALF1  = HALF-CONE ANGLE OF HUB                      (DEG)    BD2   36
C.          ALF2  = ANGLE OF BLADE LEADING EDGE LOCUS           (DEG)    BD2   38
C.          FSR   = FEEDLINE UPSTREAM RADIUS                    (IN)     BD2   40
C.          HL    = FORWARD HUB RADIUS                          (IN)     BD2   42
C.          HX    = HUB EQUIVALENT LENGTH                       (IN)     BD2   44
C.        CARD 5    S1,S2,XSCLFC                          (5F10.4 FORMAT) BD2   46
C.          S1    = LOCATION OF INNERMOST BLADE SECTION         (IN)     BD2   48
C.          S2    = LOCATION OF OUTERMOST BLADE SECTION         (IN)     BD2   50
C.          XSCLFC= FLAG TO CORRECT INPUT DATA IF Z MEASURED             BD2   52
C.                  PARALLEL TO CENTERLINE                     (NO)      BD2   54
C.        CARD 6    BNUM,DGINC,ENC,BNC,STWNOM             (5F10.4 FORMAT) BD2   56
C.          BNUM  = NUMBER OF BLADES                                     BD2   58
C.          DGINC = NUMBER OF GRID INCREMENTS                            BD2   60
C.          ENC   = UPSTREAM EXTENSION OF FLOWFIELD SOLUTION             BD2   62
C.          BNC   = DOWNSTREAM EXTENSION OF FLOWFIELD SOLUTION           BD2   64
C.          STWNOM= NOMINAL WIDTH OF STREAMTUBE                          BD2   66
C.        CARD I    X,Y11,Y12,Y21,Y22                     (5F10.4 FORMAT) BD2   68
      READ (5,255) TITL1                                                 BD2   70
10    READ (5,255) TITL2                                                 BD2   72
      IF (TITL2.EQ.STOP) GO TO 205                                       BD2   74
      READ (5,280) IPUNCH,INTERP                                         BD2   76
C.        READ IN INDUCER GEOMETRY DATA                                  BD2   78
      READ (5,260) ALF1,ALF2,FSR,HL,HX                                   BD2   80
      RAD=57.29578                                                       BD2   82
      ANGL1=ALF1/RAD                                                     BD2   84
      ANGL2=ALF2/RAD                                                     BD2   86
      TMLTAN=ABS(TAN(ANGL1))                                             BD2   88
      TMLCSN=ABS(COS(ANGL1))                                             BD2   90
      FSL=FSR-HL                                                         BD2   92
      HT=HX*TMLTAN+HL                                                    BD2   94
      FST=FSR-HT                                                         BD2   96
      READ (5,260) S1,S2,XSCLFC                                          BD2   98
C.        READ IN INDUCER ANALYSIS DATA                                  BD2  100
      READ (5,260) BNUM,DGINC,ENC,BNC,STWNOM                            BD2  102
      DO 15 I=1,50                                                       BD2  104
      READ (5,260) X(I),Y11(I),Y12(I),Y21(I),Y22(I)                      BD2  106
      IF (X(I).LT.0.) GO TO 20                                           BD2  108
15    CONTINUE                                                           BD2  110
20    NPTS=I-1                                                           BD2  112
C.        ALL INPUT COMPLETE - PRODUCE ECHO PRINTOUT                     BD2  114
      WRITE (6,265) TITL1,TITL2                                          BD2  116
      WRITE (6,270) S1,S2                                                BD2  118
```

```
      WRITE (6,260) (X(I),Y11(I),Y12(I),Y21(I),Y22(I),I=1,NPTS)      BD2
      IF (XSCLFC.LE.0.) GO TO 30                                      BD2
C.        CORRECT INPUT DATA FOR Z MEASURED PARALLEL TO CENTERLINE    BD2
      DO 25 I=1,NPTS                                                  BD2
      Y11(I)=Y11(I)/TMLCSN                                            BD2
      Y12(I)=Y12(I)/TMLCSN                                            BD2
      Y21(I)=Y21(I)/TMLCSN                                            BD2
      Y22(I)=Y22(I)/TMLCSN                                            BD2
25    CONTINUE                                                        BD2
      WRITE (6,265) TITL1,TITL2                                       BD2
      WRITE (6,210)                                                   BD2
      WRITE (6,270) S1,S2                                             BD2
      WRITE (6,260) (X(I),Y11(I),Y12(I),Y21(I),Y22(I),I=1,NPTS)      BD2
30    CONTINUE                                                        BD2
      TP1=X(NPTS)                                                     PD2
      TY1=Y12(NPTS)                                                   BD2
      TP2=X(NPTS)                                                     BD2
      TY2=Y22(NPTS)                                                   BD2
      WRITE (6,275) TP1,TY1,TP2,TY2                                   BD2
C.     ECHO OF INPUT COMPLETE                                         BD2
C.                                                                    BD2
C.        LINEARIZE R/Z VERSUS ANGULAR DISPLACEMENT                   BD2
      RMAX=FSL/TMLCSN                                                 BD2
      RMIN=FST/TMLCSN                                                 BD2
      XLSQ(1)=X(1)                                                    BD2
      XLSQ(2)=X(NPTS)                                                 BD2
      YLSQ(1)=RMAX                                                    BD2
      YLSQ(2)=RMIN                                                    BD2
      CALL LSQ1 (2,XLSQ,YLSQ,RNAUT,RSLOPE,PE,SRSQ)                    BD2
C.        LINEARIZATION COMPLETE *** R(PHI) = RNAUT + RSLOPE*PHI      BD2
C.                                                                    BD2
C.        PLOT INPUT DATA NON-NORMALIZED                             BD2
      CALL PLOTR1 (X,Y11,Y12,Y21,Y22,NPTS,TITL1,TITL2,1)            BD2
C.                                                                    BD2
C.        NORMALIZE ALL INPUT TO TRAILING EDGE COORDINATES           BD2
      DO 35 I=1,NPTS                                                  BD2
      JEND=NPTS+1-I                                                   BD2
      X1(I)=X(NPTS)-X(JEND)                                           BD2
      Y1DUM(I)=Y12(NPTS)-Y11(JEND)                                    BD2
      Y2DUM(I)=Y12(NPTS)-Y12(JEND)                                    BD2
      Y3DUM(I)=Y22(NPTS)-Y21(JEND)                                    BD2
      Y4DUM(I)=Y22(NPTS)-Y22(JEND)                                    BD2
35    CONTINUE                                                        BD2
      DO 40 I=1,NPTS                                                  BD2
      X(I)=X1(I)                                                      BD2
      Y11(I)=Y1DUM(I)                                                 BD2
      Y12(I)=Y2DUM(I)                                                 BD2
      Y21(I)=Y3DUM(I)                                                 BD2
      Y22(I)=Y4DUM(I)                                                 BD2
40    CONTINUE                                                        BD2
C.     WRITE NORMALIZED INPUT DATA                                    BD2
      WRITE (6,265) TITL1,TITL2                                       BD2
      WRITE (6,215)                                                   BD2
      WRITE (6,260) (X(I),Y11(I),Y12(I),Y21(I),Y22(I),I=1,NPTS)      BD2
C.     NORMALIZATION COMPLETE                                         BD2
C.                                                                    BD2
C.        PLOT NORMALIZED INPUT DATA                                 BD2
      CALL PLOTR1 (X,Y11,Y12,Y21,Y22,NPTS,TITL1,TITL2,2)            BD2
      IF (INTERP.LE.0) GO TO 150                                     BD2
C.                                                                    BD2
```

```
C.          NON-DIMENSIONALIZE ALL INPUT DATA WITH RESPECT TO CHORD LENGTH BD2 240
            DO 45 I=2,NPTS                                                  BD2 242
            IF (Y11(I).EQ.Y12(I)) GO TO 50                                  BD2 244
45          CONTINUE                                                        BD2 246
50          NPAIRS1=I                                                       BD2 248
            DO 55 I=2,NPTS                                                  BD2 250
            IF (Y21(I).EQ.Y22(I)) GO TO 60                                  BD2 252
55          CONTINUE                                                        BD2 254
60          NPAIRS2=I                                                       BD2 256
            DO 65 I=1,NPTS                                                  BD2 258
            X1(I)=X(I)/X(NPAIRS1)                                           BD2 260
            X2(I)=X(I)/X(NPAIRS2)                                           BD2 262
            IF (X2(I).GT.1.) X2(I)=1.0                                      BD2 264
65          CONTINUE                                                        BD2 266
C.          STORE LEADING EDGE AXIAL COORDINATES FOR LATER CURVE FIT        BD2 268
            YLDG1=Y11(NPAIRS1)                                              BD2 270
            YLDG2=Y21(NPAIRS2)                                              BD2 272
C.          NON-DIMENSIONALIZE ALL INPUT DATA WITH RESPECT TO AXIAL COORD   BD2 274
            DO 70 I=1,NPTS                                                  BD2 276
            Y11(I)=Y11(I)/Y11(NPAIRS1)                                      BD2 278
            Y12(I)=Y12(I)/Y12(NPAIRS1)                                      BD2 280
            Y21(I)=Y21(I)/Y21(NPAIRS2)                                      BD2 282
            Y22(I)=Y22(I)/Y22(NPAIRS2)                                      BD2 284
            IF (Y21(I).GT.1.) Y21(I)=1.                                     BD2 286
            IF (Y22(I).GT.1.) Y22(I)=1.                                     BD2 288
70          CONTINUE                                                        BD2 290
C.          WRITE NON-DIMENSIONALIZED INPUT DATA                            BD2 292
            WRITE (6,265) TITL1,TITL2                                       BD2 294
            WRITE (6,220)                                                   BD2 296
            WRITE (6,225) (X1(I),Y11(I),Y12(I),X2(I),Y21(I),Y22(I),I=1,NPTS) BD2 298
C.          PLOT NON-DIMENSIONALIZED DATA                                   BD2 300
            CALL PLOTR2 (X1,Y11,Y12,X2,Y21,Y22,NPAIRS1,NPAIRS2,TITL1,TITL2,1) BD2 302
C.          NON-DIMENSIONALIZATION IS NOW COMPLETE                          BD2 304
C.                                                                          BD2 306
C.          BEGIN INTERPOLATION SCHEME                                      BD2 308
            YT11(1)=Y11(1)                                                  BD2 310
            YT12(1)=Y12(1)                                                  BD2 312
            YT21(1)=Y21(1)                                                  BD2 314
            YT22(1)=Y22(1)                                                  BD2 316
            NSEX=51                                                         BD2 318
            DO 95 J=2,NSEX                                                  BD2 320
            XINC=J-1                                                        BD2 322
            XT(J)=.0+.02*XINC                                               BD2 324
            DO 75 I=1,NPAIRS1                                               BD2 326
            IF (X1(I).GE.XT(J)) GO TO 80                                    BD2 328
75          CONTINUE                                                        BD2 330
80          YT11(J)=Y11(I-1)+(Y11(I)-Y11(I-1))*(XT(J)-X1(I-1))/(X1(I)-X1(I-1))BD2 332
            YT12(J)=Y12(I-1)+(Y12(I)-Y12(I-1))*(XT(J)-X1(I-1))/(X1(I)-X1(I-1))BD2 334
            DO 85 I=1,NPAIRS2                                               BD2 336
            IF (X2(I).GE.XT(J)) GO TO 90                                    BD2 338
85          CONTINUE                                                        BD2 340
90          YT21(J)=Y21(I-1)+(Y21(I)-Y21(I-1))*(XT(J)-X2(I-1))/(X2(I)-X2(I-1))BD2 342
            YT22(J)=Y22(I-1)+(Y22(I)-Y22(I-1))*(XT(J)-X2(I-1))/(X2(I)-X2(I-1))BD2 344
95          CONTINUE                                                        BD2 346
            WRITE (6,265) TITL1,TITL2                                       BD2 348
            WRITE (6,230)                                                   BD2 350
            WRITE (6,260) (XT(I),YT11(I),YT12(I),YT21(I),YT22(I),I=1,NSEX)  BD2 352
            CALL PLOTR2 (XT,YT11,YT12,XT,YT21,YT22,NSEX,NSEX,TITL1,TITL2,2) BD2 354
            DO 105 I=1,NSEX                                                 BD2 356
            RSTREAM(I)=RNAUT+RSLOPE*XT(I)*X(NPAIRS1)                        BD2 358
```

```
      RSTREAM(2)=RNAUT+RSLOPE*XT(I)*X(NPAIRS2)                           BD2 360
      RAD(1)=S1/RSTREAM(1)                                              BD2 362
      RAD(2)=S2/RSTREAM(2)                                              BD2 364
      YLSQ(1)=YT11(I)                                                   BD2 366
      YLSQ(2)=YT21(I)                                                   BD2 368
      CALL LSQ1 (2,RAD,YLSQ,YZER1,YSLP1,PE,SRSQ)                        BD2 370
      YLSQ(1)=YT12(I)                                                   BD2 372
      YLSQ(2)=YT22(I)                                                   BD2 374
      CALL LSQ1 (2,RAD,YLSQ,YZER2,YSLP2,PE,SRSQ)                        BD2 376
      DO 100 J=1,5                                                      BD2 378
      RINC=J-1                                                          BD2 380
      RADIUS=.10+.20*RINC                                              BD2 382
      Y1(J,I)=YZER1+YSLP1*RADIUS                                        BD2 384
      Y2(J,I)=YZER2+YSLP2*RADIUS                                        BD2 386
100   CONTINUE                                                         BD2 388
105   CONTINUE                                                         BD2 390
      WRITE (6,265) TITL1,TITL2                                        BD2 392
      WRITE (6,235)                                                    BD2 394
      DO 110 I=1,NSEX                                                   BD2 396
      WRITE (6,240) (XT(I),Y1(J,I),Y2(J,I),J=1,5)                      BD2 398
110   CONTINUE                                                         BD2 400
C.        PLOT NON-DIMENSIONALIZED DATA FOR INTERPOLATED BLADE SECTIONS BD2 402
C.                                                                     BD2 404
      CALL PLOTR3 (XT,Y1,Y2,NSEX,TITL1,TITL2,1)                        BD2 406
C.        LSQ FIT TO LEADING EDGE COORDINATES                          BD2 408
C.                                                                     BD2 410
      YLSQ(1)=X(NPAIRS1)                                               BD2 412
      YLSQ(2)=X(NPAIRS2)                                               BD2 414
      RSTREAM(1)=RNAUT+RSLOPE*X(NPAIRS1)                               BD2 416
      RSTREAM(2)=RNAUT+RSLOPE*X(NPAIRS2)                               BD2 418
      XLSQ(1)=S1/RSTREAM(1)                                            BD2 420
      XLSQ(2)=S2/RSTREAM(2)                                            BD2 422
      CALL LSQ1 (2,XLSQ,YLSQ,YLEZ,YLES,PE,SRSQ)                        BD2 424
      DO 115 J=1,5                                                      BD2 426
      XM=J-1                                                           BD2 428
      XINC=.10+.20*XM                                                 BD2 430
      XLEDG(J)=YLEZ+YLES*XINC                                          BD2 432
115   CONTINUE                                                         BD2 434
C.        LSQ FIT TO LEADING EDGE AXIAL COORDINATES                    BD2 436
      YLSQ(1)=YLDG1                                                    BD2 438
      YLSQ(2)=YLDG2                                                    BD2 440
      CALL LSQ1 (2,XLSQ,YLSQ,YLDZ,YLDS,PE,SRSQ)                        BD2 442
      DO 120 J=1,5                                                      BD2 444
      XM=J-1                                                           BD2 446
      XINC=.10+.20*XM                                                 BD2 448
      YLEDG(J)=YLDZ+YLDS*XINC                                          BD2 450
120   CONTINUE                                                         BD2 452
C.        COMPUTE INTERPOLATED BLADE SECTIONS                          BD2 454
      DO 130 J=1,5                                                      BD2 456
      DO 125 I=1,NSEX                                                   BD2 458
      XBS(J,I)=XT(I)*XLEDG(J)                                          BD2 460
125   CONTINUE                                                         BD2 462
130   CONTINUE                                                         BD2 464
      DO 140 J=1,5                                                      BD2 466
      DO 135 I=1,NSEX                                                   BD2 468
      Y1(J,I)=Y1(J,I)*YLEDG(J)                                         BD2 470
      Y2(J,I)=Y2(J,I)*YLEDG(J)                                         BD2 472
135   CONTINUE                                                         BD2 474
140   CONTINUE                                                         BD2 476
      WRITE (6,265) TITL1,TITL2                                        BD2 478
```

```
      WRITE (6,245)                                                  BD2 480
      DO 145 I=1,NSEX                                                BD2 482
      WRITE (6,250) (XBS(J,I),Y1(J,I),Y2(J,I),J=1,5)                 BD2 484
145   CONTINUE                                                       BD2 486
C        PLOT NORMALIZED INTERPOLATED DATA                          BD2 488
      CALL PLOTR4 (XBS,Y1,Y2,NSEX,TITL1,TITL2,1)                     BD2 490
150   CONTINUE                                                       BD2 492
      IF (IPUNCH.EQ.0) GO TO 10                                      BD2 494
      NSEX=NPTS                                                      BD2 496
C        SET UP STREAMTUBE COORDINATES                              BD2 498
C                                                                   BD2 500
C        LINEARIZE R/Z VERSUS AXIAL DISPLACEMENT                    BD2 502
      XLSQ(1)=0.                                                     BD2 504
      XLSQ(2)=HX                                                     BD2 506
      YLSQ(1)=FST                                                    BD2 508
      YLSQ(2)=FSL                                                    BD2 510
      CALL LSQ1 (2,XLSQ,YLSQ,RAXZ,RAXS,PE,SRSQ)                      BD2 512
C     LINEARIZATION COMPLETE *** R(AX)=RAXZ+RAXS*AX                 BD2 514
C                                                                   BD2 516
C        SET UP AX MATRIX OF AXIAL DISPLACEMENTS                    BD2 518
C                (-33 PRCNT TO +66 PRCNT SECTIONAL SPAN)            BD2 520
      AX(1)=-HX/3.                                                   BD2 522
      AX(NSEX)=6.*HX/3.                                             BD2 524
      XNPT=NSEX-1                                                    BD2 526
      AXDELT=(AX(NSEX)-AX(1))/(XNPT)                                 BD2 528
      DO 155 I=2,NSEX                                                BD2 530
      AX(I)=AX(I-1)+AXDELT                                          BD2 532
155   CONTINUE                                                       BD2 534
C                                                                   BD2 536
C        COMPUTE RX MATRIX OF FREESTREAM RADIAL DIMENSIONS AS F(AX) BD2 538
      DO 160 I=1,NSEX                                                BD2 540
      RX(I)=RAXZ+RAXS*AX(I)                                         BD2 542
160   CONTINUE                                                       BD2 544
C                                                                   BD2 546
C        PUNCH INPUT FOR CAVITATION PROGRAM *** Y1=PRESSURE,Y2=SUCTION BD2 548
      BRAD=2.*FSR                                                    BD2 550
      NDUM=1                                                         BD2 552
      BANG=6.28318/BNUM                                              BD2 554
      PUNCH255,TITL1                                                 BD2 556
      PUNCH255,TITL2                                                 BD2 558
      KSTPRI=5                                                       BD2 560
      IF (INTERP.GT.0) GO TO 170                                     BD2 562
      KSTPRI=2                                                       BD2 564
      K=1                                                            BD2 566
      DO 165 I=1,NPTS                                                BD2 568
      Y1(K,I)=Y11(I)                                                BD2 570
      Y2(K,I)=Y12(I)                                                BD2 572
      XBS(K,I)=X(I)                                                  BD2 574
165   CONTINUE                                                       BD2 576
      K=2                                                            BD2 578
      DO 170 I=1,NPTS                                                BD2 580
      Y1(K,I)=Y21(I)                                                BD2 582
      Y2(K,I)=Y22(I)                                                BD2 584
170   CONTINUE                                                       BD2 586
      DO 200 K=1,KSTPRI                                              BD2 588
      INC=10+(K-1)*20                                                BD2 590
      PUNCH295,INC                                                   BD2 592
      PUNCH290,NSEX,NSEX,NSEX,NDUM,NDUM,NSEX,BANG,DGINC,BRAD,ENC,BNC BD2 594
C        PUNCH PRESSURE R,Z COORDINATES                             BD2 596
      PUNCH295,(Y1(K,I),I=1,NSEX)                                    BD2 598
```

```
C.           PUNCH SUCTION   R,Z COORDINATES                                    BD2 6
        PUNCH295,(Y2(K,I),I=1,NSEX)                                             BD2 6
C.           COMPUTE CHORD COORDINATES                                          BD2 6
        DO 175 I=1,NSEX                                                         BD2 6
        YCC(I)=(Y1(K,I)+Y2(K,I))/2.                                            PD2 6
175     CONTINUE                                                               BD2 6
C.           PUNCH CHORD      R,Z COORDINATES                                   BD2 6
        PUNCH295,(YCC(I),I=1,NSEX)                                             BD2 6
C.           PUNCH SUCTION THETA COORDINATES                                    BD2 6
        PUNCH295,(XBS(K,I),I=1,NSEX)                                           BD2 6
C.           COMPUTE PRESSURE ANGULAR COORDINATES                               BD2 6
        DO 180 I=1,NSEX                                                         BD2 6
        TPAC(I)=XBS(K,I)+360./BNUM                                             BD2 6
180     CONTINUE                                                               BD2 6
C.           PUNCH PRESSURE THETA COORDINATES                                   BD2 6
        PUNCH295,(TPAC(I),I=1,NSEX)                                            BD2 6
C.           PUNCH CHORD      THETA COORDINATES                                 BD2 6
        PUNCH295,(XBS(K,I),I=1,NSEX)                                           BD2 6
C.           COMPUTE RD MATRIX OF STREAMTUBE RADII FOR FRONT BLADE SECTION      BD2 6
        XJ=K-1                                                                  BD2 6
        XINC=.10+.20*XJ                                                        BD2 6
        DO 185 I=1,NSEX                                                         BD2 6
        RD(I)=RX(I)*XINC+HL+(HX-AX(I))*TMLTAN                                  BD2 6
185     CONTINUE                                                               BD2 6
C.           COMPUTE BD(I) = STREAMTUBE WIDTH AS F(AX)                          BD2 6
        NMID=NSEX/2                                                            BD2 6
        RMID=RX(NMID)                                                          BD2 6
        DO 190 I=1,NSEX                                                         BD2 6
        BD(I)=STWNOM*RX(I)/RMID                                                BD2 6
190     CONTINUE                                                               BD2 6
        DYBETA=RD(1)-RD(NSEX)                                                  BD2 6
        DXBETA=2.*HX                                                           BD2 6
        BETA=ATAN2(DYBETA,DXBETA)                                              BD2 6
        SIAD=SIN(BETA)                                                         BD2 6
        DO 195 I=1,NSEX                                                         BD2 6
        PUNCH300,RD(I),BD(I),SIAD,AX(I)                                        BD2 6
195     CONTINUE                                                               BD2 6
200     CONTINUE                                                               BD2 6
        GO TO 10                                                               BD2 6
205     STOP                                                                   BD2 6
C                                                                              BD2 6
210     FORMAT (//2X51HCORRECTED INPUT DATA FOR Z MEASURED PARALLEL TO C/L/BD2 6
       1)                                                                      BD2 6
215     FORMAT (2X40HNORMALIZED INPUT DATA FOR SECTIONAL DATA,/6X2HX ,2(8XBD2 6
       12HY1,8X2HY2)/)                                                         BD2 6
220     FORMAT (2X78HNON-DIMENSIONALIZED INPUT DATA NORMALIZED TO TRAILINGBD2 6
       1 EDGE FOR SECTIONAL INPUT,/2(8X2HX ,8X2HY1,8X2HY2)/)                   BD2 6
225     FORMAT (5F10.4)                                                       BD2 6
230     FORMAT (2X45HINCREMENTAL PERCENT CHORD DERIVED DATA POINTS,/8X2HX  BD2 6
       1,2(8X2HY1,8X2HY2)/)                                                    BD2 6
235     FORMAT (2X48HBLADE SECTIONAL DATA EXTRAPOLATED FOR 5 SECTIONS,/5(6BD2 7
       1X2HXT,6X2HY1,6X2HY2)/)                                                 BD2 7
240     FORMAT (15F8.4)                                                       BD2 7
245     FORMAT (2X53HNORMALIZED INPUT DATA FOR INTERPOLATED BLADE SECTIONSBD2 7
       1,/5(6X2HX ,6X2HY1,6X2HY2)/)                                           BD2 7
250     FORMAT (5(F8.2,2F8.4))                                                BD2 7
255     FORMAT (6A10)                                                         BD2 7
260     FORMAT (5F10.4)                                                       BD2 7
265     FORMAT (1H1,8A10//8A10//)                                             BD2 7
270     FORMAT (4X53HINPUT DATA FOR CONTINUOUS BLADE SECTIONS AT LOCATIONSBD2 7
```

```
1./16X5HR1 = .F5.3.10X5HR2 = .F5.3./5X3HPHI.2H8X2HY1.8X2HY2)/)      BD2 720
'75   FORMAT (4X31HINPUT TRAILING EDGE COORDINATES./F10.4.F15.4./F10.4.2SD2 722
     10X.F15.4)                                                         BD2 724
:80   FORMAT (10I5)                                                     BD2 726
 285  FORMAT(4X32HINPUT DATA FOR BLADE SECTION AT .I3.1X14HPERCENT RADIABD2 728
     $L)                                                                BD2 730
 290  FORMAT(6I5.5F10.4)                                                BD2 732
 295  FORMAT(10F8.3)                                                    BD2 734
 300  FORMAT(4E10.3)                                                    BD2 736
      END                                                               BD2 740*


      SUBROUTINE LS01 (N.X.Y.A.B.PE.SRSQ)                               LQ1    1
      LINEAR LEAST SQUARES SUBROUTINE FIT                              LQ1    2
      R A ZEHNLE.....NOVEMBER 1968                                     LQ1    3
      EQUATION...Y=A+BX                                                LQ1    4
      PROGRAM VARIABLES                                                LQ1    5
          N      NUMBER OF PAIRS OF DATA POINTS (X.Y)                  LQ1    6
          X      ARRAY OF INDEPENDENT VARIABLES                       LQ1    7
          Y      ARRAY OF DEPENDENT VARIABLES                         LQ1    8
          A.B  CONSTANTS OF STANDARD FIRST ORDER EQUATION             LQ1    9
          PE     PROBABLE ERROR OF FIT OF DATA TO CURVE               LQ1   10
          SRSQ SUM OF THE RESIDUALS SQUARED                           LQ1   11
      DIMENSION X(1). Y(1)                                             LQ1   12
      IF (N.LE.1) GO TO 15                                             LQ1   13
      SX=0.                                                            LQ1   14
      SXSQ=0.                                                          LQ1   15
      SY=0.                                                            LQ1   16
      SXY=0.                                                           LQ1   17
      SRSQ=0.                                                          LQ1   18
      DO 5 I=1.N                                                       LQ1   19
      SY=SY+Y(I)                                                       LQ1   20
      SXY=SXY+X(I)*Y(I)                                                LQ1   21
      SX=SX+X(I)                                                       LQ1   22
      SXSQ=SXSQ+X(I)**2                                                LQ1   23
      D=N*SXSQ-SX*SX                                                   LQ1   24
      A=(SXSQ*SY-SX*SXY)/D                                             LQ1   25
      B=(N*SXY-SX*SY)/D                                                LQ1   26
      DO 10 I=1.N                                                      LQ1   27
  10  SRSQ=SRSQ+(Y(I)-A-B*X(I))**2                                     LQ1   28
      PE=.675*SQRT(SRSQ/(N-2))                                         LQ1   29
      RETURN                                                           LQ1   30
      ERROR MESSAGE INDICATOR                                          LQ1   31
   5  WRITE (6.20) N                                                   LQ1   32
      RETURN                                                           LQ1   33
                                                                       LQ1   34
   0  FORMAT (1X36HERROR IN INPUT TO LS01    N INPUT AS .I5)           LQ1   35
      END LS01                                                         LQ1   36*
```

```
      SUBROUTINE PLOTR1(X,Y11,Y12,Y21,Y22,N,TITL1,TITL2,IS)         PLT1
      DIMENSION X(1),Y11(1),Y12(1),Y21(1),Y22(1),                   PLT1
     $TITL1(8),TITL2(8),TL1(9),TL2(9)                               PLT1
      DATA TL1(9),TL2(9)/2H$.,2H$./                                 PLT1
      DATA XSYMB,YSYMB/10HTHETA    $.,10HAXIAL Z $./                PLT1
      CALL INIT280                                                  PLT1
      DO 1 I=1,8                                                    PLT1
      TL1(I)=TITL1(I)                                               PLT1
    1 TL2(I)=TITL2(I)                                               PLT1
      XMIN=0.                                                       PLT1
      YMIN=0.                                                       PLT1
      XMAX=X(1)                                                     PLT1
      YMAX=Y12(1)                                                   PLT1
      DO 2 I=2,N                                                    PLT1
      IF(X(I).GT.XMAX) XMAX=X(I)                                    PLT1
      IF(Y12(I).GT.YMAX) YMAX=Y12(I)                                PLT1
    2 CONTINUE                                                      PLT1
      CALL MAPG (XMIN,XMAX,YMIN,YMAX,.1,.9,.15,.9)                  PLT1
      CALL LINEOPT(0,1)                                             PLT1
      CALL CHAROPT(0,0,1,0,0)                                       PLT1
      CALL ABSBEAM(.01,.98)                                         PLT1
      CALL SYMBOL(TL1)                                              PLT1
      CALL ABSBEAM(.01,.94)                                         PLT1
      CALL SYMBOL(TL2)                                              PLT1
      CALL ABSBEAM(.5,.07)                                          PLT1
      CALL SYMBOL(XSYMB)                                            PLT1
      CALL ABSBEAM (.10,.02)                                        PLT1
      IF (IS.EQ.1) CALL SYMBOL (36HECHO PLOT OF INPT DATA SECTIONS  $.)PLT1
      IF (IS.EQ.2) CALL SYMBOL (36HDATA NORMALIZED TO TRLNG EDGE    $.)PLT1
      CALL CHAROPT(0,0,1,1,0)                                       PLT1
      CALL ABSBEAM(.01,.5)                                          PLT1
      CALL SYMBOL(YSYMB)                                            PLT1
      NST=N-1                                                       PLT1
      DO 45 I=1,NST                                                 PLT1
      IF((Y11(I).EQ.0.).OR.(Y11(I+1).EQ.0.)) GO TO 44              PLT1
      IF(Y11(I).EQ.Y12(I)) GO TO 44                                 PLT1
      CALL LINE(X(I),Y11(I),X(I+1),Y11(I+1))                        PLT1
      CALL LINE(X(I),Y12(I),X(I+1),Y12(I+1))                        PLT1
   44 CONTINUE                                                      PLT1
   45 CONTINUE                                                      PLT1
      DO 47 I=1,NST                                                 PLT1
      IF((Y21(I).EQ.0.).OR.(Y21(I+1).EQ.0.)) GO TO 46              PLT1
      IF(Y21(I).EQ.Y22(I)) GO TO 46                                 PLT1
      CALL LINE(X(I),Y21(I),X(I+1),Y21(I+1))                        PLT1
      CALL LINE(X(I),Y22(I),X(I+1),Y22(I+1))                        PLT1
   46 CONTINUE                                                      PLT1
   47 CONTINUE                                                      PLT1
      CALL FRAME                                                    PLT1
      RETURN                                                        PLT1
      END                                                           PLT1
```

.

```
      SUBROUTINE PLOTR2(X1,Y11,Y12,X2,Y21,Y22,N1,N2,T1,T2,IS)          PLT2 01
      DIMENSION X1(1),Y11(1),Y12(1),X2(1),Y21(1),Y22(1),T1(8),T2(8),    PLT2 02
     $TL1(9),TL2(9)                                                     PLT2 03
      DATA TL1(9),TL2(9)/2H$.,2H$./                                     PLT2 04
      DATA XSYMB,YSYMB/10HTHETA    $.,10HAXIAL Z $./                    PLT2 05
      CALL INIT280                                                      PLT2 06
      DO 1 I=1,8                                                        PLT2 07
      TL1(I)=T1(I)                                                      PLT2 08
    1 TL2(I)=T2(I)                                                      PLT2 09
      XMIN=0.                                                           PLT2 10
      YMIN=0.                                                           PLT2 11
      XMAX=X1(1)                                                        PLT2 12
      YMAX=Y12(1)                                                       PLT2 13
      DO 2 I=2,N1                                                       PLT2 14
      IF(X1(I).GT.XMAX) XMAX=X1(I)                                      PLT2 15
      IF(Y12(I).GT.YMAX) YMAX=Y12(I)                                    PLT2 16
    2 CONTINUE                                                          PLT2 17
      CALL MAPS (XMIN,XMAX,YMIN,YMAX,.1,.9,.15,.9)                      PLT2 18
      CALL LINEOPT(0,1)                                                 PLT2 19
      CALL CHAROPT(0,0,1,0,0)                                           PLT2 20
      CALL ABSBEAM(.01,.98)                                            PLT2 21
      CALL SYMBOL(TL1)                                                  PLT2 22
      CALL ABSBEAM(.01,.94)                                            PLT2 23
      CALL SYMBOL(TL2)                                                  PLT2 24
      CALL ABSBEAM(.5,.07)                                             PLT2 25
      CALL SYMBOL(XSYMB)                                                PLT2 26
      CALL ABSBEAM (.10,.02)                                           PLT2 27
      IF (IS.EQ.1) CALL SYMBOL (36HNON-DIMEN DATA FOR INPUT DATA PTS $.)PLT2 28
      IF (IS.EQ.2) CALL SYMBOL (36HNON-DIMEN DATA FOR 51 DATA POINTS $.)PLT2 29
      CALL CHAROPT(0,0,1,1,0)                                           PLT2 30
      CALL ABSBEAM(.01,.5)                                             PLT2 31
      CALL SYMBOL(YSYMB)                                                PLT2 32
      CALL LINES(X1,Y11,N1)                                             PLT2 33
      CALL LINES(X1,Y12,N1)                                             PLT2 34
      CALL LINES(X2,Y21,N2)                                             PLT2 35
      CALL LINES(X2,Y22,N2)                                             PLT2 36
      CALL FRAME                                                        PLT2 37
      RETURN                                                            PLT2 38
      END                                                               PLT2 39*
```

```
      SUBROUTINE PLOTR3  (X,Y1,Y2,N,TITL1,TITL2,IS)                      PLT3
      DIMENSION    X(1),Y1(5,1),Y2(5,1),XP(51),YP1(51),YP2(51),         PLT3
     $TITL1(8),TITL2(8),TL1(9),TL2(9)                                   PLT3
      DATA TL1(9),TL2(9)/2HS.,2HS./                                     PLT3
      DATA XSYMB,YSYMB/10HTHETA    $.,10HAXIAL Z $./                    PLT3
      CALL INIT280                                                      PLT3
      DO 1 I=1,8                                                        PLT3
      TL1(I)=TITL1(I)                                                   PLT3
    1 TL2(I)=TITL2(I)                                                   PLT3
      XMIN=0.                                                           PLT3
      YMIN=0.                                                           PLT3
      XMAX=X(1)                                                         PLT3
      YMAX=Y1(1,1)                                                      PLT3
      DO 2 I=1,N                                                        PLT3
      IF(X(I).GT.XMAX) XMAX=X(I)                                        PLT3
      IF(Y1(1,I).GT.YMAX) YMAX=Y1(1,I)                                  PLT3
    2 CONTINUE                                                          PLT3
      CALL MAPG (XMIN,XMAX,YMIN,YMAX,.1,.9,.15,.9)                      PLT3
      CALL LINEOPT(0,1)                                                 PLT3
      CALL CHAROPT(0,0,1,0,0)                                           PLT3
      CALL ABSBEAM(.01,.98)                                             PLT3
      CALL SYMBOL(TL1)                                                  PLT3
      CALL ABSBEAM(.01,.94)                                             PLT3
      CALL SYMBOL(TL2)                                                  PLT3
      CALL ABSBEAM(.5,.07)                                              PLT3
      CALL SYMBOL(XSYMB)                                                PLT3
      CALL ABSBEAM (.10,.02)                                            PLT3
      IF (IS.EQ.1) CALL SYMBOL (36HNON-DIMEN DATA FOR INTERP SECTIONS$.)PLT3
      IF (IS.EQ.2) CALL SYMBOL (36H                                 $.)PLT3
      CALL CHAROPT(0,0,1,1,0)                                           PLT3
      CALL ABSBEAM(.01,.5)                                              PLT3
      CALL SYMBOL(YSYMB)                                                PLT3
      DO 60 J=1,5                                                       PLT3
      DO 44 I=1,N                                                       PLT3
      XP(I)=X(I)                                                        PLT3
      YP1(I)=Y1(J,I)                                                    PLT3
      YP2(I)=Y2(J,I)                                                    PLT3
   44 CONTINUE                                                          PLT3
      CALL LINES(XP,YP1,N)                                              PLT3
      CALL LINES(XP,YP2,N)                                              PLT3
   60 CONTINUE                                                          PLT3
      CALL FRAME                                                        PLT3
      RETURN                                                            PLT3
      END                                                               PLT3
```

```
      SUBROUTINE PLOTR4   (X,Y1,Y2,N,TITL1,TITL2,IS)                          PLT4 01
      DIMENSION X(5,1),Y1(5,1),Y2(5,1),XP(51),YP1(51),YP2(51),             PLT4 02
     $TITL1(8),TITL2(8),TL1(9),TL2(9)                                        PLT4 03
      DATA TL1(9),TL2(9)/2H$.,2H$./                                          PLT4 04
      DATA XSYMB,YSYMB/1OHTHETA    $.,1OHAXIAL Z $./                         PLT4 05
      CALL INIT280                                                           PLT4 06
      DO 1 I=1,8                                                             PLT4 07
      TL1(I)=TITL1(I)                                                        PLT4 08
    1 TL2(I)=TITL2(I)                                                        PLT4 09
      XMIN=0.                                                                PLT4 10
      YMIN=0.                                                                PLT4 11
      XMAX=X(1,1)                                                            PLT4 12
      YMAX=Y1(1,1)                                                           PLT4 13
      DO 2 I=1,N                                                             PLT4 14
      IF(X(1,I).GT.XMAX) XMAX=X(1,I)                                         PLT4 15
      IF(Y1(1,I).GT.YMAX) YMAX=Y1(1,I)                                       PLT4 16
    2 CONTINUE                                                               PLT4 17
      CALL MAPG (XMIN,XMAX,YMIN,YMAX,.1,.9,.15,.9)                           PLT4 18
      CALL LINEOPT(0,1)                                                      PLT4 19
      CALL CHAROPT(0,0,1,0,0)                                                PLT4 20
      CALL ABSBEAM(.01,.98)                                                  PLT4 21
      CALL SYMBOL(TL1)                                                       PLT4 22
      CALL ABSBEAM(.01,.94)                                                  PLT4 23
      CALL SYMBOL(TL2)                                                       PLT4 24
      CALL ABSBEAM(.5,.07)                                                   PLT4 25
      CALL SYMBOL(XSYMB)                                                     PLT4 26
      CALL ABSBEAM (.10,.02)                                                 PLT4 27
      IF (IS.EQ.1) CALL SYMBOL (36HNRMLZD DATA FOR 5 INTRPLTD SECTS  $.)PLT4 28
      CALL CHAROPT(0,0,1,1,0)                                                PLT4 29
      CALL ABSBEAM(.01,.5)                                                   PLT4 30
      CALL SYMBOL(YSYMB)                                                     PLT4 31
      DO 60 J=1,5                                                            PLT4 32
      DO 44 I=1,N                                                            PLT4 33
      XP(I)=X(J,I)                                                           PLT4 34
      YP1(I)=Y1(J,I)                                                         PLT4 35
      YP2(I)=Y2(J,I)                                                         PLT4 36
   44 CONTINUE                                                               PLT4 37
      JL=1                                                                   PLT4 38
   45 K=JL+1                                                                 PLT4 39
      IF((YP1(K)-YP1(JL)).GT.0.) GO TO 48                                    PLT4 40
      JL=JL+1                                                                PLT4 41
      GO TO 45                                                               PLT4 42
   48 CONTINUE                                                               PLT4 43
      NP=N                                                                   PLT4 44
      IF(JL.EQ.1) GO TO 50                                                   PLT4 45
   49 IK=I+JL-1                                                              PLT4 46
      XP(I)=XP(IK)                                                           PLT4 47
      YP1(I)=YP1(IK)                                                         PLT4 48
      YP2(I)=YP2(IK)                                                         PLT4 49
      NP=I                                                                   PLT4 50
      I=I+1                                                                  PLT4 51
      IF(IK.LT.N) GO TO 49                                                   PLT4 52
   50 CONTINUE                                                               PLT4 53
      CALL LINES(XP,YP1,NP)                                                  PLT4 54
      CALL LINES(XP,YP2,NP)                                                  PLT4 55
   60 CONTINUE                                                               PLT4 56
      CALL FRAME                                                             PLT4 57
      RETURN                                                                 PLT4 58
      END                                                                    PLT4 59*
```

TURBOPUMP INDUCER CAVITATION ANALYSIS FOR NAS8-26266 F/O, 17 JAN 1972

F-1 LOX, 2 INPUT BLADE SECTIONS INTERPOLATED TO 10,30,50,70,90 PRCNT SECTION

INPUT DATA FOR CONTINUOUS BLADE SECTIONS AT LOCATIONS

PHI	R1 = .750		R2 = 4.500	
	Y1	Y2	Y1	Y2
13.0000	.5250	.6250	0.	0.
15.0000	.6293	.6953	0.	0.
20.0000	.6306	.8514	0.	0.
25.0000	.7549	1.0031	0.	0.
30.0000	.8224	1.1502	0.	0.
35.0000	.8933	1.2927	0.	0.
40.0000	.9578	1.4307	0.	0.
45.0000	1.0460	1.5640	0.	0.
50.0000	1.1283	1.6927	0.	0.
55.0000	1.2148	1.8166	0.	0.
60.0000	1.3058	1.9359	0.	0.
65.0000	1.4015	2.0505	0.	0.
70.0000	1.5022	2.1602	1.8300	1.8300
75.0000	1.6081	2.2680	1.8806	1.9973
80.0000	1.7158	2.3760	1.9489	2.1462
85.0000	1.8257	2.4843	2.0280	2.2841
90.0000	1.9350	2.5930	2.1181	2.4110
95.0000	2.0445	2.7019	2.2196	2.5269
100.0000	2.1543	2.8111	2.3289	2.6364
105.0000	2.2643	2.9206	2.4397	2.7462
120.0000	2.5963	3.2508	2.7699	3.0773
135.0000	2.9309	3.5838	3.1037	3.4111
150.0000	3.2682	3.9197	3.4403	3.7476
165.0000	3.6083	4.2583	3.7797	4.0870
180.0000	3.9513	4.6000	4.1220	4.4293
195.0000	4.2972	4.9447	4.4673	4.7746
210.0000	4.6463	5.2926	4.8158	5.1231
225.0000	4.9986	5.6439	5.1676	5.4749
240.0000	5.3543	5.9985	5.5228	5.8300
255.0000	5.7135	6.3569	5.8816	6.1838
270.0000	6.0765	6.7190	6.2441	6.5514
285.0000	6.4435	7.0853	6.6108	6.9180
300.0000	6.8147	7.4545	6.9817	7.2830
305.0000	6.9433	7.5701	7.1063	7.4136
310.0000	7.0811	7.6779	7.2320	7.5379
315.0000	7.2286	7.7778	7.3694	7.6508
320.0000	7.3700	7.8699	7.5100	7.7433
325.0000	7.5150	7.9500	7.6350	7.8550
330.0000	7.6550	8.0150	7.7600	7.9500
335.0000	7.8500	8.0750	7.9000	8.0300
340.0000	8.0500	8.1250	8.0600	8.1150

INPUT TRAILING EDGE COORDINATES

340.0000	8.1250		
340.0000			8.1150

TURBOPUMP INDUCER CAVITATION ANALYSIS FOR NAS6-26266 F/O, 17 JAN 1972
1 LOX, 2 INPUT BLADE SECTIONS INTERPOLATED TO 10,30,50,70,90 PRCNT SECTIONS
INPUT DATA FOR BLADE SECTION AT 10 PERCENT RADIAL

					0.9444	40.0000	15.0000	2.0000	1.0000
.176	.343	.500	.761	.951	1.142	1.317	1.482	1.647	1.810
.973	2.135	2.295	2.456	2.615	2.774	2.932	3.090	3.247	3.403
.559	3.713	3.868	4.022	4.175	4.327	4.479	4.631	4.781	4.932
.031	5.231	5.179	5.526	7.675	5.922	5.969	6.115	6.261	6.406
.551	6.693	6.808	6.958	7.060	7.178	7.279	7.374	7.464	7.549
.600									
.	.008	.150	.249	.371	.503	.658	.820	.983	1.145
.307	1.459	1.625	1.783	1.946	2.106	2.263	2.420	2.576	2.731
.887	3.040	3.194	3.347	3.499	3.651	3.802	3.952	4.102	4.252
.401	4.546	4.598	4.847	4.990	5.136	5.281	5.426	5.571	5.715
.858	6.001	6.146	6.299	6.462	6.632	6.812	6.999	7.193	7.395
.600									
.035	.285	.559	.565	.661	.825	.987	1.151	1.315	1.478
.640	1.802	1.962	2.123	2.281	2.440	2.598	2.755	2.912	3.067
.223	3.377	3.521	3.684	3.837	3.989	4.140	4.292	4.442	4.592
.741	4.890	5.039	5.186	5.333	5.479	5.625	5.771	5.916	6.061
.204	6.347	6.450	6.626	6.766	6.905	7.045	7.186	7.329	7.472
.600									
	6.643	13.285	19.928	26.571	33.214	39.856	46.499	53.142	59.785
.427	73.070	79.713	86.356	92.999	99.641	106.284	112.927	119.569	126.212
.855	139.498	146.140	152.783	159.426	166.068	172.711	179.354	185.997	192.639
.282	205.925	212.569	219.210	225.853	232.496	239.139	245.781	252.424	259.067
.710	272.352	278.995	285.638	292.281	298.923	305.566	312.209	318.851	325.494
.137									
.000	126.643	133.285	139.928	146.571	153.214	159.856	166.499	173.142	179.785
.427	193.070	199.713	206.356	212.999	219.641	226.284	232.927	239.569	246.212
.855	259.498	266.140	272.783	279.426	286.068	292.711	299.354	305.997	312.639
.282	325.925	332.569	339.210	345.853	352.496	359.139	365.781	372.424	379.067
.710	392.352	398.995	405.638	412.281	418.923	425.566	432.209	438.851	445.494
.137									
	6.643	13.285	19.928	26.571	33.214	39.856	46.499	53.142	59.785
.427	73.070	79.713	86.356	92.999	99.641	106.284	112.927	119.569	126.212
.855	139.498	146.140	152.783	159.426	166.068	172.711	179.354	185.997	192.639
.282	205.925	212.569	219.210	225.853	232.496	239.139	245.781	252.424	259.067
.710	272.352	278.995	285.638	292.281	298.923	305.566	312.209	318.851	325.494
.137									

9E+00 1.750E-01 1.879E-01-2.557E+00
0E+00 1.791E-01 1.879E-01-2.263E+00
1E+00 1.813E-01 1.879E-01-1.951E+00
2E+00 1.844E-01 1.879E-01-1.643E+00
3E+00 1.915E-01 1.879E-01-1.335E+00
4E+00 1.905E-01 1.879E-01-1.027E+00
5E+00 1.938E-01 1.879E-01-7.187E-01
7E+00 1.906E-01 1.879E-01-4.107E-01
8E+00 2.000E-01 1.879E-01-1.027E-01
9E+00 2.031E-01 1.879E-01 2.053E-01
0E+00 2.062E-01 1.879E-01 5.133E-01
1E+00 2.094E-01 1.879E-01 8.213E-01
2E+00 2.125E-01 1.879E-01 1.129E+00
3E+00 2.156E-01 1.879E-01 1.477E+00
4E+00 2.188E-01 1.879E-01 1.745E+00
6E+00 2.219E-01 1.879E-01 2.053E+00
6E+00 2.250E-01 1.879E-01 2.361E+00
7E+00 2.281E-01 1.879E-01 2.669E+00
8E+00 2.313E-01 1.879E-01 2.977E+00
0E+00 2.344E-01 1.879E-01 3.285E+00
1E+00 2.375E-01 1.879E-01 3.593E+00

```
2.903E+00  2.456E-01  1.879E-01  4.203E+00
2.844E+00  2.469E-01  1.879E-01  4.517E+00
2.785E+00  2.500E-01  1.879E-01  4.825E+00
2.726E+00  2.531E-01  1.879E-01  5.133E+00
2.667E+00  2.562E-01  1.879E-01  5.441E+00
2.608E+00  2.594E-01  1.879E-01  5.749E+00
2.549E+00  2.625E-01  1.879E-01  6.057E+00
2.490E+00  2.656E-01  1.879E-01  6.365E+00
2.431E+00  2.687E-01  1.879E-01  6.673E+00
2.372E+00  2.719E-01  1.879E-01  6.981E+00
2.314E+00  2.750E-01  1.879E-01  7.289E+00
2.255E+00  2.781E-01  1.879E-01  7.597E+00
2.196E+00  2.812E-01  1.879E-01  7.905E+00
2.137E+00  2.844E-01  1.879E-01  8.213E+00
2.079E+00  2.875E-01  1.879E-01  9.521E+00
2.019E+00  2.906E-01  1.879E-01  8.829E+00
1.960E+00  2.937E-01  1.879E-01  9.137E+00
1.901E+00  2.969E-01  1.879E-01  9.445E+00
1.842E+00  3.000E-01  1.879E-01  9.753E+00
1.783E+00  3.031E-01  1.879E-01  1.006E+01
1.724E+00  3.062E-01  1.879E-01  1.037E+01
1.665E+00  3.094E-01  1.879E-01  1.068E+01
1.607E+00  3.125E-01  1.879E-01  1.098E+01
1.548E+00  3.156E-01  1.879E-01  1.129E+01
1.489E+00  3.187E-01  1.879E-01  1.160E+01
1.430E+00  3.219E-01  1.879E-01  1.191E+01
1.371E+00  3.250E-01  1.879E-01  1.222E+01
1.312E+00  3.281E-01  1.879E-01  1.253E+01
1.253E+00  3.312E-01  1.879E-01  1.283E+01
```

217

Feedline Wall

R_2

Blade Sectional Data
Supplied by Drawing

R_1

Inducer
Hub

Additional Blade
Sections Derived
From Supplied Data

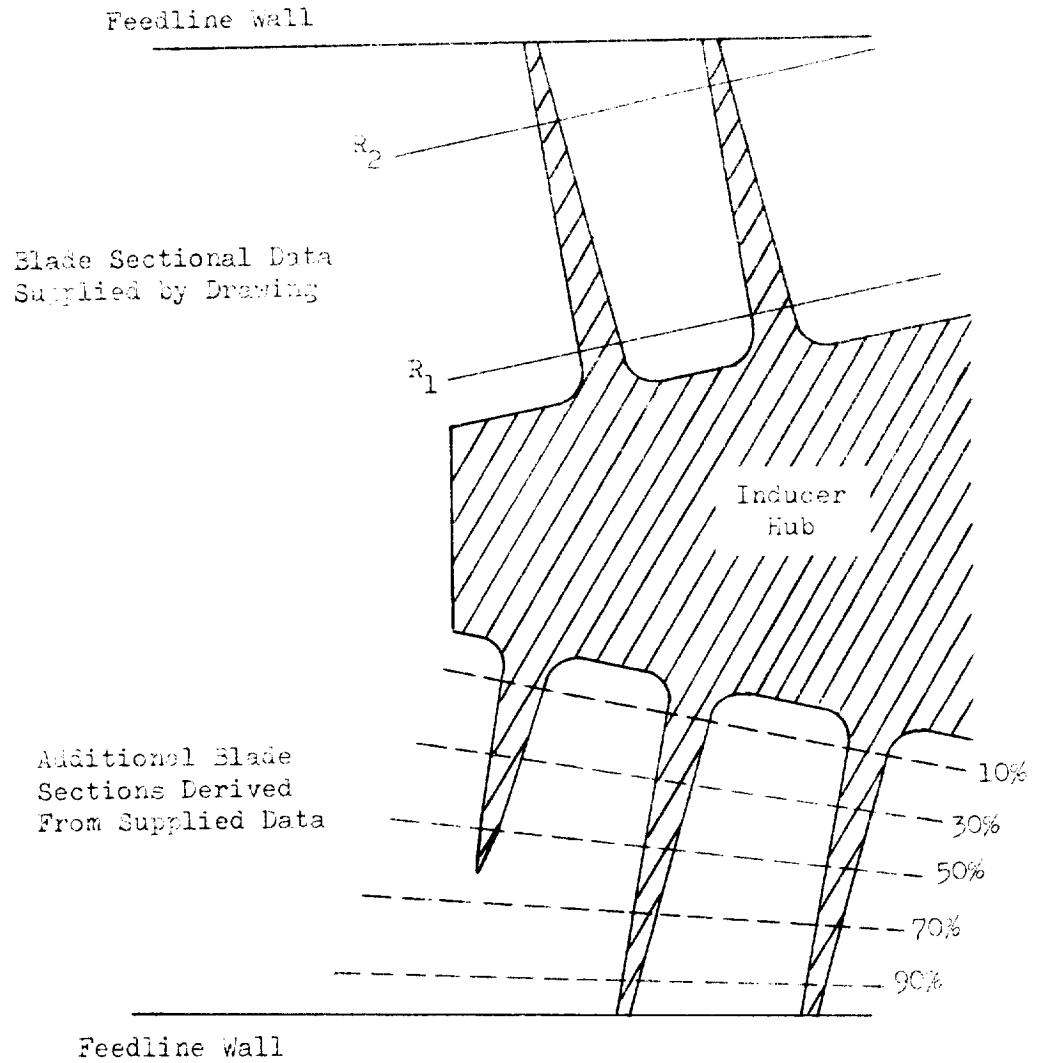— 10%

— 30%

— 50%

— 70%

— 90%

Feedline Wall

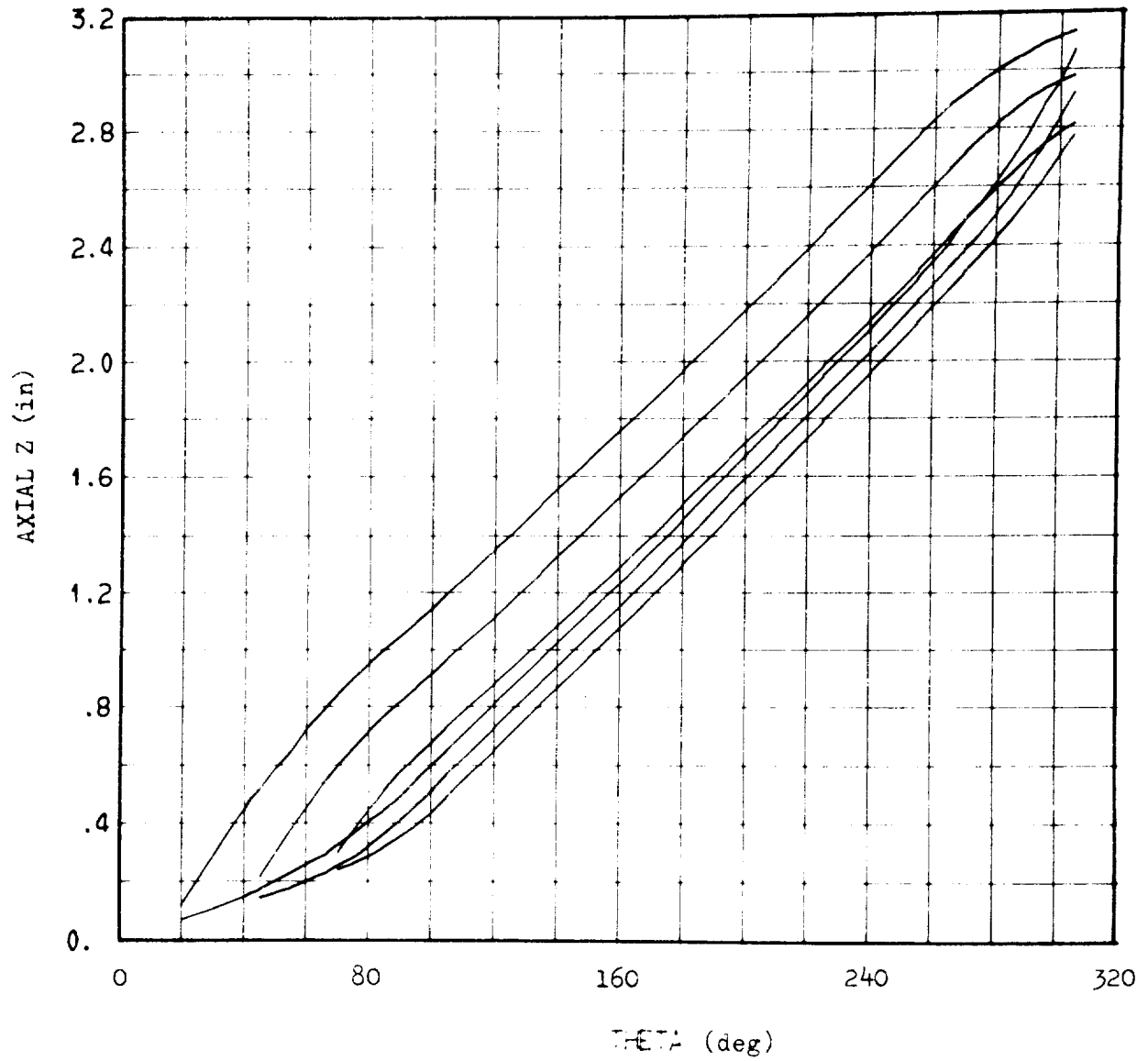Figure F.1   Typical Inducer Showing Blade Sections
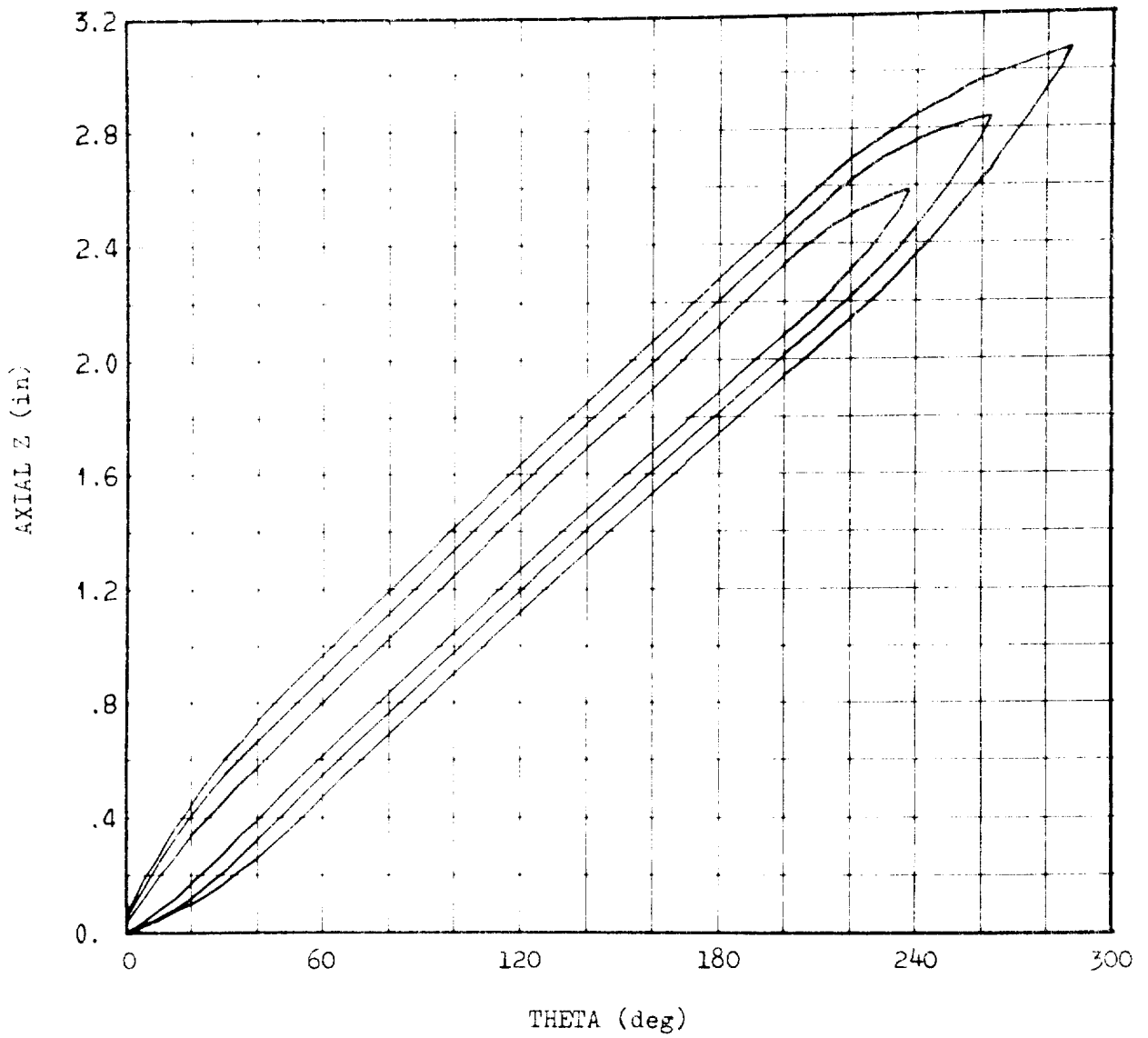
Figure F.2   Input Blade Sectional Data
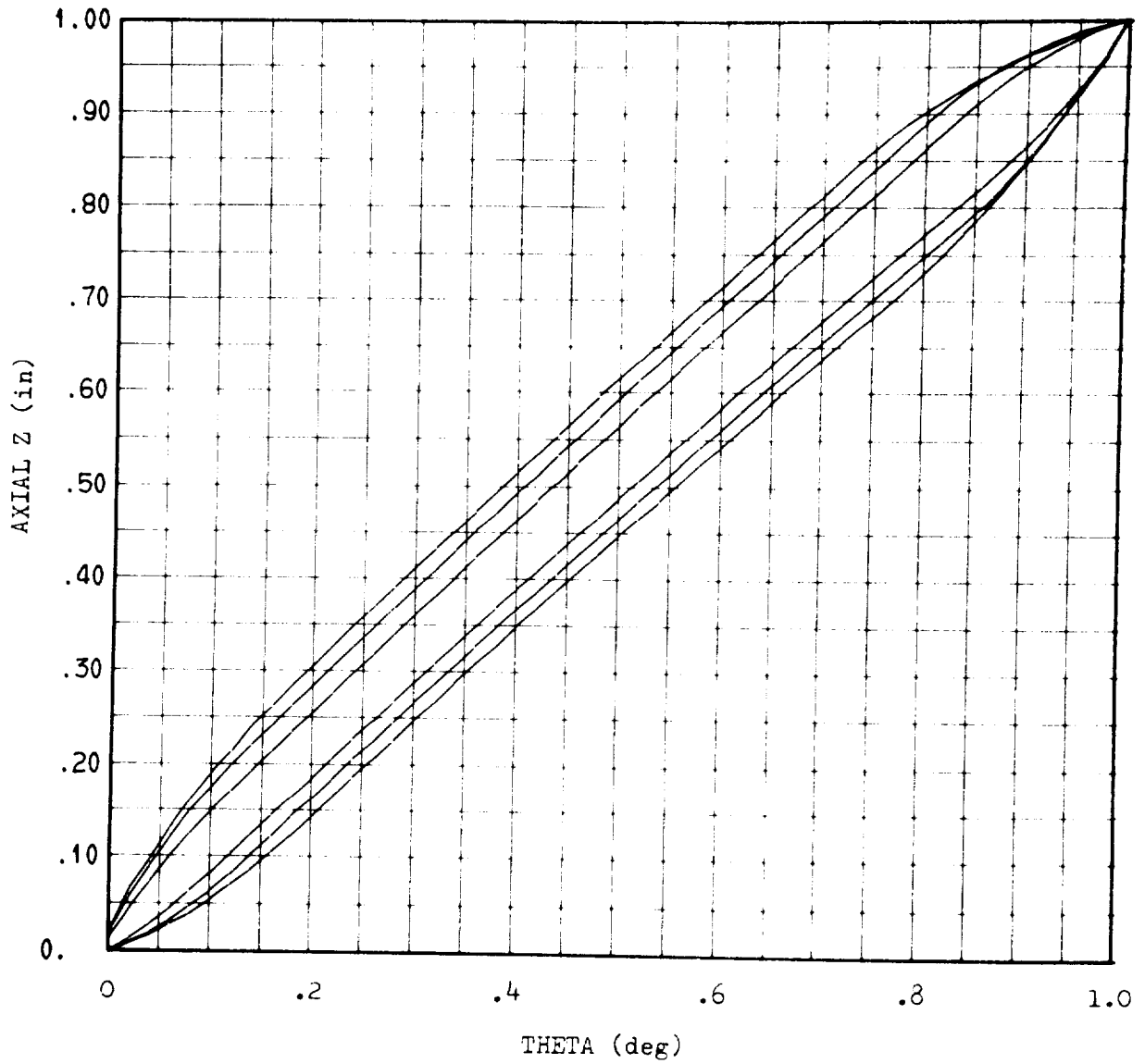
Figure F.3 Input Data Normalized To Trailing Edge

Figure F.4 Non-Dimensionalized Input Data

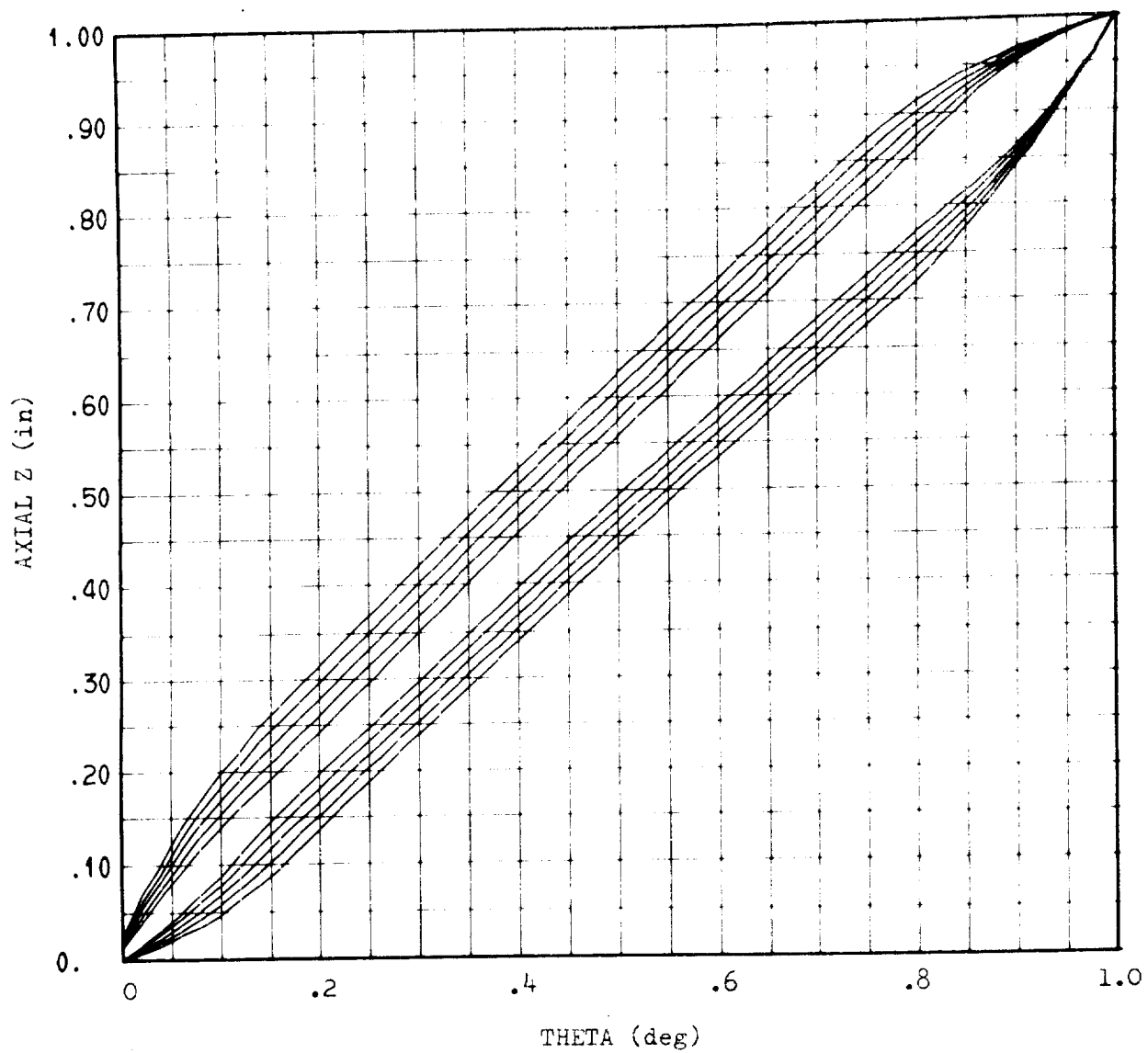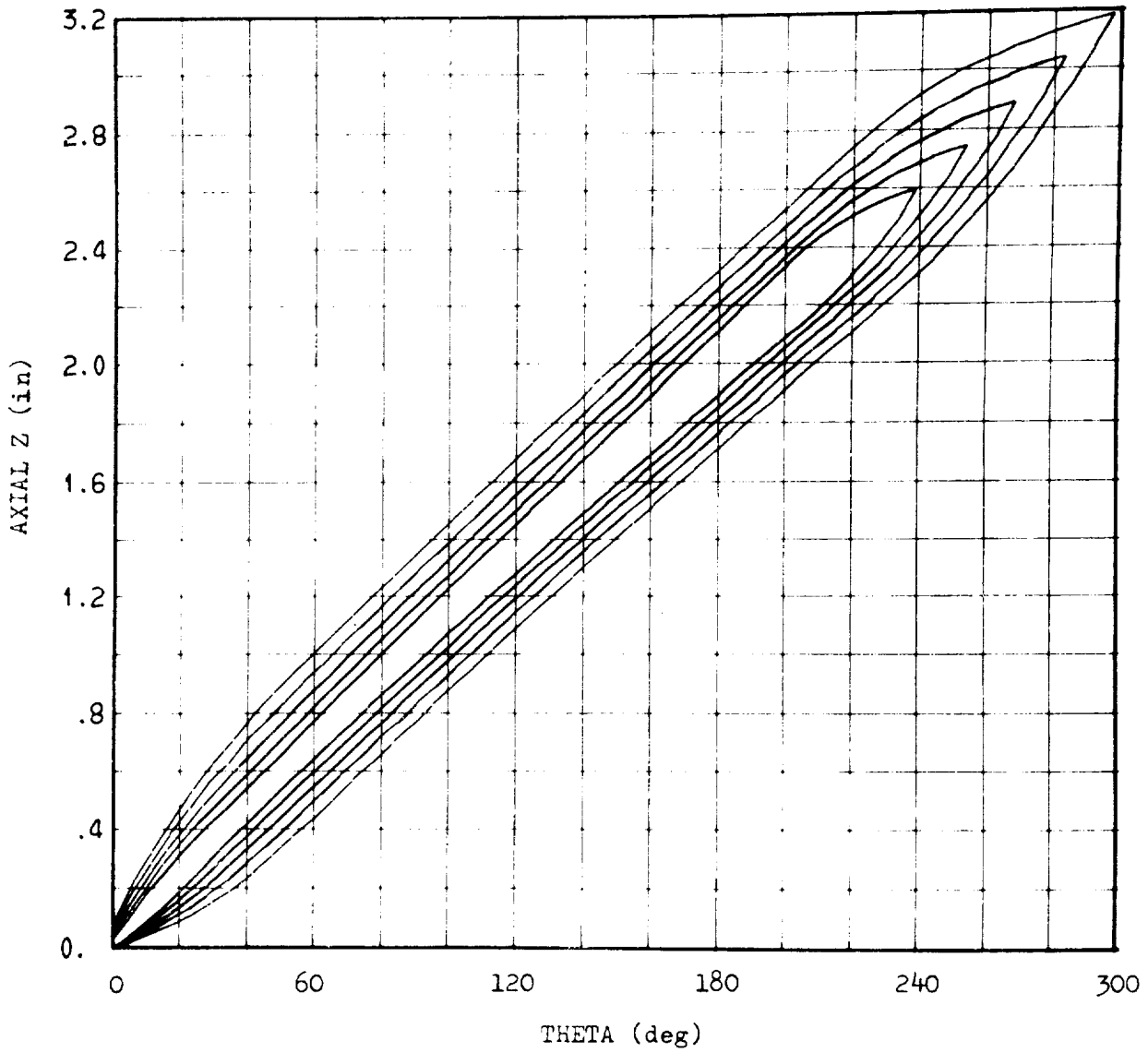Figure F.5   Non-Dimensionalized Data For 5 Blade Sections

Figure F.6   J-2 LOX Data For 5 Blade Sections Normalized To Trailing Edge